Exploring Rice Genetic Resources to Improve Nutrient Use Efficiency

Nahed Abdullah Ahmed Mohammed

PhD

University of York

Biology

February 2018

Abstract

Rice, as a major staple crop, is one of the most important targets for plant breeders in an attempt to secure enough food for a growing world population. Producing nutrient efficient crops has become essential not only to attempt securing enough food for the growing population, but also to eliminate environmental consequences of using fertilizers. Nitrogen (N), phosphorus (P) and potassium (K) are major macronutrients that are rate limiting for plant growth and crop productivity. The aims of this project were to explore the genetic diversity of rice to identify genotypes with high efficiency under N, P and K deficient conditions, to identify chromosomal loci linked to NPK use efficiency using Genome Wide Association Studies (GWAS), and to manipulate a proton pump using CRISPR/Cas9 system with the aim of improving mycorrhiza-dependent nutrient uptake. Biomass and elemental analyses revealed considerable variations among 294 rice genotypes, and a subset of genotypes was identified that were relatively tolerant to NPK nutrient limitation. GWAS study revealed novel and previously known QTLs and genes with potential importance to the use efficiency of N, P and K. Alongside with N and K transporters and regulatory proteins, unexpectedly several genes involved in Na transport were identified as candidates. The CRISPR/Cas9 system was successfully applied to manipulate several candidate genes identified from GWAS, in addition to the rice H^+-ATPase (OsHA1). Overall, the findings from this study can be used as a basis to conduct similar studies in other crops, which can all contribute to improve crop production, sustainable agriculture and food security.

Table of Contents

List of Tables

List of Figures

List of Appendices

Acknowledgements

The endless thanks to the almighty Allah for always being there for me, for all his blessings and for making me who I am today.

Words can never be enough to express my sincere gratitude to those incredible people in my life who made this thesis possible. Above all, I am deeply indebted to my supervisors Dr. Michael Schultze and Dr. Frans Maathuis, for their valuable suggestions, encouragement and help. Thanks to my advisory panel Prof. Ian Bancroft and Prof. Sue Hartley for their devoted guidance. Many thanks to those people who contributed to the success of my research, Dr. Juan Patishtan, Dr. Petra Stirnberg, Dr. Raquel Carvalho, Dr. Tom Hartley, Dr. Thomas Irving, the horticultural technicians, and to all my lab colleagues. It has been an honour to be a member of this research group.

I take this opportunity to dedicate this work to my parents, Abdullah and Fatimah. Thank you both for being a source of love, care, motivation and for giving me strength to achieve the best in my life. My heartiest thanks go to my brothers Mohammed and Ahmed, my sisters Nada, Najla and Shahad, for always offering love and support. To my dear husband Mohammed, thank you for being a great supporter and for your unconditional love and care. I also thank my friends Manuela Iovinella, Samra Irem, Laziana Ahmad and Nurashikin Ihsan for the unforgettable memories. Special thanks to Dr. Juan Patishtan, for being a great friend and supporter.

Finally, I gratefully acknowledge the financial support received from my government ruled by King Salman Bin Abdul-Aziz Al-Saud and previously by king Abdullah Bin Abdul-Aziz Al-Saud. I would like to express my deepest appreciation for giving me this great opportunity to continue my higher education abroad.

Declaration

I declare that this thesis is a presentation of original work and I am the sole author. This work has not previously been presented for an award at this, or any other, University. All sources are acknowledged as references.

Chapter 1: Introduction

1.1 Crop production and food security

By the middle of this century, it is estimated that the world population will be around 9 billion (Godfray et al., 2010). Increasing crop production is important to secure enough food for the growing population, but this is challenged by the decline in land and water resources (Godfray et al., 2010), biotic stress factors such as diseases, weeds, pests and pathogens (Atkinson and Urwin, 2012; Hammond-Kosack and Jones, 2000), abiotic stresses including climate change and extreme temperatures, drought and salinity, flooding, nutrient stresses or toxicities (Atkinson and Urwin, 2012; Chapman et al., 2012). One of the most important aspects that affect plant growth is providing sufficient amounts of mineral nutrients. Mineral nutrient deficiencies have an effect on plant growth and root morphology (Baligar et al., 1998) which subsequently influence the ability of the plant to take up and make use of these nutrients to fulfil the plant's needs (Fageria, 2012). It has been proposed that abiotic stresses account for more than 50% reduction in average crop yields (Wang et al., 2003).

1.2 Plant requirements for mineral nutrients

Plant roots take up mineral nutrients from the soil solution in inorganic form, as ions. Nutrients are classified as macronutrients and micronutrients based on the amount required by the plant (Maathuis, 2009). Six out of 14 vital nutrients are considered as macronutrients due to the large amounts they are needed in, while the others are known as micronutrients since they are needed in smaller amounts. Nitrogen (N), phosphorus (P), potassium (K), magnesium (Mg), calcium (Ca) and sulfur (S) are macronutrients, micronutrients include: Zinc (Zn), manganese (Mn), molybdenum (Mo), chloride (Cl), cobalt (Co), copper (Cu), iron (Fe) and nickel (Ni). Sodium (Na) and silicon (Si) are included in the micronutrient list by some authors (Maathuis, 2013). Beside mineral nutrients, three non-mineral elements are also required which are carbon (C), oxygen (O) and hydrogen (H).

1.2.1 Importance of nitrogen, phosphorus and potassium for plants

N, P and K are classified as macronutrients because of the large amounts of these nutrients that are needed by plants. They are building blocks of life that are required for healthy and optimum growth. Nitrogen plays central roles in providing amino groups in amino acids, photosynthesis, plant metabolism, building purine and pyrimidine bases, protein synthesis and non-protein compounds like coenzymes (Maathuis, 2013; Maathuis, 2009). Other than that, N nutrition is interlinked with that of potassium and carbon specifically. One of the most important roles of potassium is its ability to activate enzymes, providing electro-neutrality during NO_3^- transport, water homeostasis, cell turgor and movement of cells and organs in plants, cell expansion and the growth of plants, enhancing the size, shape, colour and taste of the plants (Maathuis, 2013; Nath and Tuteja, 2016). Reduced turgor pressure is observed in plants lacking K, causing reductions in growth rates (Maathuis, 2013), reductions in crop yield and also in plant health (Maathuis and Podar, 2011). Phosphorus is a component of sugar phosphate, nucleic acids and phospholipids (Taiz and Zeiger, 2010). It is important due to its role in the transfer of energy, protein metabolism, plant growth and health, root development and crop yield improvement (Fageria and Press, 2009). It is used in the build-up of DNA and is required during cell division and in the development of new tissues (Nath and Tuteja, 2016).

1.2.2 Interactions between N, P, K and other nutrients

Nutrient interaction in crop plants is measured in terms of uptake or yield level. Nutrient interactions may be positive (when application of a particular nutrient increases uptake of other essential plant nutrients), negative (when application of a particular nutrient decreases uptake of other essential plant nutrients), or neutral (when application of a particular nutrient has no effect on uptake of other essential plant nutrients). These interactions are also called synergistic, antagonistic or neutral, respectively (Aulakh and Malhi, 2005; Fageria, 2008; Malvi, 2011). Generally, nutrient concentration depends on the part of the

plant being analysed, plant age, plant species or genotype within species, and other factors (Fageria et al., 2005; Fageria, 1992; Fageria et al., 2006).

Positive interactions of K with N and P have been reported. Optimum supply of N ensures optimum uptake of K and P (Malvi, 2011). Often, yield response to K fertilizer is observed only when the supplies of other nutrients, especially N and P, are sufficient. Vice versa, a higher amount of K in the soil is needed with the application of N and P to increase crop yield (Dibb and Thompson Jr, 1985). Additionally, grain yield increased in response to NPK fertilization in upland rice (Fageria and Baligar, 2005). A study comparing the effect of fertilizing rice using N only, N with P, and N with P and K, revealed that grain yield increased up to 81.6% when P was added, and up to 9.8% with NPK compared to NP (Duan et al., 2014). Furthermore, P and PK addition has led to significant decrease in N loss to the environment (via leaching, denitrification and volatilization) when compared to the use of sole N (Duan et al., 2014).

Wilkinson et al. (2000) reported that P, K, S, Ca, and Mg uptake increased in response to N application, as long as these nutrients were present in adequate quantities in the growth medium. On the other hand, N addition can have negative interactions with micronutrients. For example, zinc deficiency was observed in upland rice and corn as a result of N application which led to higher demand for micronutrients and hence to micronutrient deficiencies (Fageria and Gheyi, 1999). Negative interactions between K and Mg and Ca uptake have been reported, which might be an effect of competition between these ions as their physiological properties are quite similar (Dibb and Thompson Jr, 1985; Fageria, 1983; Johansen et al., 1968). In crop plants, high levels of K decreased B uptake and increased B deficiency (Hill and Morrill, 1975). In contrast, addition of K improved Cu, Mn and Zn uptake (Dibb and Thompson Jr, 1985). Generally, P has positive interaction with N, K, and Mg. Conversely, P and Zn show antagonistic interaction (Wilkinson et al., 2000).

1.2.3 Uptake and distribution of N, P, K in plants

The movement of solutes and metabolites into and out of cells is ultimately facilitated by electrochemical H^+ gradients which are created by the activity of plasma membrane H^+-ATPases (Sondergaard et al., 2004).The plasma membrane in plants separates the cells from the surrounding environment. While it regulates the transport of molecules and ions into and out of the cells, internal membranes regulate solute transport within each cell. If the movement is from areas of higher (electro) chemical potential to lower chemical potential areas, the process is called passive transport (diffusion) as it occurs without the direct need for energy and is mediated by channels and uniporters. Active transport is the movement of substances against the (electro) chemical-potential gradient and it requires energy which is often provided by the hydrolysis of ATP. Primary active transport is against the direction of electrochemical gradient and the energy here is often derived directly from the breakdown of ATP, this type of transport is mediated by pumps. Secondary active transport is also against the direction of electrochemical gradient, but the energy here is derived secondarily from a stored free energy in the form of the H^+ gradient known as proton motive force (PMF), and is mediated by symporters and antiporters.

1.2.3.1 Nitrogen uptake and distribution

Plants utilize nitrogen in the form of ammonium (NH_4^+) and nitrate (NO_3^-) (Malvi, 2011). N is taken up through root specific high (HATs) and low (LATs)- affinity transporters for both ammonium and nitrate. HATs mediate the uptake in low N concentrations while LATs mediate under high concentrations (Huang et al., 2018). Genes encoding NH_4^+ and NO_3^- transporters in different plant cell compartments are shown in Figure 1.1.
Uptake and translocation of nitrate in rice is mediated by four protein families: chloride channel family (CLC), slow anion channel-associated homologues (SLAC/SLAH) (Krapp et al., 2014), and the NPF nitrate transporter 1/peptide transporter family (also known as the NRT1/PTR family) which in rice comprises at least 80 proteins. Of the latter, most are involved in low affinity transport of nitrate except OsNPF6.5 (NRT1.1b) which has dual affinity (Bin et al., 2015; Tsay et al., 2007). Lastly, the fourth family is the nitrate

transporter 2 family NRT2 which consists of five members, including OsNRT2.1, OsNRT2.2, OsNRT2.3a, OsNRT2.3b, and OsNRT2.4, and the NAR2 family which includes two members (OsNAR2.1, OsNAR2.2) (Araki and Hasegawa, 2006; Fan et al., 2016; Feng et al., 2011; Hu et al., 2015; Tang et al., 2012; Yan et al., 2011; Yang et al., 2017b). High affinity transport systems (HATS) in rice consist of two gene families: NRT2 and NAR2. All three OsNRT2.1/2.2/2:3a transporters require OsNAR2.1 as a partner to mediate nitrate transport. Moreover, knockdown of OsNAR2.1 resulted in supressed expression in OsNRT2.1, OsNRT2.2 and OsNRT2.3 transporters (Yan et al., 2011). OsNRT2.1 and 2.2 are believed to have a key role in nitrate uptake (Araki and Hasegawa, 2006). OsNRT2.3 has two mRNA splice variants: OsNRT2.3a and OsNRT2.3b. It has been observed that OsNRT2.3a plays a major part in long distance nitrate transport from root to shoot specifically under low nitrate (Tang et al., 2012).

In rice, there are four AMT families that mediate ammonium transport. Family 1, 2 and 3 have 3 members in each whereas the AMT4 family has only one member. AMT1 members are considered to be high affinity transporters, the other 3 families are characterized as low affinity transporters (Bao et al., 2015; Gaur et al., 2012; Li et al., 2012; Li and Shi, 2006; Loqué, 2004; Ranathunge et al., 2014; Sonoda et al., 2003a; Sonoda et al., 2003b; Suenaga et al., 2003).

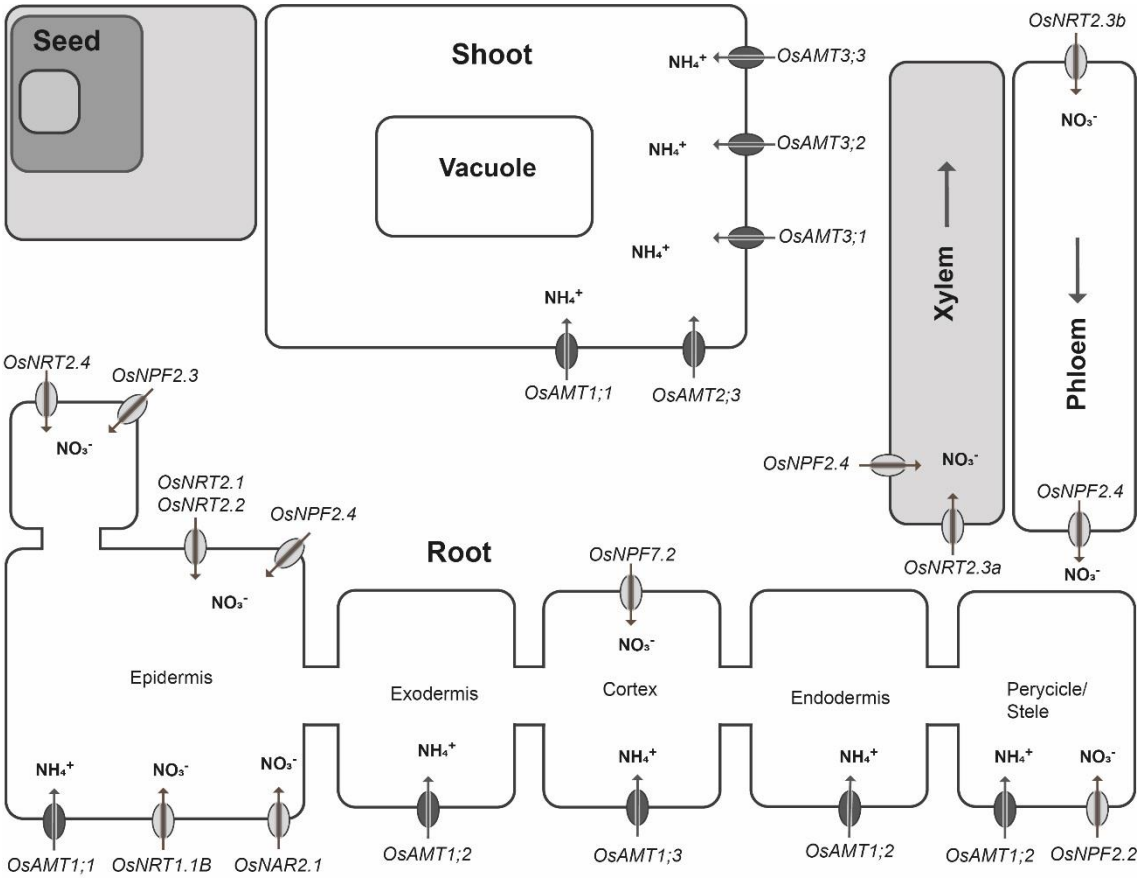

Figure 1. 1: The genes encoding NH_4^+ and NO_3^- transporters in different plant cell compartments including root, xylem, phloem, shoot and seed.

1.2.3.2 Phosphorous uptake and distribution

P is taken up in the form of inorganic orthophosphate (Pi, HPO_4^{2-}, $H_2PO_4^-$) (Malvi, 2011). Various phosphate ion transport systems are taking part in the assimilation of Pi (Nath and Tuteja, 2016). Direct uptake from soil takes place through $Pi:2H^+$ cotransporters (Nath and Tuteja, 2016). Phosphate transporters (PHT) play pivotal roles in the uptake of inorganic phosphate from the soil (Maruyama and Wasaki, 2018). Genes encoding inorganic phosphate ($H_2PO_4^-$) transporters in different plant cell compartments are shown in Figure 1.2. High affinity symporters belonging to the PHT1 family comprise a total of 13 members that are located in the plasma membrane and take part in Pi uptake from the soil and translocation and root-shoot mobilization (Ai et al., 2009; Jeong et al., 2015; Jia et al., 2017; Kobae and Hata, 2010; Lin et al., 2009; Paszkowski et al., 2002; Smith et al., 2011;

Sun et al., 2012; Wang et al., 2014b; Ye et al., 2015a; Zhang et al., 2015a). PHT2 is located in the chloroplast, PHT3 in the mitochondria and PHT4 in the Golgi apparatus and non-photosynthetic plastids (Nath and Tuteja, 2016).

PHT activity is regulated by the phosphate starvation response 1 (PHR1) transcription factor. AtPHR1 in rice regulates the activity of PHT (Chiou and Lin, 2011). High and low-affinity transporters are used to maintain Pi homeostasis under stress conditions in plants. Also, the plasma membrane Pi transporter and phosphate transporter traffic facilitator 1 (PHF1) maintains Pi homeostasis. In low P conditions, Pi high affinity transporters are expressed in roots (Nath and Tuteja, 2016). Further proteins that may be involved in phosphate homeostasis are found in the PHR (Guo et al., 2015; Ruan et al., 2017; Wu and Wang, 2008), PHO (Secco et al., 2010; Secco et al., 2012a) and SPX domain-containing protein families (Chen et al., 2011; Liu et al., 2010b; Secco et al., 2012b; Wang et al., 2012; Wang et al., 2017; Wang et al., 2009).

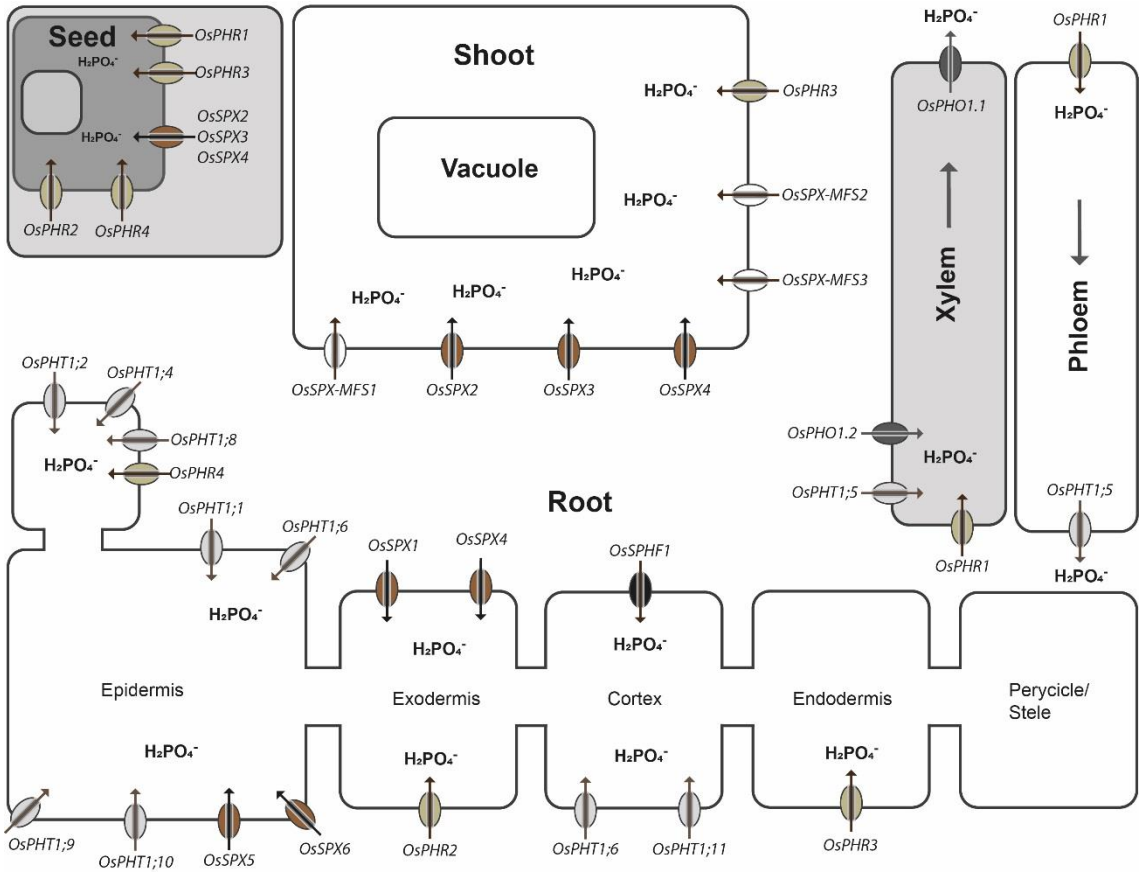

Figure 1. 2: The genes encoding inorganic phosphate ($H_2PO_4^-$) transporters in different plant cell compartments including: root, xylem, phloem, shoot and seed.

1.2.3.3 Potassium uptake and distribution

Potassium is taken up in its ionic form (K^+) (Malvi, 2011). Uptake of potassium ions from the soil is against the K^+ concentration gradient and is powered by the membrane potential and maintained by the H^+-ATPase (Nath and Tuteja, 2016). Genes encoding potassium (K^+) transporters in different plant cell compartments are shown in Figure 1.3. Various gene families including KT/HAK/KUP, HKT, NHX and CHX are involved in K^+ transport in plants (Chen et al., 2015a; Chen et al., 2015b; Fukuda et al., 2004; Yang et al., 2014a). High-affinity potassium transporter family (HKTs) consists of 2 classes: Class 1 includes 4 members and mediates Na transport only, while class 2 can transport both K and Na and consists of 4 members (Garciadeblás et al., 2003; Horie et al., 2011b; Lan et al., 2010a;

Suzuki et al., 2016; Waters et al., 2013; Yao et al., 2010). In rice, 27 genes belonging to the KT/HAK/KUP potassium transporter family are distributed among 8 chromosomes and they cluster in four major groups based on their amino acid sequences (Chen et al., 2015a; Chen et al., 2015b; Gupta et al., 2008; Yang et al., 2014a). Functions of HAK cluster III and IV members are less well understood compared to cluster I and II members (Grabov, 2007). In general, the majority of cluster I members in plants tends to have a role in high affinity K uptake, and cluster II members are likely to function as low affinity K transporters (Okada et al., 2008). However, physiological functions of these transporters not only differ between plant species but also between members of the same cluster within the same species (Li et al., 2017).

To release K+ from the vacuole rice has two-pore potassium channels (OsTPKa and OsTPKb) that are highly similar in their protein sequences and function as they both play an important role in K homeostasis. However, they are different in their location. While OsTPKa is located in the tonoplast of the large lytic vacuole (LV), OsTPKb is located in smaller protein storage vacuoles (PSVs) (Isayenkov et al., 2011). Outward-rectifying shaker-like potassium channels include OsSKOR and OsSGOR. SKOR channels are important for K distribution in tissues and cells through its secretion from the root cortical cells to the xylem (Jarzyniak and Jasiński, 2014; Kim et al., 2015; Nguyen et al., 2017). Inward rectifying potassium channels include OsAKT1 and OsAKT2 (Ahmad et al., 2016b; Deeken et al., 2002; Li et al., 2014; Obata et al., 2007). The AKT2 channel takes part in the loading and unloading of K in the phloem (Gajdanowicz et al., 2011). Inward rectifying shaker-like potassium channels include OsKAT1, OsKAT2, and OsKAT3 (Hwang et al., 2013; Obata et al., 2007).

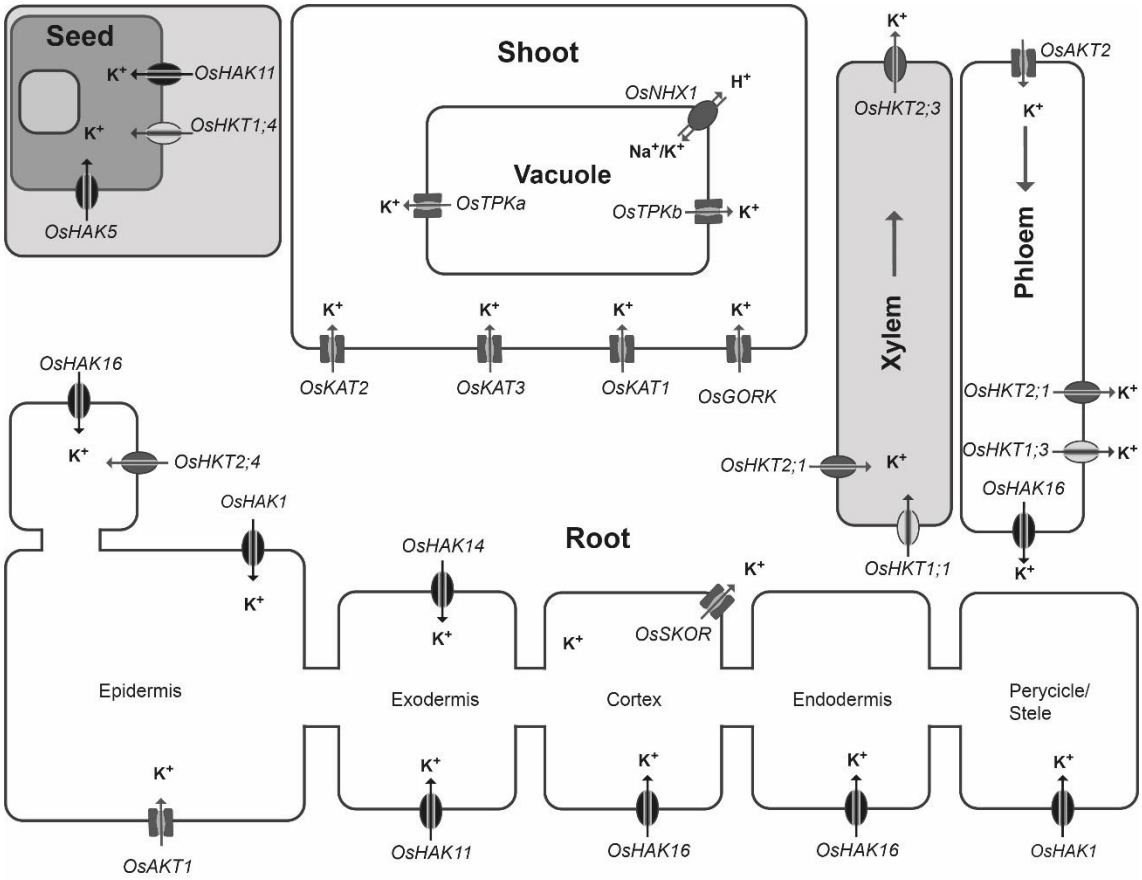

Figure 1. 3: The genes encoding potassium (K^+) transporters in different plant cell compartments including root, xylem, phloem, shoot and seed.

1.3 Nutrient deficiency and the use of fertilizers

Nitrogen, phosphorus and potassium are the most common nutrients that are considered as rate limiting for plant growth and crop productivity (Taiz and Zeiger, 2010). Despite the abundance of inorganic, organic and atmospheric N, large amounts of N fertilizers are applied in agricultural areas. Also, K deficiency is becoming increasingly common and potash fertilizers are widely used to get the best plant production. In addition, P fertilizers are applied as more than 90% of the phosphorus in the soil is tightly fixed in minerals and not available for plants to take up.

Many world soils have deficiencies in several essential nutrients. Application of fertilizers in agricultural soils is needed to provide adequate supply of essential nutrients in case of

deficiency in one or more of these nutrients. During the 20th century, around 50% of the increase in global crop production was due to the application of chemical fertilizers (Borlaug, 1994). Over the past five decades, a 20-fold increase in the use of N fertilizers worldwide positively affected crop production (Glass, 2003). Currently, the world uses around 105 million tons of N, 20 million tons of P, and 23 million tons of K fertilizers for crop production (FAO, 2013). However, the overall uptake efficiency of applied fertilizer is about or lower than 50 % for N (Raun and Johnson, 1999) , less than 10 % for P and about 40 % for K (Baligar and Bennett, 1986a, b). The demand for N, P, and K fertilizers is estimated to increase by 1.5%, 2.2%, and 2.4%, respectively, per annum from 2015 to 2020 (FAO, 2017). A further disadvantage of low uptake efficiency is the risk of minerals to either leach into groundwater or to increase air pollution (Taiz and Zeiger, 2010). Over 60% of soil N is being leached, volatilized, consumed by microbes, surface run off or lost by denitrification (Kant et al., 2011). In rice, it is estimated that 10% of N fertilizer is lost as a result of denitrification (De Datta et al., 1991). In addition, fertilizer production is costly, especially for N as it requires a large amount of energy to produce (Rothstein, 2007; Sanyal et al., 2015). The price of nitrogen, phosphorus and potassium fertilizers dramatically increased by ~60%, 360%, and 170% respectively, between mid-2007 and 2008 (Huang, 2009). Therefore, to respond to limitations in fertilizer supply and to reduce environmental impact, there is scope for increasing nutrient use efficiency in crop plants.

1.3.1 The use of NPK fertilizers in the rice production

Rice can grow in both dry and wet environments under varying climatic and soil conditions, but mainly grown in the humid tropics. More than 90% of the total rice production is harvested from irrigated and rainfed lowland rice systems (Dobermann, 2000). NPK fertilizer for rice production accounted for 14.3 % of the global fertilizer consumption during 2010/11, and percentages of NPK were 15.4, 12.8, and 12.6, respectively (Heffer, 2013). Application of N fertilizer is usually split into at least two doses per growing season, where the first application (basal dose) represents up to 75% of the total plant requirement (Chauhan et al., 2017). For the basal dose and at planting stage, NH4+ based fertilizers should be applied, but during panicle initiation stage the preferred

nitrogen source is NO3- (Wilson et al., 1994). Due to variability in soil fertility, different N management practices are recommended for different soil conditions, also optimum levels of NPK fertilizers for different countries have been proposed considering the variation of different field conditions (Halliday and Trenkel, 1992). To reach optimum rice yields, balanced fertilization is required together with the right source, rate, place and time of application. Balanced fertilization of N with appropriate amounts of P and K is required to achieve optimal yield. A study on rice-wheat cropping system with variable NPK rates revealed that the lowest yield obtained was under sole N fertilization, while the highest yield obtained when NPK fertilizer was applied at a rate of 40, 35, and 33kg ha−1, respectively (Kumar and Yadav, 2001). Application of P fertilizer is normally as early as planting stage due to its importance in root elongation, however, late applications might be provided before tillering stage (De Datta, 1981). Most, if not all, of the total amount of the required K fertilizer is generally applied at or around seeding/transplanting stage, but split doses are applied sometimes (Jian-chang, 2004). For rice production, the most commonly used N fertilizers are ammonium sulfate, urea and diammonium phosphate. To supply K to rice, potassium chloride or potassium sulfate are usually applied. As P source, di- or mono-ammonium phosphate fertilizers, or single and triple super phosphates are applied (Chauhan et al., 2017).

1.4 The role of mycorrhizal symbiosis in nutrient acquisition

In addition to the application of nutrient fertilizers, symbiotic relations between plants and soil microorganisms may enhance nutrient acquisition. Around 80% of monocots and dicots form mycorrhizal symbiotic relations (Taiz and Zeiger, 2010). Arbuscular mycorrhiza (AM) is a symbiotic relationship between plants and a phylum of soil fungi known as Glomeromycota (Parniske, 2008). Mycorrhizal fungi are present widely under natural conditions. They consist of thin, tube-shaped filaments known as hyphae and the hyphal network, or mycelium, forms the fungal body. The name arbuscular comes from the arbuscules, which are distinctive structures resembling branches or tunnels, formed within the cortical cells of plant roots colonized by mycorrhizal fungi. Storage vesicles are other distinctive structures that indicate establishment of mycorrhizal symbiosis in addition to the

formation of intracellular coils of hyphae (Smith and Read, 2008). Mycorrhizal fungi associate with the plant root system forming a symbiotic relationship to improve the ability of the plant to acquire nutrients such as phosphorus, zinc and copper as the fine hyphae have the ability to reach the surrounding soil areas which plant roots cannot reach because hyphae are much thinner. These areas are farther away from the roots than depletion zones (Taiz and Zeiger, 2010). The key advantage of AM symbiosis is its ability to enhance phosphate uptake of the plants (Leon, 2012). In rice, 70% of total phosphorus uptake owed to AM symbiosis (Yang et al., 2012). Mycorrhizal symbioses also help the plant to become more tolerant to biotic and a biotic stresses (Wang et al., 2014a) and more resistant to pathogens, drought and salinity (Bhattacharjee and Sharma, 2011). Thus, the arbuscular mycorrhizal symbiosis (AM) has the potential to contribute significantly to crop yield and worldwide food security (Bethlenfalvay, 1992; Hu et al., 2009). Under AM colonization, proton pumps (H^+-ATPases) work as energizers for the peri-arbuscular membrane to facilitate nutrient exchange between the plant acquiring mineral nutrients and the fungus acquiring fixed carbon by creating a H^+ gradient (Krajinski et al., 2014; Wang et al., 2014a).

1.5 Nutrient use efficiency

Nutrient use efficiency (UE) generally is the maximum yield or dry matter produced per nutrient uptake (Baligar et al., 2001). (Gourley et al., 1994) defined nutrient efficient plants as “germplasm that requires fewer nutrients than an insufficient one for normal metabolic processes”. More recently, (Fageria et al., 2008) defined efficient plant as one “that produces higher economic yield with a determined quantity of applied or absorbed nutrient compared to other or a standard plant under similar growing conditions”. Nutrient use efficiency is based on three factors: uptake efficiency, incorporation efficiency and utilization efficiency (Baligar et al., 2001). Uptake efficiency is based mainly on root parameters including the ability to acquire nutrients from soil, influx level and transport in roots. Incorporation efficiency is based on shoot parameters including transfer of nutrients to shoot and leaves. Finally, utilization efficiency is based on both shoot and root parameters including remobilization from older to younger leaves and from vegetative to

reproductive tissues and ability to utilize the absorbed nutrients in grain or dry matter production (Baligar et al., 2001).

Producing plants with high nutrient use efficiency (UE) under varying environmental circumstances, especially in crop plants, is highly important not only as an attempt to increase food production but also to reduce the use of fertilizers, reduce losses of nutrients (Baligar et al., 2001), reduce environmental pollution and cost of production (Fageria et al., 2013b). For example, a 1% increase in nitrogen use efficiency is estimated to result in an annual saving of around $1.1 billion (Kant et al., 2011).

1.6 Approaches to improve crop yields

Crop yield can be increased either by improving nutrient use efficiency or fertilizer use efficiency through the development of varieties that produce high yields with less fertilizer inputs. This can be achieved by exploiting genetic variation between genotypes to identify superior genotypes, and/or genes that might play a role in nutrient use efficiency. Mapping approaches such as quantitative trait loci (QTL) and genome wide association studies (GWAS) can be exploited to identify regions in the genome that can be targeted to improve desirable traits in crops (Spindel and McCouch, 2016). Following gene identification through mapping approaches, functional analysis using forward and reverse genetics, and transgenic approaches can also be employed to improve crop yield (Wan et al., 2017).

As plants vary in their ability to take up and utilize nutrients, improving nutrient use efficiency can be achieved by using genotypes that have higher levels of tolerance to biotic and abiotic stresses. Using more efficient genotypes in absorbing nutrients at higher rate at low nutrient conditions leads to the achievement of maximum crop yield and better quality food material (Baligar et al., 2001; Fageria et al., 2008). Using improved cultivars together with applying best management practices for different soil types would also reduce cost of production and increase nutrient use efficiency (Baligar et al., 2001; Clark and Baligar, 2000). Enhanced fertilizer use efficiency can be achieved by increasing the uptake capacity of the roots, for example, by overexpressing the genes that relate to the absorption and

transport of the nutrients (Huang et al., 2018). Another way to improve fertilizer recovery efficiency is using appropriate types of fertilizers, e.g. single- or multi-nutrient slow release fertilizers (SRF) and controlled release fertilizers (CRF) which allow stable and continuous provision of nutrients throughout the whole growth period (Baligar et al., 2001).

1.6.1 Transgenic approaches to improve crop yield

Nutrient use efficiency can be improved by engineering root growth to enhance the response of the roots to nutrient availability (Wan et al., 2017). For example, overexpressing OsTOND1 in rice enhanced the primary root length and nitrogen uptake as well as the nitrogen shoot concentration, leading to an increase of grain yield (Zhang et al., 2015b). The manipulation of different genes that code for transporters in plants enhanced roots ability to grow and absorb ions from low macronutrient conditions. For example, overexpression of the transporter genes such as OsNRT2.3b and OsNAR2 in rice increased grain harvest under standard and low nitrogen conditions (Fan et al., 2016). The ammonium transporter OsAMT1 can be used to modify nitrogen use efficiency in rice, a species that utilizes ammonium as the major N resource in paddy fields (Ranathunge et al., 2014). Under phosphorous deficiency, the activation of the expression of PHT1 genes increased the capability of the roots to obtain the macronutrient from the soil (Raghothama and Karthikeyan, 2005). Also, P transporters can be enhanced by overexpressing their genes such as OsPHT1.1 in roots and shoots to increase their activity. Overexpression of OsPHT1.4 increased Pi accumulation in roots while OsPHT1.6 increased the uptake rate and accumulation of Pi (Wan et al., 2017).

The utilization of potassium can be enhanced by its translocation into different organs and enhanced ability to substitute Na for K (White, 2013). Manipulation of the expression of potassium channels and transporters such as KUP/HAK/KT using transcription factors improved the use efficiency of the macronutrient and increased stress tolerance in *Arabidopsis thaliana* (Nieves - Cordones et al., 2010). Overexpression of OsHAK5 in rice increased the net K influx rate in roots and the transport to distant parts (Nath and Tuteja, 2016). Furthermore, nutrient use efficiency can be improved by engineering transcription

factors (TFs) and regulatory proteins. For example, overexpression of transcription factors such as DDF2, TFIIA and bHLH121 enhanced the growth of roots under low potassium conditions in *Arabidopsis thaliana* (Hong et al., 2013). Rice plants under high nitrate showed increased root length, shoot biomass, shoot N accumulation and the expression level of nitrate transporters when OsMAD25 transcription factor was overexpressed (Yu et al., 2015). It has been shown in rice that the expression of the majority of genes that are induced by P starvation are controlled by OsPHR1, OsPHR2 and OsPHR3 transcription factors. Moreover, overexpression of OsPHR3 led to enhanced tolerance of rice plants under P deficiency (Guo et al., 2015).

1.7 Importance of rice and rice as a model of choice

Rice is a staple food for over half of the world's population (Nguyen, 2002), and it is the main source of nutrition in developing countries (Toriyama, 2005). It is estimated that in order to meet the world's demand, 60 million tons of rice should be added to the current production every year (Muthayya et al., 2014). Rice is a monocotyledonous plant belonging to the grass family (Poaceae) with other grasses such as wheat, maize and barley. Two out of 22 recognized species of *Oryza* genus are known to be cultivated, the Asian rice *Oryza sativa*, and the African rice *Oryza glaberrima*, the rest are wild species (Vaughan et al., 2003). Cultivated Asian rice *O. sativa* is divided into two major groups each of which is divided into well differentiated sub-populations. Indica includes indica and australis, and japonica includes the tropical japonica, temperate japonica and aromatic (Glaszmann, 1987).

Rice was chosen as a model in this project because of the small size of its genome (430 Mb) which has been fully sequenced, self-fertilization, ease of cultivation and ease of transformation by *Agrobacterium*. These factors contribute to the significance of the research of the cultivation of rice and ways that can increase its production. Research done on rice has led to the production of varieties with desirable traits and it contributed to increased rice production globally from 260 to 700 million tons during the past 5 decade (Maclean et al., 2013). Additionally, information gained from studies on rice allow us to

study other grasses and cereal crops that are shown to have a monophyletic origin (Itoh et al., 2005) and plentiful of genomic resources (Wang et al., 2013).

1.8 Aims

The overall aim of this project was to contribute to improving crop production by producing nutrient efficient crop that can produce high yield with less fertilizer inputs. The first research chapter aimed to test if genetic diversity among rice genotypes would enhance nutrient use efficiency by identifying high performing genotypes under stress conditions where major multiple elements (N, P and K) are limiting. The second research chapter aimed to link differences in phenotypes with genotypes using genome wide association studies (GWAS) to identify markers linked to the use efficiency of N, P and K. For the third research chapter, the aim was to test if increasing the activity of the rice H^+-ATPase (OsHA1) by manipulating the regulatory domain using one of the latest genome editing tools (CRISPR/Cas9 system), would improve P uptake and growth under mycorrhizal colonization.

Chapter 2: Characterisation of rice cultivars under Nitrogen, Potassium and Phosphorus deficiency

2.1 Introduction

Abiotic stresses including extreme temperatures, drought, salinity and nutrient stresses account for more than 50% reduction in average crop yields (Wang et al., 2003). Change in physiological, developmental and morphological characteristics are observed in plants in response to nutrient supply. On a morphological basis, nutrient deficiency symptoms can be visually analysed by monitoring changes in plant size, leaf colour and root architecture. For example, P deficient rice plants are short, have narrow dark green erect leaves and thin stems (Fageria et al., 2013b). In rice, chlorosis is observed in K deficient plants with brown leaf margins, while leaves of N deficient plants are yellowish (Chen et al., 2014; Taiz and Zeiger, 2010). Changes in root growth and architecture in *O. sativa* are found to be an adaptive trait in response to nutrient deficiencies (Sales et al., 2011) together with other adaptive mechanisms that occur in plants in general such as changes in expression patterns of ion transporters (Ashley et al., 2006) or soil acidification for nutrient mobilization (Ryan et al., 2001). Biomass analysis is an indicator to determine the efficiency of using (absorbing, translocating, and utilizing) nutrients under different conditions. It has been shown that plants generally allocate more biomass in roots as a response to nutrient shortage, and macronutrient deficiencies lead to variations in the shoot to root ratio (Hermans et al., 2006). Plant growth is greatly influenced by nutrient uptake (Sinclair, 1992) and reduction of growth was observed under P, K and N deficiency in *Arabidopsis thaliana*, sorghum and other plants (Ashley et al., 2006; Lopez-Bucio et al., 2005; Poirier and Bucher, 2002; Zhao et al., 2005).

Observation of deficiency symptoms only is not a sufficient method of diagnosis for nutrient disorders, since deficiency symptoms of one nutrient can be confused with other nutrients. In addition, ionomic traits would provide better understanding of plant growth as better distribution of nutrients in parts of the plant (root, shoot and grain) reflects their use

efficiency. A study on *Arabidopsis thaliana* plants grown under different supplies of P and K revealed that 85% of the growth variations were explained by variation in ion content (Prinzenberg et al., 2010). Generally, nutrient concentration depends on the part of the plant being analysed, plant age, plant species or genotype within species, and other factors (Fageria et al., 2005; Fageria, 1992; Fageria et al., 2006). A study on N concentrations in rice revealed that N uptake in the shoot as well as in the grain was significantly related to shoot dry weight and grain yield (Fageria, 2003).

Nutrient use efficiency can be defined and measured in various ways (Baligar et al., 2001), but overall it reflects the ability of the plant to use the available nutrients sufficiently in producing maximum yield or dry matter. There is an urgent need to increase crop yield in order to meet the world demand of food. Taking into consideration the drawbacks of the increased fertilizer application, the development of varieties that produce high yields with less fertilizer input is important for improving crop yield and sustainable agriculture. One of the reasons behind the differences in the use efficiency of nutrients is genetic variability between genotypes. These differences can be based on differences in nutrient uptake, translocation, dry matter production/unit nutrient absorbed and plant ecological interactions (Baligar et al., 2001). Better performance of some genotypes may be associated with better root geometry, ability of plants to take up sufficient nutrients from lower subsoil concentrations, better transport or distribution and utilization within plants (Fageria et al., 2008). Genetic variation among rice cultivars has been reported for nitrogen (Ju et al., 2006; Namai et al., 2009; Samonte et al., 2006), potassium (Fageria et al., 2013c; Liu et al., 2009; Yang et al., 2003) and phosphorus (Fageria and Baligar, 1997; Fageria et al., 2013a, 2014; Wissuwa and Ae, 2001).

Rice cultivation is the largest use of land for food production, with over 144 million farms around the world (Maclean et al., 2013). Most of these farms are in low-income developing countries where significant fertilizer inputs are not affordable by farmers. Even if fertilizers are applied, the use efficiency of these fertilizers is less than 50% for N (Raun and Johnson, 1999), less than 10 % for P and about 40 % for K (Baligar and Bennett, 1986a, b). Although previous studies in rice were conducted to evaluate different varieties and

improve use efficiency for nitrogen, phosphorus and potassium separately, no previous studies focused on identifying efficient genotypes when multiple elements (NPK) are reduced in parallel. This study was conducted to identify rice genotypes that are more efficient to grow under low supply of NPK. The diverse genotypes used from the Rice Diversity Panel 1 (RDP1) represent all five sub-populations of rice (*Oryza sativa* L.) including indica, australis, temperate japonica, tropical japonica and aromatic, and this panel have been selected from different geographical regions around the world (Zhao et al., 2011). Due to the positive interactions between N, P and K and the critical roles they play in terms of plant growth and yield, identifying varieties that are able to grow well and produce yield with a minimum amount of these nutrients would enormously contribute to increasing crop production while reducing fertilizer inputs and their consequences. Even if these varieties would show lower yield compared to standard varieties under optimal conditions, a small growth advantage under nutrient limiting conditions would have a great impact. For example, a 1% increase in nitrogen use efficiency is estimated to result in an annual saving of around $1.1 billion (Kant et al., 2011).

2.2 Materials and methods

2.2.1 Growth conditions and biomass analysis

A total of 317 rice accessions were examined to find out which lines are more tolerant to low nutrient conditions (reduced N, P, and K concentrations). These lines are from the rice diversity panel 1 (RDP1) which encompasses accessions representing all subpopulations of rice (Table 2.1). The seed stock was obtained from The National Rice Research Centre (https://www.ars.usda.gov/southeast-area/stuttgart-ar/dale-bumpers-national-rice-research-center/docs/genetic-stocks-oryza-gsor-collection-home/). A minimum of 3 seeds from each accession was placed in one compartment in P40 trays filled with sand (obtained from https://www.aggregate.com) for germination. Two weeks after sowing, initial fresh weight was measured, then seedlings were transferred to hydroponics (9L boxes with 54 places each) where two test conditions were applied for 3 weeks. Plants were either grown in full strength modified Yoshida medium (Yoshida et al., 1976) or in the same nutrient solution except that the concentration of N, P, K was reduced to 1/10. One plant from each

accession was grown under each condition. Medium was replaced once a week and the pH of the medium was set at 5.5 and was not adjusted during the week. In the glasshouse, plants were supplemented with light to provide a minimum of 12 h daylight; minimum 28 °C day, minimum 24 °C night temperature.

The accessions were divided into two batches: the first batch included 204 accessions and the second batch had around 113 accessions. As some accessions failed to germinate and some had less than 3 replicates, we ended up with a total of 294 accessions. Each batch was repeated 4 times, with randomizing the accessions each time. Three Nipponbare plants in each box were used as a reference. The first batch was grown during Aug, Sep and Oct 2014, and the second batch during Nov, Dec 2014 and Jan 2015.

Plants were kept in test conditions for 3 weeks, then fresh weight, dry weight and relative growth rate were measured. The relative growth rate was calculated using the formula: RGR = (ln W2 - ln W1)/(t2-t1), where: ln = natural logarithm, t1 = time one (in days), t2 = time two (in days), W1 = Fresh weight of plant at time one (in grams), W2 = Fresh weight of plant at time two (in grams) (Hoffmann and Poorter, 2002).

Table 2. 1: Rice diversity population used in this study and the number of accessions in each subpopulation of rice.

Subpopulation	Number of accessions
Indica	55
Australis	46
Tropical japonica	82
Temprate japonica	65
Aromatic	10
Admixed	6
Admixed-indica	4
Admixed-japonica	26

2.2.1.1 Yoshida medium preparation

The original recipe of Yoshida medium (Yoshida et al., 1976) was modified by replacing some salts in the original recipe with others in order to keep the concentrations of the other elements the same while reducing N, P, K concentrations to 1/10 (Table 2.2). In brief, the following macronutrients were modified: potassium sulfate (K_2SO_4) was replaced with potassium chloride (KCl). In full strength medium (1 NPK) the total concentrations of N, P and K were: 2.86 mM, 0.32 mM and 1.02 mM respectively. In 1/10 medium (0.1 NPK), the total concentration of N was 0.29 mM, P was 0.03 mM and K was 0.10 mM. The total sodium concentration was about 0.59 mM and 0.059 mM, under 1 NPK and 0.1 NPK, respectively.

Table 2. 2: Components and concentrations of elements in 1 NPK Yoshida medium used in hydroponics.

	Component	Element	Element concentration (mM)
Macronutrient	NH_4NO_3	N	2.86
	NaH_2PO_4	P	0.32
	KCl	K	1.02
	$CaCl_2$	Ca	1.00
	$MgSO_4 \cdot 7\ H_2O$	Mg	1.64
Micronutrient	$CuSO_4$	Cu	0.00016
	$ZnSO_4$	Zn	0.00038
	$MnSO_4$	Mn	0.0018
	H_3BO_3	B	0.045
	$(NH_4)_6Mo_7O_{24}$	Mo	0.00002
	NaFeEDTA	Fe	0.04358
	(Na_2O_3Si)	Silica	0.02

2.2.1.2 Testing growth reductions for a subset of accessions under low NPK condition

Based on relative growth rate reduction (RGRRED) results from the growth experiment which included 294 genotypes (I will refer to as 1st experiment from here onwards), a number of candidate genotypes was selected for re-testing as follows: 22 genotypes were selected as they appeared to have less reduction in growth rates (tolerant) compared to

others and 19 genotypes with large reductions (sensitive). Seeds were germinated in sand for 2 weeks then transferred to test conditions for 3 weeks. Three seedlings from each genotype were transferred to 0.1 NPK condition for retesting. Three seedlings were also transferred to 0.01 NPK condition to test their performance under more severe nutrient stress. RGR of these genotypes under 1 NPK condition from the 1st experiment was used to calculate RGRRED when re-testing. Ion data was from plants in the 1st experiment, not from re-tested plants. Data from genotypes with fewer than 3 replicates were excluded from the experiment. At the end, 15 tolerant and 11 sensitive genotypes were tested.

2.2.2 Elemental analysis

Due to the large number of plants used in this experiment, analysing content of elements in each replicate and accession was not feasible. In total, 294 pooled samples from each condition (control and 0.1 NPK) were processed. The entire dry shoot was milled using a robot that is custom-made by (https://www.labmanautomation.com) to grind plant biomass and dispense specified amounts of material into the corresponding tubes. Equal amounts from each plant in each replicate were measured and then pooled to have a total of 80 mg (4 replicates: 20 mg each, 3 replicates: 26.7 mg each). For inductively coupled plasma optical emission spectrometry (ICP-OES) analysis, around 20 mg were weighed out from each pooled sample into 2 ml Eppendorf tubes and 1 ml of concentrated nitric acid was added. The tubes were placed in a heating block and left overnight at 70 °C to digest. Digests were diluted by adding 19 ml of deionised water to a final concentration of 5% HNO_3. Elements were measured using ICP-OES at wavelengths (nm) and plasma view as follows: P (177.495, Axial), K (766.490, Radial), Na (589.592, Radial), Mg (279.553, Radial), Ca (396.847, Radial), Zn (213.856, Axial), Fe (259.940, Axial) and B (249.773, Axial). A commercial ICP multi element standard solution IV (1000 mg/l) was used to make a working stock of 100 mg/l which was used then to make a range of calibration standards: 0.1, 0.2, 0.3, 0.5, 1, 2.5, 5, and 10 mg/l to cover both trace and macro elements. Calibration standard for phosphorus was prepared separately using KH_2PO_4, as P was not included in the multi element solution. All the calibration standards were made with 5% HNO_3. Merck ICP standard IV from (https://uk.vwr.com) was used as Certified Reference Material

(CRM) for accuracy and precision. Combustion analysis using a CN elemental analyser was used to measure total N and C. For the CN analyser, around 20 mg tissue was weighed out into tin capsules and folded. The same amount of glutamic acid was weighed out to be used as calibrating standard, and of birch leaf organic analytical standard (OAS) obtained from (http://www.elementalmicroanalysis.com) as CRM. Then, average shoot element concentration relative to dry weight and fresh weight was calculated for the whole set of accessions. In order to assess the nutrient use efficiency of different genotypes, nutrient efficiency ratio or nutrient utilization ratio (NER= mg shoot dry weight/mg element in shoot) was calculated (Baligar et al., 2001).

Although pooling samples gives more robust data it does not provide information on the variation between replicates. Therefore, Nipponbare plants were analysed individually to obtain an estimate of plant-to-plant variability and also to get an indication of element concentrations in root tissues. The 3 reference Nipponbare plants (shoot, root) in each box were milled and equal amounts were weighed out to make 1 pooled sample (10 mg) representing each box. As each replicate had 4 boxes in the 1st batch and 3 boxes in the 2nd batch for each condition, a total of 16 Nipponbare plants from the 1st batch and 12 plants from 2nd batch were tested. The types of phenotypic data collected from control and low NPK treatments are summarised in Table 2.3.

Table 2. 3: Summary of the types of phenotypic data collected from growth and elemental analysis. Abbreviations are as follows: CT for control treatment (1 NPK), LT for low treatment (0.1 NPK).

	Trait	Abbreviation	Calculation	Unit
Growth	Initial weight	IW	-	g
	Total final fresh weight	FW	-	g
	Total dry weight	DW	-	g
	Relative growth rate	RGR	(ln(FW)-ln(IW))/21	d^{-1}
	RGR reduction	RGRRED	$(1-(RGR_{LT}/RGR_{CT}))x100$	%
	Shoot fresh weight	SFW	-	g
	Root fresh weight	RFW	-	g
	Fresh weight shoot to root ratio	FWSR	shoot FW/root FW	-
	Shoot dry weight	SDW	-	g
	Root dry weight	RDW	-	g
	Dry weight shoot to root ratio	DWSR	shoot DW / root DW	-

	Fresh weight reduction	FWRED	$(1-(FW_{LT}/FW_{CT}))x100$	%
	Dry weight reduction	DWRED	$(1-(DW_{LT}/DW_{CT}))x100$	%
	Shoot fresh weight reduction	SFWRED	$(1-(SFW_{LT}/SFW_{CT}))x100$	%
	Root fresh weight reduction	RFWRED	$(1-(RFW_{LT}/RFW_{CT}))x100$	%
	Fresh weight shoot to root ratio reduction	FWSRRED	$(1-(FWSR_{LT}/FWSR_{CT}))x100$	%
	Shoot dry weight reduction	SDWRED	$(1-(S\ DW_{LT}/S\ DW_{CT}))x100$	%
	Root dry weight reduction	RDWRED	$(1-(R\ DW_{LT}/R\ DW_{CT}))x100$	%
	Dry weight shoot to root ratio reduction	DWSRRED	$(1-(\ DWSR_{LT}/\ DWSR_{CT}))x100$	%
Element content- DW basis	Zn	Zn(DW)	-	(µmol/g DW)
	K	K(DW)	-	(µmol/g DW)
	Mg	Mg(DW)	-	(µmol/g DW)
	Ca	Ca(DW)	-	(µmol/g DW)
	Fe	Fe(DW)	-	(µmol/g DW)
	B	B(DW)	-	(µmol/g DW)
	Na	Na(DW)	-	(µmol/g DW)
	P	P(DW)	-	(µmol/g DW)
	N	N(DW)	-	(µmol/g DW)
	C	C(DW)	-	(µmol/g DW)
	Zn reduction	Zn(DW)RED	$(1-(Zn(DW)_{LT}/\ (Zn(DW)_{CT}))x100$	%
	K reduction	K(DW)RED	$(1-(K(DW)_{LT}/\ (K(DW)_{CT}))x100$	%
	Mg reduction	Mg(DW)RED	$(1-(Mg(DW)_{LT}/\ (Mg(DW)_{CT}))x100$	%
	Ca reduction	Ca(DW)RED	$(1-(Ca(DW)_{LT}/\ (Ca(DW)_{CT}))x100$	%
	Fe reduction	Fe(DW)RED	$(1-(Fe(DW)_{LT}/\ (Fe(DW)_{CT}))x100$	%
	B reduction	B(DW)RED	$(1-(B(DW)_{LT}/\ (B(DW)_{CT}))x100$	%
	Na reduction	Na(DW)RED	$(1-(Na(DW)_{LT}/\ (Na(DW)_{CT}))x100$	%
	P reduction	P(DW)RED	$(1-(P(DW)_{LT}/\ (P(DW)_{CT}))x100$	%
	N reduction	N(DW)RED	$(1-(N(DW)_{LT}/\ (N(DW)_{CT}))x100$	%
	C reduction	C(DW)RED	$(1-(C(DW)_{LT}/\ (C(DW)_{CT}))x100$	%
	Zn/RGR	Zn(DW)/RGR	-	-
	K/RGR	K(DW)/RGR	-	-
	Mg/RGR	Mg(DW)/RGR	-	-
	Ca/RGR	Ca(DW)/RGR	-	-
	Fe/RGR	Fe(DW)/RGR	-	-
	B/RGR	B(DW)/RGR	-	-
	Na/RGR	Na(DW)/RGR	-	-
	P/RGR	P(DW)/RGR	-	-
	N/RGR	N(DW)/RGR	-	-
	C/RGR	C(DW)/RGR	-	-
	Zn	Zn(FW)	-	(µmol/g FW)
	K	K(FW)	-	(µmol/g FW)

Element content- FW basis	Mg	Mg(FW)	-	(µmol/g FW)
	Ca	Ca(FW)	-	(µmol/g FW)
	Fe	Fe(FW)	-	(µmol/g FW)
	B	B(FW)	-	(µmol/g FW)
	Na	Na(FW)	-	(µmol/g FW)
	P	P(FW)	-	(µmol/g FW)
	N	N(FW)	-	(µmol/g FW)
	C	C(FW)	-	(µmol/g FW)
	Zn reduction	Zn(FW)RED	$(1-(Zn(FW)_{LT}/ (Zn(FW)_{CT}))x100$	%
	K reduction	K(FW)RED	$(1-(K(FW)_{LT}/ (K(FW)_{CT}))x100$	%
	Mg reduction	Mg(FW)RED	$(1-(Mg(FW)_{LT}/ (Mg(FW)_{CT}))x100$	%
	Ca reduction	Ca(FW)RED	$(1-(Ca(FW)_{LT}/ (Ca(FW)_{CT}))x100$	%
	Fe reduction	Fe(FW)RED	$(1-(Fe(FW)_{LT}/ (Fe(FW)_{CT}))x100$	%
	B reduction	B(FW)RED	$(1-(B(FW)_{LT}/ (B(FW)_{CT}))x100$	%
	Na reduction	Na(FW)RED	$(1-(Na(FW)_{LT}/ (Na(FW)_{CT}))x100$	%
	P reduction	P(FW)RED	$(1-(P(FW)_{LT}/ (P(FW)_{CT}))x100$	%
	N reduction	N(FW)RED	$(1-(N(FW)_{LT}/ (N(FW)_{CT}))x100$	%
	C reduction	C(FW)RED	$(1-(C(FW)_{LT}/ (C(FW)_{CT}))x100$	%
	Zn/RGR	Zn(FW)/RGR	-	-
	K/RGR	K(FW)/RGR	-	-
	Mg/RGR	Mg(FW)/RGR	-	-
	Ca/RGR	Ca(FW)/RGR	-	-
	Fe/RGR	Fe(FW)/RGR	-	-
	B/RGR	B(FW)/RGR	-	-
	Na/RGR	Na(FW)/RGR	-	-
	P/RGR	P(FW)/RGR	-	-
	N/RGR	N(FW)/RGR	-	-
	C/RGR	C(FW)/RGR	-	-
Nutrient use Efficiency (UE)	Zn	ZnUE	$1/Zn_{LT}$	-
	K	KUE	$1/K_{LT}$	-
	Mg	MgUE	$1/Mg_{LT}$	-
	Ca	CaUE	$1/Ca_{LT}$	-
	Fe	FeUE	$1/Fe_{LT}$	-
	B	BUE	$1/B_{LT}$	-
	Na	NaUE	$1/Na_{LT}$	-
	P	PUE	$1/P_{LT}$	-
	N	NUE	$1/N_{LT}$	-
	C	CUE	$1/C_{LT}$	-

2.2.3 Testing the response of rice genotypes to single and multiple element deficiencies

This experiment was carried out to check which element was the most limiting among the three under 0.1 NPK condition by reducing one element, N, P, or K, at a time and multiple

elements (NPK) at the same time. NPK concentration was further reduced to 0.01 to check the response of plants under more severe nutrient stress. In this experiment Nipponbare and a subset of 7 tolerant and 6 sensitive lines were used. In 0.01 NPK condition, the total concentration of N was 0.029 mM, P was 0.003 mM and K was 0.01 mM. Three seedlings from each genotype were transferred to hydroponics after 2 weeks germination in sand. Plants were kept in test conditions for 3 weeks. Then fresh weight (total, shoot, root), RGR and RGRRED were measured.

2.2.4 Statistical Analyses

To reduce seasonal variation, data were normalized for effects of replicates and seasonal variability by using a linear mixed effect package (LME4) in R software (Bates et al., 2014). R software (version 3.1.3), SAS statistical analysis system (SAS, version 9.4) and SPSS Statistics software package (version 24.0.0.1) were used to carry out statistical tests including: Two-tailed t-test to compare means of phenotypic traits (growth and ion parameters, table 2.3) between different treatments, and to compare means of tolerant and sensitive genotypes under low treatment, one-way ANOVA to check the association between phenotypic traits and genotypes or sub-populations, post-hoc test using Tukey's honest significant test (Tukey HSD; $P<0.05$) to determine significant differences between means produced from ANOVA. Correlation matrices were generated using corrplot library in R software (version 3.1.3). Correlations were declared statistically significant if *P* value was < 1%. A cut-off value of at least 0.5 was considered for pairwise Pearson's correlation coefficients (> 0.5 for positive correlations and < –0.5 for negative correlations).

2.3 Results

2.3.1 Morphological differences between plants in low and adequate supply of NPK

A total of 294 rice accessions was examined to find out which lines are more efficient when grown in low nutrient conditions (0.1x NPK concentrations). It was expected to see differences in terms of the observable characteristics between plants in different treatments

and between accessions in each treatment in response to the reduction in NPK concentrations. Overall, accessions grown in low N, P, K conditions were shorter, leaves had pale green colour, and stems were thinner compared to the ones grown in adequate N, P, K supply. On the other hand, roots of plants grown in 0.1x NPK supply were longer and thinner than those of plants grown in 1 NPK supply. However, differences between accessions varied. Figure 2.1 shows an example of the observed morphological differences.

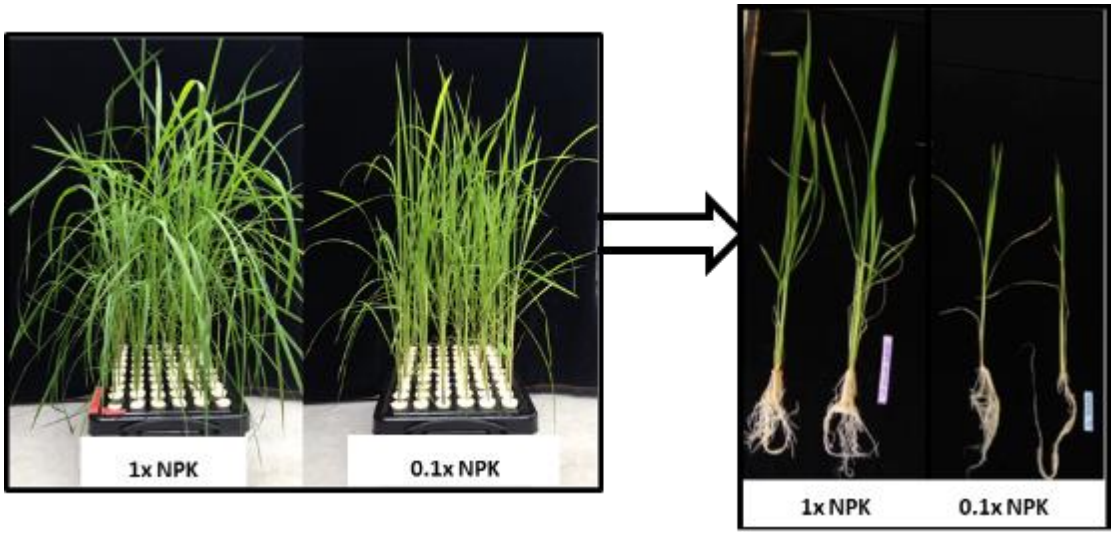

Figure 2.1: Morphological differences between plants grown for 3 weeks under adequate and low supply of NPK.

2.3.2 Growth and biomass analysis

The average of 4 replicates for the whole set of accessions was calculated for each of these variables (initial weight, final weight, dry weight, relative growth rate (RGR) and RGR reduction) in both conditions (1 NPK and 0.1 NPK). Average initial weight before transferring to hydroponics varied between 0.08 and 0.28 g, which is a 3.5 fold difference between the extremes. The bulk of the plants was between 0.12 and 0.22 g. The average final total fresh weight and shoot fresh weight of plants in control condition was significantly higher than that in 0.1 NPK (Two-tailed t-test, $P < .0001$). The latter showed almost 2 fold decrease in average total weight, shoot fresh weight and shoot to root ratios

compared to control plants. However, average fresh root weight was almost the same and not significantly different between treatments (Figure 2.2). Distribution of fresh weight parameters in control plants was shifted to the higher end, except for root fresh weight where the two treatments mostly overlapped. Using two-tailed t-test, all growth parameters were statistically significantly different between control and 0.1 NPK treatments ($P<0.05$), except for average initial weight and fresh root weight.

The same trend as seen with fresh weight was observed for all dry weight parameters, except for root dry weight where the difference was significant between the two treatments (Two-tailed t-test, $P < .0001$) and roots had relatively higher weight in low NPK plants (Supplementary Figure 2.1). The average relative growth rate was significantly greater in 1 NPK plants (Two-tailed t-test, $P < .0001$), within the range of 0.070 and 0.140 ($g\ g^{-1}\ d^{-1}$), than in 0.1 NPK plants, where it was between 0.056 and 0.106 ($g\ g^{-1}\ d^{-1}$) (Supplementary Figure 2.2). To check which lines were more efficient to grow in the low nutrient supply, RGR reduction was calculated. Growth reductions varied between 6% and 40%. The lowest values indicate that these accessions were more tolerant to grow under low N, P, K supply (Supplementary Figure 2.2).

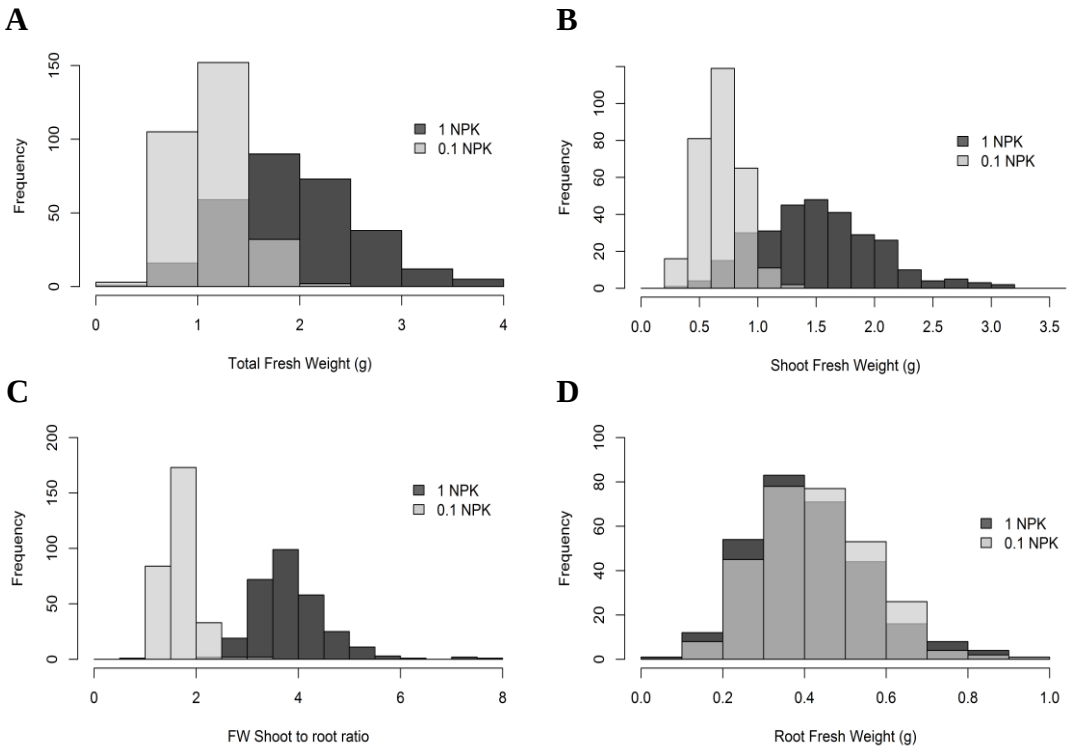

Figure 2.2: Average final fresh weight distribution among 294 accessions grown in 1 and 0.1 NPK conditions. Total FW (A), shoot FW (B) and shoot to root FW ratio (C) were significantly different in the two treatments. Root FW (D) was not significantly different in the two treatments. The significance was identified by two-tailed t-test ($P < 0.05$). The transparent colour indicates overlaps between the two treatments.

2.3.2.1 Genotypic variation on sub-population level in rice under low NPK based on growth parameters

Based on growth parameters (materials and methods, table 2.3), variations were observed not only between different genotypes, but also between sub-populations. Under 0.1 NPK, the sub-population factor was statistically significantly associated with almost all growth parameters except total fresh weight and shoot fresh weight (one-way ANOVA; $P<0.05$). For example, means of RGR under 0.1 NPK condition were significantly different between admixed indica and temperate japonica sub-populations. Admixed indica showed significantly higher growth rates compared to temperate japonica (Tukey's honest significant test HSD, $P<0.05$; Figure 2.3). Means of RGR under control conditions did not show significant differences between subpopulations. Also, admixed indica sub-population showed significantly lower RGRRED compared to indica, temperate japonica, australis and admixed (Figure 2.3). To conclude, admixed indica cultivars on average were more tolerant to grow under low NPK supply.

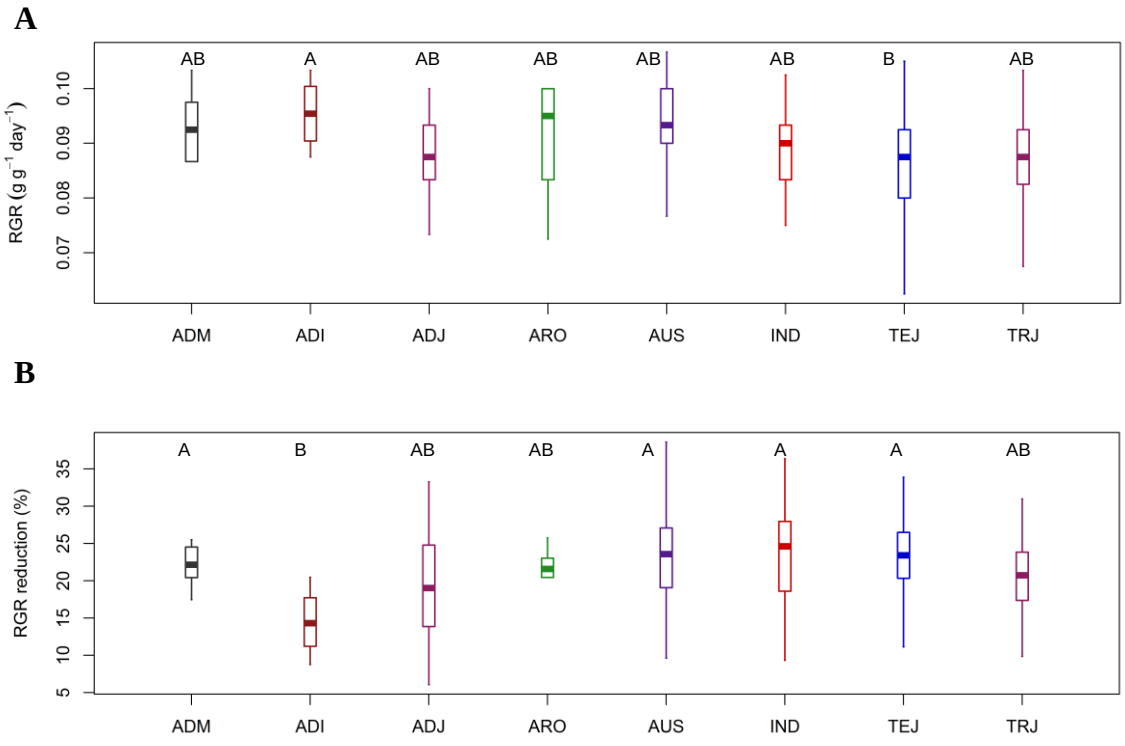

Figure 2. 3: Means for: A) Relative growth rate; B) Reduction in relative growth rate for each rice sub-population under 0.1 NPK condition. Letters above boxplots denote statistically significant differences between sub-populations (Tukey's honest significant test HSD, $P<0.05$). Sub-population abbreviations are as follows: ADM for admixed, AUS for Australis, IND for Indica, ADI for Admixed Indica, ARO for Aromatic, TEJ for Temperate Japonica, TRJ for Tropical Japonica, and ADJ for Admixed Japonica.

2.3.2.2 Differences in growth reductions for a subset of accessions under low NPK condition

A total of 15 tolerant and 11 sensitive genotypes (Table 2.4) was re-tested under 0.1 NPK condition to confirm their level of tolerance. They were also tested under 0.01 NPK condition to check their performance under more severe nutrient stress. Percentages of reduction in growth rates were compared for tolerant and sensitive genotypes between the 1st experiment and the re-test. In general, plants grew better in the retest. However, average reduction in growth rates in sensitive genotypes was 4 times bigger than for tolerant genotypes and this difference was significant (Two-tailed t-test, $P < 0.05$; Figure 2.4). RGRRED for the subset of lines ranged between 6 and 10% for tolerant lines and between 24 and 34% for sensitive ones, which is comparable to RGRRED for the whole set of lines which ranged between 6 and 40%. For the subset, tolerant lines had growth reductions closer to the lower end of the whole set of lines, while sensitive lines had values closer to the higher end. There was still genotype to genotype variation.

Under more severe nutrient stress (0.01 NPK), average RGRRED was around 60 % which was bigger than that under 0.1 NPK. Although the difference between tolerant and sensitive genotypes was small (1.2 fold), it was statistically significant (Two-tailed t-test, $P < 0.05$; Supplementary Figure 2.3). Although identifying tolerant and sensitive genotypes using different parameters like RGRRED and use efficiency (UE) is expected to give different outputs, it was interesting to test if there is an overlap between the top 10 tolerant and sensitive genotypes identified using these two parameters. The results showed that the tolerant genotype (301158) based on RGRRED showed high use efficiency for K. Interestingly, a tolerant genotype (301100) was considered as inefficient for using P, while a sensitive genotype (301199) was having high efficiency for P. Another sensitive genotype based on RGRRED (301072) showed high efficiency for N. Suggesting that efficient genotypes in using one element don't necessarily have low RGRRED, and vice versa.

Table 2. 4: List of candidate tolerant and sensitive genotypes based on reduction in relative growth rate. Abbreviations are as follows: IND for Indica, Aus for australis, TEJ for Temperate Japonica, TRJ for Tropical Japonica.

Tolerant-GSORID	Sub-population	Sensitive-GSORID	Sub-population
301325	Admixed-jap	301224	Ind
301100	Trj	301199	Ind
301405	Trj	301052	Tej
301227	Admixed-jap	301241	Trj
301259	Ind	301169	Aus
301345	Aus	301256	Admixed-jap
301158	Trj	301265	Tej
301214	Trj	301273	Tej
301374	Trj	301167	Trj
301341	Aus	301177	Tej
301141	Trj	301072	Tej
301299	Trj	-	-
301209	Admixed-jap	-	-
301171	Tej	-	-
301310	Aus	-	-

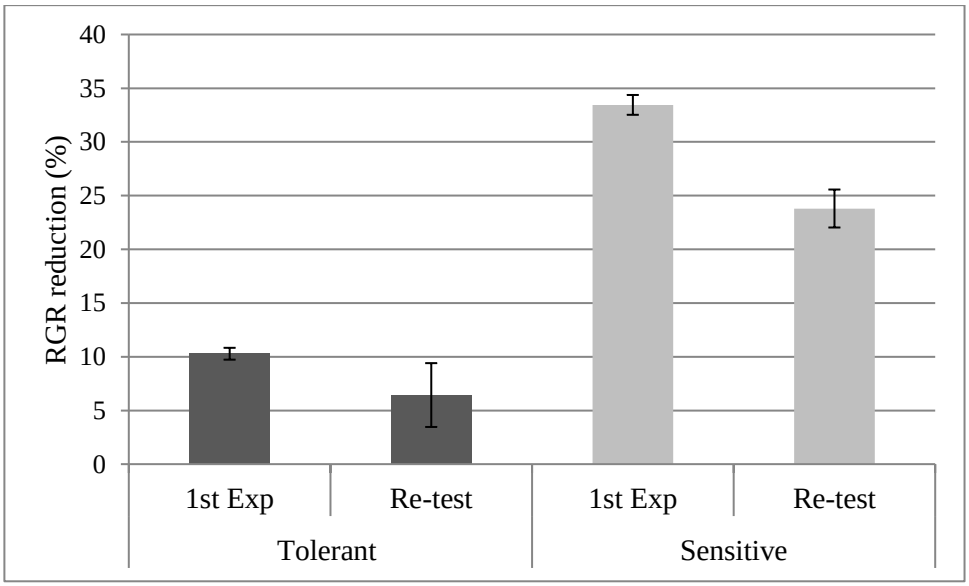

Figure 2. 4: Average reduction in growth rates in tolerant lines was smaller than for sensitive lines under 0.1 NPK (Two-tailed t-test, $P = 0.001$). Mean ± SE (n = 45 tolerant, 33 sensitive).

2.3.3 Elemental analysis

2.3.3.1 Shoot concentration of elements on dry and fresh weight basis

The average shoot content of elements was calculated for the whole set of accessions. Shoot N, P and K content was reduced to nearly half when plants were grown under 0.1 NPK condition (Figure 2.5). Distribution of N, P and K concentrations between the two treatments was split into two distinguishable clusters where control plants shifted to the higher end.

Other nutrients were also measured because nutrient interactions can have positive or negative effects on the uptake of others. Under 0.1 NPK condition, a slight increase in Ca, Na and Fe shoot concentrations was found (18 %, 16% and 14%, respectively) (Figure 2.6). The increase was bigger in Mg and Zn concentrations (29 % and 50%, respectively). On the other hand, B and C concentrations in 0.1 NPK plants were reduced by 14% and 3%, respectively (Figure 2.6). Although the distribution of some elements was almost completely overlapping between the two treatments, the difference was significant. On fresh weight basis, the general trends for most of the shoot elements were the same as on dry weight basis, except B and C concentrations in 0.1 NPK plants where there was a slight increase (Supplementary Figure 2.4 and 2.5). All ion concentrations significantly differed between treatments based on two-tailed t-test (<0.05).

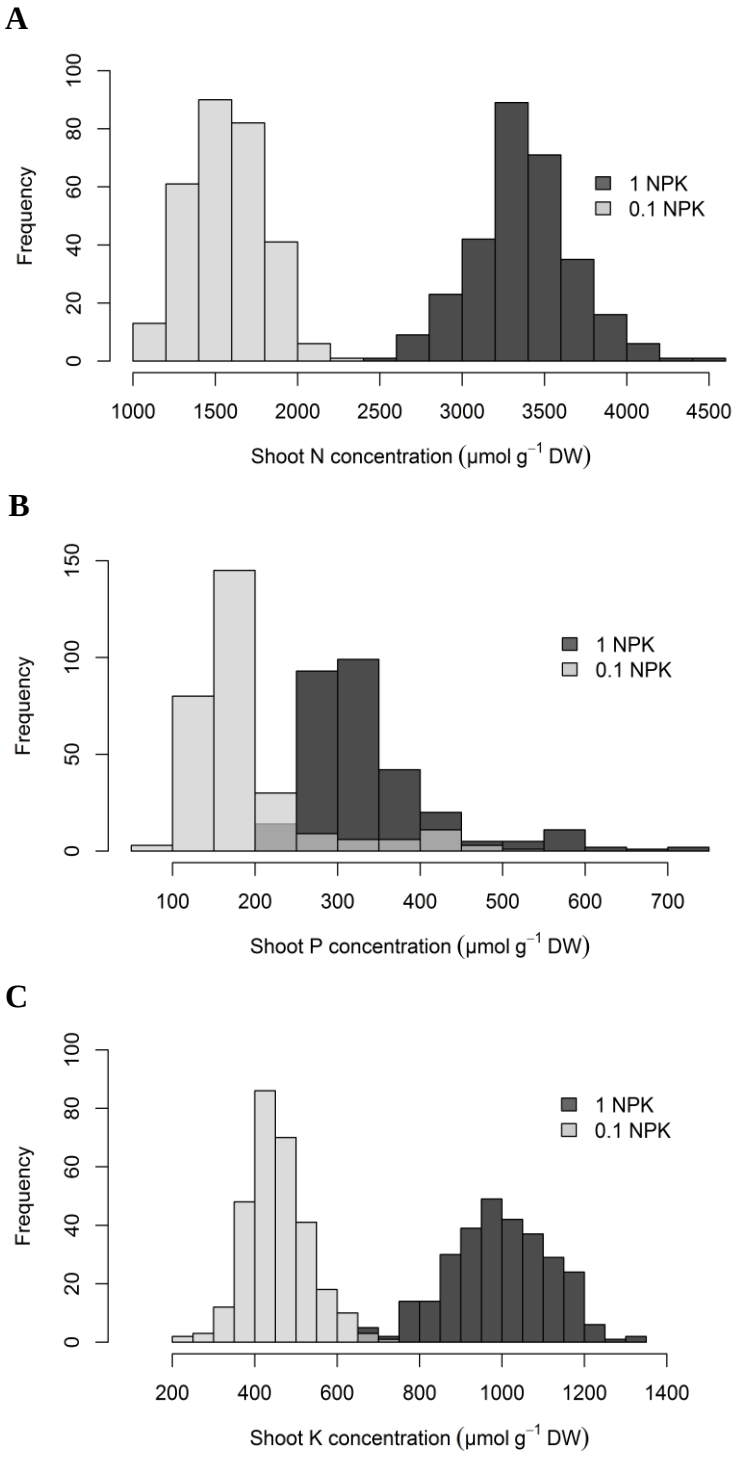

Figure 2. 5: Shoot concentration of elements based on dry weight in 0.1 NPK plants compared to 1 NPK plants. Significant reduction in: (A) average N concentration; (B) average P concentration; (C) average K concentration. The significance was identified by two-tailed t-test ($P < 0.05$). The transparent colour indicates overlaps between the two treatments.

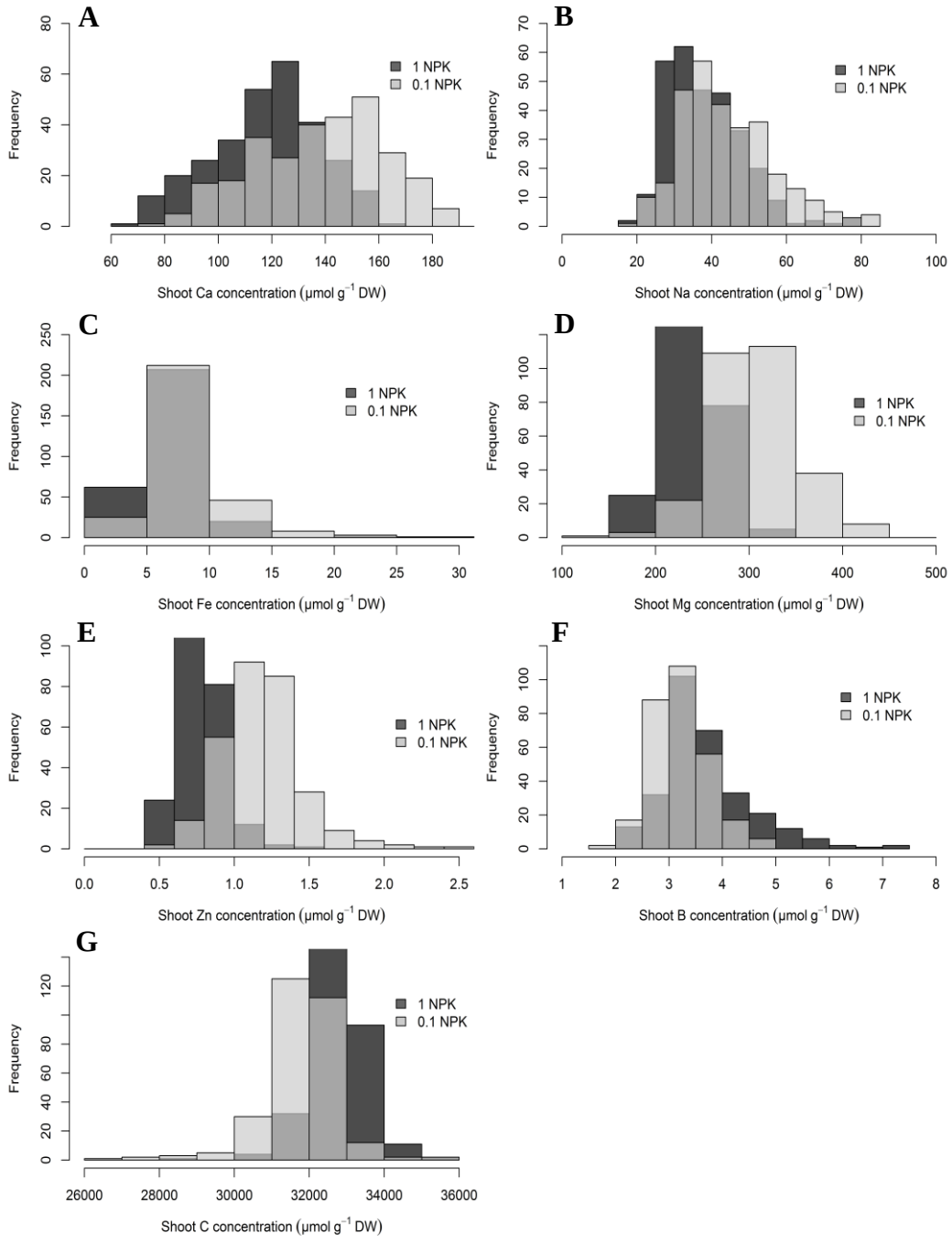

Figure 2. 6: Shoot concentration of elements based on dry weight in 0.1 NPK plants compared to 1 NPK plants. Significant increase in the average concentration of: (A) Ca, (B) Na, (C) Fe, (D) Mg, (E) Zn. Significant decrease compared to 1 NPK plants in the concentration of: (F) B; (G) C. The significance was identified by two-tailed t-test ($P < 0.05$). The transparent colour indicates overlaps between the two treatments.

2.3.3.2 Shoot and root element concentrations in reference Nipponbare plants

Due to time and material limitation for some genotypes, root samples of the 294 accessions were not analysed for ion content. Also, sample pooling does not allow an estimation of the variation between replicates. For these reasons, the average element concentration in dry shoot and root tissues was calculated for a total of 28 reference Nipponbare plants.

The general trends of element contents in Nipponbare shoots agree with those observed for the whole set of accessions. When comparing Nipponbare root and shoot, N, P, K, Ca, Mg and B concentration was relatively higher in shoots than in the root in both conditions. In contrast, Fe concentration was much higher in the root compared to the shoot in both conditions. The same was true for Na but only under low NPK. Zn concentration in the root of 1 NPK plants was higher than the in the shoot and the opposite was true for 0.1 NPK plants.

In 0.1 NPK plants, root N, P, K was reduced to nearly half compared to 1 NPK plants which agrees with the shoot trend (Figure 2.7). As in shoots, the concentration of Ca, Mg, Zn, Fe and B did not vary much between the treatments (Figure 2.8). There was, however, a more than two-fold increase in Na concentration in the roots of 0.1 NPK plants, which contrasts with little change in the shoot.

Since average shoot concentrations in Nipponbare were relatively similar to that of all genotypes, it is possible to assume that using Nipponbare reference plants was a good way to get an indication of root ion concentrations. Furthermore, these differences in ion distribution between shoot and root under different treatments might explain the different mechanisms in response to low supply of nutrients. The increased concentration of Na in roots under limited nutrient supply might compensate for reduced K uptake.

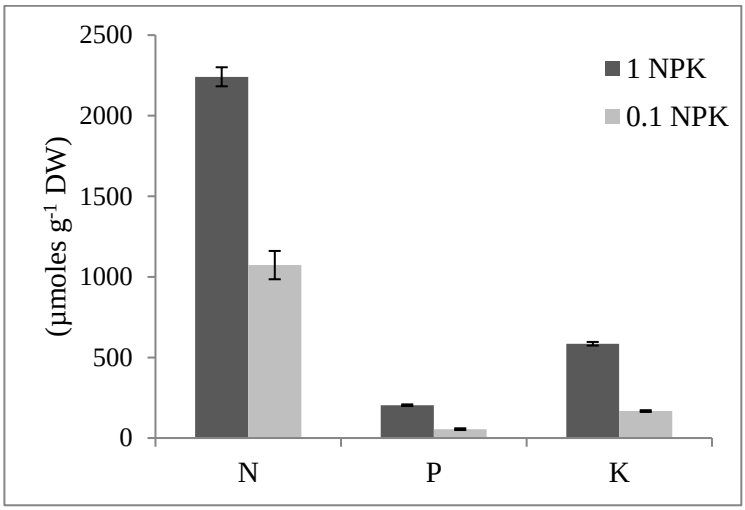

Figure 2. 7: Root N, P and K concentration in 0.1 NPK and 1 NPK Nipponbare plants. Mean ± SE (n = 28).

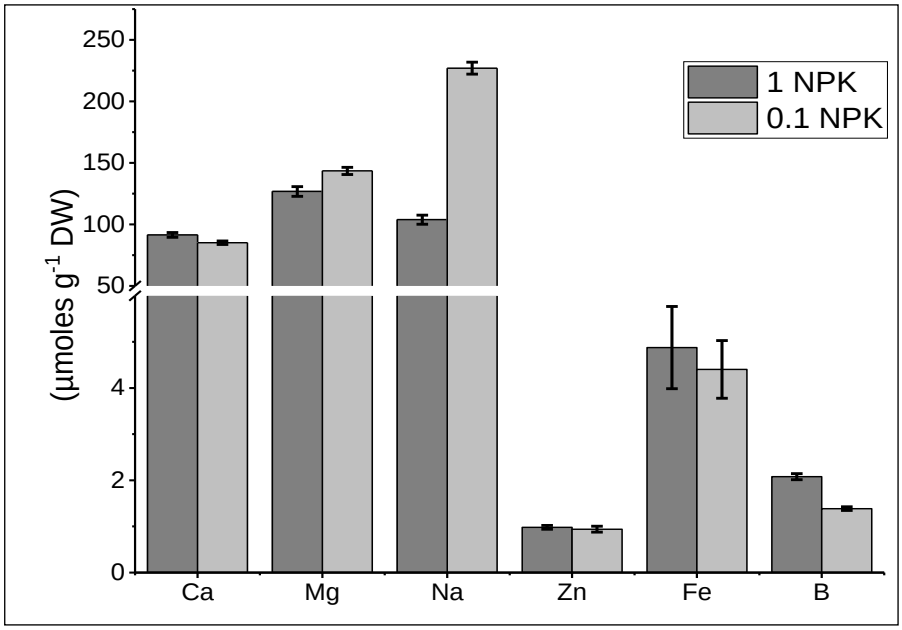

Figure 2. 8: Root Ca, Mg, Na, Zn, Fe and B concentration in 0.1 NPK and 1 NPK Nipponbare plants. Mean ± SE (n = 28).

2.3.3.3 Differences in nutrient use efficiencies under low NPK condition

To be able to evaluate the performance of the genotypes and identify those that were more efficient in nutrient use under low NPK treatment, nutrient use efficiency was calculated using shoot dry weight of plants. Since shoot tissues from 4 replicates were pooled prior to performing the elemental analysis, no replicate data were available and hence no standard errors. Use efficiency values for N, P and K were higher under low treatment compared to high treatment (Figure 2.9), which is explained by the higher tissue concentration of elements under 1 NPK. Differences in use efficiency for N, P and K were observed among the accessions in both treatments. Pearson's pairwise correlation was performed. Moderate positive correlation between high and low treatment was observed for nitrogen use efficiency (NUE, r =0.48), strong positive correlation for PUE (r =0.72) and weak positive correlation for KUE (r =0.2). This suggests that different genotypes have variable use efficiency for different elements, and some might be efficient for one element but not the other. Also, the strong positive correlation between PUE under both treatments suggests that same genotypes that were efficient in using P under high treatment were also efficient under low treatment. Alternatively, it could mean that P was not limiting.

Under 0.1 NPK, genotypes with high and low efficiency in using N, P, K were identified. Genotypes with higher efficiency had the ability to grow better with a smaller amount of nutrients. There was about two-fold difference in use efficiency of N between the most efficient and inefficient genotypes. The difference was around 7 and 3 fold, for P and K, respectively. The top 10 accessions for highest and lowest use efficiency for N, P and K under low treatment are summarised in Supplementary Table 2.1. Of the top 10 genotypes with lowest P efficiency, 6 overlapped between high and low treatment, and 3 out of 10 genotypes with highest P use efficiencies overlapped between high and low treatments. This might explain the strong correlation between both treatments. However, 3 out of 10 genotypes with lowest K use efficiency overlapped between high and low treatments, although the correlation was very weak. No genotypes overlapped for NUE. Genotypes that overlapped between the two treatments are highlighted in Supplementary Table 2.1.

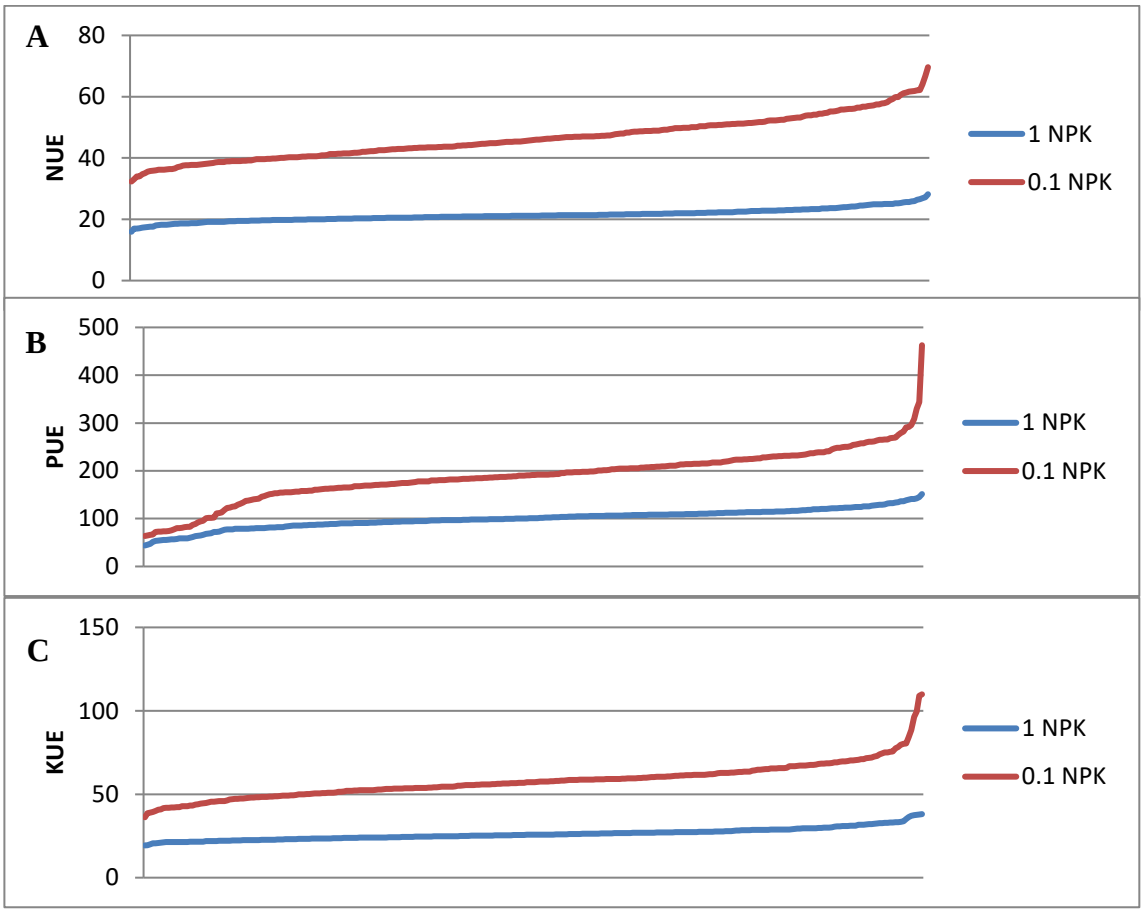

Figure 2. 9: Distribution of use efficiency in control treatment (red line) and low treatment (blue line) for: A) nitrogen (NUE); B) phosphorus (PUE); C) potassium (KUE). The values were ordered from lowest to highest for each treatment separately, genotypes at either ends do not correspond to each other.

2.3.3.4 Genotypic variation on sub-population level in rice under low NPK based on tissue element concentration

Under 0.1 NPK, the sub-population factor was statistically significantly associated with almost all parameters related to shoot element content (materials and methods, Table 2.3) except: Fe content on dry weight basis, C content on dry weight basis, N content on fresh weight basis, K content on fresh weight basis, Fe content on fresh weight basis, Fe use efficiency and C use efficiency (One-way ANOVA; $P<0.05$).

Regarding element concentrations, as N and K were not significantly associated with sup-population factor, only P is presented. Under 0.1 NPK, means for P concentration in dry, and fresh shoot tissue showed that Aromatic accumulated the highest P concentration among all sub-populations. Aromatic had the lowest P use efficiency that was significant compared to Indica which showed the highest P use efficiency (Figure 2.10). Interestingly, Aromatic was significantly associated with P under control as well (Supplementary Figure 2.6).

To conclude, variations were observed not only between genotypes but also between sub-populations. As P content in low and control treatment correlated significantly positive, it was interesting to find that the same subpopulation had accumulated more P in both conditions. This might also suggest that P was not limiting under low supply.

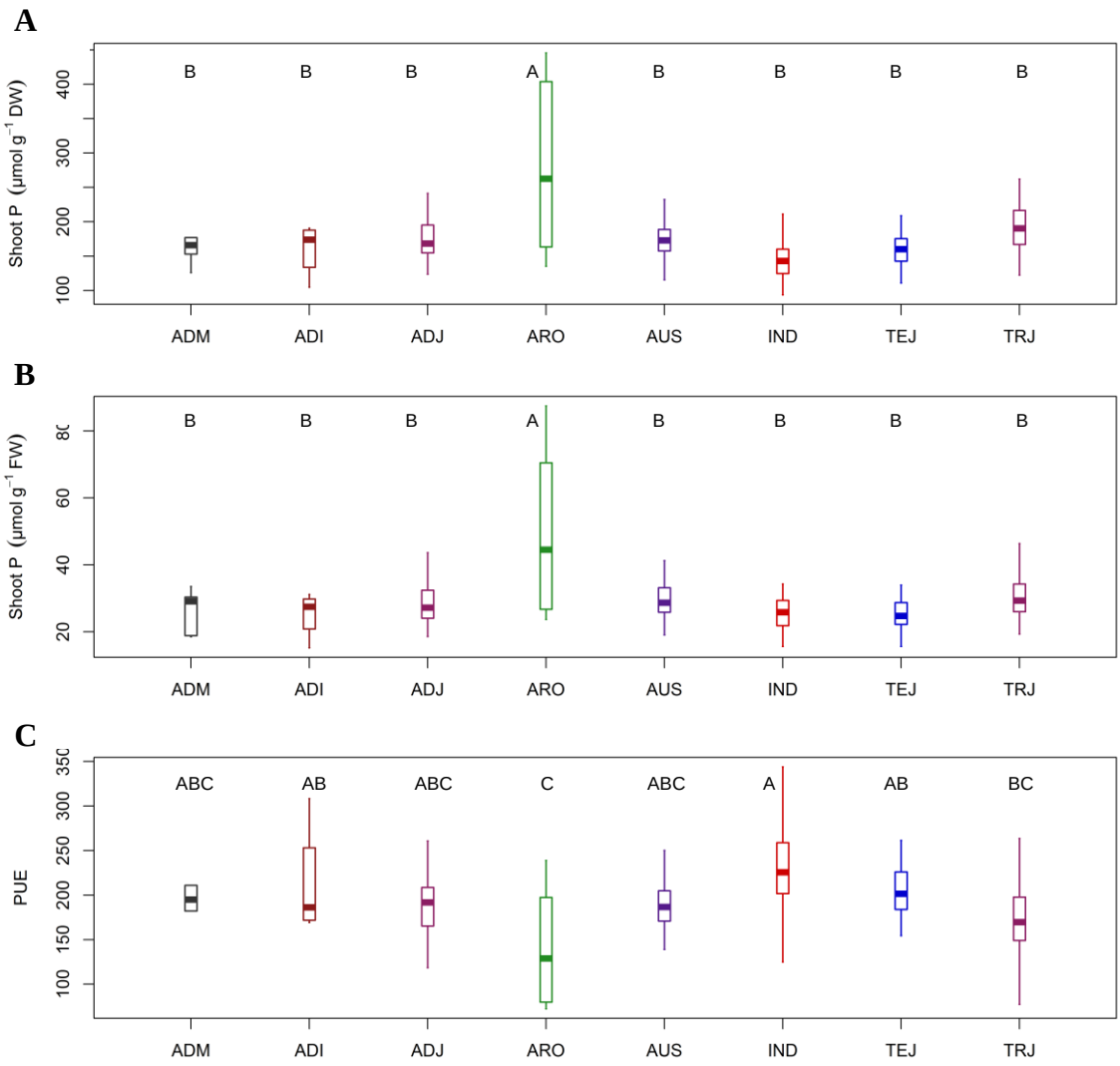

Figure 2. 10: Means under 0.1 NPK condition for: A) P concentration on DW basis; B) P concentration on FW basis; C) P use efficiency for each rice sub-population. Letters above boxplots denote statistically significant differences between sub-populations (Tukey's honest significant test HSD, $P<0.05$). Sub-population abbreviations are as follows: ADM for admixed, AUS for australis, IND for Indica, ADI for Admixed Indica, ARO for Aromatic, TEJ for Temperate Japonica, TRJ for Tropical Japonica, and ADJ for Admixed Japonica.

2.3.4 Correlation between phenotypes of plants grown in low and adequate NPK supply

2.3.4.1 Growth parameters

The correlation between the different growth parameters was tested. The correlation tests were based on an average of 4 replicates. Overall, there were significant positive correlations between initial weight, fresh weight (total, shoot, root) and dry weight (total, shoot, root) in both control and 0.1 NPK conditions (Figure 2.11).

One might expect that plants that have grown better during the first two weeks, hence have higher RGR during that time, would also grow faster later in hydroponics. However, there was only a very weak positive correlation between the initial fresh weight of plants and the relative growth rate in control (*r=0.18*) and low treatment (*r=0.17*) (Figure 2.11). There was a significant positive correlation between relative growth rates of plants in control and low conditions (Figure 2.11). This suggests that the accessions whose relative growth rates were highest in 1 NPK condition have relative growth rates that are less depressed in the low NPK condition. However, though this assumption might be true as an overall trend, there were still variations between individuals. Five accessions with highest relative growth rates were selected from the control condition and compared to their relative growth rates in 0.1 NPK condition. As shown in Figure 2.12, accessions that have grown better under adequate supply of nutrients have not always done better under low NPK supply. Overall, growth parameters correlated fairly well within and between treatments. Under 0.1 NPK only, shoot to root ratio was significantly and negatively correlated with root weight, suggesting that as the ratio was decreasing, root weight increased, and that was true for both FW and DW (Figure 2.11).

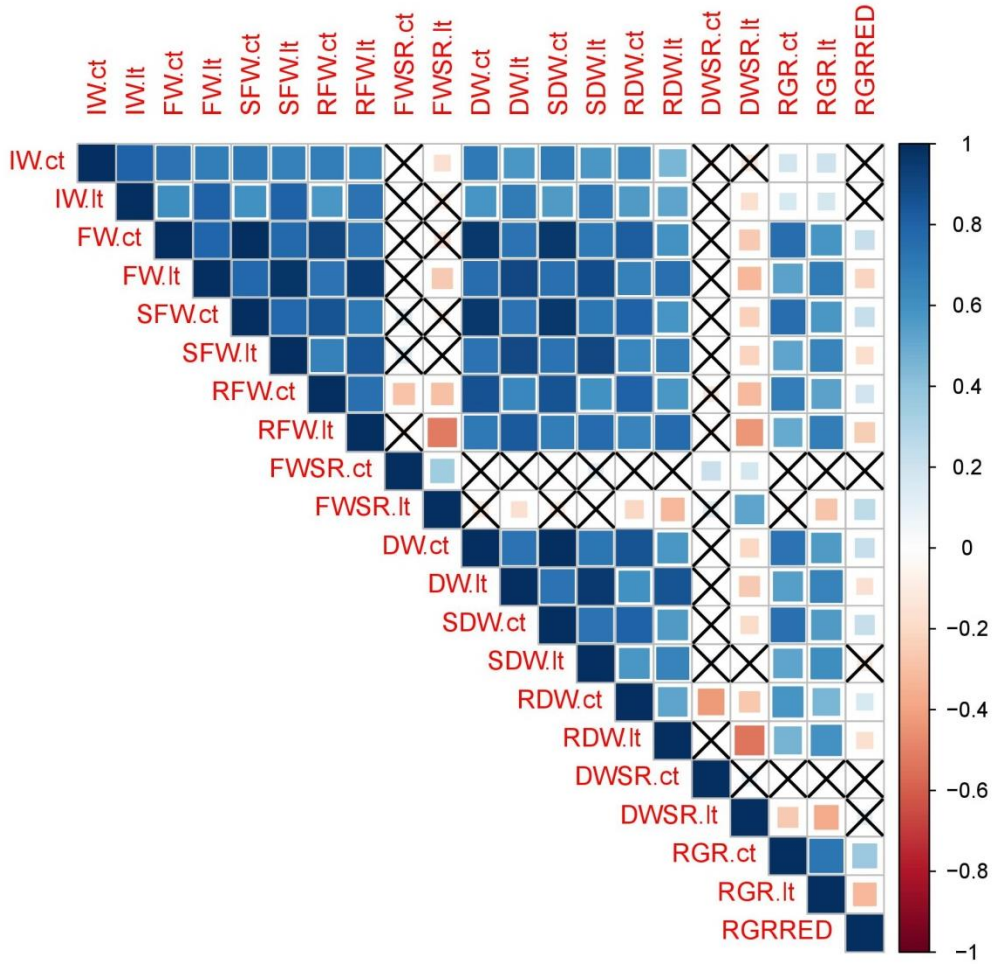

Figure 2. 11: Correlation matrix between growth parameters. Positive and negative correlations are displayed in blue and red respectively. Correlations with p-value > 0.01 are crossed. Abbreviations are as follows: CT for control treatment (1 NPK), LT for low treatment (0.1 NPK), IW for initial weight, FW for fresh weight, SFW for shoot fresh weight, RFW for root fresh weight, FWSR for fresh weight shoot to root ratio, DW for dry weight, SDW for shoot dry weight, RDW for root dry weight, FWDR for dry weight shoot to root ratio, RGR for relative growth rate and RGRRED for relative growth rate reduction.

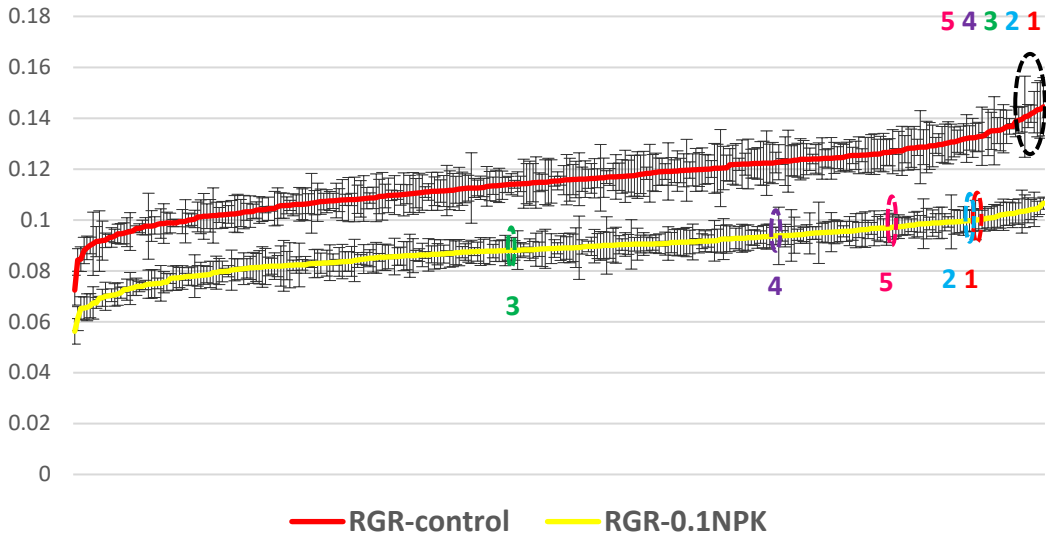

Figure 2. 12: Relative growth rates of the same accessions in different conditions: control and 0.1 NPK. Numbers represent the top 5 accessions with highest RGR values in control condition and their corresponding positions in 0.1 NPK treatment.

2.3.4.2 Shoot element concentrations

P concentration based on dry weight was strongly positive and significantly correlated between control and 0.1 NPK treatment (r = 0.85), suggesting that plants having high P concentration in control also have high P under low treatment (Supplementary Figure 2.7). The same was true for P concentration on fresh weight basis (Supplementary Figure 2.8) and for P use efficiency (Supplementary Figure 2.10). This suggests that P was not limiting under 0.1 NPK condition. This finding was confirmed by another experiment where N, P and K were reduced separately. Plants under 0.1 P showed lowest reduction in growth compared to 0.1 N or 0.1 K. Also, Ca concentration based on dry weight, fresh weight and Ca use efficiency correlated positively and significantly between control and 0.1 NPK treatment (Supplementary Figure 2.7, 2.8 and 2.9). Although Ca was not limiting this might suggest that it was a useful element under low NPK.

Under 0.1 NPK, a positive correlation was observed between shoot N and Ca on dry weight basis (Supplementary Figure 2.7), fresh weight basis (Supplementary Figure 2.8) and use efficiency (Supplementary Figure 2.9), suggesting that plants having high N concentration

also had high Ca content (Supplementary Figure 2.7, 2.8 and 2.9). Under 0.1 NPK, positive correlation was observed between N concentration based on fresh weight and other elements including K and C (Supplementary Figure 2.8). Not only under 0.1 NPK, N based on FW correlated significantly and positively with C, but it did also under control condition (Supplementary Figure 2.8). Under control, Mg correlated positively with Ca, Na and C (Supplementary Figure 2.8). Under control only, it has been shown that plant having high N efficiency were also having high C efficiency (Supplementary Figure 2.9).

2.3.4.3 Growth and shoot ion concentration

Correlations analysis between growth parameters and shoot ions on DW basis did not reveal any significant correlations. The same was true for correlations between growth parameters and nutrient use efficiencies. This might be explained by the different efficiencies of different genotypes in using nutrients under the same condition. On fresh weight basis, shoot C correlated negatively and significantly with fresh weight under low treatment only (r = -0.57). This might be related to N as C:N ratio can be an indicator for N deficiency.

2.3.4.4 Correlation between RGRRED and ion concentration in a subset of accessions

To test if growth reduction was influenced by the concentrations of any of the shoot elements in dry weight under low NPK, correlation analyses were carried out. Correlations were deemed statistically significant if the P value was < 1%. A cut-off value of at least 0.5 was considered for pairwise Pearson's correlation coefficients (> 0.5 for positive correlations and < –0.5 for negative correlations).

Results revealed that there was no significant correlation between RGRRED with any of the shoot ions either in tolerant (Supplementary Figure 2.10) or in sensitive lines (Supplementary Figure 2.11). This is in agreement with the overall trend in the whole set of accessions which did not reveal any significant correlations between growth and element parameters. However, in tolerant lines, there was significant positive correlation between

shoot N and Ca concentrations, K with Mg and B, Ca and Mg, and finally Mg and B (Supplementary Figure 2.10). Correlations between shoot ions were different for sensitive lines, P correlated positively with Zn, while B correlated negatively with B (Supplementary Figure 2.11).

In general, tolerant lines had relatively higher shoot N, P, K, Ca and Mg concentrations compared to sensitive ones. Shoot Na, Zn, B concentrations were comparable in tolerant and sensitive lines. In contrast, shoot Fe was higher in sensitive lines. The difference was only significant in shoot N, K, Ca, Mg and Fe concentrations between tolerant and sensitive lines (Two-tailed t-test, $P < 0.05$). Taking into account these differences in growth reductions and their correlation with shoot ions in tolerant and sensitive lines might possibly explain the differences in tolerance. For example, the accumulation, distribution and interactions between elements for tolerant lines might explain their better performance under nutrient stress. In this case, maybe by allocating more macronutrients in shoots.

2.3.5 Response of rice genotypes to single and multiple element deficiencies

For the whole set of accessions, deficiency symptoms were observed on morphological basis, growth and element concentrations in shoot tissues under 0.1 NPK condition. Now the question is whether this response was to all three elements (NPK) or whether one of them contributed the most to the observed phenotypes.

To test which element was the most limiting among the three under 0.1 NPK condition, one element, N, P, or K, was reduced at a time and tests were conducted using Nipponbare. NPK concentration was further reduced to 0.01 to check the response of the plant to more stressed conditions and these tests included Nipponbare and a subset of 7 tolerant and 6 sensitive lines. To see the treatment effect, the average of all plants was calculated regardless their tolerance. Then the average of Nip, tolerant and sensitive genotypes was compared.

On morphological basis, when single elements were further reduced to 0.01, deficiency symptoms became stronger and more distinguishable. Low N plants had very pale green colour, while low K plants started to show brown leaf margins and bending, low P plants were less affected compared to N and K (Figure 2.13). Differences in the size of plants in response to different treatments including control (1 NPK), 0.01 NPK, 0.01 N, 0.01 P and 0.01 K are presented in figure 2.14. Plants in control were much bigger than the ones grown under deficient conditions in either single or multiple elements. Plants deficient for 3 elements were smaller than the ones with single element deficiencies, however, size of plants under low N were slightly bigger than the low NPK ones, followed by low K plants which were bigger and then low P plants.

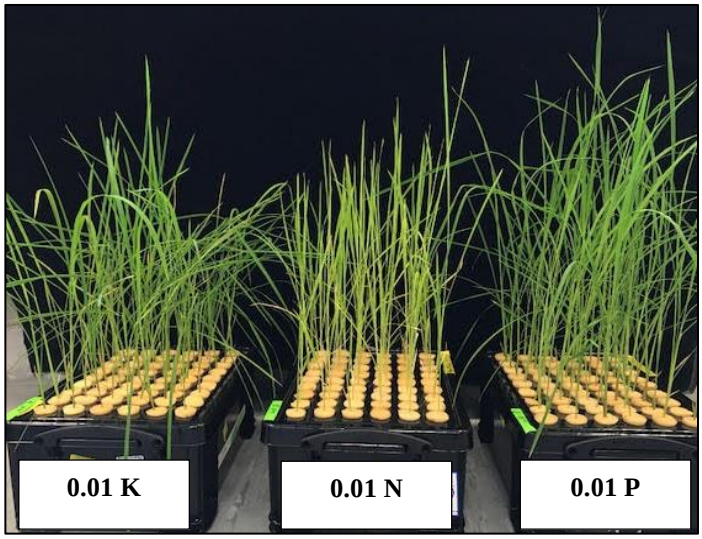

Figure 2. 13: Morphological differences between plants grown under 0.01 reduction of N, P and K.

Figure 2. 14: Differences in plant sizes in response to different treatments: control (1 NPK), parallel reduction of NPK (0.01 NPK), and individual reduction of N, P and K.

2.3.5.1 Relative growth rate

Based on the average of all plants (Nipponbare, tolerant and sensitive), RGR was significantly different between 1 NPK and both 0.1 and 0.01 NPK. The difference was also significant between 0.1 NPK and 0.01 NPK (Figure 2.15). When comparing single and multiple elements, difference in average RGR between 0.1 NPK and 0.1 of separate elements was roughly the same but slightly higher for 0.1 P. Difference was only significant between 0.1 NPK and 0.1 P, meaning that when either N or K was reduced, RGR of plants was affected roughly to the same level as when all together were reduced. This suggests that N and K were more dominant to affect growth compared to P. On the other hand, under more stress (0.01 NPK), the difference in RGR between single and multiple elements was only significant under 0.01 P and 0.01 K (Supplementary data 2.13), meaning that growth rates of plants under reduced N only are comparable to those when multiple elements are reduced. This indicates that N is the most limiting factor for growth

under more severe stress. When comparing single elements, the difference in RGR was significant between 0.1N and 0.01 N, and between 0.1 K and 0.01 K, meaning that further reduction of N and K had great impact on growth. However, the difference was not significant between 0.1 and 0.01 P, suggesting that further reduction of P didn't have an impact on growth (Figure 2.15). The overall trend of fresh weight was similar to that of relative growth rate (not shown). Significance was identified using Tukey's honest significant test HSD ($P<0.05$).

2.3.5.2 RGR reduction

Compared to 1 NPK, there was around 15% and 58% reduction in average growth rates of plants under 0.1 NPK and 0.01 NPK, respectively and this difference was significant (Tukey's honest significant test HSD, $P<0.05$; Figure 2.16). As expected, reduction in growth rates of plants exposed to reduced NPK together were relatively larger than those when only a single element was reduced. When reduced to 1/10, there was 10%, 1% and 12% reduction in average plants' growth rate for N, P and K respectively, compared to 1 NPK. However, the difference was only significant between 0.1 NPK and 0.1 P (Tukey's honest significant test HSD, $P<0.05$; Figure 2.16). RGRRED of plants under 0.1 N and 0.1 K was nearly similar to that of 0.1 NPK and the difference was not significant. On the other hand, under more stress, the RGR reduction under 0.01 N was highest (52%) and nearly as much as for 0.01 NPK, whereas for K and P RGR was reduced to a much lesser extent (35% and 11%, respectively). This suggests that reducing only N was sufficient to result in growth reductions similar to those where all elements were limiting and that N is the most limiting factor for growth under more stress. When comparing single elements, the difference in RGRRED was significant between 0.1 and 0.01 N (10% and 52%, respectively), and between 0.1 and 0.01 K (12% and 35%, respectively), meaning that further reduction of N and K had great impact on growth. However, the difference was not significant between 0.1 and 0.01 P (1% and 11%, respectively), suggesting that further reduction of P did not have a great impact on growth (Figure 2.16).

To conclude, when NPK were individually reduced to 1/10, N and K seem to contribute equally to the reduction in growth rates. On the other hand, under more severe stress (0.01 condition), N was the most limiting factor, followed by K. In all cases, P was the least limiting factor.

2.3.5.3 Comparison between tolerant and sensitive lines based on RGR and RGRRED

The overall trend for the 3 genotype groups (Nipponbare, tolerant and sensitive) was similar to that of the average of all genotypes. There was a significant difference in RGR between tolerant and sensitive genotypes under 0.01 NPK and 0.01 N (Supplementary Figure 2.12). Since N was the most limiting factor, this suggests that the tolerance to low NPK was because these genotypes were tolerant to N. Also, the difference in RGR between tolerant and sensitive genotypes under 0.1 P and 0.01 P conditions was significant (Supplementary Figure 2.12). Nipponbare was used as a reference, but based on RGRRED, it turned out to be more sensitive than the average of sensitive lines (Supplementary Figure 2.13). However, the difference was not significant.

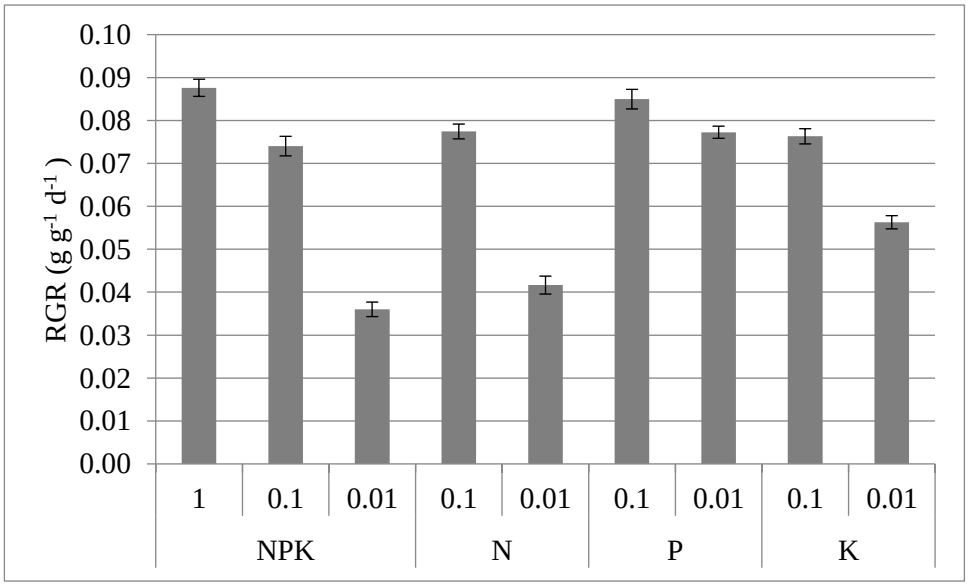

Figure 2. 15: Average RGR of plants under varying NPK treatments. Mean ± SE (n = 42).

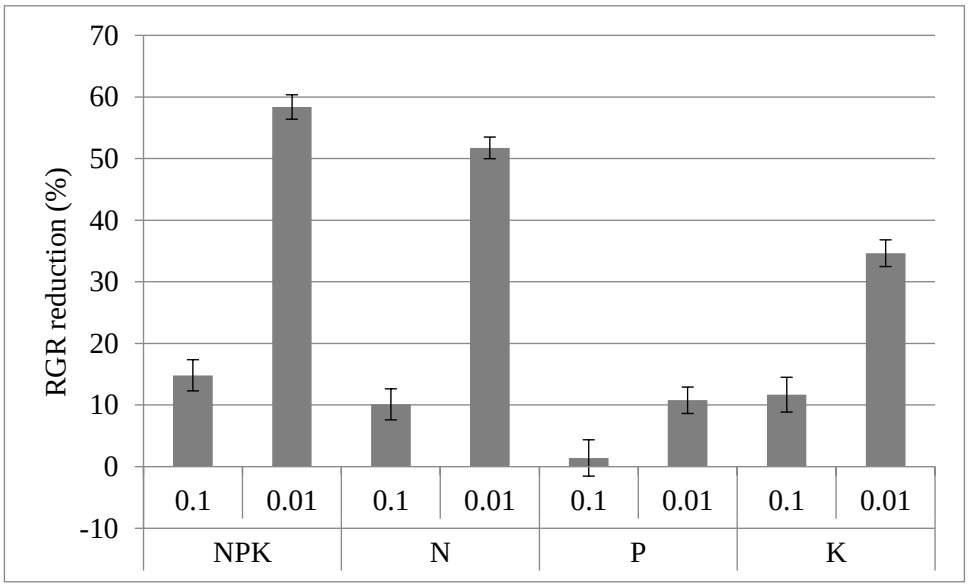

Figure 2. 16: Percentage of growth reduction of plants under varying NPK treatments compared to control (1 NPK) treatment. Mean ± SE (n = 42).

2.4 Discussion

2.4.1 Morphological differences between plants in low and adequate supply of NPK

Growing plants in hydroponics where a nutrient solution with adjustable elemental composition is used, has been widely used in research for the ease of achieving the required experimental conditions (Gericke, 1937; Taiz and Zeiger, 2010). A large number of diverse rice accessions was examined to find out which lines are more efficient to use the available nutrients and grow under low nutrient supply (0.1 NPK). On a morphological basis, it was observed that plants grown in full strength medium are much bigger than the ones with reduced amounts of N, P, and K. According to (Fageria et al., 2013b), plants lacking phosphorus have narrow erect leaves, fine stems, and are short in height. Stunted growth in young plants and delay in maturation might be observed as well (Taiz and Zeiger, 2010). Potassium deficient plants show chlorosis which might develop later to necrosis, have dark green colour with yellowish brown leaf margins or dark brown necrotic spots, stems are weak and thin, leaves may curl and the plant might bend to the ground. Also nitrogen deficiency in plants would inhibit growth and lead to chlorosis (yellowing of the leaves),

formation of thin and woody stems, leaves are narrow, short and erect (Taiz and Zeiger, 2010). Morphological traits of plants in this experiment were as expected. Plants have pale green colour (yellowish), finer and weaker stems, small and erect leaves, also they are shorter compared to the ones with higher N, P, and K concentrations. The lack of N might have been the cause of the observed chlorosis, due to loss of chlorophyll. Longer treatments would probably have led to further deficiency symptoms but since deficiency symptoms are quite similar, it is hard to tell which nutrient was the most limiting for these plants. Since N and K turned out to be equally limiting under 0.1 condition, this might suggest that, the morphological differences observed when reducing NPK to 0.1 was a result of a combined effect of N and K, but not P which was the least limiting factor. Another possibility is that P was limiting to some extent under 0.1 NPK and reducing single elements did not reflect what was happening when all three were reduced as that might result in nutrient imbalance and it is known that nutrient ratio and balancing is more important than the concentration of each nutrient (Malvi, 2011). Therefore, reducing NPK to levels where deficiency for each individual element is reached rather than reducing them by the same proportion relative to controls might have shown a different response as some elements are needed in larger amounts. Also, reducing multiple elements at a time introduces complexity and confounding variables not only on morphological basis but also based on the response of genotypes as some might be tolerant to one or two elements but not to all together. This was evident when tolerant lines differed significantly from the sensitive ones only under low P. When single elements were reduced 100-fold, deficiency symptoms became stronger and more distinguishable, and they were as expected. Low N plants had very pale green colour, while low N plants started to show brown leaf margins. Comparing ion content for the plants that are deficient in one or multiple elements would be useful.

2.4.2 Correlation between phenotypes of plants grown in low and adequate NPK supply

There was a weak correlation between the initial fresh weight of plants and the relative growth rate in both conditions. This suggests that the initial weight had only a minor effect on relative growth rates. During the two weeks before treatment, larger plants did not

necessarily have larger RGR as it was not the only contributor to plant size during that time. Other factors such as seed reserves and germination speed might have contributed as well. On the other hand, the positive correlation between relative growth rates in both conditions and total final plant weights indicates that plants with higher relative growth rates have subsequently larger final fresh weights. Also, the initial weight was positively correlated with final fresh weight. To summarize, final weight was positively correlated with initial weight and RGR, meaning that to end up with larger final weight plants have had either larger initial weight, or larger relative growth rate, or both. Initial weight had only a minor effect on RGR, and the differences in plant size during the first two weeks might be a result of varying germination times and seed reserves.

Although the overall correlation (based on average of 4 replicates) was positive between relative growth rate in full and 0.1 NPK supply, individual accessions responded differently to adequate and limited supply of NPK. One reason for that might be the genetic variation between these accessions which makes them have different tolerance abilities to limited supply of nutrients. Moreover, plants grown under NPK deficient conditions might have different mechanisms and different genes regulated in response to stress compared to plants that have adequate supply of nutrients. Also tolerant (efficient) genotypes may employ different sets of genes compared to sensitive ones.

High levels of variation observed among the phenotypes tested in this study at both genotype and subpopulation level, might be partially explained by the large and diverse set of rice accessions used. Variation in growth rates might be an important indicator for the efficiency of some genotypes in using the nutrients supplied for growth and biomass production. Therefore, fast growing genotypes that showed improved performance compared to others under low nutrient conditions could possibly have a positive impact on crop development when exploited in breeding programs. Furthermore, a particular sub-population with higher growth rates (e.g. admixed indica in my study) can be further analysed to check for differences within rather than between subpopulations as differences within subpopulations have been reported in rice for many agricultural traits (Samuel et al., 2016; Zhao et al., 2011). Identifying more efficient genotypes in using the nutrients

sufficiently to grow under low NPK conditions would have a great impact in reducing inputs and cost of production once introduced to breeding programs either by selecting these cultivars for propagation or crossing with the better performing cultivars. Since the tolerant cultivars in this study haven't been tested for yield, it would be beneficial to test them for grain yield production. If they turned out to be low yield cultivars, they can be crossed with other cultivars known for high yields, or they can be genetically manipulated. Combining genetic engineering techniques with conventional breeding programmes would allow the introgresssion of the desirable traits into commercial crops, however, extensive testing is required for the improved varieties before they can be used. The large variation in performance among genotypes under low NPK condition might be a result of superior alleles controlling the genes involved in uptake and transport of these nutrients. For example, the rice sodium transporter *OsHKT1;1* was found to be important in accumulating more sodium in the roots of genotypes belonging to indica group compared to japonica genotypes under salt stress (Campbell et al., 2017). Therefore, allelic variations of the genes identified to be involved in nutrient use efficiency or other important traits, should be utilized in breeding programs.

2.4.3 Root architecture modifications in response to low NPK supply

Root growth and root system architecture (RSA) are affected by water and nutrient provision (Chapman et al., 2012). In order to increase access of roots to nutrients, changes in the architecture occur as an adaptive trait in response to less nutrient supply (Sales et al., 2011). In my experiments, roots of plants grown in 0.1 NPK supply were longer and thinner than those of plants grown in full supply. Also, the shoot-to-root ratio was smaller in 0.1 NPK plants. That might be either an effect of low P, as plants usually develop modifications to root morphology in response to low P availability (Faye et al., 2006; He et al., 2003; Lynch and Brown, 2001). Also, (Clark, 1982) stated that roots of plants lacking phosphorus were long and spindly, with little fibrousness.

In addition, the observed change in RSA could be the result of K deficiency. A study by Jia et al. (2008) on 6 rice genotypes with variable K efficiencies grown in hydroponics, showed a reduction in root growth under low K level (5 mg/L, which is similar to the 0.1x concentration that I used) for all genotypes, while moderate K deficiency (10 mg/L) led to an increase in root length of the efficient genotypes. Additionally, all the efficient genotypes in their study formed more fine roots than the inefficient ones under low and moderate K supply and also had higher K concentrations in shoots, suggesting that root morphology parameters are important for K uptake by roots and in the translocation of K up to shoots. Root modifications can also be caused by N deficiency which has previously been shown to make radical changes to root architecture, to increase the root biomass leading to decrease of the shoot-to-root ratio (Hermans et al., 2006; Krapp et al., 2011; Scheible et al., 1997). Since all three, N, P and K are reduced in my study, it is not surprising to find a reduced shoot-to-root ratio. It has been found that N and P deficient plants have increased root to shoot ratio, while in K deficient plants that was rarely observed (Hermans et al., 2006), suggesting that N being the cause of allocating more biomass to the root is a more sensible scenario, since P did not appear limiting in my experiments.

2.4.4 Nutrient accumulation in tissues as an indicator for nutrient use efficiency

In general, better distribution of nutrients in parts of the plant (root, shoot and grain) reflects their use efficiency. A study on upland rice revealed that accumulation of K was the highest compared to other nutrients. Results have shown that total K accumulation was 206 kg ha^{-1}, total N accumulation was 126 kg ha^{-1} and total P accumulation was 13 kg ha^{-1}. K accumulation was higher in the shoot, whereas N and P accumulation was higher in the grain. Also, to produce 1 metric ton of grain of upland rice, the requirement for K was the highest among the nutrients with 40 kg, while N requirement was 28 kg and P was 3 kg (Fageria et al., 2004). It has been reported that uptake of K is higher than N uptake in lowland and upland rice (Fageria and Baligar, 2001; Fageria et al., 2003; Fageria et al., 2010). These reported amounts of mineral nutrient requirement relate to molecular ratios

(N/P/K) of about 1.7 / 0.08 / 1.0. The ratio of N/P/K in Yoshida medium was 2.9 / 0.3 / 1.0, while in shoot tissues were as follows: 3.4 / 0.3/ 1 (in 1 NPK) and 3.5 /0.4 / 1 (in 0.1 NPK). This indicates that the ratios of the elements are more like in the medium, not as reported in the literature field-grown plants. Also, the ratio does not dramatically change when NPK is reduced 10-fold. Therefore, when reducing all 3 elements to 1/10, P is far less limiting when comparing to what is actually needed: 0.03 compared to 0.08. Hence, this perfectly agrees with the observations of P being the least limiting element. This is under the assumption that the ratios matter.

On the other hand, my results showed that both N and K were limiting to the same extent as they equally affected FW, RGR and RGRRED, while under more stress (0.01 condition), N was the most limiting factor among the three. This could explain why genes related to N and K deficiency show up as best candidates in GWA analysis (chapter 3). In this context, it is interesting to note that a parallel GWA study in the lab (Hartley, 2018) that tested the same rice lines under conditions where only K was reduced to 1/10, did not produce the SNPs that showed up as significant in my analysis. This suggests that N and P limitation influence the way how K deficiency is perceived by the plant.

2.4.5 Ion analysis and interaction between nutrients

In my experiment, low supply of K (under 0.1 NPK) might be the cause of the increase in Mg and Ca. The antagonistic relationship between K with Mg and Ca was reported previously (Malvi, 2011). Under low NPK supply, although shoot and root Na was expected to be much higher than that in 1 NPK condition, only a slight increase in shoot Na occurred. The increase in root Na (from Nipponbare data) was much higher. Usually, when K is deficient, plants take up Na to compensate for K (Malvi, 2011). Although under 0.1 NPK external Na concentration was higher than K in the medium (0.29 mM and 0.1 mM, respectively), the increase of Na in shoot was not significant. The parallel study by Hartley (2018) where K alone was reduced to 0.1 mM, shoot Na was 7.1 times higher compared to control. However, external Na in his case was around 0.7 mM under control and low K supply, which can explain the comparatively higher Na uptake. Increase of Na and the other

elements was much higher when ions were measured on a fresh weight basis. Boron under low NPK supply was slightly decreased, which might be a response to low K as their relationship is synergistic (Malvi, 2011). Under 0.1 NPK condition, the increase in Zn might be a result of N decrease as they have negative relation (Malvi, 2011). In rice, as N supply increased, Zn deficiency became more severe (Singh and Singh, 1985). Calculating ion content on dry weight basis does not consider water status in tissues which is an important influencer on transport and biochemical processes. Therefore ion concentration was calculated on fresh weight basis as well.

A study on N concentrations in rice revealed that N uptake in the shoot as well as in the grain was significantly related to shoot dry weight and grain yield (Fageria, 2003). The difference in uptake and utilization of nutrients may be associated with better root geometry, ability of plants to take up sufficient nutrients from lower or subsoil concentrations, better transport or distribution and utilization within plants (Fageria et al., 2008). This indicates that plants grown in adequate supply of nutrients and having high biomass and high ion content in shoot tissues, must have utilized the acquired nutrients sufficiently for dry matter production. On the other hand, if plants have low dry weight but high accumulation of nutrients the utilisation efficiency is low. However, correlation between growth and ion parameters in my study was not significant which suggests that nutrient accumulation in the shoot did not explain the higher relative growth rates under low NPK. Analysing the effect of reducing three elements in parallel is more complicated, because some interactions are contradicting between each element and between high and low supply.

To conclude, studying the effect of reducing NPK in parallel was done for the first time on large number of rice genotypes. Efficient genotypes that showed smaller reduction in growth rates compared to those under optimal nutrient supply were identified which can be of potential importance to crop improvement and reducing the use of fertilizers. Also, among the three elements reduced, some were more limiting than others under different degrees of nutrient stress.

Chapter 3: Genetic diversity of rice under low nitrogen, phosphorus and potassium

3.1 Introduction

With rice being a staple food for many people, an important goal for rice breeding programs is to develop rice varieties that produce high yields with less fertilizer inputs. The emergence of contemporary sequencing technologies has built an opportunity to improve genetic approaches for enhancing production in crops. Ways to improve the soil culture, nutrient use efficiency, pest and disease resistance, have been developed through gene identification and mapping (Spindel and McCouch, 2016).

There are many genetic approaches that have been exploited to create a link between genotype and phenotype, either by identifying genes or analyzing gene functions, such as microarray analysis, mutant analysis using forward and reverse genetics methods, quantitative trait locus (QTL) mapping and genome wide association studies. These approaches have contributed enormously in improving nutrient use efficiency and other desirable traits in plants.

3.1.1 Transcriptomics studies

Studies on the transcriptome and differences in expression patterns of genes in response to environmental stimuli such as nutrient deficiencies have been conducted. For example Fan et al. (2016) reported that when the high-affinity nitrate transporter *NRT2;3b* was overexpressed, there was a 40% increase in nitrogen use efficiency (NUE) in rice upon fertilizer application in the range of 0 to 300 kg N ha^{-1}. In the rice Kaybonnet cultivar, overexpression of the ammonium transporter gene *OsAMT1.1* has resulted in an increase in N uptake and accumulation in shoot and root under adequate supply of N (Ranathunge et al., 2014). It has been reported that up-regulation of high affinity Pi transporters has led to increased root Pi uptake (Raghothama and Karthikeyan, 2005). Transgenic lines overexpressing the phosphate transporter gene *OsPht1;6* gene have shown an increased P uptake and accumulation (Zhang et al., 2014a). Overexpression of *OsPHT1;2* and

OsPHT1;4 has increased Pi accumulation in shoot and root, respectively (Liu et al., 2010a; Ye et al., 2015b). Under K deficiency, overexpression of *OsHAK5* potassium transporter resulted in improved K influx rate in rice roots (Yang et al., 2014b). When *KUP3* potassium transporter of *Alternanthera philoxeroides* was overexpressed in rice, improved growth and K uptake was observed under different levels of K (Song et al., 2014). Overexpression of the potassium channel *TPKb*, improved growth and increased K uptake and concentration in rice shoots and roots under low K supply (Ahmad et al., 2016a).

3.1.2 Quantitative Trait Loci (QTL) mapping

Quantitative Trait Locus (QTL) analysis is a statistical method that joins two types of information; genotype information (mainly molecular markers) and phenotype data (trait measurements), with the aim of explaining the reasons for the genetic variation involving complex traits (Samuel et al., 2016). In rice, QTLs for several agronomically important traits have been identified such as biomass yield (Matsubara et al., 2016), initial growth rate (Sun et al., 2014), growth and grain yield (Hittalmani et al., 2003; Venuprasad et al., 2012), nutrient deficiency tolerance and use efficiency for nitrogen (Wei et al., 2012), potassium (Miyamoto et al., 2012), and phosphorus (Nishida et al., 2017). For example, for nitrogen deficiency tolerance traits, a total of 14 QTLs has been identified for relative shoot and root weight and relative plant height (Lian et al., 2005), and 7 QTLs for relative biomass yield, relative plant height, relative root length and relative chlorophyll content (Feng et al., 2010). A QTL in chromosome 6 was found to be associated with nitrogen use efficiency (Shan et al., 2005). Under low N supply, one main-effect QTL on chromosome 9 was also linked to NUE (Cho et al., 2007). Related to low phosphorus tolerance, a QTL in chromosome 12 was detected (Nishida et al., 2017). Under control and low K treatments, 30 QTLs have been identified for total biomass, shoot and root dry weight, shoot height and root length, and 52 QTLs for shoot and root Na, K, Ca and Mg concentrations (Fang et al., 2015).

3.1.3 Genome-wide association studies

Genome-wide association study (GWAS) has recently become the method of choice for linking genetic markers with phenotypes and is widely used in the identification of QTLs that underlie the quantitative traits. GWAS is a mapping approach used to identify genetic variants or single nucleotide polymorphisms (SNPs) in the genome which are associated with a particular phenotype or a trait. The association between each genotyped marker and a certain phenotype is evaluated by GWAS (Korte and Farlow, 2013). In the DNA sequence, common single base-pair changes are known as SNPs. They are a form of genetic variation used as markers of a genomic region (Bush and Moore, 2012). GWAS can be conducted to spot causative factors for a trait of interest and also to find out aspects of a trait's genetic architecture, for example how many loci contribute to the phenotype. Linkage Disequilibrium (LD) can be explained as a non-random association of alleles between genetic loci or at linked loci (Yu and Buckler, 2006). LD between functional sites and markers is the key to association mapping. The density of marker coverage required depends on how rapid the LD decays over physical distance, the more rapid the LD decays, the higher the needed marker density. In rice, the estimated window of linkage disequilibrium (LD) decay is between 50 and 500 kb (Mather et al., 2007; McNally et al., 2009; Rakshit et al., 2007). The LD decay in Arabidopsis thaliana is estimated to range between 10 and 250 kb (Magnus et al., 2002; Sung et al., 2007). In other crops such as spring barley, the extent of LD is approximately 10 centimorgan (Kraakman et al., 2004), while in bread wheat and durum wheat it is estimated to extend to 41.2 and 25.5 centimorgan, respectively (Somers et al., 2007). The distance of LD decay was smaller as in commercial maize is estimated to range between 1 and 10 kb (Inghelandt et al., 2011). It is possible to use GWAS to investigate genetic and phenotypic variations related to different complex traits in a large number of rice cultivars, whereby the genetic data of the characterized lines can be used again and again to test many phenotypes (Zhao et al., 2011). Results from GWAS can be compared with earlier studies such as quantitative trait loci (QTLs) and mutant analysis (Zhao et al., 2011).

The production of rice across the globe has been boosted by the genome-wide association studies using diversity panels encompassing hundreds of inbred rice accessions where associations are established for important complex traits such as grain length and size, and resistance to prevailing grain diseases and resilience to abiotic stress among other important traits (McCouch et al., 2016; Zhao et al., 2011). The rice diversity panel 1 (RDP 1) was phenotyped in previous GWAS studies for more than 34 traits related to stress tolerance such as blast resistance; morphological traits such as leaf length and width; yield components including plant height and panicle length; and developmental traits such as flowering time (Zhao et al., 2011). Other GWAS studies conducted in rice included a variety of important traits such as tolerance to salinity (Kumar et al., 2015), drought (Xuehui et al., 2010), Root traits (Ristova and Busch, 2014; Wissuwa et al., 2016), yield (Liang et al., 2016). Candidate genes for other important traits were revealed using GWAS on other crops such as grain yield, nitrogen use efficiency, plant height, biomass, flowering time and grain yield in wheat (Cormier et al., 2014; Neumann et al., 2011; Sukumaran et al., 2015), plant height, heading date, grain weight, protein and starch content in spring barley (Pasam et al., 2012), disease resistance, leaf architecture and oil biosynthesis in maize (Hui et al., 2012; Kristen et al., 2011; Tian et al., 2011)

3.1.4 Genome editing using CRISPR/Cas9 system

Genetic manipulation is one of the approaches used to analyze gene function. The CRISPR/Cas9 system is a genome editing tool that enables alteration of the genomic DNA by using customizable single guide RNA to specifically target a nucleic acid sequence. (Belhaj et al., 2013; Bortesi and Fischer, 2015). Cas9 is a protein complex that has a nuclease activity for the cleaving of double-stranded DNA. The enzyme cleaves the complementary strand by following the guide RNA for complementary target site recognition in the DNA sequence, which introduces double strand breaks (DSB) into the target region. These can cause gene modifications by DNA repair mechanisms such as non-homologous end joining (NHEJ) and homology- directed repair (HDR) (Belhaj et al., 2013). NHEJ utilizes DNA ligase IV to rejoin the broken ends, while HDR uses template strands for the repair (Belhaj et al., 2015). Repair by NHEJ may lead to frame shift

mutations by the introduction of insertions or deletions, altering the functioning of genes (Song et al., 2016). Chromosomal deletions can be obtained when the NHEJ mechanism is combined with multiple gRNAs targeting the region. Similarly, HDR mechanisms can lead to the creation of insertions, base substitutions or deletions (Belhaj et al., 2015). The NHEJ repair mechanism might be preferred in plant genome editing (Belhaj et al., 2013).

3.1.5 Rice diversity panel

Rice has been a favourite to GWAS mainly because of its broad history of domestication and evolution (Halewood et al., 2018; Zhao et al., 2011). Two out of 22 recognized species of the *Oryza* genus are known to be cultivated, the Asian rice *Oryza sativa*, and the African rice *Oryza glaberrima*, the rest are wild species (Vaughan et al., 2003). Cultivated Asian rice *O. sativa* is divided into two major groups each of which is divided into well differentiated sub-populations. Indica includes indica and aus, and japonica includes the tropical japonica, temperate japonica and aromatic cultivars (Glaszmann, 1987). Since the rice genome has been fully sequenced (Itoh et al., 2005) and genotypes of around 400 *O. sativa* accessions are accessible (Zhao et al., 2011), in this study we took the opportunity to make use of these accessions to explore the links between genotype and phenotype using GWAS. The rice diversity panel 1 (RDP1) encompasses 400 *O. sativa* accessions which have been selected from different geographical regions around the world, representing all five sub-populations of rice (Zhao et al., 2011). Also, the panel has shown variability in several important traits such as resistance to diseases and insects, tolerance to drought, low mineral nutrition, high salt concentrations and flooding, and other less important traits such as cooking quality, grain colors, lengths and textures (Zhao et al., 2011). In this study, GWAS was used to identify chromosomal loci linked to nitrogen, phosphorus and potassium use efficiency in rice using RDP1. By doing so, novel associations were identified in addition to those that overlapped with previous QTL studies. Also, some genes within QTLs that were previously known to be involved in nutrient uptake, transport and use efficiency were detected, together with other candidates with potential importance in improving NPK use efficiency. Some of the candidate genes identified were further analysed using the CRISPR/Cas9 system.

3.2 Materials and methods

3.2.1 Phenotypic data

Phenotypic data were obtained from 294 diverse accessions from the rice diversity panel 1 (RDP1) (Zhao et al., 2011) grown for 3 weeks under adequate (1 NPK) and low supply of nutrients (0.1 NPK), and included growth traits and element concentrations. For plant growth conditions and elemental analysis see (Chapter 2, methods). Details of all the phenotypic traits included in GWAS analysis are summarised in Chapter 2 (Table 2.3).

3.2.2 Genome Wide Association Studies

GWAS analysis was performed on trait data using mean values of four replicates. Genome wide associations between genotypes and phenotypes were performed in R software (version 3.1.3) using GenABEL package (Aulchenko et al., 2007). All the GWAS analysis was done using the high density rice array (HDRA) which includes information for 700,000 SNPs and provides a better resolution compared to the previous 44,000 SNP chip, with higher SNP density of around 1 SNP per 0.54 kb within the rice genome (McCouch et al., 2016). To reduce seasonal variation, data were normalized for effects of replicates and seasonal variability by using a linear mixed effect package (LME4) (Bates et al., 2014). GenABEL package can run GWAS with different models including: Naïve, FASTA (Family-Based Score Test for Association) and EIGENSTRAT (Chen and Abecasis, 2007; Price et al., 2006). The FASTA model was used for data analysis because it applies mixed linear model (MLM) to control false positives in GWAS (Yu et al., 2006) such as those derived from spurious genetic associations produced by population structure (Shin and Lee, 2015). Also, it accounts for both within and between family structures (Li and Zhu, 2013). In contrast, software like EIGENSTRAT does not model family structure which may lead to inflation in test statistics (Price et al., 2010) and similarly Naive does not account for population structure.

The genomic control λ (λGC) measures the departure of the median p-value from its expected position. The inflation rate λ <1.03-1.05 is believed to sufficiently explain the

relatedness between individuals (Li and Zhu, 2013), although it is related to sample size (Price et al., 2010). Another reason for using FASTA is that the genomic control λGC obtained from this model were around 1 unlike other approaches which yielded much higher values. Four principal components were included in all GWAS analyses. A false discovery rate (FDR) of 10% was applied as a threshold criterion to correct for multiple tests conducted by GWAS (Benjamini and Hochberg, 1995). Associations between SNPs and phenotypic traits were defined as significant if they exceeded the FDR threshold.

3.2.3 Quantitative trait loci and candidate gene identification

A total of 89 individual and combined traits was analysed for associations (see chapter 2, table 2.3). Traits without significant association signals were excluded from further analysis. Signals that contained at least 3 significant SNPs not farther than 20 kb away from each other, were deemed genuine QTLs while signals based on single significant SNP were ignored for down-stream analysis. Major peaks were divided into minor regions after zooming-in the genomic region surrounding the peak. If two or more QTLs overlapped fully or partially between several traits, they were grouped into a single QTL. Each QTL was given a number to differentiate between QTLs in the same chromosome.
Within QTLs, genes were identified by interrogating a genomic area of 100 kb on either side of the most significant SNP. The 200 kb interval was chosen to fall within the estimated window of linkage disequilibrium (LD) decay in rice which is between 50 and 500 kb (Mather et al., 2007; McNally et al., 2009; Rakshit et al., 2007) though it has to be noted that LD is subpopulations dependent (e.g. ~100 kb for indica, ~200 kb for aus and temperate japonica, and ~300 kb for tropical japonica; (Zhao et al., 2011). Genes were obtained by using the Rice Genome Annotation Project (http://rice.plantbiology.msu.edu/pub/data/Eukaryotic_Projects/o_sativa/annotation_dbs/pseudomolecules/version_7.0/) browser. The genes that were duplicated or have an annotation of retrotransposons, or expressed proteins with no additional information were excluded. AgriGO gene ontology analysis tool (http://bioinfo.cau.edu.cn/agriGO/analysis.php) was used to perform GO singular enrichment analysis for the whole set of genes to get an indication of which functional

classes were overrepresented in this study. Genes were also checked for the presence of non-synonymous SNPs (nsSNPs) significantly associated with a trait using the Rice Diversity Allele Finder: (http://rs-bt-mccouch4.biotech.cornell.edu/AF/). Comparison of the QTLs identified from GWAS with previous QTL studies was performed.

3.2.4 Evaluation of candidate genes using mutational analysis

3.2.4.1 Using loss of function (knockout) mutants

Among the candidates identified by GWAS two HKT transporters were selected for further evaluation. Rice functional genomic database (http://signal.salk.edu/cgi-bin/RiceGE) was checked for available mutant lines. One mutant line (T34523T) was found for OsHKT1;1 (LOC_Os04g51820) but not for OsHKT1;4 (LOC_Os04g51830). A retrotransposon (Tos17) insertion mutant of OsHKT1;1 (line NF7030) was obtained from (Wang et al., 2015). The Tos17 retrotransposon insertion resided within the first intron region of OsHKT1;1.

To identify homozygous mutants, plants were genotyped for the insertion. Leaf tissues were frozen in liquid nitrogen, then ground with plastic mortar before adding 400 µl of extraction buffer (200 mM Tris pH 7.5, 250 mM NaCl, 25 mM EDTA, 0.5% SDS) (Edwards et al., 1991). PCR with Phire Hot Start II DNA Polymerase contained: 10 µl Phire reaction buffer (5x), 1 µl dNTP mix (10 mM), 2.5 µl forward primer (10 µM), 2.5 µl reverse primer (10 µM), 25 ng DNA template, 1 µl Phire Hot Start II DNA Polymerase (Thermo Scientific), nuclease-free water to a total of 50 µl. PCR was performed using primers to the right and left of the insertion in OsHKT1;1 gene as described in (Wang et al., 2015). The expected product size was 1080 bp. Rice actin primers were used for control reactions (expected product size was 409 bp). The PCR program used was: 98°C 30 sec, 35 cycles of: 98°C; 5 sec, 50°C 5 sec, 72°C 15 sec; 72°C 1 min. Primer sequences used are presented in Supplementary Table 3.1. PCR products were run in 1.2% agarose gels and 100bp Generuler DNA ladder was used.

3.2.4.2 Phenotypic characterisation of putative KO lines

Seeds of HKT1;1 mutant plants and wild type (Nipponbare) were germinated for 2 weeks in sand. A total of 9 mutant and 5 Nipponbare seedlings was grown for 3 weeks under 1 NPK and 0.1 NPK conditions (for medium preparation, see methods in chapter 2). Fresh weight, dry weight and relative growth rate were measured.

3.2.4.3 Generating loss of function mutation using CRISPR/Cas9

Using Knock-Out feature in DESKGEN software (https://www.deskgen.com), suitable gRNA sequences (20 nt) were designed to target the HKT1;1 and HKT1;4 genes (Supplementary Table 3.2). Guides with highest possible on-target and off-target scores were selected as described (Doench et al., 2014). Two guides for the 1st exon of HKT1;4 were picked for single knockout. Multiple gRNAs were used to increase the chance of obtaining a deletion. To produce a double knockout, one guide targeting the 1st exon of HKT1;4 and one targeting the 2nd exon of HKT1;1 were picked to simultaneously disrupt these two genes through introducing a large deletion.

3.2.5 Assembly of CRISPR/Cas9 constructs using Golden Gate cloning

Components of the Golden Gate MoClo plant parts kit (Addgene #1000000047) and MoClo toolkit (Addgene #1000000044) (Engler et al., 2008; Engler et al., 2014) were used to assemble plasmid constructs. Plasmids containing components of the CRISPR/Cas9 system were kindly provided by Nicola Patron (The Sainsbury Laboratory, Norwich). See Supplementary Table 3.3 for details of plasmids. DNA fragments were cloned to level 1 then Level M acceptors via one step restriction/ligation with type II restriction enzymes, *BsaI* and *BpiI* , respectively. To make level 1 plasmids (transcriptional units), promoter, coding sequence and terminator were cloned from donor plasmids into level 1 acceptor. Based on their position in level M constructs, appropriate acceptors were chosen from the kit. Transcriptional units were assembled in the following order: selection cassette in

position 1, Cas9 cassette in position 2, gRNA1 cassette in position 3, gRNA2 cassette in position 4, and finally a suitable end-linker. In order to knock out genes, level M plasmids containing gRNAs were assembled to target a specific sequence at genes of interest. SnapGene (www.snapgene.com) was used for the in silico assembly of the constructs.

3.2.5.1 Level 1 constructs

To assemble level 1 fragments, PCR was performed first to join the 20 bp gRNA sequence to the gRNA scaffold contained within pICSL90010. Primers used are listed in Supplementary Table 3.4. PCR reactions contained: 10 µl Q5 reaction buffer (5x), 1 µl dNTP mix (10mM), 2.5 µl forward primer (10 µM), 2.5 µl reverse primer (10 µM), 25 ng template (pICSL90010), 0.5 µl Q5 DNA polymerase (New England Biolabs), nuclease-free water to a total of 50 µl. The PCR program used was: 98°C 30 sec; 30 cycles of 98°C 10 sec, 72°C 30 sec; 72°C 2 min. 5 µl of each reaction were analysed on 2% agarose gel containing 2 µl SYBR Safe DNA Gel Stain. The remaining 45 µl were purified using MinElute PCR purification Kit (Qiagen) and the concentration was measured using Nanodrop spectrophotometer. Constructs were assembled with *Triticum aestivum* U6 promoter (TaU6) from plasmid pICSL90003. One step digestion/ligation reaction was performed following the long protocol in ligase buffer from the Golden Gate assembly manual (Engler et al., 2014). Two hundred ng of acceptor plasmid were mixed with the inserts to a 2:1 molar ratio of insert(s): acceptor. Then, 1.5 µl T4 ligase buffer, 1.5 µl Bovine Serum Albumin (10x), 200 units T4 DNA ligase (0.5 µl of 400 U/µl), 5 units *BsaI* (0.5 µl of 10U/µl) were added and the volume was made up to 20 µl with nuclease free water. The program used was: 37 °C 20 sec; 26 cycles of 37 °C 3 min, 16°C 4 min; 50°C 5 min; 80°C 5 min. 2 µl of the reactions were transformed into competent *E.coli,* plating 150 µl of bacterial suspension on X-gal (40 µg/ml)/ IPTG (0.1 mM) containing LB agar plates with carbencillin (50 µg/ml). White colonies containing the ligated plasmid were streaked to new LB agar plates with the appropriate antibiotic and incubated overnight at 37 °C. Plasmid DNA was extracted from 2 ml bacterial culture using Macherey-Nagel's NucleoSpin Plasmid kit. Plasmid concentrations were measured with Nanodrop photometer. Constructs were validated using restriction digests and sequencing. Each

purified plasmid (500 ng) was digested with 1 µl of one or a combination of restriction enzymes and run on 1% agarose gel with 1 kb DNA ladder (Invitrogen).

3.2.5.2 Level M constructs

The same steps were followed to assemble level M constructs except for using *BpiI* instead of *BsaI* in the digestion/ligation reaction and using spectinomycin instead of carbencillin for selection. Three level M constructs were assembled to target HKT1;1, HKT1;4, and both. Diagnostic digestion with *SacI* and with a combination of *NcoI* + *SacI* and *BamHI* + *NcoI* was performed.

3.2.5.3 Rice transformation

Constructs were introduced into japonica Nipponbare using *A tumefaciens* strain AGL1 transformation following the protocol of (Nishimura et al., 2006). Briefly, around 100 seeds per batch were de-husked and placed on a suitable medium to produce calli. Around 1 month later, the calli were infected with the *Agrobacterium* carrying the vector of interest. Three days post-infection, calli were transferred to a selection medium for 4 weeks and then to a medium for shoot regeneration for 4-6 weeks. After that, shoots were placed into glass jars for a few days, then rooted seedlings were placed to soil pots and left to grow.

3.2.5.4 Identification of mutations in T0 plants

Tissues were collected randomly from multiple leaves of the same regenerated T0 plant. Leaf tissues were frozen in liquid nitrogen, then ground with mortar and pestle before DNA was extracted using the Macherey-Nagel NucleoSpin^{TM} Plant II kit. PCR was used to check for possible insertions or deletions in the targeted region. PCR reaction contained: 10 µl Q5 reaction buffer (5x), 1 µl dNTP mix (10 mM), 2.5 µl forward primer (10 µM), 2.5 µl reverse primer (10 µM), 100 ng template DNA , 0.5 µl Q5 High-Fidelity DNA Polymerase (New England Biolabs), nuclease-free water to a total of 50 µl. The PCR program used was: 98°C 30 sec; 40 cycles of: 98°C 5 sec, 50°C (for HKT1;1 primers) or 68°C (for

HKT1;4 primers) 5 sec, 72°C 20 sec; 72°C 2 min. Primers used are listed in Supplementary Table 3.5. PCR products were run in 2% agarose gel and 100 bp Generuler DNA ladder was used. PCR products were purified using MinElute PCR purification Kit (Qiagen). 3'A overhangs were added to PCR products using the following reaction mix: 1–4 µl of the purified PCR product, 2 µl of GoTaq Reaction Buffer (5x) (Promega), 2 µl of dATP (1 mM), 1 µl GoTaq Flexi DNA Polymerase (5 u/µl), 0.6 µl of $MgCl_2$ (25 mM), and nuclease-free water to a final volume of 10 µl. The mixture was incubated at 70°C for 30 minutes in a thermal cycler.

The PCR products were then ligated into the pGEM-T Easy Vector I (Promega) using T4 DNA ligase. After incubation at 4 °C overnight, ligated product was used to transform *E.coli* (DH5α) mix and go cells prepared by using the transformation buffer set (T3002) from Zymo Research Corp. The mixture was plated on LB/ampicillin/IPTG/X-Gal plates and incubated overnight at 37 °C. Plasmid DNA was extracted from 5 colonies for each cloned PCR product using Macherey-Nagel's NucleoSpin Plasmid kit. Plasmids were then analysed using restriction digests and Sanger sequencing. Each purified plasmid (500 ng) was digested with 1 µl of one or a combination of restriction enzymes and run on 1% agarose gel with 1 kb DNA ladder (Invitrogen). Sequencing was done using GATC Bitech barcode service (www.gatc-biotech.com). Snapgene software was used to align sequence traces with unmodified DNA.

3.3 Results

3.3.1 GWAS on growth and ion content parameters

A 700k SNP-chip (McCouch et al., 2016) was used to analyse phenotypic data. After applying genotypic quality controls using GenABEL package, 598,678 (85.5%) markers were used since those with call rates < 80% (n=7017) and/or a minor allele frequency of <1% (n=94325) were excluded. GWAS was performed on all the phenotypic data summarized in Chapter 2 (Table 2.3). GWAS results on all phenotypes under 0.1 NPK condition are summarized in Table 3.1. Manhattan plots and quantile-quantile plots for all

phenotypes analysed by GWAS are summarized in the supplementary figures 3.1 to 3.87. Information on one growth parameter is provided as an example.

Table 3. 1: Summary of GWAS results of all phenotypic traits under 0.1 NPK condition. Trait name is followed by chromosome number and the number of significant SNP positions.

	Trait	Chromosome	Significant peaks (SNP positions)	
			Peak 1	Peak 2
Growth	Total final fresh weight	4	31184058	-
		6	21820752	24975205
		8	3002115	-
		10	17129594	-
	Relative growth rate	4	30464183	30772771
		10	20556687	-
		12	21660849	-
	Shoot fresh weight	3	16552163	-
		5	8401535	-
		6	25006916	-
		8	3002115	-
		10	16525036	-
	Root fresh weight	4	31184058	-
		7	28318143	-
		10	17129594	-
	Fresh weight shoot to root ratio	6	10018271	-
		10	2120093	-
	Fresh weight reduction	1	43115311	-
	Shoot fresh weight reduction	1	42369736	-
		5	645981	-
	Fresh weight shoot to root ratio reduction	6	11010207	-
Element Content- DW basis	Mg	4	21426950	-
		12	6942014	-
	Na	1	11054118	22203914
		6	22223580	29540591
		8	9206953	27088677
		10	21526441	-
	P	2	5383487	-
		4	13866768	-
		8	10364518	-
		10	16298434	-
	K reduction	1	29231879	29309405
		7	23344427	-

		8	3776462	-
		12	24274703	-
	K/RGR	2	20631168	-
		10	88521	-
	Na/RGR	1	11054118	-
		6	29540591	-
		8	9206953	27088677
	P/RGR	4	13866768	-
		8	10364518	-
		10	16298434	-
	N/RGR	2	683345	8905285
		3	31210808	-
		5	1407184	-
	C/RGR	2	21792130	29300008
		4	30482186	-
		5	16088422	23793160
		6	28554495	-
		7	1050153	-
		8	9591468	-
		9	19188564	-
Element Content- FW basis	K	2	20631168	-
	Mg	1	24957110	-
		4	21426950	-
	Fe	12	21104861	-
	Na	1	11054118	22203914
		6	29476763	-
		8	9206953	27088677
		9	7472543	-
	P	2	5383487	-
		4	13866768	-
		8	10364518	-
		10	15637076	-
	N	2	8548363	-
		3	31006533	-
		10	7819452	-
		11	17671985	-
	C	2	21123989	-
		4	12818578	14706057
		5	8297036	-
		12	21103899	-
	K reduction	1	29231879	-
	Mg reduction	4	31184058	-
		8	7615516	-

		11	2032303	-
	Na reduction	8	3457036	17430264
	N reduction	3	31006533	-
	Zn/RGR	6	13341013	-
	K/RGR	2	20631168	-
		6	28079760	-
		7	1050153	-
		8	9591468	-
		9	10349285	-
		11	23911043	-
	Na/RGR	1	11054118	-
		2	22853692	-
		6	10281351	6719213
		8	27088677	9176203
	P/RGR	1	37710728	-
		4	13865907	-
		5	26598956	-
		8	10364518	-
		10	15637076	-
	N/RGR	2	8548363	-
		3	31006533	-
		5	23793160	-
	C/RGR	8	9591468	-
Nutrient use Efficiency	Fe	3	31674182	-
		6	15982420	-
	B	6	27129592	-
		8	5258341	-
		12	26075612	22029281
	Na	1	11336511	-
		6	29461156	-
		8	8609327	-
	N	10	13257618	-

3.3.1.1 Relative growth rate (RGR)

As an example of the analysis pipeline, Figure 3.1 shows the Q-Q plot and Manhattan plot from the mixed linear model using relative growth rates of plants grown in 0.1 NPK as phenotypic data. SNPs above the threshold line are significant at using a 10% FDR rate. In quantile-quantile plots, the line produced based on observed P-values should lie along the

diagonal line of the expected P-values for most SNPs. The Q-Q plot value of around one suggests that no confounders (population structure, or family relatedness) occurred in the GWAS. Based on RGR data, a number of QTLs was identified in different chromosomes (Figure 3.1). The QTL in chromosome 4 included around 20 significant SNPs distributed among ~1Mb genomic region. Zooming into this region (Figure 3.2) shows a complex QTL which encompasses a total of 45 unique genes after removing transposons, expressed proteins and duplicates. For a peak to be considered a QTL, it has to encompass a minimum of 3 significant SNPs not farther than 20 kb away from each other. Two minor peaks only fulfilled this criterion, and genes within 200 kb from the top SNP in each minor peak were identified. Candidate genes identified in the QTL in chromosome 4 are summarized in table 3.2.

From this collection, candidate genes that might play a role in nutrient transport and use efficiency were identified, for example, cation transporters OsHKT1;4 (LOC_Os04g51830) and OsHKT1;1 (LOC_Os04g51820). These HKTs are permeable to Na only (Jabnoune et al., 2009; Su et al., 2015; Suzuki et al., 2016) and may be involved in regulation of K/Na homeostasis. OsHKT1;1 seems to act as a low-affinity sodium transporter (Garciadeblas et al., 2003) and it is highly expressed in the shoot while its expression in the root is induced by potassium starvation (Garciadeblas et al., 2003). Wang et al. (2015) reported that OsHKT1;1 in rice has an important role in salt tolerance by reducing Na concentration in shoots and preventing sodium toxicity in leaf blades as it is probably involved in the control of Na concentrations in the phloem and xylem sap under salt stress. The *Oshkt1;1* mutant plants displayed hypersensitivity to salt stress, they contained less Na in the phloem sap and accumulated more Na in the xylem compared with the wild type. HKT1;1 is expressed mainly in the phloem of leaf blades and it is regulated by the OsMYBc transcription factor (Wang et al., 2015). HKT1;4 is highly expressed in leaf sheaths (Suzuki et al., 2016) and it controls leaf sheath-to-blade Na transfer under salt stress (Cotsaftis et al., 2012). A recent study on rice revealed that OsHKT1;4 has a function in limiting Na accumulation particularly in leaf blades under salt stress in reproductive growth stage (Suzuki et al., 2016).

Na is known to have a positive influence on plant growth under limited K supply (Flowers and Lauchli, 1983; Takahashi and Maejima, 1998; Takahashi et al., 1997) as it can replace K to some extent, in carrying out some functions due to similar chemical properties between them (Wakeel et al., 2011). A study on rice plants revealed that shoot Na accumulation had increased under K deficient conditions but differed among cultivars (Akai et al., 2012). Additionally, it has been proven that Na improved the growth of rice plants under K deficiency and another HKT family member, OsHKT2;1, had a role in uptake and allocation of Na as a useful element in K deficient rice root (Horie et al., 2007). This gene was identified from GWAS analysis on another trait. The HKT genes were chosen as best candidates among others to potentially have a role in the transport and use efficiency of K.

Transcription factors are known to regulate cellular processes and some TFs were found such as WRKY transcription factor 68 and MYB protein. Other genes such as calcium-transporting ATPase which is a Mg-ATP dependent enzyme that catalyses the transport of calcium (Bañuelos et al., 2002; Yang et al., 2009). Similar analyses were carried out for all other traits listed in (Table 2.3, Chapter 2) and the full list of genes is in (Supplementary Table 3.7).

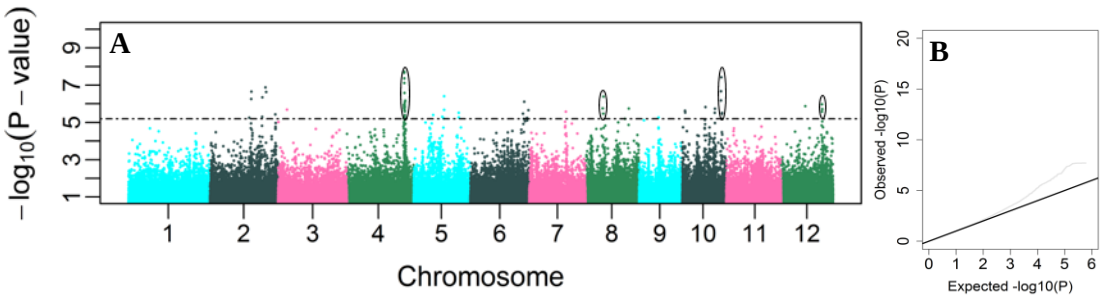

Figure 3. 1: A) Genome-wide P-values from the mixed model method based on relative growth rate in 0.1 NPK plants. The X-axis shows the location of the identified SNPs along the 12 chromosomes of the rice genome, the Y-axis indicates the -log10 (P-value) which determines the significance of the association between SNPs and traits. The horizontal line indicates the genome-wide significance threshold (FDR <10%). Circles indicate peaks that fulfilled the criteria for QTL definition. B) A Q-Q plot for relative growth rate in 0.1 NPK plants shows the distribution of the observed P-values alongside their expected values. Genomic control λ_{GC}= 1.056436.

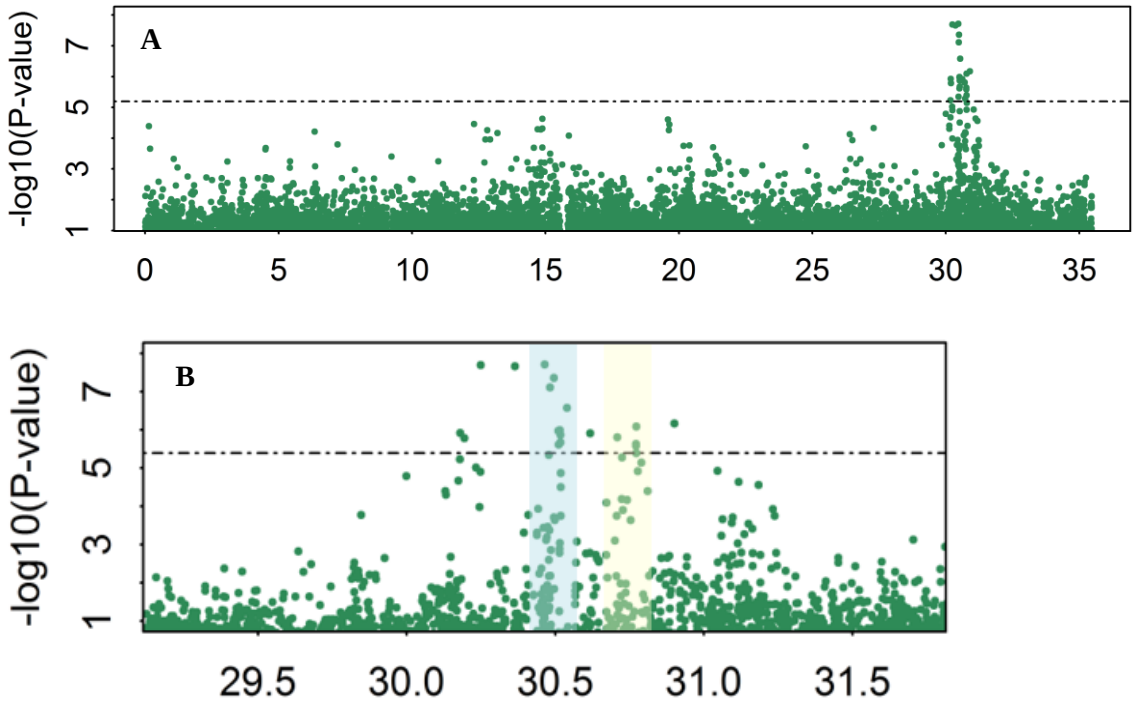

Figure 3. 2: A) Chromosomal view showing the peak in chromosome 4 identified from RGR in 0.1 NPK plants. B) Zoom-in of around 2 Mb covering the peak in chromosome 4. Blue and yellow shading indicate 200 kb interval of the two peaks analysed.

Table 3. 2: Summary of the candidate genes identified in the QTL in chromosome 4 associated with RGR.

Locus ID	Gene
LOC_Os04g51240	EF hand family protein, putative, expressed
LOC_Os04g51270	vacuolar ATPase G subunit, putative, expressed
LOC_Os04g51280	DAG protein, chloroplast precursor, putative, expressed
LOC_Os04g51300	peroxidase precursor, putative, expressed
LOC_Os04g51310	putrescine-binding periplasmic protein-related, putative, expressed
LOC_Os04g51320	transcription factor TF2, putative, expressed
LOC_Os04g51330	maltose excess protein 1-like, chloroplast precursor, putative, expressed
LOC_Os04g51340	pectinacetylesterase domain containing protein, expressed
LOC_Os04g51350	pentatricopeptide, putative, expressed
LOC_Os04g51360	oxidoreductase, 2OG-Fe oxygenase family protein, putative, expressed
LOC_Os04g51370	protein kinase, putative, expressed
LOC_Os04g51380	protein-S-isoprenylcysteine O-methyltransferase. tax, putative, expressed
LOC_Os04g51390	aldose 1-epimerase, putative, expressed
LOC_Os04g51400	zinc finger, C3HC4 type domain containing protein, expressed
LOC_Os04g51440	villin protein, putative, expressed
LOC_Os04g51450	glycosyl hydrolases family 16, putative, expressed
LOC_Os04g51460	glycosyl hydrolases family 16, putative, expressed
LOC_Os04g51510	glycosyl hydrolases family 16, putative, expressed
LOC_Os04g51520	glycosyl hydrolases family 16, putative, expressed
LOC_Os04g51560	WRKY68, expressed
LOC_Os04g51570	tyrosine phosphatase, putative, expressed
LOC_Os04g51580	leucine rich repeat containing protein, expressed
LOC_Os04g51610	calcium-transporting ATPase, plasma membrane-type, putative, expressed
LOC_Os04g51630	60S ribosomal protein L7, putative, expressed
LOC_Os04g51660	transferase family protein, putative, expressed
LOC_Os04g51690	glycosyl hydrolase family 47 domain contain protein, expressed
LOC_Os04g51700	DNA ligase I, ATP-dependent family protein, expressed
LOC_Os04g51786	containing DUF163, putative, expressed
LOC_Os04g51792	PAP fibrillin family domain containing protein, expressed
LOC_Os04g51794	DNA binding protein, putative, expressed
LOC_Os04g51796	DNA repair ATPase-related, putative, expressed

LOC_Os04g51800	MYB protein, putative, expressed
LOC_Os04g51820	OsHKT1;1 - Na+ transporter, expressed
LOC_Os04g51830	OsHKT1;4 - Na+ transporter, expressed
LOC_Os04g51880	GHMP kinases ATP-binding protein, putative, expressed
LOC_Os04g51890	OsSAUR20 - Auxin-responsive SAUR gene family member, expressed
LOC_Os04g51910	proteasome/cyclosome repeat containing protein, expressed
LOC_Os04g51920	protein disulfide isomerase, putative, expressed
LOC_Os04g51940	YT521-B, putative, expressed
LOC_Os04g51950	serine/threonine-protein kinase HT1, putative, expressed
LOC_Os04g51970	synaptic vesicle 2-related protein, putative, expressed
LOC_Os04g51980	transferase family domain containing protein, expressed
LOC_Os04g51990	transferase family domain containing protein, expressed
LOC_Os04g52000	protein phosphatase 2C, putative, expressed
LOC_Os04g52020	PHD-finger domain containing protein, putative, expressed

3.3.2 Quantitative trait loci linked to NPK nutrition in rice

Based on GWAS analyses carried out on all traits a total of 84 QTLs was detected which covered a total of 3540 genes (Supplementary Table 3.6). After removal of duplications and of genes that were annotated as (retro)transposons, or as expressed proteins with no additional information, a total of 1462 unique genes remained (Supplementary Table 3.7). Some of the 84 QTLs identified in this analysis overlapped with previously identified QTLs (Figure 3.3). In total, 16 QTLs from this GWAS analysis were found to be localized within previously identified genomic regions. These were 10 QTLs associated with K deficiency tolerance in rice in all chromosomes except for 2, 3, 5, 6, 9 and 10 (Fang et al., 2015), three known QTLs for N deficiency tolerance and use efficiency in chromosome 4 and 9 (Wei et al., 2012), and three QTLs in chromosome 6, 10 and 12 linked to P deficiency tolerance (Nishida et al., 2017; Shimizu et al., 2008; Wissuwa et al., 2002; Wissuwa et al., 1998). Novel QTLs linked to NPK use efficiency were found in other parts of the genome across almost all the chromosomes.

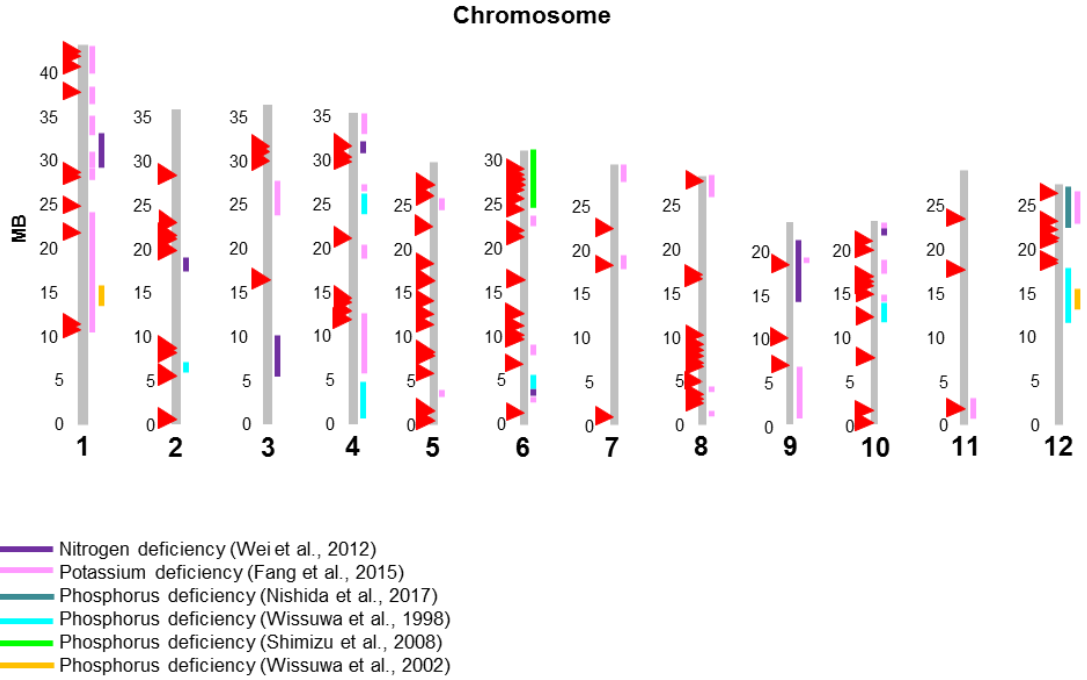

Figure 3. 3: Summary of QTLs identified in this study. SNP positions are shown using red triangles to the left of grey bars which represent rice chromosomes. Coloured rectangles represent QTLs identified in previous studies in rice.

3.3.3 Genes within Quantitative Trait Loci

3.3.3.1 General classification of genes

AgriGO gene ontology analysis tool (http://bioinfo.cau.edu.cn/agriGO/analysis.php) was used to perform GO singular enrichment analysis for the curated list of 1462 genes (Du et al., 2010). A total of 109 GO terms was statistically significantly (FDR <5%) enriched relative to their background abundance in the rice genome, these included secondary level terms of the parent ones under 3 categories: biological process, molecular function and cellular component. Significance was calculated using Fisher's exact test with a Yekutieli adjustment for multiple testing. Considering only parent terms within the 3 categories, we ended up with a total of 13 significant overrepresented Go terms (7 in biological process category, 4 in molecular function and 2 in cellular components categories). Overrepresented GO terms in all 3 categories are summarized in figure 3.4. To conclude, metabolic and cellular processes together with response to stimulus related terms are

overrepresented in biological process category. Based on molecular function, catalytic activity and binding related terms are overrepresented. This suggests that genes with regulatory roles, such as kinases and transcription factors, might be potentially important to the use efficiency of NPK. However, these categories encompass hundreds of genes which will need further evaluation. In the molecular function category, transporter activity GO terms were also overrepresented. This is not surprising since many transporters have been previously identified to be involved in improving the use efficiency of nutrients (N, P and K) (Teng et al., 2017).

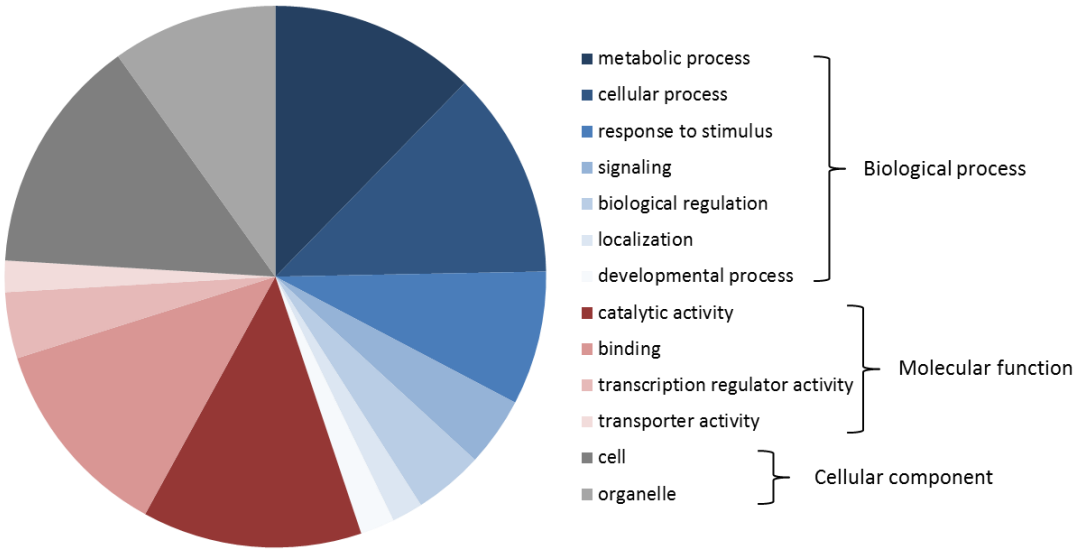

Figure 3. 4: Summary of overrepresented GO terms in the curated list of genes.

3.3.3.2 SNPs associated with traits and within genes

Candidates were checked for the presence of non-synonymous SNPs (nsSNPs) using the Rice Diversity Allele Finder: (http://rs-bt-mccouch4.biotech.cornell.edu/AF/). Within the peaks included and amongst the SNPs that were significantly associated with any of the traits, 176 SNPs were found to be within genes. Of these, 36 nonsynonymous SNPs were found within 32 different genes as listed in Table 3.3 with two nonsense mutations in OsWAK35a - OsWAK short gene (LOC_Os04g24300) and in OsWAK126 - OsWAK receptor-like protein kinase (LOC_Os12g42040). Two nsSNPs were found within the cation transporter OsHKT2;4 (LOC_Os06g48800).

Table 3. 3: Non-synonymous single nucleotide polymorphisms (SNPs) identified using GWAS.

Gene	Chr	SNP position (bp)	Amino acid change
LOC_Os01g19548: pentatricopeptide, putative, expressed	chr1	11090319	Thr->Ser
LOC_Os02g34490: Leucine Rich Repeat family protein, expressed	chr2	20668145	Leu->Ser
LOC_Os03g54084: phytochrome C, putative, expressed	chr3	31006533	Cys->Tyr
LOC_Os03g54780: STE_PAK_Ste20_KHSh_GCKh_HPKh.1 - STE kinases include homologs to sterile 7, sterile 11 and sterile 20 from yeast, expressed	chr3	31147642	Met->Ile
LOC_Os04g24220: OsWAK32 - OsWAK receptor-like protein kinase, expressed	chr4	13866768	Glu->Asp
LOC_Os04g35250: MONOCULM 1, putative, expressed	chr4	21425711	Lys->Thr
LOC_Os04g24220: OsWAK32 - OsWAK receptor-like protein kinase, expressed	chr4	13865907	Ala->Ser
LOC_Os04g24300: OsWAK35a - OsWAK short gene, expressed	chr4	13924025	Arg->Stop
LOC_Os05g40520: OsFBT8 - F-box and tubby domain containing protein, expressed	chr5	23793160	Thr->Lys
LOC_Os06g37540: hypothetical protein	chr6	22223580	Arg->Cys
LOC_Os06g48800: OsHKT2;4 - Na+ transporter, expressed	chr6	29535779	Leu->Phe
LOC_Os06g48800: OsHKT2;4 - Na+ transporter, expressed	chr6	29536340	Ile->Val
LOC_Os06g48870: methyl-binding domain protein MBD, putative, expressed	chr6	29593765	Ala->Thr
LOC_Os06g12390: galactosyltransferase family protein, putative, expressed	chr6	6719213	Gln->Lys
LOC_Os06g48860: OsSAUR28 - Auxin-responsive SAUR gene family member, expressed	chr6	29580806	Asp->Glu
LOC_Os06g48650: OsSub52 - Putative Subtilisin homologue, expressed	chr6	29435494	Ala->Val
LOC_Os06g44880: type II intron maturase protein, putative, expressed	chr6	27129592	Ala->Ser
LOC_Os06g47210: oligopeptidase, putative, expressed	chr6	28623106	Asp->Asn
LOC_Os08g05600: aquaporin protein, putative, expressed	chr8	2997985	Phe->Val
LOC_Os08g42840: leucine rich repeat protein, putative, expressed	chr8	27088677	Val->Gly
LOC_Os08g43010: disease resistance RPP13-like protein 1, putative, expressed	chr8	27184186	Glu->Asp
LOC_Os08g43000: CC-NBS-LRR, putative, expressed	chr8	27178314	Gln->Arg
LOC_Os08g42840: leucine rich repeat protein, putative, expressed	chr8	27088956	Tyr->Phe
LOC_Os08g15149: oxidoreductase, 2OG-Fe oxygenase family protein, expressed	chr8	9167154	Ala->Val

LOC_Os08g43000: CC-NBS-LRR, putative, expressed	chr8	27178176	Leu->Arg
LOC_Os08g15180: 60S acidic ribosomal protein, putative, expressed	chr8	9181356	Ile->Val
LOC_Os08g09030: hypothetical protein	chr8	5250384	Ile->Asn
LOC_Os08g28830: pentatricopeptide, putative, expressed	chr8	17630078	Lys->Met
LOC_Os08g09020: Cupin domain containing protein, expressed	chr8	5249103	Val->Ile
LOC_Os08g08990: Cupin domain containing protein, expressed	chr8	5234303	Gly->Ser
LOC_Os10g31510: glycine-rich cell wall structural protein 2 precursor, putative, expressed	chr10	16508164	Ala->Val
LOC_Os10g31620: glycine-rich cell wall structural protein 2 precursor, putative, expressed	chr10	16567557	Ala->Val
LOC_Os10g25670: hypothetical protein	chr10	13288466	Phe->Leu
LOC_Os11g40090: A49-like RNA polymerase I associated factor family protein, expressed	chr11	23912892	Arg->His
LOC_Os11g40080: lipin, N-terminal conserved region family protein, expressed	chr11	23904581	Ser->Phe
LOC_Os12g42040: OsWAK126 - OsWAK receptor-like protein kinase, expressed	chr12	26075612	Ser->Stop

3.3.3.3 Novel candidate genes with potential importance for NPK use efficiency

Among the 1462 genes, 6 genes were identified to potentially be involved directly in the use efficiency of NPK. These genes included: 1 ammonium transporter, 3 nitrate transporters and 2 potassium transporters. Unexpectedly, several Na transporters were identified that might be potentially important in the use efficiency of K. Other genes that might be potentially important are regulatory genes and transcription factors. Associated traits and putative roles in PKN nutrition of the most promising candidate genes are briefly discussed in the next section.

The low affinity ammonium transporter AMT3;1 (LOC_Os01g65000) was associated with P(FW)/RGR_{LT} and it is expressed more in shoots than roots (Gaur et al., 2012). Two high-affinity nitrate transporters OsNRT2.1 (LOC_Os02g02170) and OsNRT2.2 (LOC_Os02g02190) were associated with N(FW)/RGR_{LT}. OsNRT2.1 and 2.2 are believed to have a key role in nitrate uptake (Araki and Hasegawa, 2006). Under low nitrate,

enhanced growth was observed in rice plants when OsNRT2.1 was overexpressed (Katayama et al., 2009). OsNRT2.1/2.2 are mainly and abundantly expressed in most cell types of the roots (primary and lateral) but also expressed in the leaves (Feng et al., 2011). The High-affinity nitrate transporter 2.3 (NRT2.3) (LOC_Os01g50820) was associated with K(DW)RED_{LT} and K(FW)RED_{LT}. OsNRT2.3 have two mRNA splice variants: OsNRT2.3a and OsNRT2.3b. It has been observed that OsNRT2.3a plays a major part in long distance nitrate transport from root to shoot specifically under low nitrate, additionally, knockdown of this gene led to impairment in xylem loading of nitrate and reduction in growth at under low nitrate (Tang et al., 2012). OsNRT2.3 is expressed in the stelar cells of both primary and lateral roots (Feng et al., 2011; Tang et al., 2012). All the three OsNRT2.1/2.2/2:3a genes require OsNAR2.1 as a partner to mediate nitrate transport, moreover knockdown of OsNAR2.1 resulted in supressed expression in all of the above mentioned OsNRT2 transporters (Yan et al., 2011).

Linked to RGR, two sodium transporters were identified, OsHKT1;1 (LOC_Os04g51820) and OsHKT1;4 (LOC_Os04g51830) as mentioned previously. Linked to the same trait, the high affinity potassium transporter 14 (HAK14) was identified (LOC_Os07g32530). From the same family, another transporter HAK11 (LOC_Os04g52390) was found to be associated with FW and with Mg(FW)REDLT. In rice, 27 genes belonging to the KT/HAK/KUP potassium transporter family are distributed among 8 chromosomes and they cluster in four major groups based on their amino acid sequences (Gupta et al., 2008). Although both OsHAK11 and OsHAK14 belong to cluster III, they are subdivided into cluster IIIA and B respectively. However, functions of cluster III and IV members are less understood compared to cluster I and II members (Grabov, 2007). Cluster III genes are not highly expressed in roots, but OsHAK11 expression in the root was found to be induced by salt stress (Okada et al., 2008). In general, the majority of cluster I members in plants tends to have a role in high affinity K uptake, and cluster II members are likely to function as low affinity K transporters (Okada et al., 2008). However, physiological functions of these transporters not only differ between plant species but also between members of the same cluster within the same species (Li et al., 2017).

Two Na transporters were found to be related to many traits including: Na(DW)LT, Na(DW)/RGRLT and NaUELT. These are: OsHKT2;1 (LOC_Os06g48810) and OsHKT2;4 (LOC_Os06g48800). OsHKT2;1 is a high affinity Na transporter which has a role in uptake and allocation of Na in rice roots under K deficiency (Garciadeblás et al., 2003; Horie et al., 2007) and the expression in roots is induced by K starvation (Garciadeblás et al., 2003; Horie et al., 2001). Under low K provision, OsHKT2;1 expression was up-regulated (Ma et al., 2012; Takehisa et al., 2013) and shoot Na accumulation increased when OsHKT2;1 was overexpressed (Miyamoto et al., 2015). Furthermore, OsHKT2;4 selectively transports K under low external Na concentration , but mediates Na transport when Na concentration is high (>10 mM). Its K selectivity is dominant over Na (Sassi et al., 2012) and other divalent cations such as Mg and Ca (Horie et al., 2011a; Lan et al., 2010b). Expression of OsHKT2;4 was down-regulated under K deficiency (Shankar et al., 2013) and it is expressed more in shoots than roots (Miyamoto et al., 2015) .

The Na transporter OsHKT1;5 (LOC_Os01g20160) was associated with NaUELT. OsHKT1;5 is a selective sodium transporter and it has been shown that a loss of function of this gene has led to higher Na accumulation in shoots under salt stress as it has a role in recirculating Na from shoots to roots by excluding Na in the phloem (Kobayashi et al., 2017; Mekawy et al., 2015) and also in retrieving Na from the xylem to reduce the accumulation in shoots (Zhong-Hai et al., 2005).

3.3.4 Evaluation of candidate genes using available mutants

Among the candidates identified by GWAS two HKT transporters were selected for further evaluation as they might have a role in K use efficiency. A mutant of OsHKT1;1 (line NF7030) obtained from (Wang et al., 2015) had the Tos17 retrotransposon insertion within the first intron of OsHKT1;1. Published data confirmed that this insertion had an effect on gene function and showed that the plants had a phenotype when tested under salinity stress (Wang et al., 2015). The seed stock obtained was homozygous for the insertion (Figure.3.5).

Although HKT1;1 is highly expressed in the shoot (leaf blade specifically), the expression in the root is induced by potassium starvation (Garciadeblás et al., 2003) suggesting that this gene might have a role in transport of Na to compensate for K under K deficiency. In this case, by disrupting HKT1;1 gene function, it was expected that the knockout lines would be limited in their Na transport/uptake, assuming there is little or no redundancy. Therefore, under low NPK, plants would perform less well since K cannot be efficiently replaced by Na. In standard NPK conditions, it was expected that there is no difference between wild type and mutant. On the other hand, HKT1;1 plays a role in reducing Na accumulation in the shoot under salt stress (Wang et al., 2015), meaning that this gene would act negatively under normal conditions by limiting Na transport to the shoot. In this case, disrupting the gene function would be expected to have a positive effect. Mutant plants would not reduce Na accumulation in the shoot and therefore plants would still benefit from Na as a useful element under K deficiency. However, testing mutant HKT1;1 seeds together with Nipponbare under 1 NPK and 0.1 NPK condition revealed that mutant plants had lower final fresh weights and relative growth rates (Figures 3.6 and 3.7) in both conditions which does not confirm the first assumption we had. Moreover, RGR reduction showed no difference between wild-type and mutant plants (Figure 3.8), meaning that knocking out HKT1;1 did not reveal any effect. This is possibly due to redundancy and more than one gene contributing to give a phenotype, or this gene might act differently under different conditions.

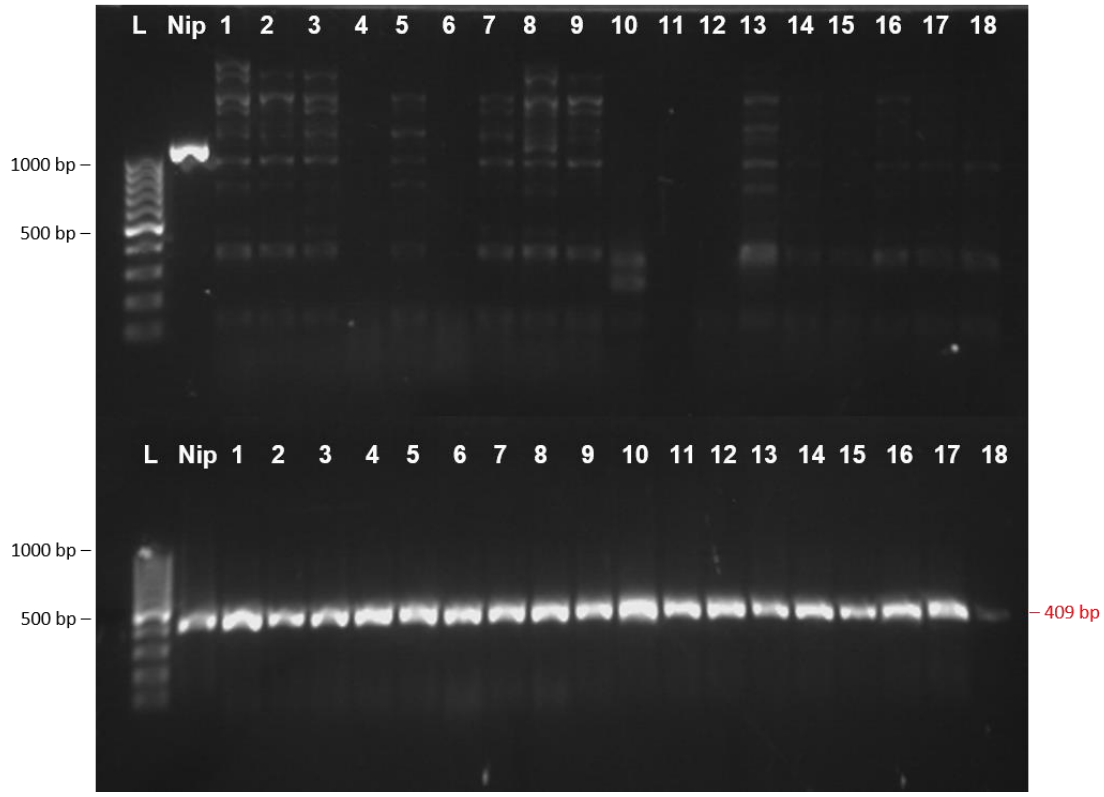

Figure 3.5: PCR product after amplification with OsHKT1;1 F and R primers shows a wild-type band at the expected size of 1080 bp for Nipponbare and not for plants with Tos17 insertion (Top). Using rice actin primers, bands at size of 409 bp were observed in both wild type and mutant plants confirming a successful PCR (Bottom). L: 100bp DNA ladder, lane 1: Nipponbare, 1-18: HKT1;1 mutant plants.

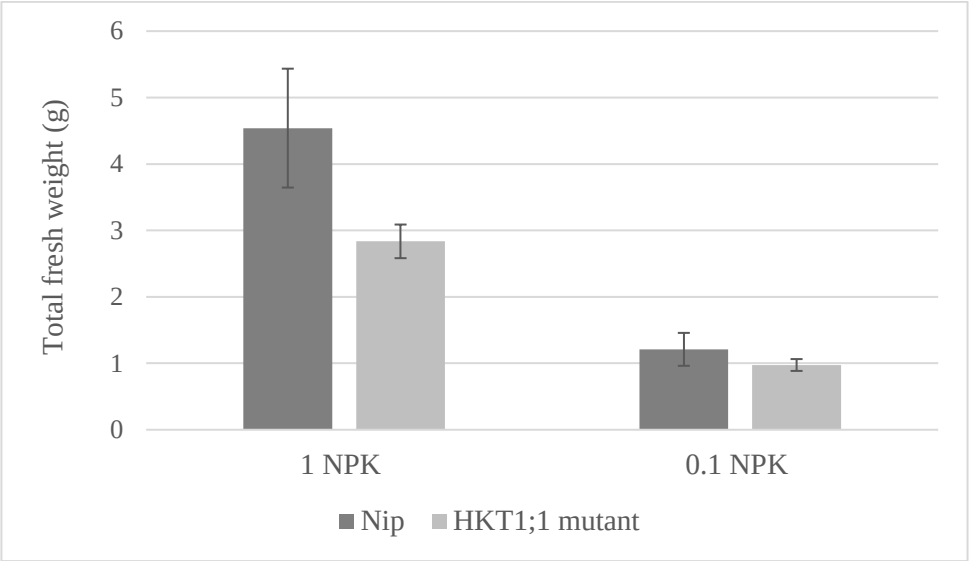

Figure 3. 6: Average fresh weight of HKT1;1 mutant plants was smaller than Nipponbare plants under 1 NPK and 0.1 NPK conditions. Error bars: SE (n=9 HKT1;1 mutant, n=5 Nip).

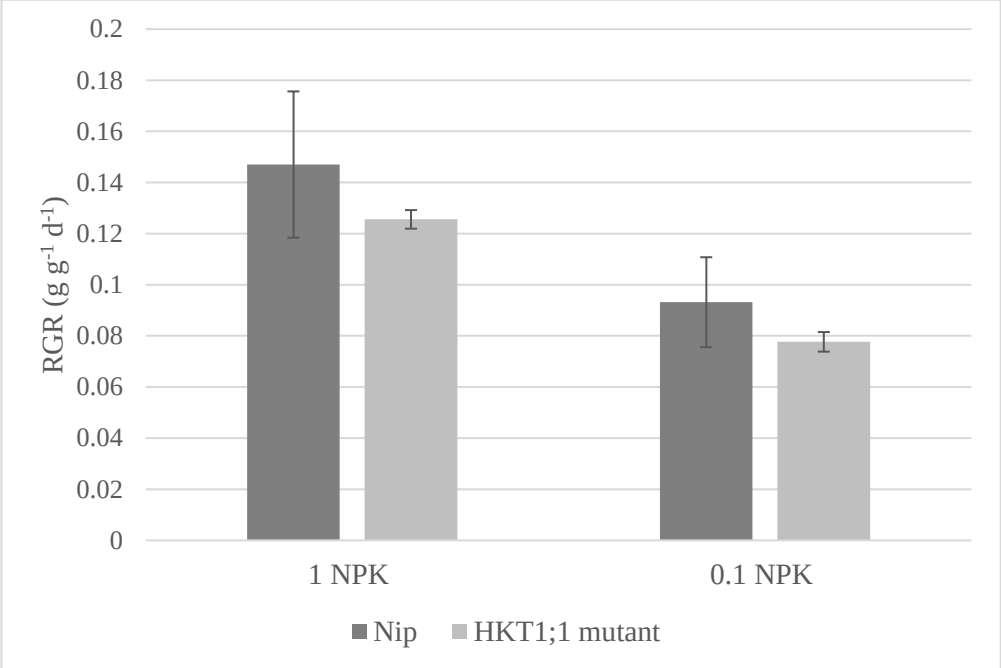

Figure 3. 7: Relative growth rates of mutant plants were lower than Nipponbare plants under 1 NPK and 0.1 NPK conditions. Error bars: SE (n=9 HKT1;1 mutant, n=5 Nip).

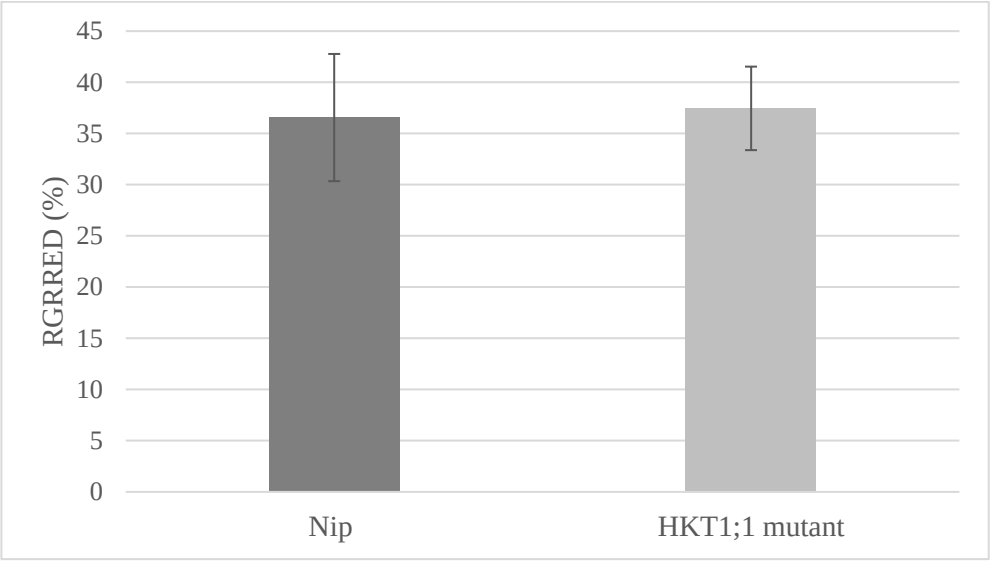

Figure 3. 8: RGR reduction shows no difference between Nipponbare and mutant plants.

3.3.5 Evaluation of candidate genes using CRISPR/Cas9 system

Two guides on the 1st exon of HKT1;4 were chosen for generating single knockout mutants, through small indels at either target site or by deleting the segment in between the targets. To produce a double knockout, 1 guide targeting the 1st exon of HKT1;4 and one targeting the 2nd exon of HKT1;1 were designed to simultaneously disrupt these two genes by deleting the region in between the targeted sites (Fig 3.9).

To make level 1 constructs, gRNA scaffolds were amplified and the expected sizes of 140 bp or 141 bp depending on the gRNA length were observed (Figure 3.10a). Level 1 constructs were tested by diagnostic digestions and bands of correct sizes were observed (Figure 3.10b). Level M constructs were also confirmed by diagnostic restriction digests (Figure 3.11). The structure of the final construct is shown in Figure 3.12.

A)

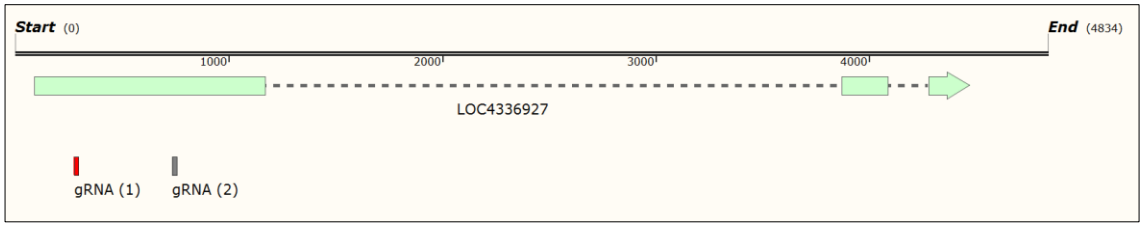

B)

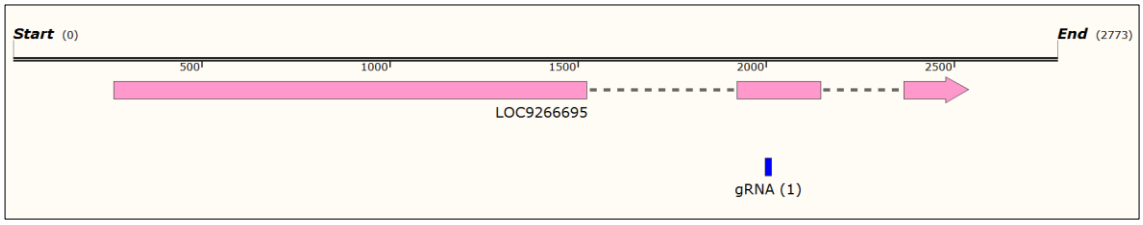

C)

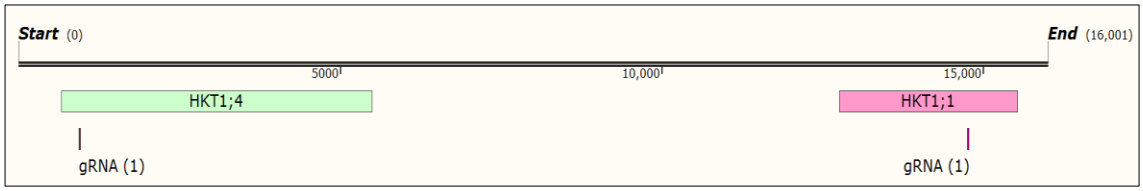

Figure 3. 9: Graphical overview illustrating the exon-intron structure of A) HKT1;4, B) HKT1;1. Red and grey bars in (A) indicate target sites for HKT1;4. Blue bar in (B) indicates the target site of HKT1:1 when simultaneously targeted with HKT1;4. C) The location of the gRNAs used for double targeting within the 1st exon of HKT1;4 and 2nd exon of HKT1;1.

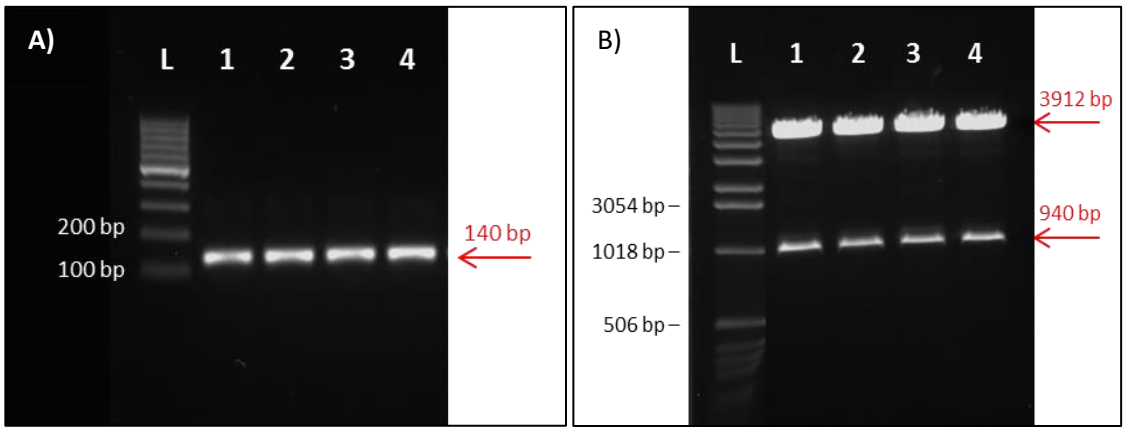

Figure 3. 10: (A) PCR products after scaffold amplification at expected size. From the left: (L) 100 bp DNA ladder, (1) TaU6-gRNA1-HKT1;1, (2) TaU6-gRNA2-HKT1;1, (3) TaU6-gRNA1-HKT1;4, (4) TaU6-gRNA2-HKT1;4. (B) Restriction digests for level 1 plasmids with *NcoI* + *SacI* shows bands at expected sizes. (L) 1 kb DNA ladder, (1) gRNA1 cassette-HKT1;1, (2) gRNA2 cassette-HKT1;1, (3) gRNA1 cassette-HKT1;4, (4) gRNA2 cassette-HKT1;4.

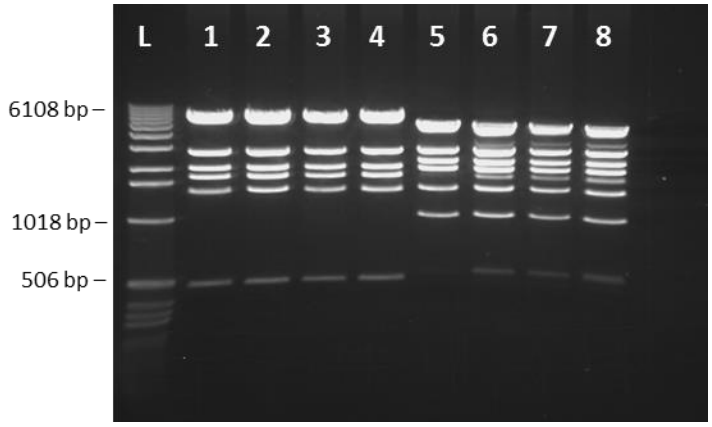

Figure 3. 11: Diagnostic restriction digests to confirm level M consctructs. Bands were observed at the expected sizes after digestion with a combination of *NcoI* + *SacI* (1-4) and *BamHI* + *NcoI* (5-8). (L) 1 kb DNA ladder. Level M constructs: (1 and 5) HKT1;1, (2 and 6) HKT1;4, (3 and 7, 4 and 8) HKT1;1 and HKT1;4.

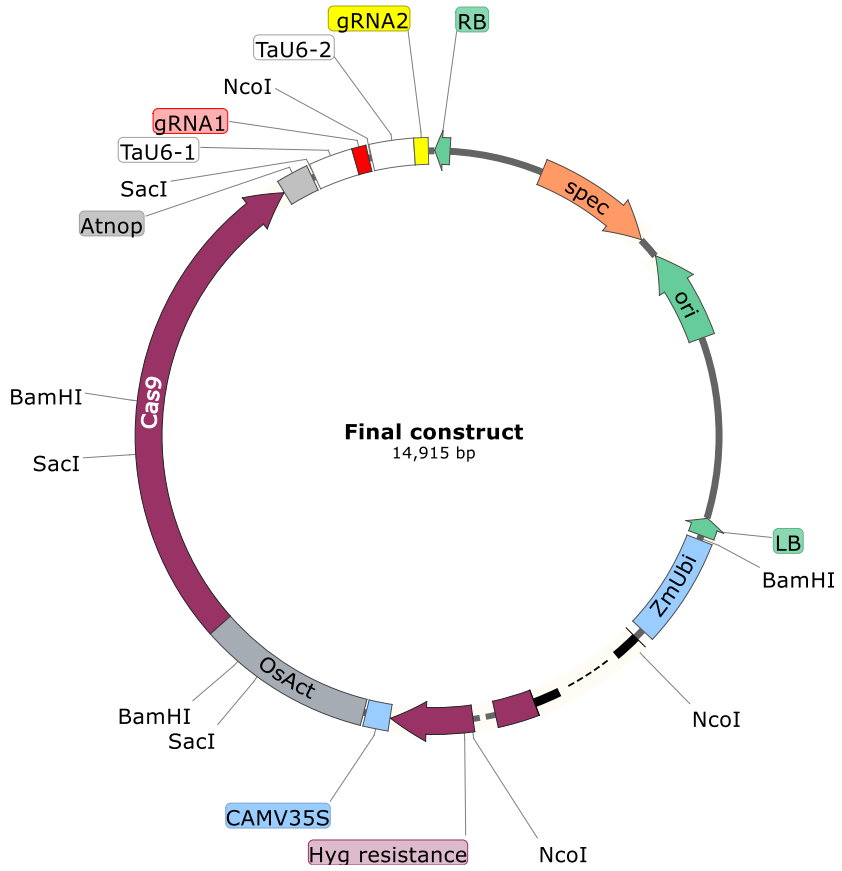

Figure 3. 12: Map of level M constructs. Abbreviations are as follows: RB for right border, spec for spectinomycin resistance, Ori for origin of replication, LB for left border, ZmUbi for *Zea mays* Ubiquitin promoter, Hyg for hygromycin phosphotransferase resistance, CAMV35S for Cauliflower mosaic virus 35S terminator, OsAct for *Oryza sativa* Actin promoter, Atnop for *Arabidopsis thaliana* nopaline synthase terminator, TaU6 for *Triticum aestivum* U6 promoter. Sites of *NcoI*, *SacI* and *BamHI* enzymes used for diagnostic digests.

3.3.5.1 Rice transformation

All steps to regenerate transgenic plants following the (Nishimura et al., 2006) protocol were successfully accomplished (Figure 3.13).

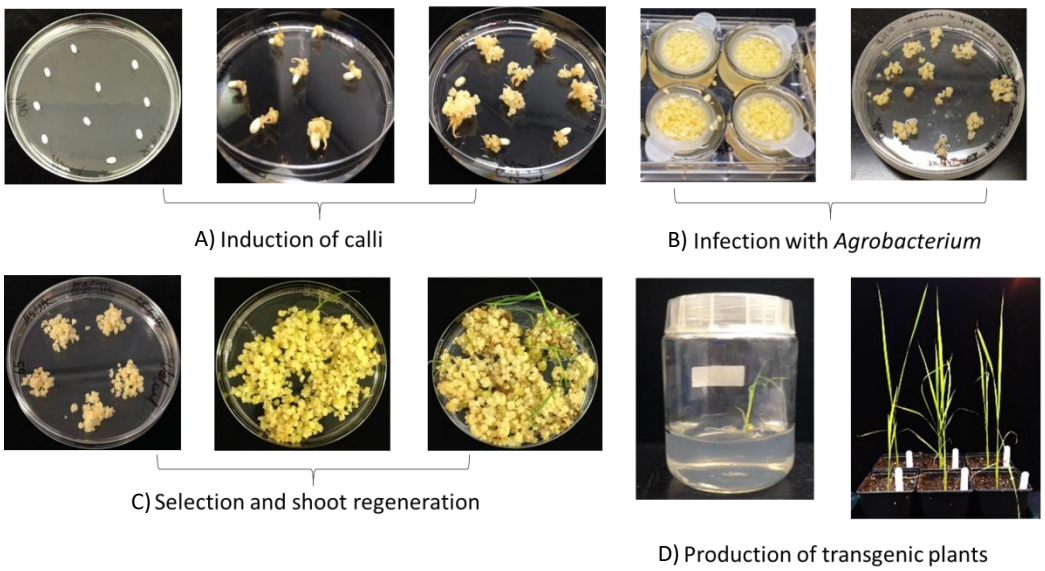

Figure 3. 13: Rice transformation and production of transgenic plants. A) Induction of calli from placing de-husked seeds (left) to calli formation (right) takes 4 weeks; B) Pre-culture of calli with *Agrobacterium* (3 days), inoculation of *Agrobacterium* and co-cultivation (3 days); C) Selection of transformed cells (4 weeks) and regeneration of shoot (4-6 weeks); D) Growth of transgenic plants in soil pots.

3.3.5.2 Identifying mutations in the T0 plants

For each construct 7 to 18 plants were regenerated (Table 3.4). Some of these were obtained from the same callus and could therefore originate from a single transformation event. 7 to 10 plants for each construct were tested by PCR and sequencing of cloned PCR products to identify mutations. In some lines, large deletions were detected by PCR. These are plants 7, 9 and 10 from construct OsHKT1;4 (Figure 3.14) and plant 3 from construct OsHKT1;1+OsHKT1;4 (Figure 3.16a). These deletions were confirmed by sequencing. Also, sequencing revealed a high rate of success in generating small deletions or insertions (Figures 3.15, 3.17, 3.18; Table 3.4). Sequencing results for the 2nd target site of OsHKT1;4

were not obtained, as this region was downstream the amplified region using PCR. Hence, mutation types for this plants are not confirmed before sequencing the 2nd target. Many of the sequenced cloned represented failed insertions of the PCR fragment into the plasmid. Therefore, there is often only one sequence trace available. Hence, in most cases it is not yet possible to tell whether a plant was homozygous or biallelic. However, wt sequences were recovered only in 4 out 19 plants, whereas mutant sequences were detected in 16 plants. Hence, the success rate of mutagenesis was about 80%. The biallelic cases are the most likely not to contain wt sequence. For others, more sequencing data are needed before testing plants for phenotypes. In the case of targeting OsHKT1;1 and OsHKT1;4 together, so far only plants 3, 4 and 5 carry mutant alleles in both genes. Unfortunately, the mutations found in OsHKT1;4 in these three plants result in the deletion of a single amino acid. This is unlikely a knockout mutation. However, it is worth sequencing more clones from these plants and from plants 2 and 6 to see if additional mutant alleles can be found.

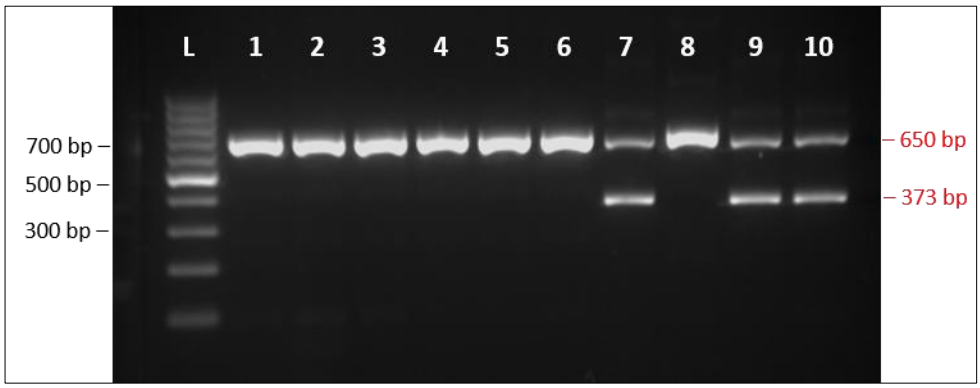

Figure 3. 14: PCR products for construct HKT1;4. (L): 100 bp DNA ladder. Numbers above lanes indicate plant IDs. The expected PCR product size for unmodified HKT1;4 was 650 bp. The expected deletion size from cuts at both target sites for HKT1;4 is 474 bp. Additional band in sample 7, 8 and 10 indicate deletion of 277 bp.

Figure 3. 15: Mutations in the1st target site of HKT1;4 in T0 generation. Sequence corresponding to the gRNA is shown in blue, PAM sequence in bold and underlined. Grey highlighted circumflex accents added to wild-type sequence indicate insertions occurred in these sites. Deletions and insertions are indicated by red dashes and red letters, respectively. Numbers on the left side indicate plant ID. Numbers on the right side indicate types of mutation and numbers of nucleotides involved, followed by number of sequence traces in brackets. Plants generated from the same callus are 7, 9 and 10. Plant 4 and 6 were excluded due to cloning artefact.

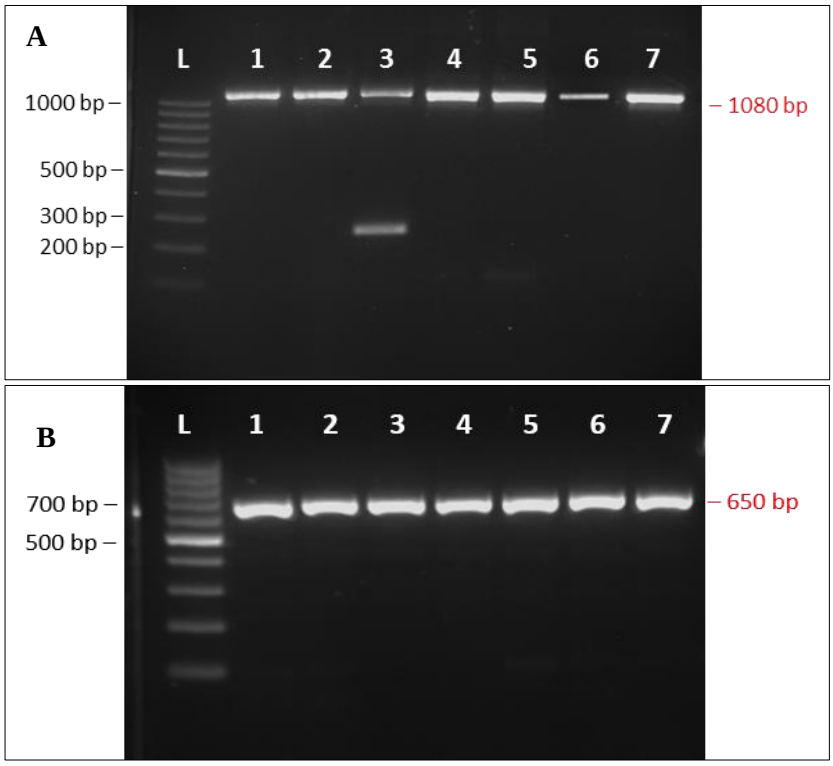

Figure 3. 16: PCR products for construct HKT1;1 and HKT1;4 using : A) HKT1;1 primers, B) HKT1;4 primers. (L): 100 bp DNA ladder, Numbers above lanes indicate plant IDs. The expected PCR product size for unmodified HKT1;4 was 650 bp. A) Additional band in sample 3 indicate deletion of around 830 bp.

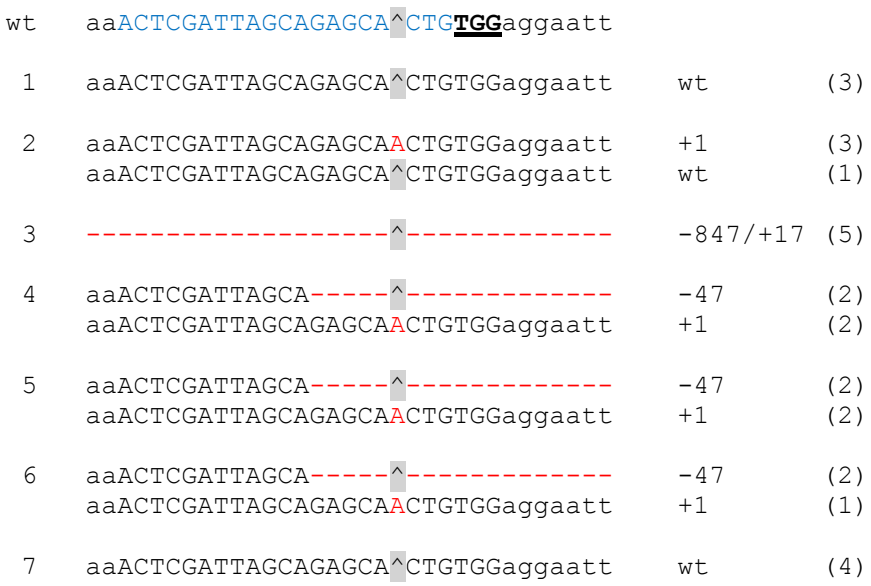

Figure 3. 17: Mutations in T0 generation of HKT1;1 gene simultaneously targeted with HKT1;4. Sequence corresponding to the gRNA is shown in blue, PAM sequence in bold and underlined. Grey highlighted circumflex accents added to wild-type sequence indicate insertions occurred in these sites. Deletions and insertions are indicated by red dashes and red letters, respectively. Numbers on the left side indicate plant ID. Numbers on the right side indicate types of mutation and numbers of nucleotides involved, followed by number of sequence traces in brackets. Plants generated from the same callus are 4 and 5.

```
wt   gaGAACACCTCCATCTCG^ACGGTGGacatgct
 3   gaGAACACCTCCATCT--^-CGGTGGacatgct    -3  (1)
 4   gaGAACACCTCCATCT--^-CGGTGGacatgct    -3  (2)
 5   gaGAACACCTCCATCT--^-CGGTGGacatgct    -3  (1)
 7   gaGAACACCTCCATCTCGAACGGTGGacatgct    +1  (1)
```

Figure 3. 18: Mutations in T0 generation of HKT1;4 gene simultaneously targeted with HKT1;4. Sequence corresponding to the gRNA is shown in blue, PAM sequence in bold and underlined. Grey highlighted circumflex accents added to wild-type sequence indicate insertions occurred in these sites. Deletions and insertions are indicated by red dashes and red letters, respectively. Numbers on the left side indicate plant ID. Numbers on the right side indicate types of mutation and numbers of nucleotides involved, followed by number of sequence traces in brackets. Plants generated from the same callus are 4 and 5. Plant 1, 2 and 6 were excluded due to cloning artefact.

Table 3. 4: Summary of HKT1;4 and HKT1;1+HKT1;4 mutants in the T0 generation. Number of plants generated for each construct, mutations in each target site and the overall mutant type. Small letters indicate plants generated from the same callus. (+) and (–) indicate insertions and deletions, respectively. Abbreviations are as follows: wt for wild type, bi for bi-allelic mutant, hom for homozygous mutants, het for heterozygous plants for wt/mutant, na for plants excluded due to cloning artefact. Question marks indicate uncertainty due to limited number of available sequences.

Construct	Plant	Callus	Site 1	overall
HKT1;4	1		wt	wt?
	2		-2	?
	3		-1	?
	4		na	
	5		+1	?
	6		na	
	7	a	-277, -16	bi
	8		-21	?
	9	a	-277, -16	bi
	10	a	-277	?
HKT1;1 double targeting	1		wt	wt
	2		+1, wt	het
	3		-847, +17 (= -830)	bi
	4	b	-47, +1	bi
	5	b	-47, +1	bi
	6		-47, +1	bi
	7		wt	wt
HKT1;4 double targeting	1		na	
	2		na	
	3		-3	?
	4	b	-3	?
	5	b	-3	?
	6		na	
	7		+1	?

3.4 Discussion

The physiological and genetic response of 294 rice varieties to low supply of multiple elements (NPK) in parallel was studied for the first time. In this GWAS study, a total of 84 QTLs was found to be associated with different traits under low NPK. Different GWAS outputs were observed among treatments and traits, with some overlapping. The vast majority of QTLs presented for low NPK traits was absent in the same traits under control condition, suggesting that these genetic variations were treatment specific. An important goal for crop breeders is to develop varieties that produce high yields with less fertilizer input. Identifying genes that are responsible for the differences in use efficiency of nutrients therefore has a potential to be exploited for crop improvement.

Of the 84 QTLs from the GWAS analysis, 16 SNPs were found to overlap with known QTLs related to N, P and K deficiency. Other SNPs from GWAS overlapped with QTLs related to other traits. These findings suggest that co-localisation between GWAS outputs and previous QTL studies serves as a good complementary approach, and they both can be exploited to improve desirable traits in crops. Furthermore, QTLs appearing in more than one trait and overlapping in different studies might indicate their potential importance as a target to for crop improvement.

Gene ontology enrichment analysis on the curated list of 1324 genes, revealed 109 GO terms that were statistically significantly overrepresented relative to their background abundance in the rice genome. Such a large number of overrepresented GO terms makes it inconvenient to identify genes as candidates based on their GO terms. Another issue is that results generated from different GO analysis tools could be incompatible and slightly different conclusions can be drawn by using different tools. Thus, GO analysis at best provides a complementary analysis to other analyses such as comparison of QTL overlap. Non-synonymous SNPs are found to cause alteration in amino acid sequences which can lead to phenotypic differences (Ramensky et al., 2002). Two nsSNPs were found within Wall-Associated Kinase OsWAK32 - OsWAK receptor-like protein kinase (LOC_Os04g24220). Wall-Associated Kinases (WAK) generally have a role in signal reception and sensing the extracellular environment while triggering intracellular signals

(de Oliveira et al., 2014). This might indicate the importance of these kinases as they might work as sensors for nutrient stress. Possibly, these kinases are disabled in some genotypes making them sensitive and less efficient to grow under low NPK. It was interesting to see that a good number of the genes containing nsSNPs encodes proteins with regulatory functions, such as OsWAK receptor-like protein kinase, OsFBT8 - F-box and tubby domain containing protein, OsSAUR28 - Auxin-responsive SAUR gene family member, which might explain the overrepresentation of GO terms of these categories. This could possibly indicate the importance of these genes as targets for crop improvement.

Two nsSNPs were found within the cation transporter OsHKT2;4. OsHKT2;4 selectively transports K under low external Na concentration , and its selectivity is dominant for K over Na (Sassi et al., 2012). Expression of OsHKT2;4 was down-regulated under K deficiency (Shankar et al., 2013) and it is expressed more in shoots than roots (Miyamoto et al., 2015) . A nearby gene, OsHKT2;1 has a role in uptake and allocation of Na in rice roots under K deficiency (Garciadeblás et al., 2003; Horie et al., 2007) and the expression in roots is induced by K starvation (Garciadeblás et al., 2003; Horie et al., 2001). Under low K provision, OsHKT2;1 expression was up-regulated (Ma et al., 2012; Takehisa et al., 2013) and shoot Na accumulation increased when OsHKT2;1 was overexpressed . Interestingly, these two Na transporters, OsHKT2;1 and OsHKT2;4, appeared as candidate genes in another GWAS study done by my colleague (Hartley, 2018), where only K was limiting. This supports the finding that K was a limiting factor when N, P and K were reduced in parallel. This might point to the importance of these two candidates in K use efficiency.

Since N and K were limiting in the growth experiment, identifying genes with roles in transport of N and K would be expected. The lack of P transporters in the candidate genes might be explained by the notion that P was not limiting in this study. On the other hand, the abundance of HKT transporters might be owed to K stress leading to the replacement of K with Na as useful element (Gattward et al., 2012; Subbarao et al., 1999), or might be due to K and N interaction. Na could stimulate taking up nitrate as it has been found that nitrate uptake is stimulated by cations with positive correlation between nitrate and cation uptake rates(Ivashikina and Feyziev, 1998). A study on wheat revealed that nitrate uptake was

similar with either Na or K as the only cation in the medium. However, accumulation of N in leaves was reduced by 75% with almost no Na accumulated when Na was the only ion in the medium (Barneix and Breteler, 1985).

A couple of candidate genes identified by GWAS were successfully manipulated using CRISPR/Cas9 system, and the success rate of mutagenesis was about 80%. Single knockout for HKT1;4 was successfully obtained. However, more genotyping is required to confirm the achievement of double knockouts for OsHKT1;1 and OsHKT1;4. Since more genes from the same family were identified later, simultaneous knock out can be performed using CRISPR/Cas9. Previous studies confirmed the efficiency of the system in producing simultaneous knockouts for multiple genes in rice and Arabidopsis (Ma et al., 2015). Transgenic plants produced in this study can be phenotyped to check their performance under low NPK conditions. As both genes play a role in reducing Na accumulation in the shoot under salt stress (Suzuki et al., 2016; Wang et al., 2015), knocking out these genes would be expected to have a positive effect by transporting Na to the shoot which can be used to replace K under K deficiency. If these plants showed better growth compared to wt plants, that might indicate their potential role in K use efficiency under low K conditions. Also, the produced seeds can be made available for researchers, which would be beneficial due to the lengthy process of producing these lines.

In conclusion, the GWAS study revealed QTLs linked to use efficiency of NPK for the first time. Some of these QTLs were novel and others overlapped with previously known QTLs for the use efficiency of N, P and K separately. Candidate genes that might be directly involved in the use efficiency of NPK such as N and K transporters were identified. Unexpectedly, several candidate genes identified were found to be involved in Na transport. Other genes not directly linked to NPK transport and distribution were also identified such as transcription factors and regulatory proteins involved in metabolic processes. This serves as a base for further characterisation of these genes which can then be targeted to improve crops under low NPK stress. A couple of candidate genes were successfully manipulated using the CRISPR/Cas9 system and mutant seed stock is now ready for testing.

Chapter 4: Towards improving mycorrhiza-dependent nutrient uptake by engineering the rice H+-ATPase (OsHA1)

4.1 Introduction

Genome editing techniques have been widely used lately to enhance desirable traits in plants and in crop production, and they have been gradually replacing the classical breeding methods which are lengthy and complicated (Sharma et al., 2017). There are several genome editing techniques that are used in the genetic manipulation of plants. These techniques vary in efficiency as different studies indicate. Zinc Finger Nucleases (ZFN) were the first generation editing tools, and they use chimerically engineered nucleases (Kamburova et al., 2017). Another technique is Transcription Activator-like Effector Nucleases (TALENs) which are used for selective and effective modification of target genomic DNA (Kamburova et al., 2017). Oligonucleotide-Directed Mutagenesis (ODM) uses an oligonucleotide that is similar to the target sequence although it has a single base pair change to achieve gene editing (Sauer et al., 2016). In early 2013, genome editing using CRISPR/Cas 9 system was first reported (Cong et al., 2013). According to (Song et al., 2016),the CRISPR/Cas 9 system is superior to the other genome editing technologies such as ZFNs and TALENs, mainly for the ease of construct design.-CRISPR/Cas 9 has been successfully applied in different plants such as Arabidopsis, tobacco and wheat (Feng et al., 2014; Jian-Feng et al., 2013; Jin et al., 2013; Qiwei et al., 2013; Xie and Yang, 2013).

One of the strategies plants adapted to nutrient limiting conditions is the creation of symbiotic relationships with microbes such as Arbuscular mycorrhizal (AM) fungi and rhizobia (Marschner and Dell, 1994; Smith and Read, 2010). AM symbiosis is known for enhancing the supply of not just water but also nutrients like nitrogen and phosphorus to the plant (Fellbaum et al., 2012; Leon, 2012). A large interphase between fungus and plant is

provided within root cells by the highly branched arbuscules, which are surounded by the periarbuscular membrane (PAM). This membrane separates arbuscules from the cytoplasm of the plant cells. P transport from the fungus to the plant is believed to be dependent on the proton gradient across the PAM (Krajinski et al., 2014). In rice, 70% of total phosphorus uptake owed to AM symbiosis (Yang et al., 2012), suggesting that AM has the potential to contribute significantly to crop yield and worldwide food security (Bethlenfalvay, 1992; Hu et al., 2009).

The superfamily of P-type ATPases plays a role in transporting ions and possibly phospholipids coupled with the breakdown of ATP (Baxter et al., 2003). They are named so because of the formation of phosphorylated intermediate by the enzyme during the catalytic cycle (Baxter et al., 2003; Morsomme and Boutry, 2000). In the rice genome there are 43 P-type ATPase genes belonging to 5 major groups (Baxter et al., 2003). H^+-ATPases are a subfamily of the P-type ATPase large family. These proton pumps drive the movement of ions and metabolites into and out of cells by creating an electrochemical H^+ gradient which is used to drive secondary transport (Morsomme and Boutry, 2000; Sondergaard et al., 2004). In addition to nutrient transport, they are found to be involved in stomatal opening, regulating biotic and abiotic stress responses, and growth (Duby and Boutry, 2009; Gong et al., 2010; Janicka-Russak et al., 2013; Schaller and Oecking, 1999; Zhao et al., 2000).

The stretched C-terminal region is a characteristic of H^+-ATPases compared to the other P-type ATPase groups (Duby and Boutry, 2009). A regulatory domain of 100 residues is located on the C-terminus and it has a role in regulating pump function and inhibiting enzyme activity (Duby and Boutry, 2009; Falhof et al., 2016). The general structure of H^+-ATPase in plants and fungi is shown in Figure 4.1. There are two activity states: inactive or also known as auto-inhibited state when the regulatory domain (R) is bound to the inhibitory domain in the membrane, and the active state when R domain is bound to a regulatory 14-3-3 protein and ATP degradation is tightly linked with proton pumping (Falhof et al., 2016; Werner, 2004). In plants, several phosphorylatable residues are known by which H^+-ATPases are regulated (Falhof et al., 2016). The phosphorylation of the penultimate residue, threonine (Thr), activates the binding of 14-3-3 regulatory proteins,

which results in a stable active state (Jahn et al., 1997). The binding of 14-3-3 protein prevents de-phosphorylation of the Thr residue leading to pump activation (Duby and Boutry, 2009; Falhof et al., 2016; Werner, 2004).

OsHA1 is a member of the rice plasma membrane H^+-ATPase gene family comprising 7 other members (Wang et al., 2014a). This gene is highly induced by mycorrhizal colonization and is expressed specifically in arbusculated root cells, serving as an energizer for the plant periarbuscular membrane by generating a proton gradient to support nutrient exchange between the plant and the fungus by secondary transporters (Gianinazzi-Pearson et al., 2000; Krajinski et al., 2002; Wang et al., 2014a). Under low P supply, overexpression of OsHA1 in *Medicago truncatula* resulted in improved plasma membrane potential, increased phosphate uptake and shoot P content (Wang et al., 2014a). *M. truncatula ha1*mutated plants were impaired in building the proton gradient and hence showed reduced uptake of phosphate. Moreover, under conditions of low P supply, the growth of the mutant plants was not enhanced by AM fungi (Krajinski et al., 2014).

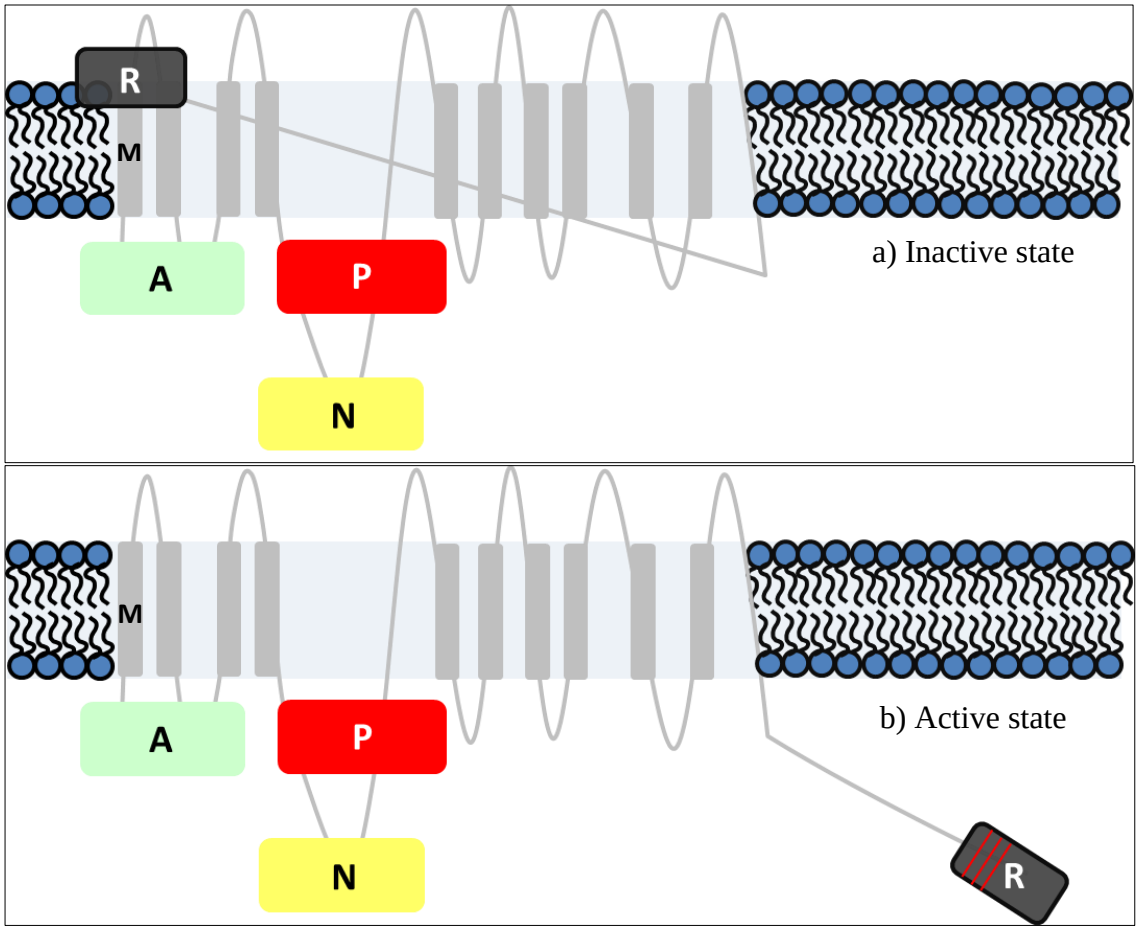

Figure 4. 1: General structure of H^+-ATPase showing two activity states modified after (Fuglsang et al., 2011). The phosphorylation domain (P) is shown in red, the nucleotide binding domain (N) in yellow, the actuator domain (A) in light green, the membrane spanning domains (M) in grey and the regulatory (R) domain in black. Of critical interest to this project is a) the inactive state when the R domain is linked to the membrane domain; b) the active state achieved when R domain is truncated, or when untruncated R domain is bound to a regulatory 14-3-3 protein. Red lines indicate cut sites to produce truncations.

Modification of pumping activity by truncating the C-terminal regulatory domain was reported in previous studies (Baunsgaard et al., 1996; Gévaudant et al., 2007; Regenberg et al., 1995; Speth et al., 2010). For example, transgenic *Nicotiana tabacum* plants lacking the regulatory domain (ΔPMA4) showed increased tolerance to salt stress and better root growth compared to wild type under saline conditions (Gévaudant et al., 2007). In another study, C-terminal deletions of *Arabidopsis thaliana AHA1* and *AHA2* genes expressed in yeast led to constitutive pumping activity, higher ATP affinity state and increased enzyme activity (Baunsgaard et al., 1996; Regenberg et al., 1995). A series of C-terminal deletions

in AHA2 ranging from 38 to 104 amino acids were produced and introduced to yeast where the orthologous gene PMA1 was knocked out. Truncated AHA2 of the sizes Δ66 to Δ92 amino acids resulted in optimal growth of yeast comparable to that when PMA1 was functional. Although lacking 38 amino acids did not affect the growth positively it was able to create a high affinity state of the enzyme. Compared to that, truncations of Δ50 amino acids and more significantly increased the enzyme activity (Regenberg et al., 1995). Conversely, yeast was not able to grow when transformed with the wild type *AHA2* as yeast lacks the regulatory 14-3-3 protein (Regenberg et al., 1995). To conclude, it was demonstrated that truncations in the regulatory domain of the C-terminus resulted in the active state of the enzyme and different sizes of deletions had variable effects on enzyme activity and growth of complemented cells.

The H^+-ATPase OsHA1 has been shown to be important for nutrient transfer in mycorrhizal symbioses (Wang et al., 2014a). However, when rice is inoculated with AM fungi under low P supply plants do not have a growth benefit compared to un-inoculated plants (Wang et al., 2014a). This is unlike *M. truncatula* where a significant increase in P uptake and shoot mass was observed (Krajinski et al., 2014; Wang et al., 2014a). By applying the same principle of introducing truncations to the C-terminus from previous studies, it might be that increasing OsHA1 activity could increase the proton gradient across the PAM, further increase the P uptake via arbuscules and therefore increase growth. This would then be directly relevant to farming in low-input agriculture. In this study, OsHA1 was manipulated using the CRISPR/Cas-9 system to manipulate the regulatory domain on the C-terminus to produce a constitutive pumping activity Considering the variable effects on pumping activity resulting from different sizes of truncations in previous studies, (Regenberg et al., 1995), three different sites upstream of the stop codon were targeted. By doing so, a series of transgenic plants differing in the length of the C-terminal truncation were generated. In many cases, the primary transformants showed mutation of both *OsHA1* alleles, i.e. were either biallelic or homozygous mutant. These plants are now ready for testing. It is expected that they show constitutive H^+ pumping activity across the periarbuscular membrane, enhanced phosphorus uptake and possibly increased growth in response to AM fungi.

4.2 Materials and methods

Using the CRISPR/Cas9 system, gRNAs were designed to target three regions within the C-terminus of the *OsHA1* gene. The three regions were at 64, 80 and 94 codons upstream of the stop codon. Codons 64 and 80 are in exon 19, whereas codon 94 is in exon 18. A total of four level M constructs were assembled to target *OsHA1* as follows (target site between brackets): construct OsHA1(94), OsHA1(80), OsHA1(64) and OsHA1(94)+(64), the latter with two target sites to increase the targeting efficiency. Detailed methods for construct assembly using Golden Gate cloning, rice transformation, and testing the T0 generation of mutant plants are explained in chapter 3 methods. Sequences of gRNAs used to target *OsHA1* (Supplementary Table 3.2). Details of plasmids used for construction of level 1 and level M plasmids (Supplementary Table 3.3). Primers used for gRNA scaffold amplification and for diagnostic PCR (Supplementary Table 3.4 and 3.5). For all constructs, the initial number of colonies sequenced from each plant was five. Ten colonies were tested for plant sample 1 and 2 only from each construct. However, some were excluded due to poor sequence quality.

4.2.1 Inoculation assays

Three OsHA1-truncated T0 plants were selected from each of the four constructs. As control, two plants carrying the construct but showing wild-type sequence in the T0 generation were chosen alongside with Nipponbare. Seeds from each T0 and control plant were germinated in sand for one week before 10 seedlings from each were transferred to a 1:1 mixture of sand and Terragreen (obtained from: http://oil-dri.co.uk). Under low P supply, half of the seedlings were inoculated with *Rhizophagus irregularis* (harvested from leek and chive co-cultures) and half without AM inoculation. In the glasshouse, plants were supplemented with light to provide a minimum of 12 h daylight; minimum 28 °C day, minimum 24 °C night temperature. A total of 30 OsHA1 truncated plants and 15 control plants were grown under each condition (+/– AM inoculation). These plants will be tested for constitutive pumping activity upon mychorrhizal colonisation, and for a positive effect on P uptake and growth.

4.3 Results

4.3.1 Construct assembly using Golden Gate cloning

The CRISPR/Cas9 system was used to create double stranded DNA breaks targeted to the region encoding the regulatory C-terminus of OsHA1. This aimed to introduce deletions or indel-based frame shift mutations resulting in the removal of a variable number of amino acids from the C-terminus of the protein. Three different sites upstream of the stop codon in the C-terminus were targeted in order to disrupt the regulatory domain which comprises the 100 amino acid from the end. Different target sites were selected to possibly result in variable effects on pumping activity as shown in previous studies where it was demonstrated that at least 50 amino acids should be truncated in order to see significant effects on the enzyme activity (Regenberg et al., 1995). The target sites in this study were approximate to the ones in the previous study. The three target sites were at -94, -80 and -64 codons upstream of the stop codon (Figure 4.2). In addition, simultaneous targeting at sites -94 and -64 was done to introduce a deletion of about 30 amino acids or simply increase the likelihood of successfully affecting at least one of the target sites (Figure 4.2). Successful cloning of level 1 and M constructs was verified by restriction digests (Figures 4.3 and 4.4). For plasmid map of level M construct see Chapter 3 (Figure 3.12).

Figure 4. 2: Graphical overview illustrating the location of the gRNAs within the region of the *OsHA1* gene encoding the C-terminus of the protein and their corresponding PAM sequences. Double targeting was done using both target sites 94 and 64.

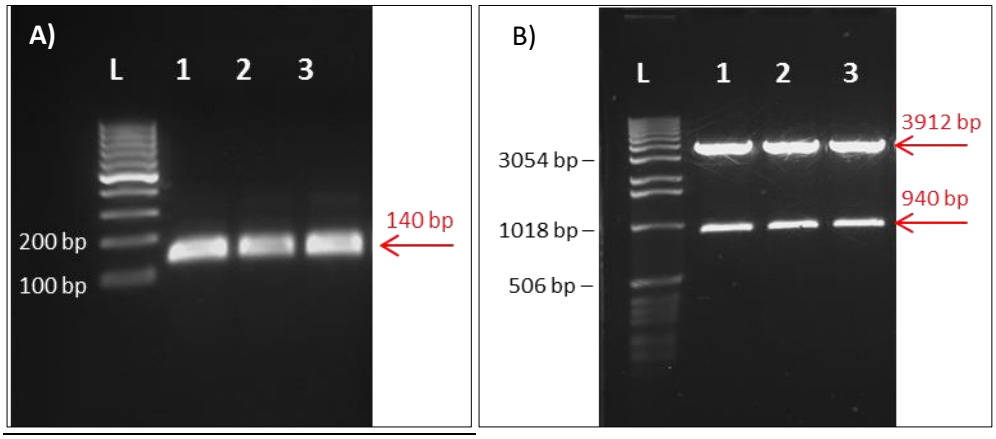

Figure 4.3: (A) PCR products after scaffold amplification at expected size. (L) 100 bp DNA ladder, (1) TaU6-gRNA1- OsHA1(94), (2) TaU6 -gRNA1-OsHA1(80), (3) TaU6-gRNA1- OsHA1(64). (B) Restriction digests with *SacI* + *NdeI* for level 1 plasmids show bands at expected sizes. (L) 1 kb DNA ladder, (1) gRNA1 cassette-OsHA1(94), (2) gRNA1 cassette-OsHA1(80), (3) gRNA1 cassette-OsHA1(64).

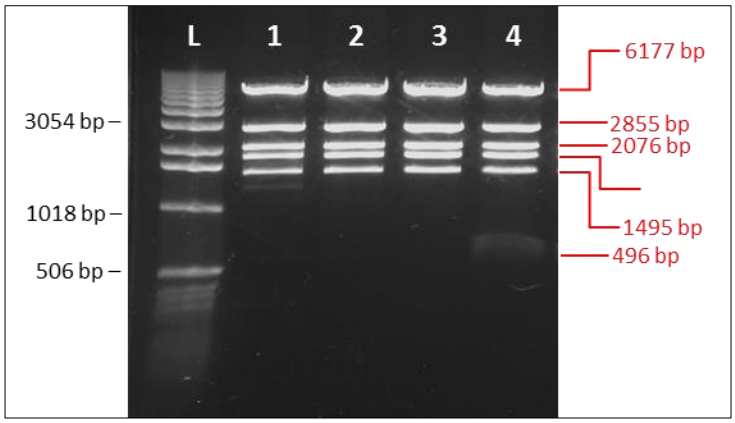

Figure 4.4: Diagnostic restriction digests to confirm level M constructs. Bands were observed at the expected sizes after digestion with a combination of *NcoI* + *SacI*. (L) 1 kb DNA ladder. Level M constructs: (1) OsHA1(94); (2) OsHA1(80); (3) OsHA1(64); (4) OsHA1(94)+(64).

4.3.2 Identifying indel mutations in the T0 plants

For each construct 10 to 30 plants were regenerated (Table 4.1). Some of these were obtained from the same callus and could therefore originate from a single transformation event. 10 to 12 plants for each construct were tested by PCR and sequencing of cloned PCR products to identify mutations. In only one of the lines a deletion large enough to be detected by PCR was found (Figure 4.5 and 4.6). However, sequencing revealed a high rate of success in generating small deletions or insertions (Figures 4.7 to 4.11; Table 4.1). About 80% of the plants did no longer carry the wt allele of OsHA1. Out of 42 plants tested a total of 33 appeared either homozygous or biallelic mutant. Targeting two sites simultaneously did not lead to a further increase in efficiency. Also, there was no obvious difference in the targeting efficiency or the type of mutation at the three sites. Most frequent were single base insertions or deletions (Table 4.1). Two plants appeared to be chimeric, i.e. more than two alleles were isolated.

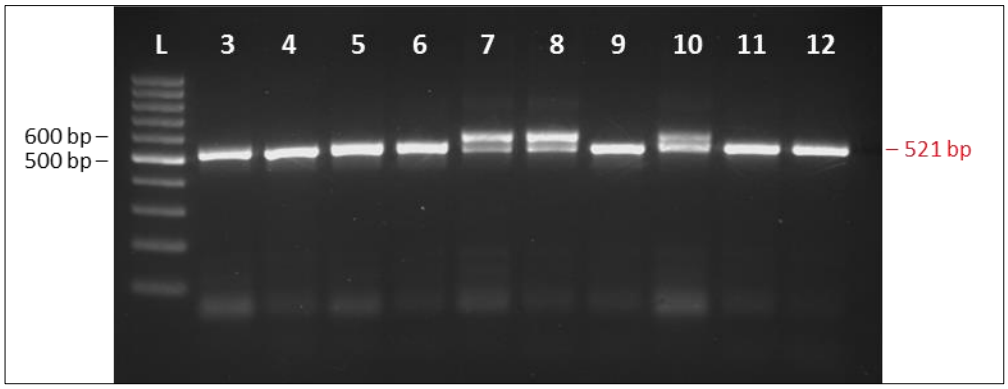

Figure 4.5: PCR products for construct OsHA1(94)+(64). (L) 100 bp DNA ladder. Numbers above lanes indicate plant IDs. Samples of plants 1 and 2 (not shown) gave the same result. The expected PCR product size for unmodified *OsHA1* was 521 bp. Additional slower moving bands in samples 7, 8 and 10 are most likely due to heteroduplex formation when single stranded PCR products of different sizes reannealed.

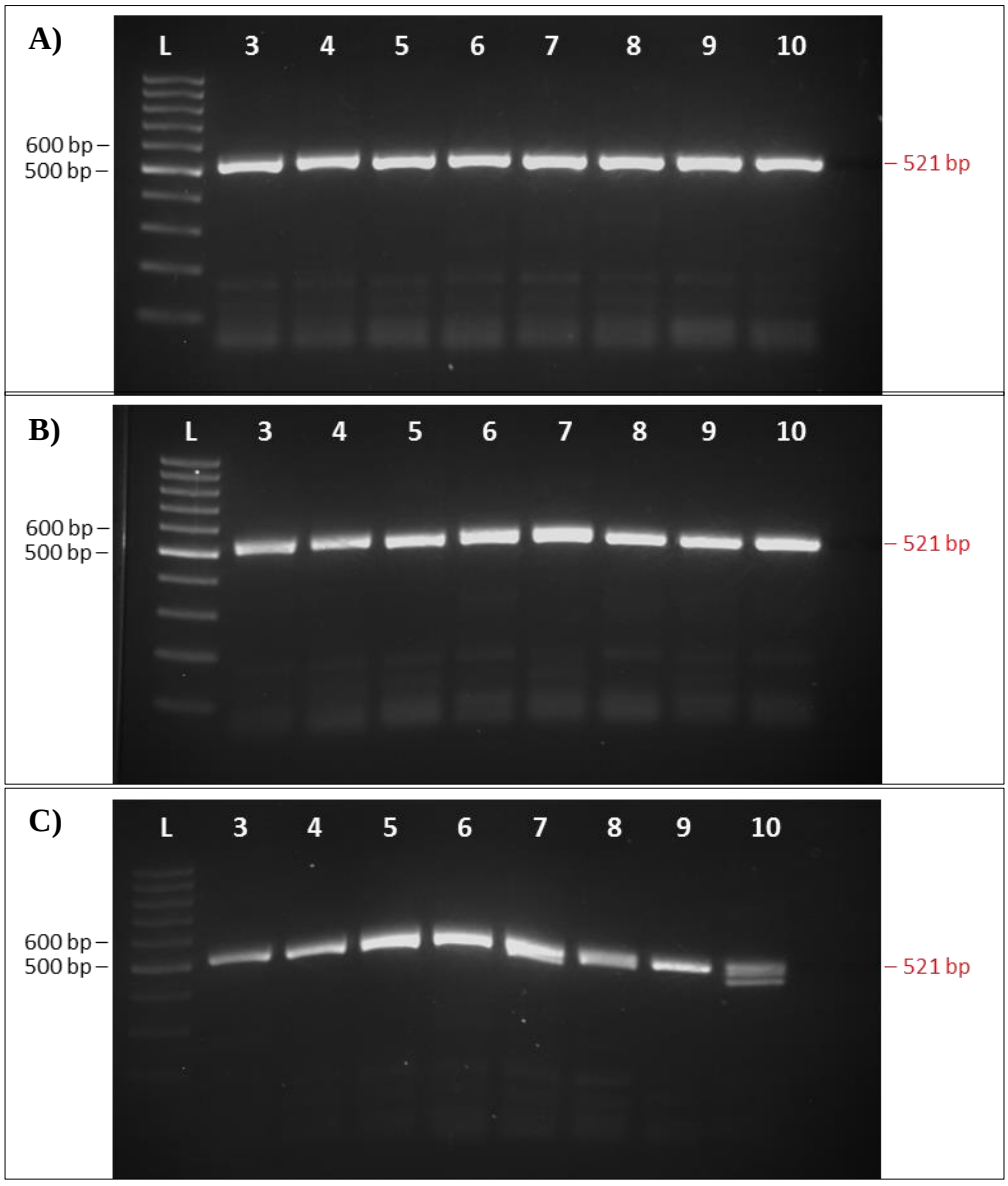

Figure 4.6: PCR products for construct: A) OsHA1(94); B) OsHA1(80); C) OsHA1(64). (L): 100 bp DNA ladder. Numbers above lanes indicate plant IDs. Samples of plants 1 and 2 (not shown) gave the same result. The expected PCR product size for unmodified *OsHA1* was 521 bp. C) The additional band in sample 10 represents a 54 bp deletion as confirmed by sequencing.

```
wt    acTAACCTTGTTATCAAT^G^^^^^^^ACAAGGttccagg

 1    acTAACCTTGTTATCAAT^GA^^^^^^ACAAGGttccagg   +1     (2)
      acTAACCTTGTTATCAAT^GT^^^^^^ACAAGGttccagg   +1     (5)

 2    acTAACCTTGTTATCAAT^G^^^^^^^ACAAGGttccagg   wt     (10)

 3    acTAACCTTGTTATCAAT^G^^^^^^^ACAAGGttccagg   wt     (3)

 4    acTAACCTTGTTATCAAT^G^^^^^^^ACAAGGttccagg   wt     (5)

 5    acTAACCTTGTTATCAAT^GT^^^^^^ACAAGGttccagg   +1     (4)

 6    acTAACCTTGTTATCAAT^GT^^^^^^ACAAGGttccagg   +1     (4)

 7    acTAACCTTGTTATCAAT^GT^^^^^^ACAAGGttccagg   +1     (2)
      acTAACCTTGTTAT----^-^^^^^^^-CAAGGttccagg   -6     (2)

 8    acTAACCTTGTTAT----^-^^^^^^^-CAAGGttccagg   -6     (3)

 9    acTAACCTTGTTATCAAT^GT^^^^^^ACAAGGttccagg   +1     (2)
      acTAACCTTGTTATCAATCG^^^^^^^ACAAGGttccagg   +1     (2)

10    acTAACCTTGTTAT----^-^^^^^^^-CAAGGttccagg   -6     (1)
      acTAACCTTGTTATCAAT^G^^^^^^^ACAAGGttccagg   wt     (4)

11    acTAACCTTGT-------^-ACTTAGTACAAGGttccagg   +7/-8  (3)

12    acTAACCTTGTTATCAAT^GA^^^^^^ACAAGGttccagg   +1     (4)
      acTAACCTTGT-------^-ACTAAGTACAAGGttccagg   +7/-8  (1)
```

Figure 4.7: Mutations at the 1st target site of OsHA1(94)+(64) in the T0 generation. Sequence corresponding to the gRNA is shown in blue, PAM sequence in bold and underlined. Grey highlighted circumflex accents added to wild-type sequence indicate insertions occurred in these sites. Deletions and insertions are indicated by red dashes and red letters, respectively. Numbers on the left side indicate plant ID. Numbers on the right side indicate types of mutation and numbers of nucleotides involved, followed by number of sequence traces in brackets. Plants generated from the same callus are 2 and 3; 5 and 6; 7, 8 and 10.

```
wt    acACGAGCAGCGCACACTA^CACGGGctgcagt

 1    acACGAGCAGCGCACACTATCACGGGctgcagt    +1    (2)
      acACGAGCAGC--------^----------agt    -18   (5)

 2    acACGAGCAGCGCACACTA^CACGGGctgcagt    wt    (10)

 3    acACGAGCAGCGCACACTA^CACGGGctgcagt    wt    (3)

 4    acACGAGCAGCGCACACTATCACGGGctgcagt    +1    (4)
      acACGAGCAGCGCACACTAACACGGGctgcagt    +1    (1)

 5    acACGAGCAGCGCACACT-^CACGGGctgcagt    -1    (4)

 6    acACGAGCAGCGCACACT-^CACGGGctgcagt    -1    (4)

 7    acACGAGCAGCGCACACTATCACGGGctgcagt    +1    (4)

 8    acACGAGCAGCGCACACTATCACGGGctgcagt    +1    (2)
      acACGAGCAG---------^----GGctgcagt    -13   (1)

 9    acACGAGCAGCGCACACTAACACGGGctgcagt    +1    (4)

 10   acACGAGCAGCGCACACTATCACGGGctgcagt    +1    (2)
      acACGAGCAGCGCACACTA^CACGGGctgcagt    wt    (3)

 11   acACGAGCAGCGCACACTATCACGGGctgcagt    +1    (3)

 12   acACGAGCAGCGCACACTATCACGGGctgcagt    +1    (4)
      acACGAGCAGCGCACACTA^CACGGGctgcagt    wt    (1)
```

Figure 4.8: Mutations at the 2nd target site of HA1(94)+(64) in the T0 generation. Sequence corresponding to the gRNA is shown in blue, PAM sequence in bold and underlined. Grey highlighted circumflex accents added to wild-type sequence indicate insertions occurred in these sites. Deletions and insertions are indicated by red dashes and red letters, respectively. Numbers on the left side indicate plant ID. Numbers on the right side indicate types of mutation and numbers of nucleotides involved, followed by number of sequence traces in brackets. Plants generated from the same callus are 2 and 3; 5 and 6; 7, 8 and 10.

Figure 4.9: Mutations in the T0 generation of HA1(94). Sequence corresponding to the gRNA is shown in blue, PAM sequence in bold and underlined. Grey highlighted circumflex accents added to wild-type sequence indicate insertions occurred in these sites. Deletions and insertions are indicated by red dashes and red letters, respectively. Numbers on the left side indicate plant ID. Numbers on the right side indicate types of mutation and numbers of nucleotides involved, followed by number of sequence traces in brackets. Plants 1 and 2 were generated from the same callus.

```
wt    acAAACCGGAAAGATTTC^^G^GAAGGGaagctcg

 1    acAAACCGGAAAG-----^^-^GAAGGGaagctcg   -6      (6)
      acAAACCGGAAAGAA---^^-^----------tcg   +1/-15  (2)

 2    acAAACCGGAAAG-----^^-^GAAGGGaagctcg   -6      (4)
      acAAACCGGAAAGAA---^^-^----------tcg   +1/-15  (2)
      acAAACCGGAAAGATTTC^^G^GAAGGGaagctcg   wt      (2)

 3    acAAACCGGAAAGATTTCTTG-------------g   +2/-13  (4)
      acAAACCGGAAAGAT---^^G^GAAGGGaagctcg   -3      (1)

 4    acAAACCGGAAAGATTT-^^-^GAAGGGaagctcg   -2      (4)
      acAAACCGGAAAGA----^^-^GAAGGGaagctcg   -5      (1)

 5    acAAACCGGAAAGATTTCTTG-------------g   +2/-13  (3)
      acAAACCGGAAAGAT---^-G^GAAGGGaagctcg   -3      (2)

 6    acAAACCGGAAAGATTTC^^GTGAAGGGaagctcg   +1      (4)
      acAAACCGGAAAGA----^^-^GAAGGGaagctcg   -5      (1)

 7    acAAACCGGAAAGATTTC^^GTGAAGGGaagctcg   +1      (3)

 8    acAAACCGGAAAGATTTC^^GAGAAGGGaagctcg   +1      (4)

 9    acAAACCGGAAAGATTT-^^-^GAAGGGaagctcg   -2      (4)
      acAAACCGGAAAGATTTC^^G^-AAGGGaagctcg   -1      (1)

10    acAAACCGGAAAGATTTC^^G^GAAGGGaagctcg   wt      (5)
```

Figure 4. 10: Mutations in T0 generation of HA1(80). Sequence corresponding to the gRNA is shown in blue, PAM sequence in bold and underlined. Grey highlighted circumflex accents added to wild-type sequence indicate insertions occurred in these sites. Deletions and insertions are indicated by red dashes and red letters, respectively. Numbers on the left side indicate plant ID. Numbers on the right side indicate types of mutation and numbers of nucleotides involved, followed by number of sequence traces in brackets. Plants generated from the same callus are 1 and 2; 3 and 5. The presence of more than two alleles in plant 2 indicate that it is chimeric.

```
wt    acACGAGCAGCGCACACTA^CACGGGctgcagt

 1    acACGAGCAGCGCACACTATCACGGGctgcagt    +1    (5)

 2    acACGAGCAGCGCACACTATCACGGGctgcagt    +1    (5)

 3    acACGAGCAGCGCACACTAACACGGGctgcagt    +1    (3)
      acACGAGCAGCGCACACTATCACGGGctgcagt    +1    (2)

 4    acACGAGCAGCGCACACTA^CACGGGctgcagt    wt    (5)

 5    acACGAGCAGCGCACAC--^CACGGGctgcagt    -2    (5)

 6    acACGAGCAGCGCACACTATCACGGGctgcagt    +1    (3)
      acACGAGCAGCGCACACT-^CACGGGctgcagt    -1    (1)

 7    acACGAGCAGCGCACACTAACACGGGctgcagt    +1    (5)

 8    acACGAGCAGCGCACACT-^CACGGGctgcagt    -1    (3)
      acACGAGCAG---------^----GGctgcagt    -13   (1)

 9    acACGAGCAGCGCACACTATCACGGGctgcagt    +1    (5)

 10   acACG--------------^----GGctgcagt    -18   (2)
      -------------------^--CGGGctgcagt    -54   (3)
```

Figure 4. 11: Mutations in T0 generation of HA1 (64). Sequence corresponding to the gRNA is shown in blue, PAM sequence in bold and underlined. Grey highlighted circumflex accents added to wild-type sequence indicate insertions occurred in these sites. Deletions and insertions are indicated by red dashes and capital letters, respectively. Numbers on the left side indicate plant ID. Numbers on the right side indicate types of mutation and numbers of nucleotides involved, followed by number of sequence traces in brackets. Plants generated from the same callus are 1 and 2.

Table 4. 1: Summary of OsHA1 mutants in T0 generation. Number of plants generated for each construct, mutations in each target site and the overall mutant type. Small letters indicate callus with more than one plant generated from. (+) and (–) indicate insertions and deletions, respectively. Abbreviations are as follows: wt for wild type, bi for bi-allelic mutant, hom for homozygous mutants, chim for chimeric plants. Question marks indicate uncertainty due to limited number of available sequences.

Construct	Plant	Callus	Site 1	Site 2	overall
94+64	1		+1, +1	+1, -18	bi
	2	a	wt	wt	wt
	3	a	wt	wt	wt
	4		wt	+1, +1	bi
	5	b	+1	-1	hom?
	6	b	+1	-1	hom?
	7	c	+1, -6	+1	bi
	8	c	-6	+1, -13	bi
	9		+1, +1	+1	bi
	10	c	-6, wt	+1, wt	chim
	11		-1 (=7-8)	+1	hom?
	12		+1, -1 (=7-8)	+1, wt	bi
94	1	d	wt		wt
	2	d	wt		wt
	3		wt		wt
	4		+1, -7		bi
	5		+1, +1		bi
	6		+1, -1		bi
	7		+1, -1		bi
	8		+1		homo
	9		+1, -12 (=2-14)		bi
	10		+1, -1		bi
80	1	e	-6, -14 (=1-15)		bi
	2	e	-6, -14 (=1-15), wt		chim
	3	f	-3, -11 (=2-13)		bi
	4		-2, -5		bi
	5	f	-3, -11 (=2-13)		bi
	6		+1, -5		bi
	7		+1		hom?
	8		+1		hom
	9		-2, -1		bi
	10		wt		wt
64	1	g	+1		hom
	2	g	+1		hom
	3		+1, +1		bi
	4		wt		wt
	5		-2		hom

	6		+1, -1		bi
	7		+1		hom
	8		-1, -13		bi
	9		+1		hom
	10		-18, -54		bi

4.3.3 Protein truncations

The introduction of insertions and deletions in the mutant plants resulted in premature stop codons and thereby different degrees of truncation at the C-terminus of the protein (Figure 4.12). These range from 32 to 92 amino acids lost. In some cases only minor changes are produced, e.g. loss of two amino acids due to the deletion of 6 bp. Three plants from each construct with different truncation sizes were selected for phenotyping (highlighted in yellow in figure 4.12). As control, two plants carrying the construct but showing wild-type sequence in the T0 generation were chosen alongside with Nipponbare. Seeds from T0 plants were obtained. A total of 30 OsHA1 truncated plants and 15 control plants were grown under each condition: (-/+AM inoculation) with low P supply. Total number of plants used in both conditions including control and truncated plants is 90. These plants will be tested for constitutive pumping activity upon mychorrhizal colonisation under low P conditions, and for the positive effect on P uptake and growth (plant mass).

Figure 4. 12: C-terminal truncations expected in the different mutant lines. Numbers between brackets indicate construct name, followed by plant ID and numbers of amino acids deleted from the original sequence of OsHA1. Small a and b letters correspond to different protein truncations in the same plant in a biallelic situation. The numbers on the right end of each line indicate the length of the predicted protein, including C-terminal variation caused by reading frame shift. Grey highlight indicates amino acids identical to the original sequence. Plants lines labelled in red were selected for phenotyping.

4.4 Discussion

In my study, about 80% of the plants did no longer carry the wt allele of *OsHA1*. Out of 42 plants tested a total of 33 appeared either homozygous or biallelic mutant. This is in an agreement with other studies where the high efficiency of the CRISPR/Cas 9 system was reported. A mutation rate of 85.4% with biallelic and homozygous mutations was obtained when CRISPR/Cas9 with optimised components was used in rice (Ma et al., 2015). Furthermore, the CRISPR/Cas9 system was efficient to produce simultaneous knockouts for multiple genes in rice and Arabidopsis (Ma et al., 2015). This system was also efficient to produce large deletions in rice chromosomes up to 245 Kb (Zhou et al., 2014). CRISPR/Cas9 targeting 11 rice genes revealed that it is specific, efficient and produces heritable mutations (Zhang et al., 2014b). The genotypes obtained in T0 generation indicated that the CRISPR/Cas9 system was effective as editing occurred even before the first cell division in more than half of cells. Also homozygous mutants were obtained in the T0 generation and stably inherited to the next generation following Mendelian genetics (Zhang et al., 2014b). Another study on rice demonstrated the high efficiency of CRISPR/Cas9 system when targeting two genes, CAO1 and LAZY1, where the efficiency of producing mutants in the T1 generation was 83.3 % and 91.6%, respectively, whereby 13.3% and 50% were bi-allelic mutants, respectively (Jin et al., 2013). Mutation frequency produced by CRISPR/Cas9 system on rice and Arabidopsis varied between 28 and 84 % (Feng et al., 2013). Also mutation frequencies in T0 wheat plants were about 65%, where 48.2% of all mutants (either homozygous, bi-allelic, or heterozygous mutants) were stably transmitted to the T1 generation with no additional mutations (Yang et al., 2017a).

Once the desired mutations are obtained in the transgenic plants it is desirable to eliminate the inserted CRISPR/Cas9 cassette by segregation in the following generation (T1). Continued presence of CRISPR/Cas9 would increase the likelihood of Cas9 cutting the genome at off-target sites, hence leading to unwanted mutations. It is expected that T0 plants are heterozygous for T-DNA insertion(s). Hence, upon selfing 25% of the T1 generation plants are expected to be transgene free (in case of single locus insertion of the T-DNA).

Another problem that we might encounter with the strategy to introduce frameshift mutations into the *OsHA1* gene is the potential degradation of mRNA by the nonsense mediated decay pathway. This may result from premature stop codons that are not in the last exon (Amrani et al., 2006; Stephanie and Allan, 2012). Therefore, it is vital to test the expression level of truncated *OsHA1* upon AM inoculation.

A question that remains to be answered is whether constitutive activation of the H^+-ATPase would be detrimental to cell function. However, given *OsHA1* in specifically expressed only in arbuscule-containing cells in the root cortex, we consider any negative effects on general plant health much less likely than in the case of a proton pump expressed throughout the plant. As different truncation sizes of the OsHA1 protein were produced in my experiment, they are expected to differently affect the enzyme activity. Therefore, there is the potential for some of the mutant lines performing better than others.
In conclusion, a large proportion of the T0 plants were successfully mutated using CRISPR/Cas9 technique resulting in different sizes of truncations which are believed to result in constitutive pumping activity, and in increased P uptake and potentially plant growth. If plants with truncated OsHA1 showed significant growth benefits this would be a novel achievement and could be exploited in low-input farming where nutrients, especially phosphorus, are not supplied in sufficient amounts.

Chapter 5: General Discussion

Producing nutrient efficient crops has become essential for food security. Efficient genotypes that perform well under nutrient stress of single elements have been identified in the past. However, in terms of observing morphological deficiency symptoms and interpreting the interaction between nutrients without confusion, reducing N, P and K in parallel rather than single elements provides a short cut to isolate efficient genotypes with direct relevance to reducing NPK fertilizer input. Although deficiency in all three elements does not resemble the conditions in agricultural fields and it might be that it is not very common to find one field that suffers from NPK stress, NPK fertilizers are heavily applied for optimum growth and yield. It should be noticed that reducing the three elements to the same level regardless the amount required by plants for each element is not ideal, as P was far less limiting than N and K in the initial growth medium used in this study. Therefore, it is fair to say that the genotypes identified here are more related to tolerance in low N and K conditions rather P limitation. In future studies one might reduce the different elements in parallel but to different extents taking into account the amount required by plants and the concentrations that are considered limiting for each element. It would be interesting to test these genotypes for yield and grain production, or other desirable traits. Information obtained from this study can be used to conduct similar studies in other crops that share a monophyletic origin with rice (Itoh et al., 2005).

Since other macro- and micro-elements were included in this study beside NPK, researchers interested in studying other elements and interaction between elements could use these results as a basis for future studies. Also, differences in shoot content of different elements between genotypes, could be potentially important not only to improve nutrient use efficiency and nutrient deficiency tolerance, but also to improve other important traits. For example, due to the role of K in response to biotic and abiotic stress, high K genotypes identified in this study could be tested for pest and disease resistance in rice and other crops (Amtmann et al., 2008; Wang et al., 2013). Also, these genotypes can be tested for drought and salinity tolerance as positive effect of K under salt stress has been reported (Cheng et

al., 2015; Gazipur, 2004; Sun et al., 2015). High N genotypes might be exploited to improve water use efficiency and tolerance to osmotic stress (Brueck, 2008; Brueck and Senbayram, 2009; Guo et al., 2008; Ren et al., 2015).

Identification of NPK efficient genotypes has a great potential to increase crop productivity with less input and to achieve sustainable agriculture. Previous work has explored nitrogen, potassium and phosphorus use efficiency in rice (Aluwihare et al., 2016; Duan et al., 2007; Yang et al., 2003), but the novelty of this study involves studying the effect of reducing NPK in parallel and identifying efficient genotypes for 3 major elements at the same time. Also, this study was done for the first time on diverse and large number of rice genotypes. The better performing genotypes identified under low NPK in this study are of breeders' interest due to their potential in reducing NPK fertilizer inputs and hence the cost of production. Also, can be tested under other conditions such as single or combined nutrient deficiencies, salt, drought and water stress conditions. Researchers might use these lines to apply genetic studies, and try to understand the physiological and molecular mechanisms behind the tolerance of these varieties under such conditions. These genotypes can be introduced to breeding programs as parental genotypes to generate more efficient lines under varying conditions. Genetic variation among rice cultivars has been reported for nitrogen (Ju et al., 2006; Namai et al., 2009; Samonte et al., 2006), potassium (Fageria et al., 2013b; Liu et al., 2009; Yang et al., 2003) and phosphorus (Fageria and Baligar, 1997; Fageria et al., 2013a, 2014; Wissuwa and Ae, 2001), and high levels of variation between inefficient and efficient cultivars have been reported. Such a diversity could be exploited in breeding programs to improve the use efficiency of crops. This can be achieved by selecting elite cultivars owing desirable traits for propagation, or producing new varieties by crossing. Additionally, identifying molecular markers through genome mapping techniques and testing a subset of lines for the allelic effect on genes controlling a particular trait can be used in marker assisted breeding to improve nutrient use efficiency and other traits. Plant breeding is important to ensure food security through the production of tolerant crops under varying environmental stresses. Rice with over 127,000 diverse accessions, has a great potential to be exploited by researchers and breeders to achieve sustainable agriculture and increase food security.

This GWAS study revealed novel and previously known QTLs for the use efficiency of N, P and K. Complex gene networks are controlling the use efficiency of NPK, starting from genes in the root responsible for efficient nutrient uptake, to genes responsible for the translocation of these nutrients from root to shoot, and the genes involved in the re-mobilization of the nutrients, and finally transcription factors and regulatory genes modulating cellular processes. As any of these genes can be potentially important, it is difficult to determine which genes are more likely to be responsible for the efficiency.

Therefore, genes identified from GWAS can be further characterised. Evaluating candidate genes from GWAS by producing knock out mutants is one of the approaches to functionally analyse genes. In some cases, where the presence of nsSNPs within the gene led to a premature stop codon and hence loss of function, this can resemble the approach of producing KO mutants. However, knock outs do not replace allelic variance. Another way to test candidates is by comparing a number of tolerant and sensitive genotypes to check if a certain allele is dominant. This can be done by using available databases for genomic variation such as rice variation map database (http://ricevarmap.ncpgr.cn). However, information is limited to a certain number of genotypes and information on a large number of the genotypes from RDP1 was not found. Alternatively, genes from high and low tolerance plants can be sequenced to check for allele differences. If variation were found, the interesting loci from one cultivar can be introduced to another cultivar by different approaches. However, validation of any QTL identified by GWAS is required before it is allowed to be used for marker-aided selection (MAS) which is applied in breeding programs (Collard and Mackill, 2008). Another approach is by direct allele swapping of small pieces using the CRISPR/Cas9 system combined with homology directed repair using variant alleles as template. Alternatively, novel techniques based on fusion of Cas9 with base editing enzymes open the possibility to introduce sequence variants more directly and without the need of homologous recombination, which is relatively inefficient in plants (Andrew, 2017).

Tolerant and sensitive lines rice accessions may differ in the level of expression of genes within the QTLs rather than amino acid sequence variation within the encoded proteins.

Therefore, future experiments should systematically analyse the expression level of the genes by QPCR, both under high and low nutrient supply and between tolerant and sensitive lines.

GWAS has contributed in increasing crop production by establishing associations with the aim of finding the genetic factors underlying important phenotypic traits such as grain yield and resistance to biotic and abiotic stresses. It also contributed in improving rice by increasing its nutrient efficiency, tolerance to nutrients deficiency and enhancing its adaptability to different environmental conditions (McCouch et al., 2016; Teng et al., 2017; Zhao et al., 2011). The GWAS of complex rice traits has improved over time due to the advancement of sequencing technologies which have utilized all the available SNP data to identifying genes. GWAS provides a high resolution as it is usually conducted in diverse panels, and results in narrower QTLs encompassing fewer genes compared to QTL mapping. This gives GWAS an advantage especially in the identification of novel QTLs as well as genes of potential importance. Overlap between QTLs and genes identified from GWAS with previous studies gives confidence and suggests the effectiveness of this method. Previous GWAS studies on different phenotypes revealed associations that were sub-species specific (Zhao et al., 2011), suggesting that it is important to re-run the GWAS based on sup-species and sub-population level, taking in account the population structure of *Oryza sativa* and the divergence between groups (Garris et al., 2005).

The CRISPR/Cas9 system was successfully applied to manipulate a couple of candidate genes identified by GWAS. Single knockout for HKT1;4 was successfully obtained. However, more genotyping is required to confirm the achievement of double knockouts for OsHKT1;1 and OsHKT1;4. Transgenic plants can be phenotyped under low NPK conditions. Since more genes from the same family were identified later, simultaneous knock out can be performed using CRISPR/Cas9. In addition, truncated *OsHA1* with variable deletion sizes was obtained. These plants are now being tested for the benefit of P uptake and growth under AM colonisation. Overall, a high mutant frequency of around 80% was obtained using the CRISPR/Cas9 system on all three targets, OsHKT1;1, OsHKT1;4 and OsHA1. It is interesting to note the mutation efficiency was very high even

though Cas9 was not codon-optimised for rice and the gRNAs were expressed from a wheat U6 promoter. Although obtaining large deletions using the CRISPR/Cas system was reported (Zhou et al., 2014), smaller indels are more frequent as reported in some studies where deletions ranging from 1-51 bp, and insertions of 1-5 bp with some point mutations were obtained (Feng et al., 2013; Jiang et al., 2013). In some cases, insertions and deletions occurred at the same time (Jiang et al., 2013). This might suggest that Cas9 does not cut simultaneously at both cut sites. A CRISPR study on *Petunia* showed that the frequency of obtaining deletions between the two cut sites of Cas9 was very low (Zhang et al., 2016). Therefore, the pattern of mutants obtained in my study are in general agreement with those reported by others. Considering the efficiency of the system, a smaller number of plants can be generated in future experiments. If plants with truncated OsHA1 showed significant growth benefits this would be a novel achievement and could be exploited in low-input farming where nutrients, especially phosphorus, are not supplied in sufficient amounts.

Appendix

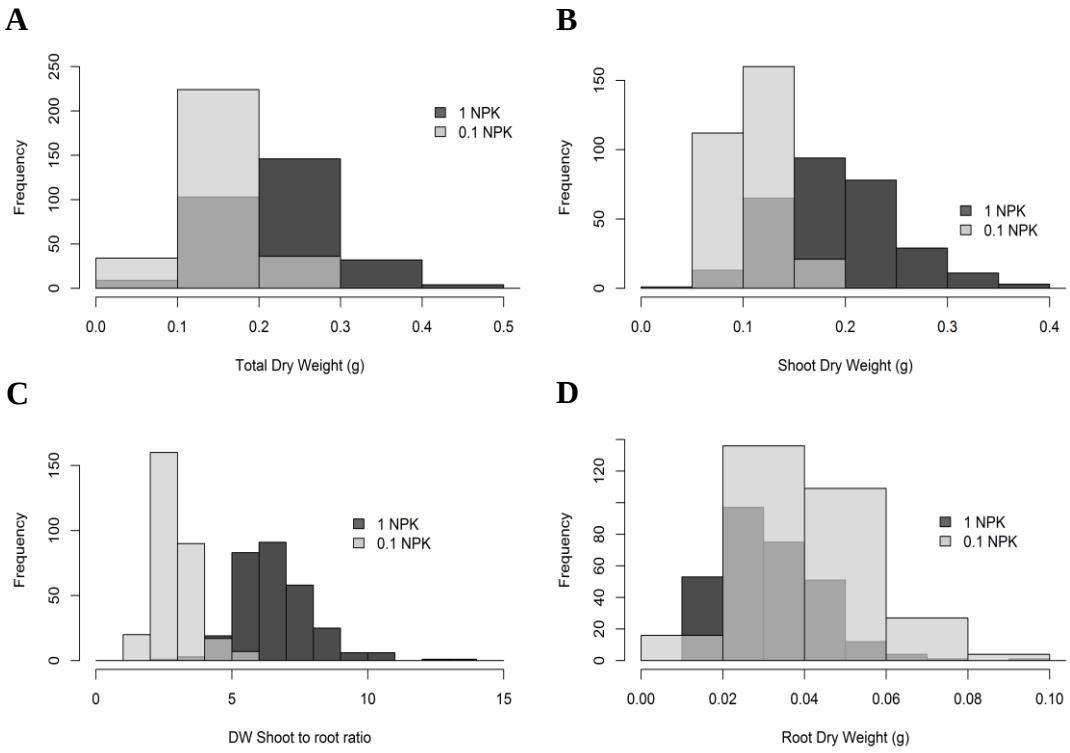

Supplementary Figure 2. 1: Average final dry weight distribution among 294 accessions grown in 1 and 0.1 NPK conditions. Total DW (A), shoot DW (B), shoot to root DW ratio (C) and Root DW (D) were significantly different in the two treatments. The significance was identified by two-tailed t-test ($P < 0.05$). The transparent colour indicates overlaps between the two treatments.

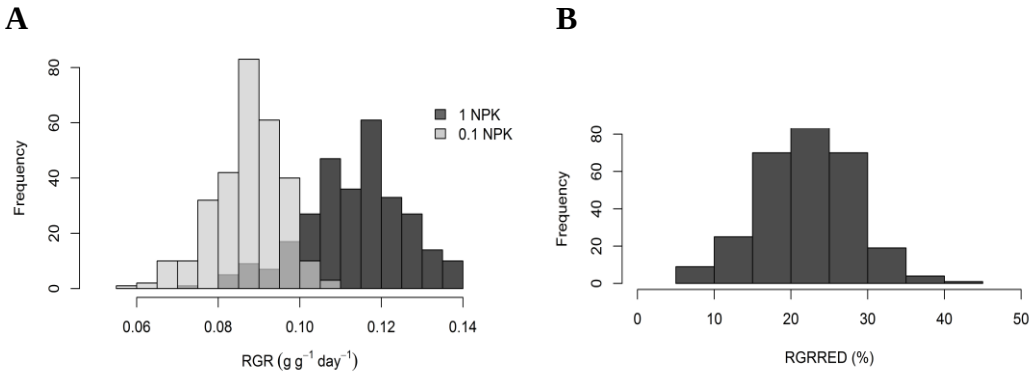

Supplementary Figure 2. 2: (A) Average relative growth rate distribution was significantly different in 1 and 0.1 NPK conditions (two-tailed t-test; P < 0.05). The transparent colour indicate overlaps between the two treatments. (B) Percentage of growth reductions in 0.1 NPK plants relative to control plants.

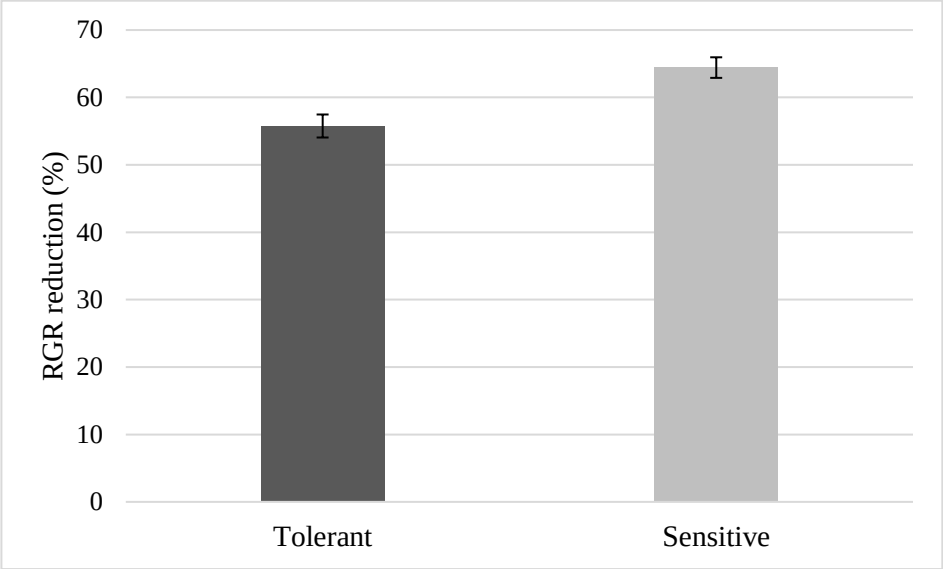

Supplementary Figure 2. 3: Average reduction in growth rates in tolerant lines was significantly smaller than sensitive lines under 0.01 NPK condition (Two-tailed t-test, *P* <0.05). Mean ± SE (n = 45 tolerant, 33 sensitive).

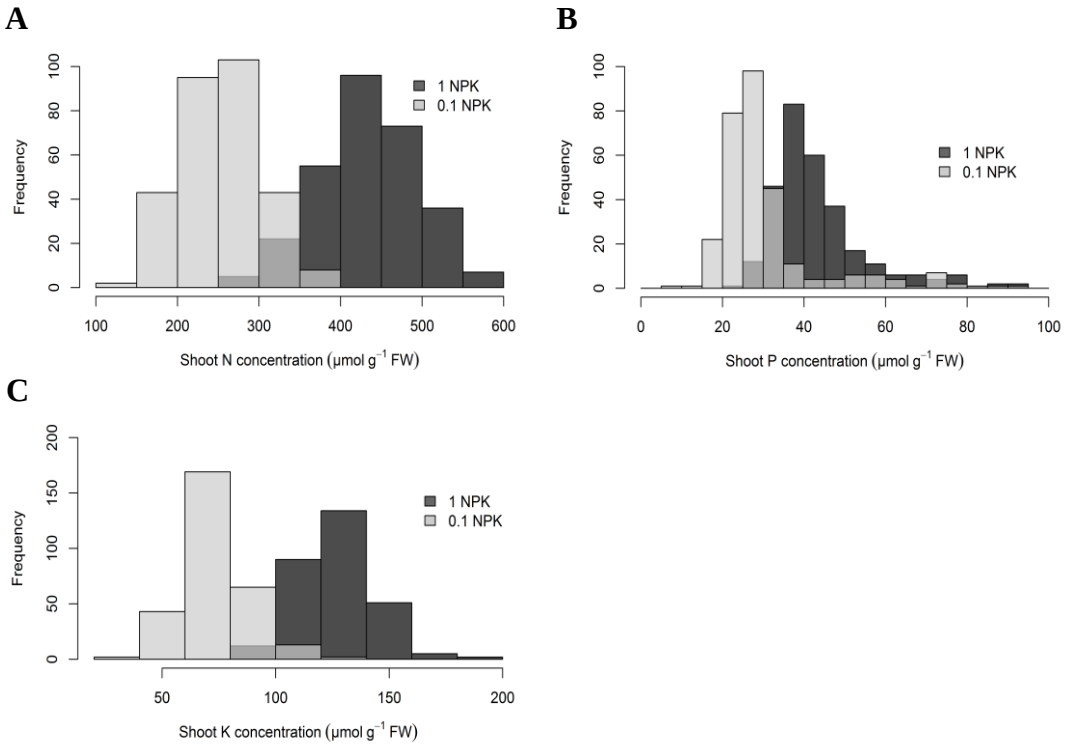

Supplementary Figure 2. 4: Shoot concentration of elements based on fresh weight in 0.1 NPK plants compared to 1 NPK plants. Significant reduction in: (A) average N concentration; (B) average P concentration; (C) average K concentration. The significance was identified by two-tailed t-test ($P < 0.05$). The transparent colour indicates overlaps between the two treatments.

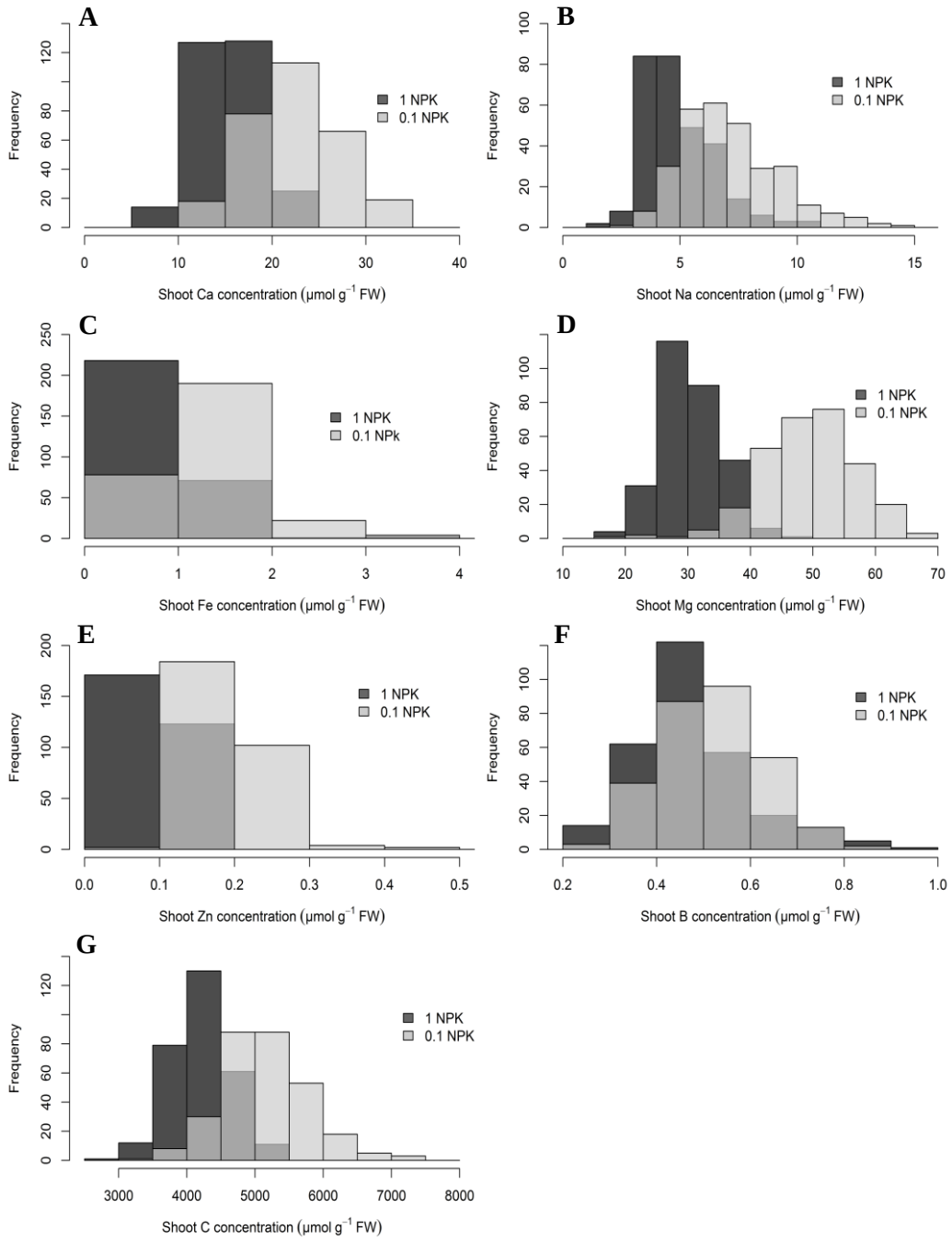

Supplementary Figure 2. 5: Shoot concentration of elements based on fresh weight in 0.1 NPK plants compared to 1 NPK plants. Significant increase in the average concentration of: (A) Ca, (B) Na, (C) Fe, (D) Mg, (E) Zn, (F) B, (G) C. The significance was identified by two-tailed t-test ($P < 0.05$). The transparent colour indicates overlaps between the two treatments.

Supplementary Table 2. 1: Top ten accessions for highest and lowest use efficiency for N, P and K under low treatment. Genotypes underlined overlapped between high and low treatment for low

PUE. Genotypes in italic overlapped between high and low treatment for high PUE. Genotypes in bold overlapped between high and low treatment for low KUE.

Efficiency	NUE	Genotype GSOR ID	PUE	Genotype GSOR ID	KUE	Genotype GSOR ID
High	70	301175	463	301163	110	301157
	67	301059	344	301180	109	301163
	64	301064	330	*301414*	100	301160
	62	301075	308	301157	96	301158
	62	301015	296	301199	89	301047
	62	301006	292	*301225*	84	301266
	62	301069	291	301160	80	301219
	62	301072	282	301067	80	301191
	61	301076	279	301266	80	301050
	61	301001	275	*301213*	78	301109
Low	36	301406	74	301210	42	**301343**
	36	301418	73	301205	42	301318
	36	301336	73	301179	42	301370
	36	301316	73	301189	41	**301353**
	35	301420	73	301212	41	301321
	35	301409	72	301005	40	301350
	34	301079	67	301079	39	301361
	34	301342	66	301206	39	301359
	33	301317	65	301138	39	301369
	32	301416	64	301100	36	**301360**

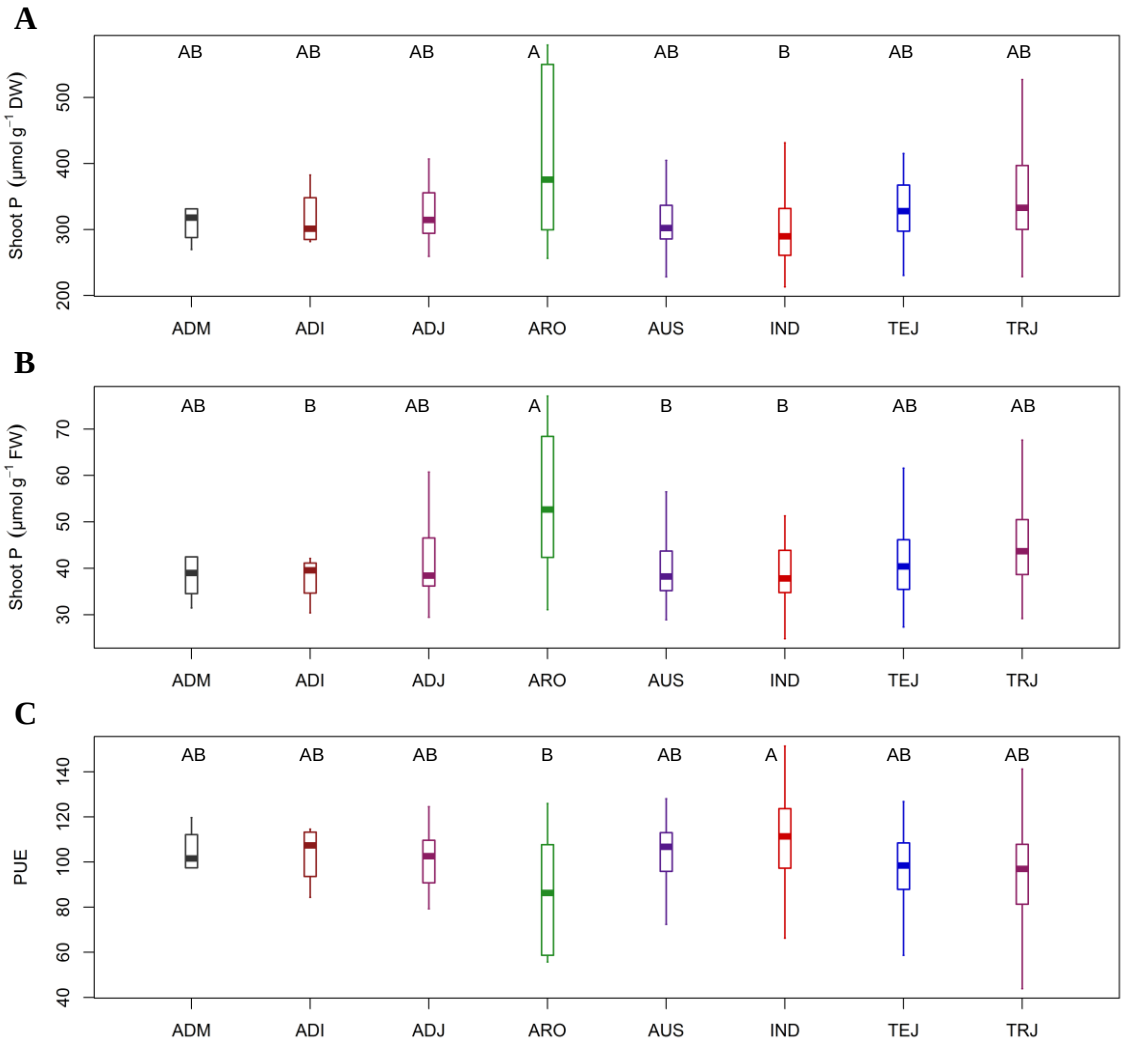

Supplementary Figure 2. 6: Means under control condition for: A) P concentration on DW basis; B) P concentration on FW basis; C) P use efficiency for each rice sub-population. Letters above boxplots denote statistically significant differences between sub-populations (Tukey's honest significant test HSD, $P<0.05$). Sub-population abbreviations are as follows: ADM for admixed, AUS for Australis, IND for Indica, ADI for Admixed Indica, ARO for Aromatic, TEJ for Temperate Japonica, TRJ for Tropical Japonica, and ADJ for Admixed Japonica.

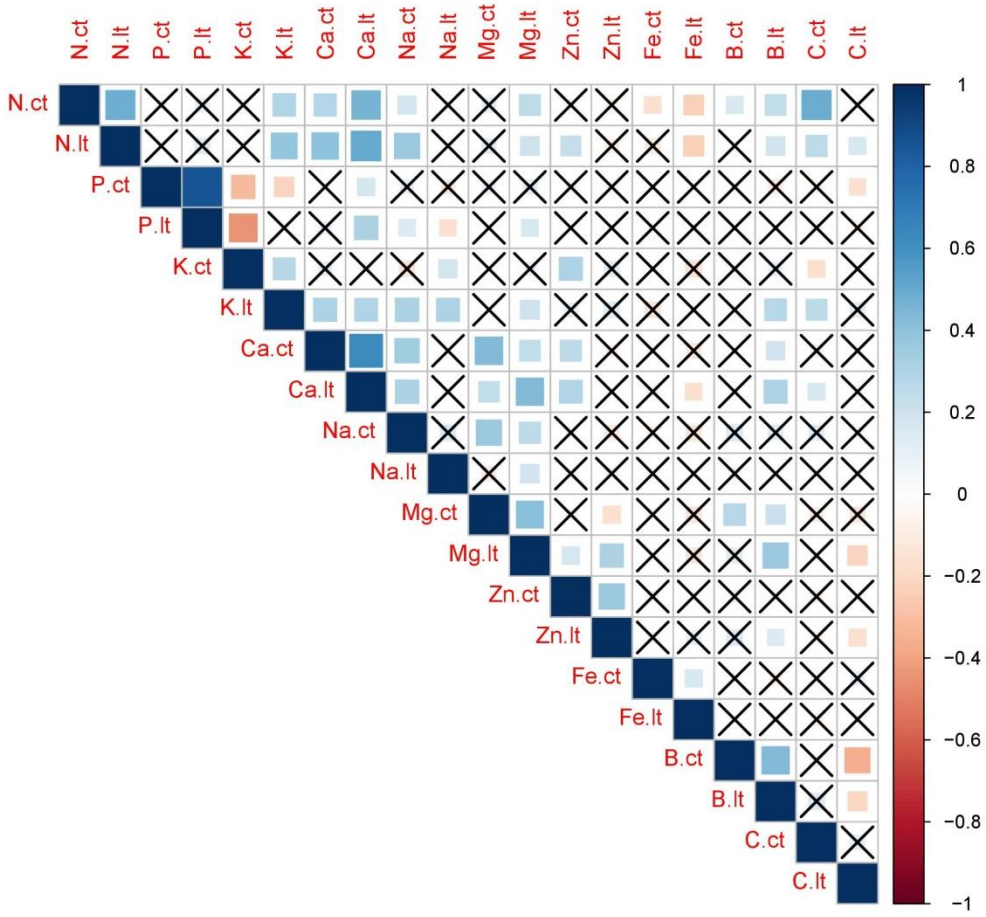

Supplementary Figure 2. 7: Correlation matrix summarising relationships between element concentrations on dry weight basis under 1 NPK and 0.1 NPK condition. Correlations with p-value > 0.01 are crossed. Abbreviations are as follows: CT for control treatment (1 NPK), LT for low treatment (0.1 NPK), N for nitrogen, P for phosphorus, K for potassium, Ca for calcium, Na for sodium, Mg for magnesium, Zn for zinc, Fe for iron, B for boron and C for carbon.

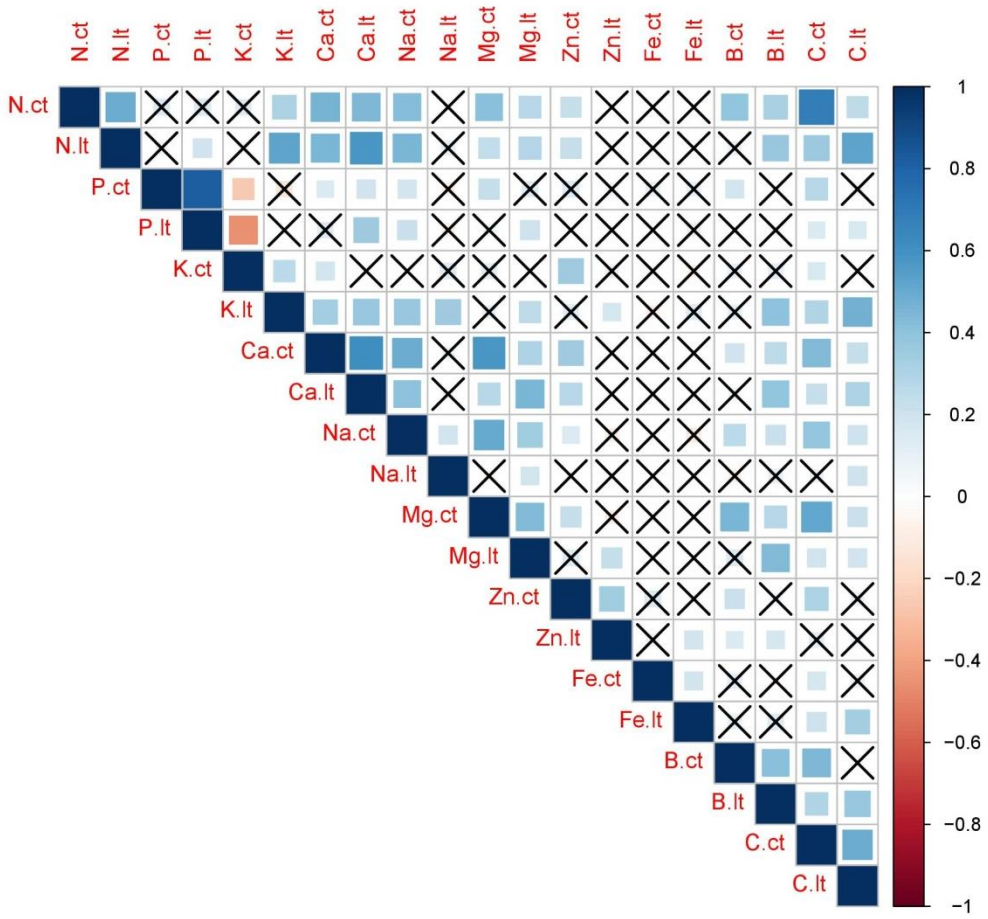

Supplementary Figure 2. 8: Correlation matrix summarising relationships between ion concentrations on fresh weight basis under 1 NPK and 0.1 NPK condition. Correlations with p-value > 0.01 are crossed. Abbreviations are as follows: CT for control treatment (1 NPK), LT for low treatment (0.1 NPK), N for nitrogen, P for phosphorus, K for potassium, Ca for calcium, Na for sodium, Mg for magnesium, Zn for zinc, Fe for iron, B for boron and C for carbon.

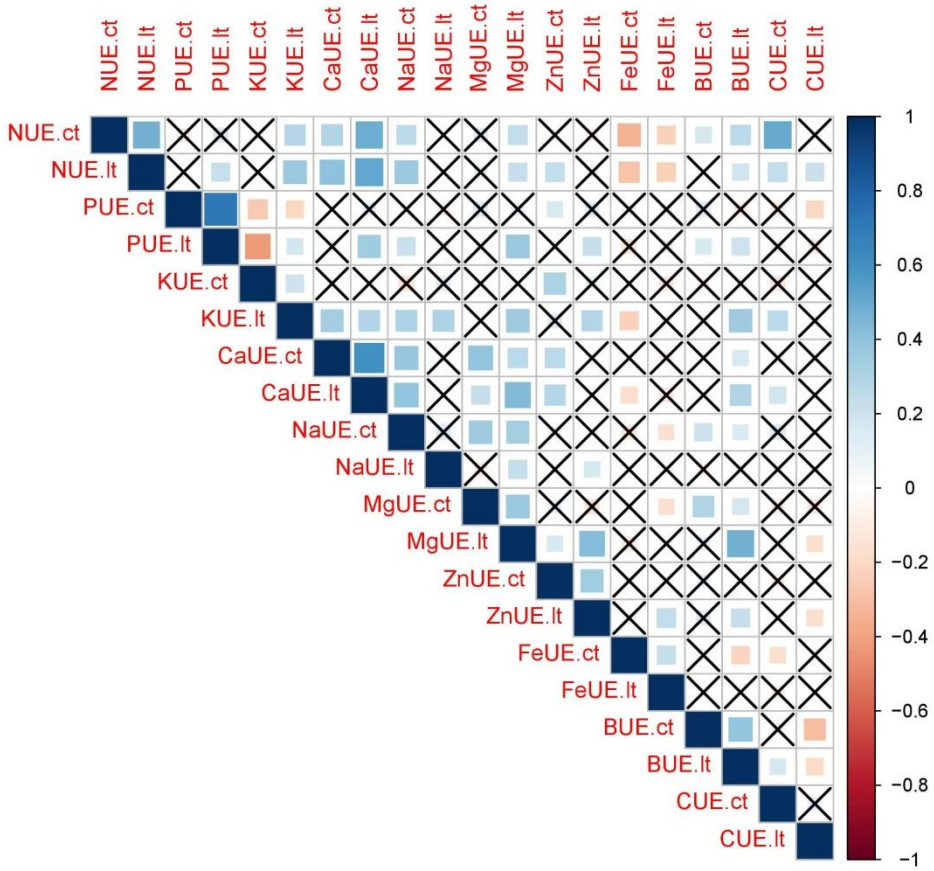

Supplementary Figure 2. 9: Correlation matrix summarising relationships between nutrient efficiency ratios under 1 NPK and 0.1 NPK condition. Correlations with p-value > 0.01 are crossed. Abbreviations are as follows: CT for control treatment (1 NPK), LT for low treatment (0.1 NPK), UE for nutrient use efficiency, N for nitrogen, P for phosphorus, K for potassium, Ca for calcium, Na for sodium, Mg for magnesium, Zn for zinc, Fe for iron, B for boron and C for carbon.

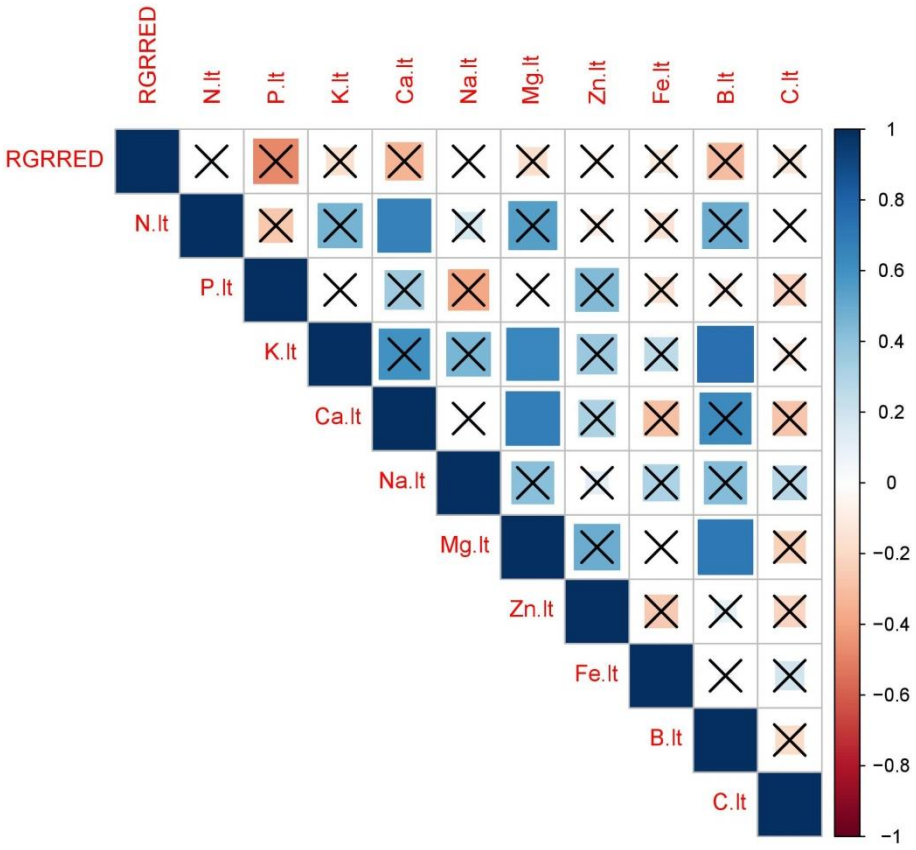

Supplementary Figure 2. 10: Correlation matrix summarising relationships between shoot element content and growth reduction for tolerant lines under 0.1 NPK condition. Correlations with p-value > 0.01 are crossed. Abbreviations are as follows: LT for low treatment (0.1 NPK), RGRRED for relative growth rate reduction, N for nitrogen, P for phosphorus, K for potassium, Ca for calcium, Na for sodium, Mg for magnesium, Zn for zinc, Fe for iron, B for boron and C for carbon.

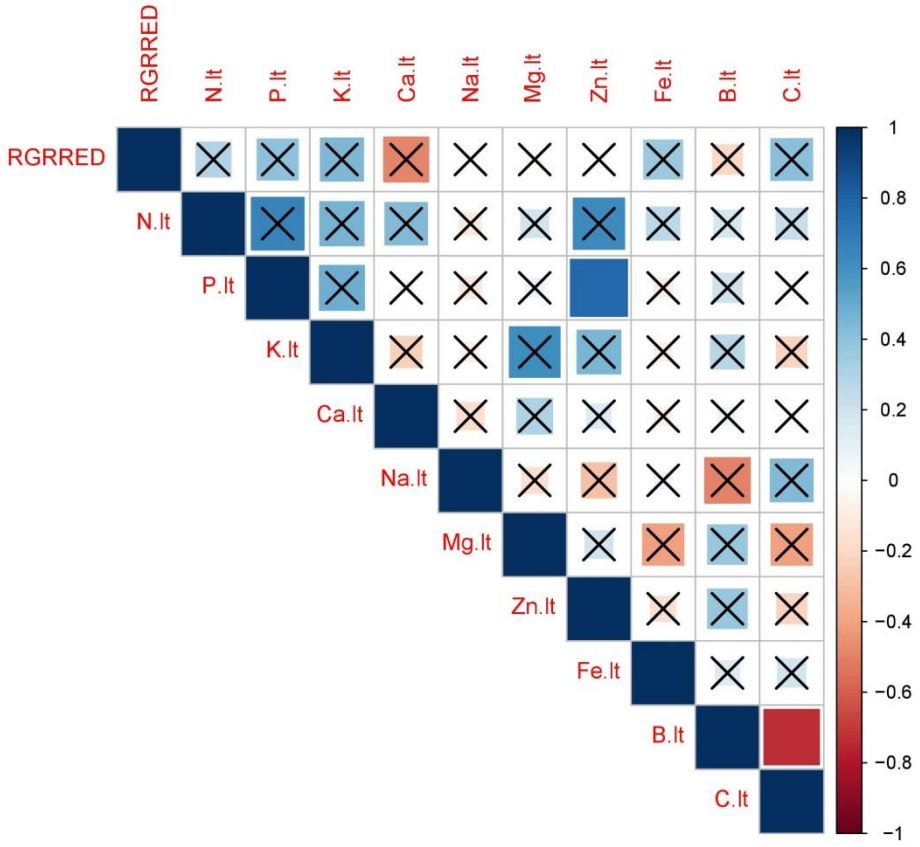

Supplementary Figure 2. 11: Correlation matrix summarising relationships between ion content and growth reduction for sensitive lines under 0.1 NPK condition. Correlations with p-value > 0.01 are crossed. Abbreviations are as follows: LT for low treatment (0.1 NPK), RGRRED for relative growth rate reduction, N for nitrogen, P for phosphorus, K for potassium, Ca for calcium, Na for sodium, Mg for magnesium, Zn for zinc, Fe for iron, B for boron and C for carbon.

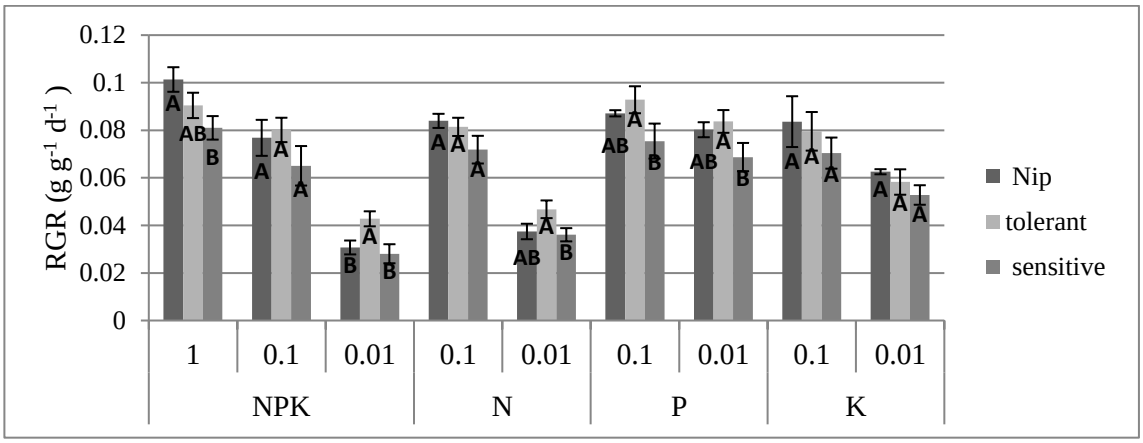

Supplementary Figure 2. 12: Average RGR based on genotype under varying NPK treatments. Mean ± SE (n = 3 Nip, 21 tolerant, 18 sensitive). Significance based on (Tukey's honest significant test HSD, P<0.05). The total number of plants in each treatment was 42 with 3 plants for each genotype (including 3 Nip, 7 tolerant and 6 sensitive).

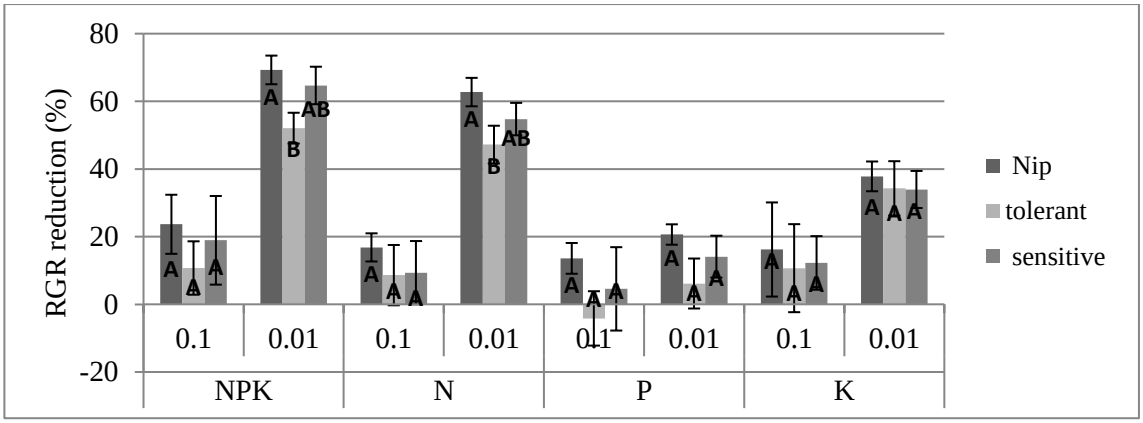

Supplementary Figure 2. 13: Percentage of growth reduction based on genotype under varying NPK treatments. Mean ± SE (n = 3 Nip, 21 tolerant, 18 sensitive). Significance based on (Tukey's honest significant test HSD, P<0.05). The total number of plants in each treatment was 42 with 3 plants for each genotype (including 3 Nip, 7 tolerant and 6 sensitive).

Supplementary Table 3. 1: Primers used for genotyping mutant HKT1;1.

Primer name	Primer sequence（5'-3'）
OsHKT1;1-F	GATCCCGCAGATTCTAGCAG
OsHKT1;1-R	GGCAATTCGGATTTTCAGTG
Rice Actin1-F	TATCCTCCGGTTGGATCTTG
Rice Actin1-R	AGCAATTCCAGGAAACATGG

Supplementary Table 3. 2: Sequences of the (20 nt) gRNAs for each target gene and their corresponding (PAM) sequence.

Target	gRNA 1	PAM	gRNA 2	PAM
HKT1;4	GAACACCTCCATCTCGACGG	TGG	GCCGACGAACGAGAACATGG	TGG
HKT1;1 and HKT1;4	ACTCGATTAGCAGAGCACTG (HKT1;1)	TGG		
HKT1;1 and HKT1;4	GAACACCTCCATCTCGACGG (HKT1;4)	TGG		
OsHA1(97)+(65)	TAACCTTGTTATCAATGACA	AGG	ACGAGCAGCGCACACTACAC	GGG
OsHA1 (97)	TAACCTTGTTATCAATGACA	AGG		
OsHA1 (80)	AAACCGGAAAGATTTCGGAA	GGG		
OsHA1 (65)	ACGAGCAGCGCACACTACAC	GGG		

Supplementary Table 3. 3: Plasmids from the Golden Gate cloning toolbox for plants used in plasmid construction. P with a number indicates the position of level 1 plasmids in the final level M construct. Abbreviations are as follows: UTR for untranslated region, Os for *Oryza sativa*, At for *Arabidopsis thaliana*, Zm for *Zea mays*, Ta for *Triticum aestivum*. Sp for *Streptococcus pyogenes*, CAMV = Cauliflower mosaic virus.

Plasmid Produced	Acceptor	Donor Plasmids (promoter, coding sequence, terminator)		
HptII Level 1(P1)	pICH47732	pICSL12009 Zm Ubiquitin + 5'UTR	pICSL80036 Hygromycin phosphotransferase	pICH41414 CAMV35S + 3'UTR
Cas9 Level 1(P2)	pICH47742	pICSL12014 Os Actin + 5'UTR	pICSL90004 *Sp* Cas9 + nuclear localisation signal	pICH41421 At nopaline synthase + 3'UTR
gRNA1 Level 1 (P3)	pICH47751	pICSL90003 TaU6	pICSL90010 gRNA sequence	-
gRNA2 Level 1 (P4)	pICH47761	pICSL90003 TaU6	pICSL90010 gRNA sequence	-
Level M	pAGM8031	Level 1(P1- P4) and pICH50900 End linker		

Supplementary Table 3. 4: Primers used for gRNA scaffold amplification and the expected resulting amplicon. Starting with forward primer containing a unique transcription start site for TaU6 promoter (underlined), followed by 20 bp sgRNA sequence indicated in red, gRNA scaffold is highlighted in grey, ending with complementary sequence for the reverse primer. BsaI restriction sites in blue.

Primer name	Primer sequence（5'-3'）
OsHKT1;1-F	TGTGGTCTCACTT(G)ACTCGATTAGCAGAGCACTGGTTTAAGAGCTATGCTGGAAACAG
OsHKT1;4-F- 1	TGTGGTCTCACTTGAACACCTCCATCTCGACGGGTTTAAGAGCTATGCTGGAAACAG
OsHKT1;4-F- 2	TGTGGTCTCACTTGCCGACGAACGAGAACATGGGTTTAAGAGCTATGCTGGAAACAG
OsHA1(94)-F	TGTGGTCTCACTT(G)TAACCTTGTTATCAATGACAGTTTAAGAGCTATGCTGGAAACAG
OsHA1(80)-F	TGTGGTCTCACTT(G)AAACCGGAAAGATTTCGGAAGTTTAAGAGCTATGCTGGAAACAG
OsHA1(65)-F	TGTGGTCTCACTT(G)ACGAGCAGCGCACACTACACGTTTAAGAGCTATGCTGGAAACAG
Scaffold-Reverse	TGTGGTCTCTAGCGAAAAAAAGCACCGACTCGGTGCCAC

Supplementary Table 3. 5: Primers used to amplify targeted region in T0 plants.

Primer name	Primer sequence（5'-3'）
OsHKT1;1- F	GATCCCGCAGATTCTAGCAG
OsHKT1;1- R	GGCAATTCGGATTTTCAGTG
OsHKT1;4- F	TGCGTGCTCCAATATGCCC
OsHKT1;4- R	AGTTGGAGAACGTCGACACC
OsHA1- F	GTGTTAGCTGCCATTGCCAC
OsHA1- R	TTCGTGAGCAGCAGATCGAG
T7 universal primer for sequencing	TAATACGACTCACTATAGGG

Supplementary Table 3. 6: Summary of quantitative trait loci (QTLs) identified in this study using GWAS of rice under 0.1 NPK condition. The table shows: the number of QTLs identified in each chromosome, QTL coordinates, and the traits associated with that QTL. Multiple traits indicate overlapping between QTLs. Abbreviations are as follows: CT for control treatment (1 NPK), LT for low treatment (0.1 NPK), FW for fresh weight, SFW for shoot fresh weight, RFW for root fresh weight, FWSR for fresh weight shoot to root ratio, DW for dry weight, SDW for shoot dry weight, RDW for root dry weight, FWDR for dry weight shoot to root ratio, RGR for relative growth rate and RGRRED for relative growth rate reduction, RED for reduction, N for nitrogen, P for phosphorus, K for potassium, Ca for calcium, Na for sodium, Mg for magnesium, Zn for zinc, Fe for iron, B for boron and C for carbon, UE for use efficiency. Further information on traits are listed in (Chapter 2, table 2.3).

Chr	QTL No.	Start (bp)	End (bp)	Traits
Chr 1	1	10934895	11163946	$Na(DW)_{LT}$, $Na(FW)_{LT}$, $Na(DW)/RGR_{LT}$, $Na(FW)/RGR_{LT}$
	2	11211845	11463442	$NaUE_{LT}$
	3	22091548	22307857	$Na(DW)_{LT}$, $Na(FW)_{LT}$
	4	24843730	25058195	$Mg(FW)_{LT}$
	5	29119761	29411376	$K(DW)RED_{LT}$, $K(FW)RED_{LT}$
	6	37595071	37816775	$P(FW)/RGR_{LT}$
	7	42265021	42471850	$SFWRED_{LT}$
	8	42893220	43217883	$FW_{LT}RED$
Chr 2	1	573100	785217	$N(DW)/RGR_{LT}$, $N(FW)/RGR_{LT}$
	2	5270236	5489303	$P(DW)_{LT}$, $P(FW)_{LT}$
	3	8446601	8652677	$N(FW)_{LT}$
	4	8801325	9007486	$N(DW)/RGR_{LT}$
	5	20529472	20737331	$K(FW)_{LT}$, $K(DW)/RGR_{LT}$, $K(FW)/RGR_{LT}$
	6	21014447	21228732	$C(FW)_{LT}$
	7	21676343	21906350	$C(DW)/RGR_{LT}$
	8	22741363	22962964	$Na(FW)/RGR_{LT}$
	9	29190864	29401373	$C(DW)/RGR_{LT}$
Chr 3	1	16449347	16658820	SFW_{LT}
	2	30711515	31318395	$N(DW)RED_{LT}$, $N(FW)_{LT}$, $N(FW)RED_{LT}$, $N(FW)/RGR_{LT}$, $N(DW)/RGR_{LT}$
	3	31566050	31781418	$FeUE_{LT}$
Chr 4	1	12707862	12924649	$C(FW)_{LT}$
	2	13760606	13980162	$P(DW)_{LT}$, $P(FW)_{LT}$, $P(DW)/RGR_{LT}$, $P(FW)/RGR_{LT}$
	3	14605163	15008150	$C(FW)_{LT}$
	4	21319617	21543010	$Mg(DW)_{LT}$, $Mg(FW)_{LT}$
	5	30361878	30584308	RGR_{LT}, $C(DW)/RGR_{LT}$
	6	30594184	30797525	RGR_{LT}
	7	31078200	31290910	FW_{LT}, $Mg(FW)RED_{LT}$
Chr 5	1	542156	750554	$SFWRED_{LT}$
	2	1306921	1511375	$N(DW)/RGR_{LT}$
	3	8195720	8509519	$C(FW)_{LT}$, SFW_{LT}
	4	15985378	16203195	$C(DW)/RGR_{LT}$
	5	23688669	23896522	$C(DW)/RGR_{LT}$, $N(FW)/RGR_{LT}$
	6	26485812	26704758	$P(FW)/RGR_{LT}$
	7	27886608	28105340	$K(DW)RED_{LT}$

Chr 6	1	6605479	6832750	$Na(FW)/RGR_{LT}$
	2	9916482	10124422	$FWSR_{LT}$
	3	10168713	10399253	$Na(FW)/RGR_{LT}$
	4	10900608	11111357	$FWSRRED_{LT}$
	5	13230119	13444616	$Zn(FW)/RGR_{LT}$
	6	15877891	16092042	$FeUE_{LT}$
	7	21708951	21922891	FW_{LT}
	8	22119339	22328915	$Na(DW)_{LT}$, $Na(DW)/RGR_{LT}$
	9	24866897	25081930	FW_{LT}
	10	27003385	27247638	BUE_{LT}
	11	27962690	28181494	$K(FW)/RGR_{LT}$
	12	28448779	28667855	$C(DW)/RGR_{LT}$
	13	29347847	29667372	$Na(FW)_{LT}$, $NaUE_{LT}$, $Na(DW)_{LT}$, $Na(DW)/RGR_{LT}$, $Na(FW)/RGR_{LT}$
Chr 7	1	945207	1152196	$C(DW)/RGR_{LT}$, $K(FW)/RGR_{LT}$
	2	19210632	19413252	RGR_{LT}
	3	23235649	23457800	$K(DW)RED_{LT}$
Chr 8	1	2895035	3105447	FW_{LT}, SFW_{LT}
	2	3337751	3576347	$Na(FW)RED_{LT}$
	3	3657275	3880233	$K(DW)RED_{LT}$
	4	5145632	5366503	BUE_{LT}
	5	7102049	7313705	$Na(FW)_{LT}$, $Na(FW)/RGR_{LT}$
	6	7488653	7719211	$Mg(FW)RED_{LT}$
	7	8497671	8715936	$NaUE_{LT}$
	8	9069082	9333729	$Na(DW)_{LT}$, $Na(DW)/RGR_{LT}$, $Na(FW)/RGR_{LT}$, $Na(FW)_{LT}$
	9	9493241	9692541	RGR_{LT}, $K(FW)/RGR_{LT}$, $C(FW)/RGR_{LT}$, $C(DW)/RGR_{LT}$
	10	10227523	10473165	$P(FW)_{LT}$, $P(DW)_{LT}$, $P(FW)/RGR_{LT}$, $P(DW)/RGR_{LT}$
	11	17320537	17678691	$Na(FW)RED_{LT}$
	12	26968542	27200388	$Na(DW)_{LT}$, $Na(FW)_{LT}$, $Na(DW)/RGR_{LT}$, $Na(FW)/RGR_{LT}$
Chr 9	1	7370444	7574210	$Na(FW)_{LT}$
	2	10246899	10560001	$K(FW)/RGR_{LT}$
	3	19074054	19296109	$C(DW)/RGR_{LT}$
Chr 10	1	3710	192593	$K(DW)/RGR_{LT}$
	2	2018955	2224867	$FWSR_{LT}$
	3	7712328	7930183	$N(FW)_{LT}$
	4	13142398	13362322	NUE_{LT}
	5	15531669	15742308	$P(FW)_{LT}$, $P(FW)/RGR_{LT}$
	6	16192110	16408077	$P(DW)_{LT}$, $P(DW)/RGR_{LT}$
	7	16426002	16626573	SFW_{LT}
	8	17018922	17237006	FW_{LT}, RFW_{LT}
	9	20449092	20654875	RGR_{LT}
	10	21406868	21636806	$Na(DW)_{LT}$
Chr 11	1	1931410	2141398	$Mg(FW)RED_{LT}$
	2	17561346	17774719	$N(FW)_{LT}$
	3	23806463	24013588	$K(FW)/RGR_{LT}$
Chr 12	1	19338780	19637985	$Mg(DW)_{LT}$

	2	21020481	21210286	$Fe(FW)_{LT}$, $C(FW)_{LT}$
	3	21557424	21766337	RGR_{LT}
	4	21889585	22133896	BUE_{LT}
	5	24163373	24391419	$K(DW)RED_{LT}$
	6	25953540	26184989	BUE_{LT}

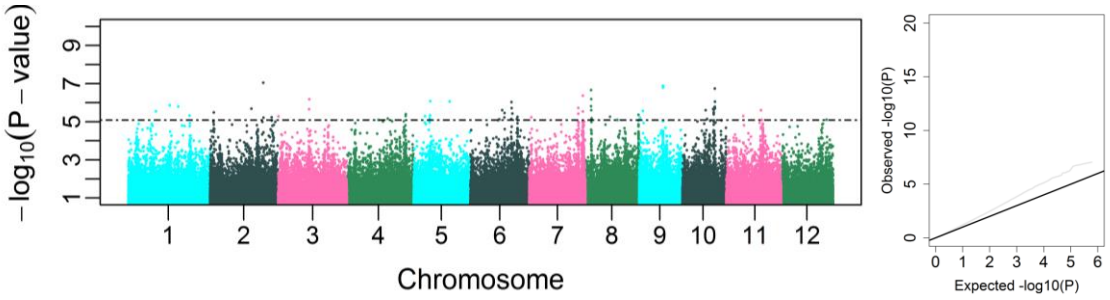

Supplementary Figure 3. 19: Genome-wide P-values from the mixed model method based on total final fresh weight in 0.1 NPK plants. The X-axis shows the location of the identified SNPs along the 12 chromosomes of the rice genome, the Y-axis indicates the -log10 (P-value) which determines the significance of the association between SNPs and traits. The horizontal line indicates the genome-wide significance threshold (FDR <10%). To the right, Q-Q plot for the corresponding trait shows the distribution of the observed P-values alongside their expected values.

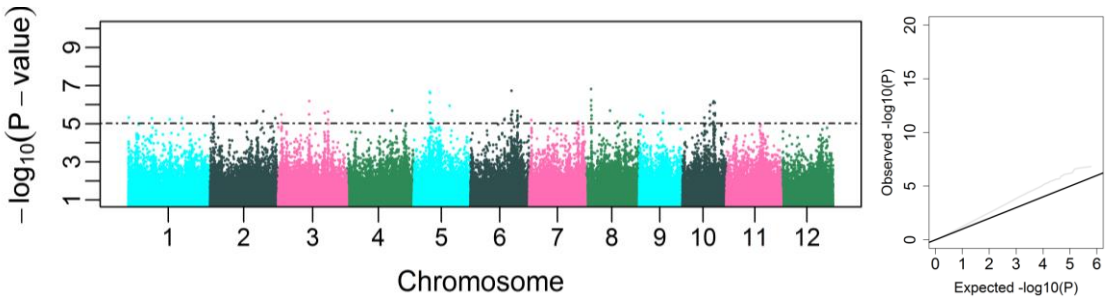

Supplementary Figure 3. 2: Genome-wide P-values from the mixed model method based on shoot fresh weight in 0.1 NPK plants. The X-axis shows the location of the identified SNPs along the 12 chromosomes of the rice genome, the Y-axis indicates the -log10 (P-value) which determines the significance of the association between SNPs and traits. The horizontal line indicates the genome-wide significance threshold (FDR <10%). To the right, Q-Q plot for the corresponding trait shows the distribution of the observed P-values alongside their expected values.

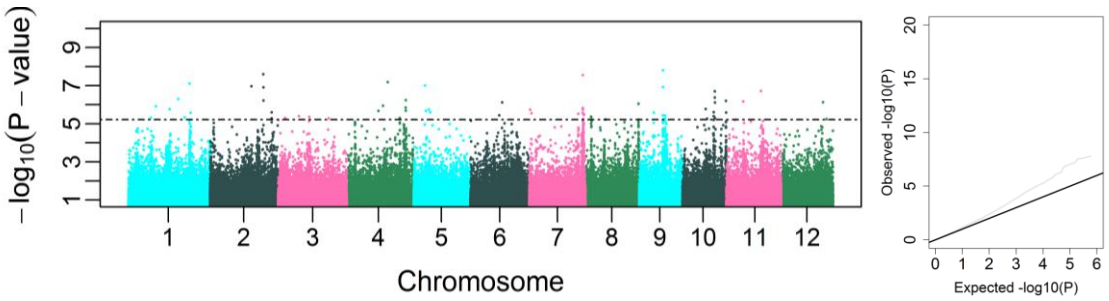

Supplementary Figure 3. 3: Genome-wide P-values from the mixed model method based on root fresh weight in 0.1 NPK plants. The X-axis shows the location of the identified SNPs along the 12 chromosomes of the rice genome, the Y-axis indicates the -log10 (P-value) which determines the significance of the association between SNPs and traits. The horizontal line indicates the genome-wide significance threshold (FDR <10%). To the right, Q-Q plot for the corresponding trait shows the distribution of the observed P-values alongside their expected values.

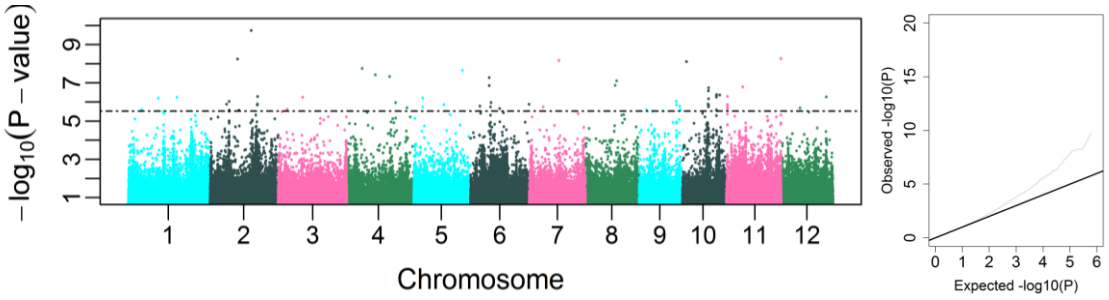

Supplementary Figure 3. 4: Genome-wide P-values from the mixed model method based on fresh weight shoot-to-root ratio in 0.1 NPK plants. The X-axis shows the location of the identified SNPs along the 12 chromosomes of the rice genome, the Y-axis indicates the -log10 (P-value) which determines the significance of the association between SNPs and traits. The horizontal line indicates the genome-wide significance threshold (FDR <10%). To the right, Q-Q plot for the corresponding trait shows the distribution of the observed P-values alongside their expected values.

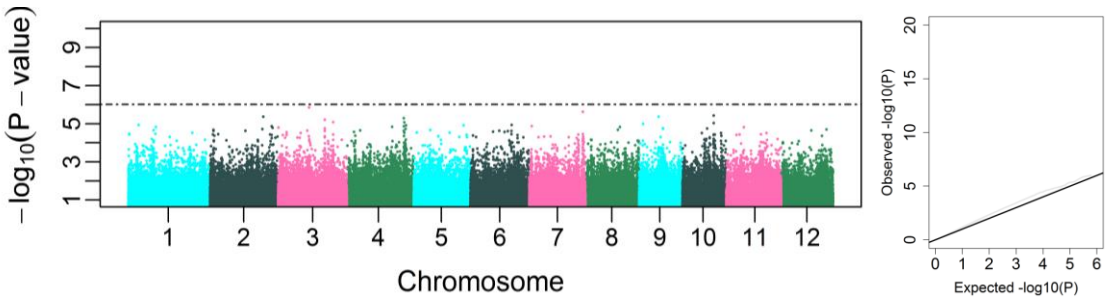

Supplementary Figure 3. 5: Genome-wide P-values from the mixed model method based on dry weight in 0.1 NPK plants. The X-axis shows the location of the identified SNPs along the 12 chromosomes of the rice genome, the Y-axis indicates the -log10 (P-value) which determines the significance of the association between SNPs and traits. The horizontal line indicates the genome-wide significance threshold (FDR <10%). To the right, Q-Q plot for the corresponding trait shows the distribution of the observed P-values alongside their expected values.

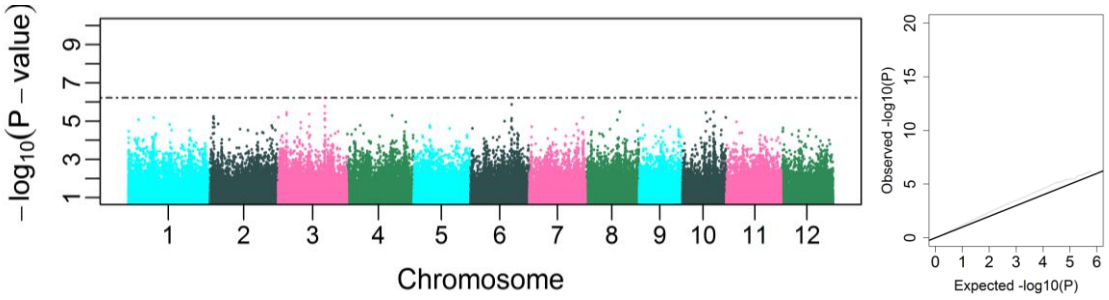

Supplementary Figure 3. 6: Genome-wide P-values from the mixed model method based on shoot dry weight in 0.1 NPK plants. The X-axis shows the location of the identified SNPs along the 12 chromosomes of the rice genome, the Y-axis indicates the -log10 (P-value) which determines the significance of the association between SNPs and traits. The horizontal line indicates the genome-wide significance threshold (FDR <10%). To the right, Q-Q plot for the corresponding trait shows the distribution of the observed P-values alongside their expected values.

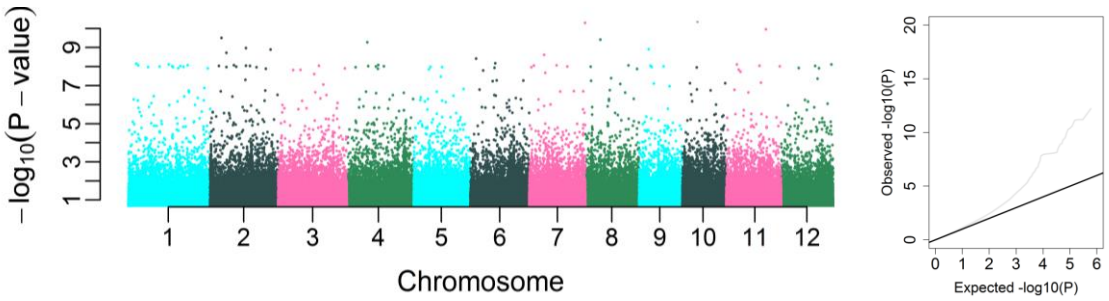

Supplementary Figure 3. 7: Genome-wide P-values from the mixed model method based on root dry weight in 0.1 NPK plants. The X-axis shows the location of the identified SNPs along the 12 chromosomes of the rice genome, the Y-axis indicates the -log10 (P-value) which determines the significance of the association between SNPs and traits. The horizontal line indicates the genome-wide significance threshold (FDR <10%). To the right, Q-Q plot for the corresponding trait shows the distribution of the observed P-values alongside their expected values.

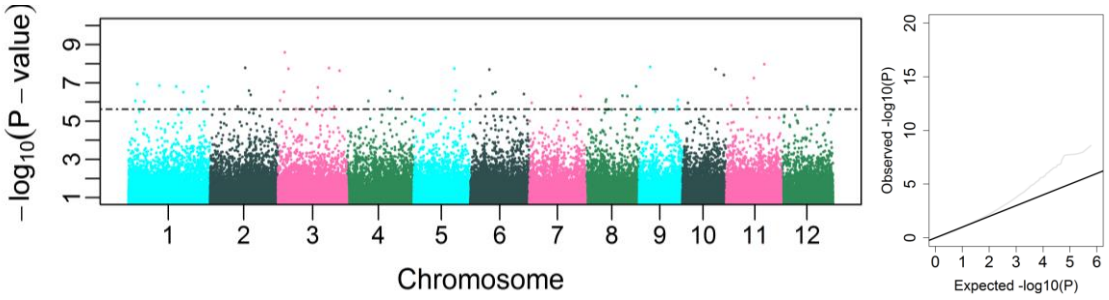

Supplementary Figure 3. 8: Genome-wide P-values from the mixed model method based on dry weight shoot-to-root ratio in 0.1 NPK plants. The X-axis shows the location of the identified SNPs along the 12 chromosomes of the rice genome, the Y-axis indicates the -log10 (P-value) which determines the significance of the association between SNPs and traits. The horizontal line indicates the genome-wide significance threshold (FDR <10%). To the right, Q-Q plot for the corresponding trait shows the distribution of the observed P-values alongside their expected values.

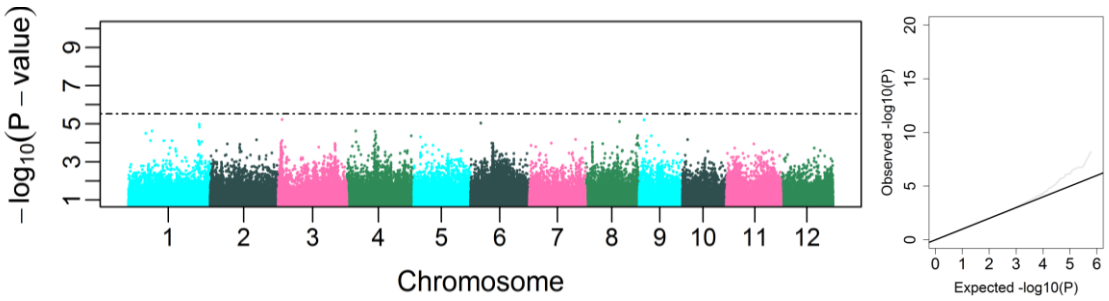

Supplementary Figure 3. 9: Genome-wide P-values from the mixed model method based on relative growth rate reduction in 0.1 NPK plants. The X-axis shows the location of the identified SNPs along the 12 chromosomes of the rice genome, the Y-axis indicates the -log10 (P-value) which determines the significance of the association between SNPs and traits. The horizontal line indicates the genome-wide significance threshold (FDR <10%). To the right, Q-Q plot for the corresponding trait shows the distribution of the observed P-values alongside their expected values.

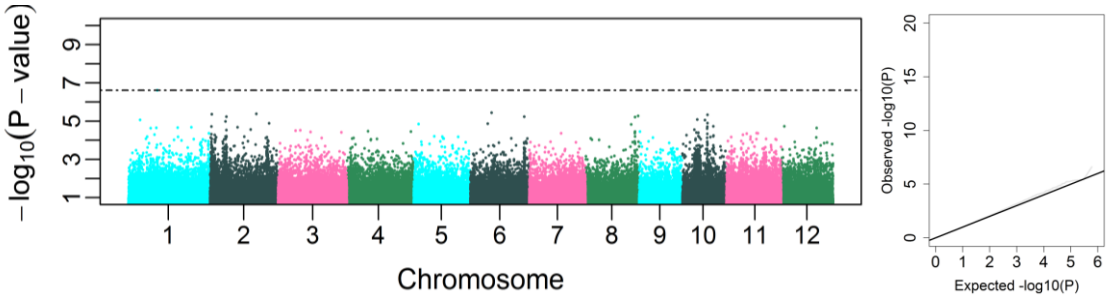

Supplementary Figure 3. 10: Genome-wide P-values from the mixed model method based on shoot nitrogen content on dry weight basis (µmoles/gDW) in 0.1 NPK plants. The X-axis shows the location of the identified SNPs along the 12 chromosomes of the rice genome, the Y-axis indicates the -log10 (P-value) which determines the significance of the association between SNPs and traits. The horizontal line indicates the genome-wide significance threshold (FDR <10%). To the right, Q-Q plot for the corresponding trait shows the distribution of the observed P-values alongside their expected values.

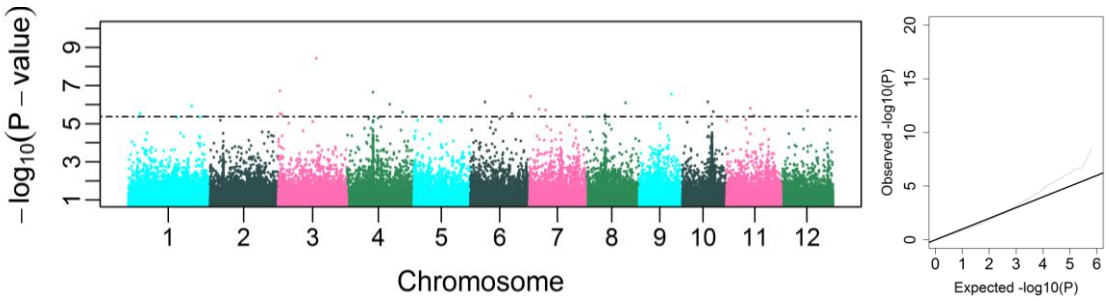

Supplementary Figure 3. 11: Genome-wide P-values from the mixed model method based on shoot phosphorus content on dry weight basis (µmoles/gDW) in 0.1 NPK plants. The X-axis shows the location of the identified SNPs along the 12 chromosomes of the rice genome, the Y-axis indicates the -log10 (P-value) which determines the significance of the association between SNPs and traits. The horizontal line indicates the genome-wide significance threshold (FDR <10%). To the right, Q-Q plot for the corresponding trait shows the distribution of the observed P-values alongside their expected values.

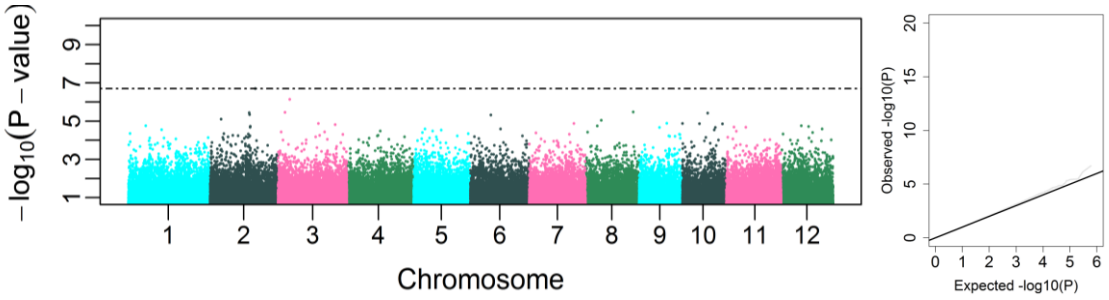

Supplementary Figure 3. 12: Genome-wide P-values from the mixed model method based on shoot potassium content on dry weight basis (µmoles/gDW) in 0.1 NPK plants. The X-axis shows the location of the identified SNPs along the 12 chromosomes of the rice genome, the Y-axis indicates the -log10 (P-value) which determines the significance of the association between SNPs and traits. The horizontal line indicates the genome-wide significance threshold (FDR <10%). To the right, Q-Q plot for the corresponding trait shows the distribution of the observed P-values alongside their expected values.

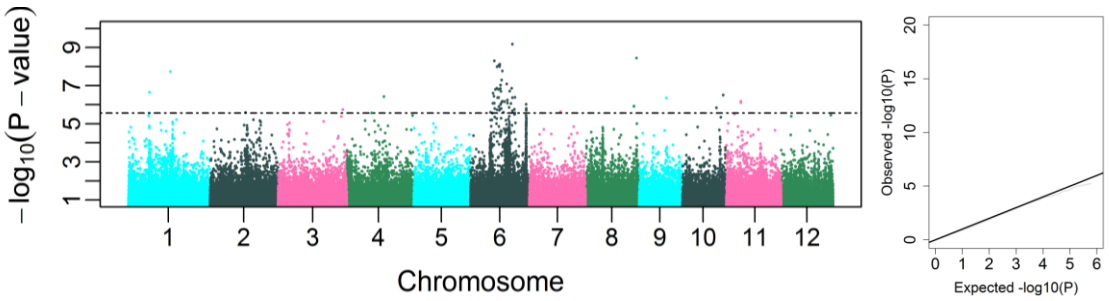

Supplementary Figure 3. 13: Genome-wide P-values from the mixed model method based on shoot sodium content on dry weight basis (µmoles/gDW) in 0.1 NPK plants. The X-axis shows the location of the identified SNPs along the 12 chromosomes of the rice genome, the Y-axis indicates the -log10 (P-value) which determines the significance of the association between SNPs and traits. The horizontal line indicates the genome-wide significance threshold (FDR <10%). To the right, Q-Q plot for the corresponding trait shows the distribution of the observed P-values alongside their expected values.

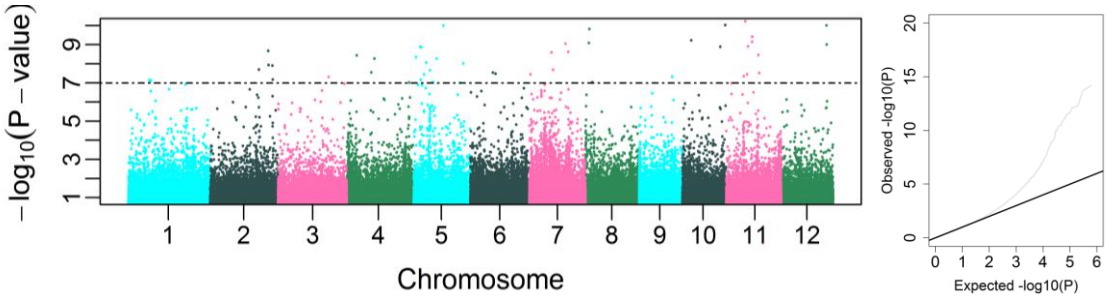

Supplementary Figure 3. 14: Genome-wide P-values from the mixed model method based on shoot zinc content on dry weight basis (µmoles/gDW) in 0.1 NPK plants. The X-axis shows the location of the identified SNPs along the 12 chromosomes of the rice genome, the Y-axis indicates the -log10 (P-value) which determines the significance of the association between SNPs and traits. The horizontal line indicates the genome-wide significance threshold (FDR <10%). To the right, Q-Q plot for the corresponding trait shows the distribution of the observed P-values alongside their expected values.

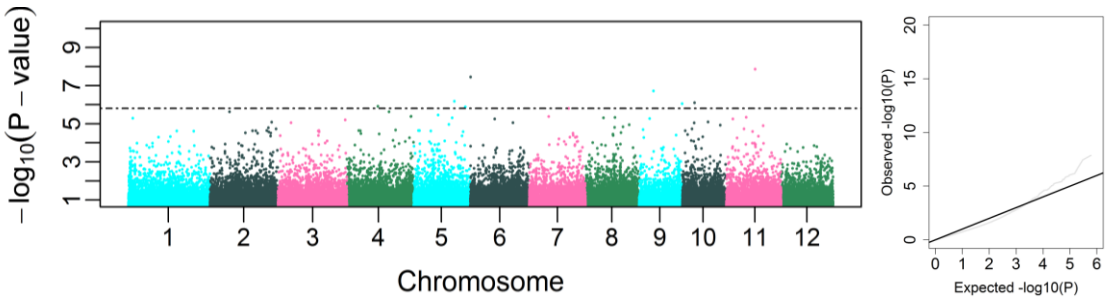

Supplementary Figure 3. 15: Genome-wide P-values from the mixed model method based on shoot iron content on dry weight basis (µmoles/gDW) in 0.1 NPK plants. The X-axis shows the location of the identified SNPs along the 12 chromosomes of the rice genome, the Y-axis indicates the -log10 (P-value) which determines the significance of the association between SNPs and traits. The horizontal line indicates the genome-wide significance threshold (FDR <10%). To the right, Q-Q plot for the corresponding trait shows the distribution of the observed P-values alongside their expected values.

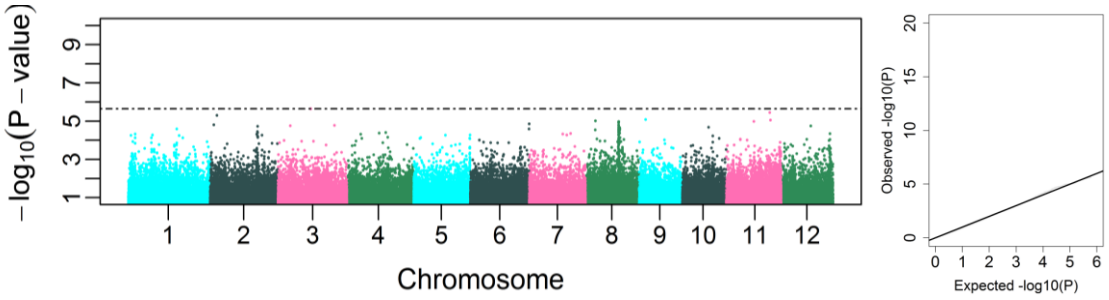

Supplementary Figure 3. 16: Genome-wide P-values from the mixed model method based on shoot boron content on dry weight basis (µmoles/gDW) in 0.1 NPK plants. The X-axis shows the location of the identified SNPs along the 12 chromosomes of the rice genome, the Y-axis indicates the -log10 (P-value) which determines the significance of the association between SNPs and traits. The horizontal line indicates the genome-wide significance threshold (FDR <10%). To the right, Q-Q plot for the corresponding trait shows the distribution of the observed P-values alongside their expected values.

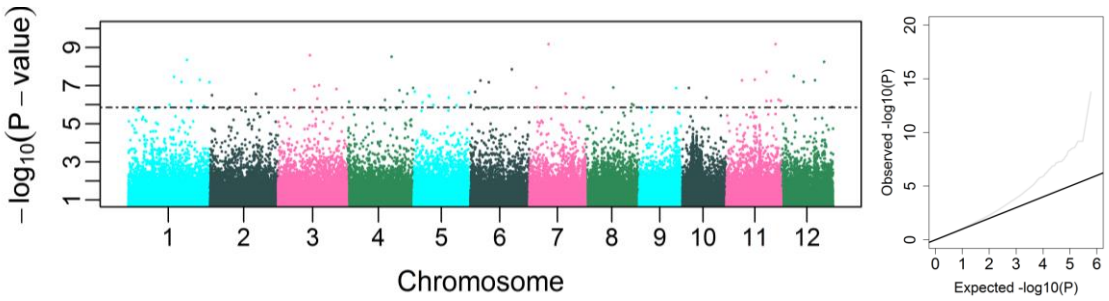

Supplementary Figure 3. 17: Genome-wide P-values from the mixed model method based on shoot carbon content on dry weight basis (µmoles/gDW) in 0.1 NPK plants. The X-axis shows the location of the identified SNPs along the 12 chromosomes of the rice genome, the Y-axis indicates the -log10 (P-value) which determines the significance of the association between SNPs and traits. The horizontal line indicates the genome-wide significance threshold (FDR <10%). To the right, Q-Q plot for the corresponding trait shows the distribution of the observed P-values alongside their expected values.

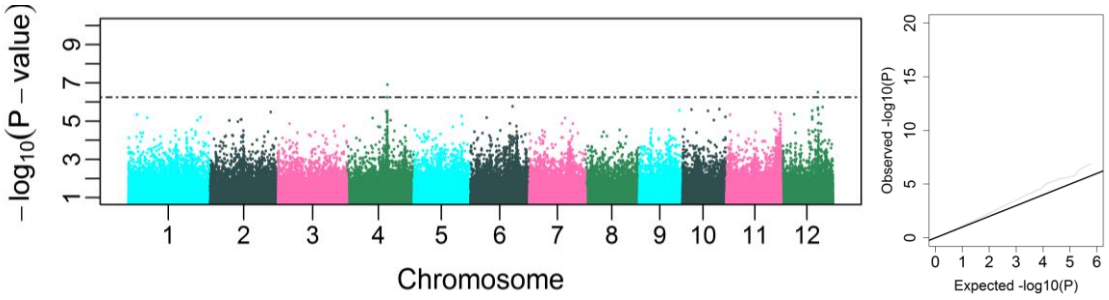

Supplementary Figure 3. 18: Genome-wide P-values from the mixed model method based on shoot magnesium content on dry weight basis (µmoles/gDW) in 0.1 NPK plants. The X-axis shows the location of the identified SNPs along the 12 chromosomes of the rice genome, the Y-axis indicates the -log10 (P-value) which determines the significance of the association between SNPs and traits. The horizontal line indicates the genome-wide significance threshold (FDR <10%). To the right, Q-Q plot for the corresponding trait shows the distribution of the observed P-values alongside their expected values.

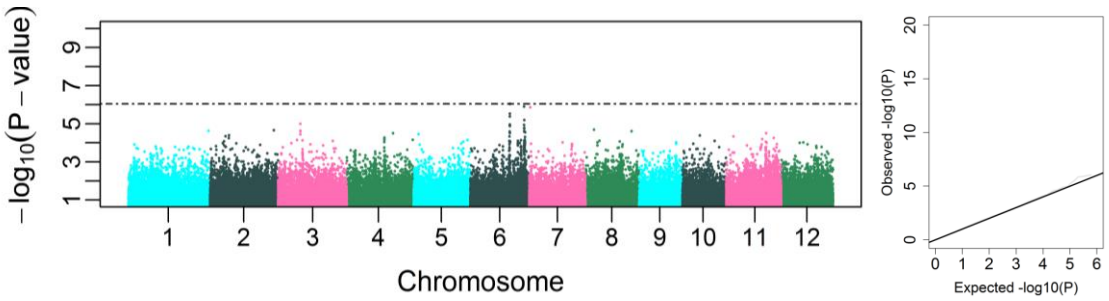

Supplementary Figure 3. 19: Genome-wide P-values from the mixed model method based on shoot calcium content on dry weight basis (µmoles/gDW) in 0.1 NPK plants. The X-axis shows the location of the identified SNPs along the 12 chromosomes of the rice genome, the Y-axis indicates the -log10 (P-value) which determines the significance of the association between SNPs and traits. The horizontal line indicates the genome-wide significance threshold (FDR <10%). To the right, Q-Q plot for the corresponding trait shows the distribution of the observed P-values alongside their expected values.

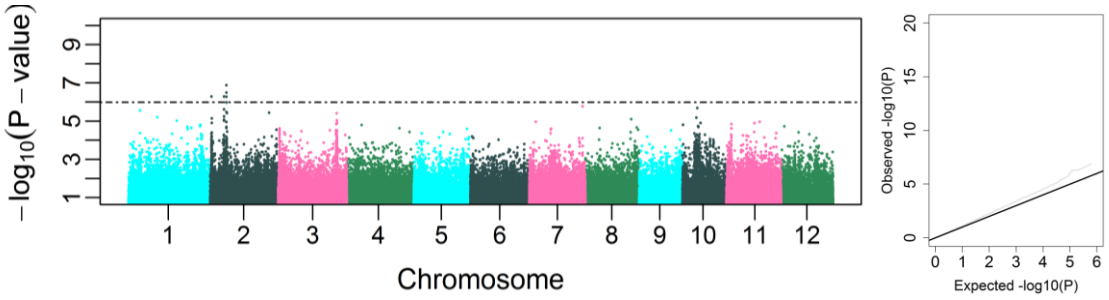

Supplementary Figure 3. 20: Genome-wide P-values from the mixed model method based on shoot nitrogen content on fresh weight basis (µmoles/gFW) in 0.1 NPK plants. The X-axis shows the location of the identified SNPs along the 12 chromosomes of the rice genome, the Y-axis indicates the -log10 (P-value) which determines the significance of the association between SNPs and traits. The horizontal line indicates the genome-wide significance threshold (FDR <10%). To the right, Q-Q plot for the corresponding trait shows the distribution of the observed P-values alongside their expected values.

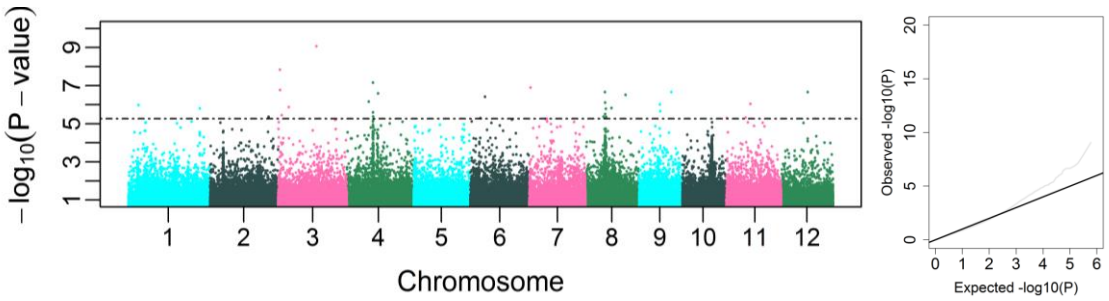

Supplementary Figure 3. 21: Genome-wide P-values from the mixed model method based on shoot phosphorus content on fresh weight basis (µmoles/gFW) in 0.1 NPK plants. The X-axis shows the location of the identified SNPs along the 12 chromosomes of the rice genome, the Y-axis indicates the -log10 (P-value) which determines the significance of the association between SNPs and traits. The horizontal line indicates the genome-wide significance threshold (FDR <10%). To the right, Q-Q plot for the corresponding trait shows the distribution of the observed P-values alongside their expected values.

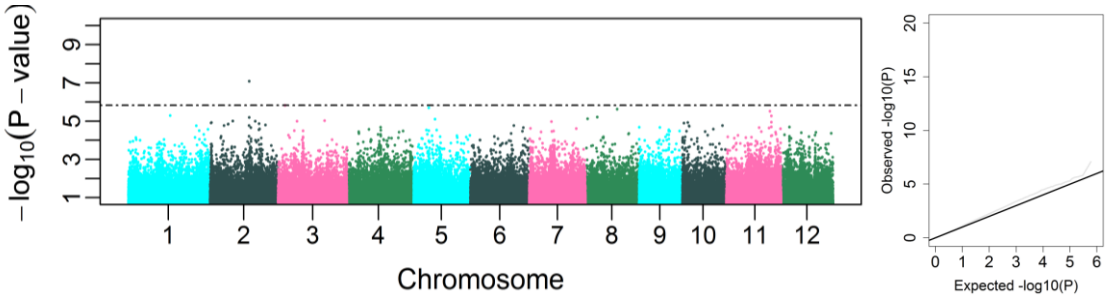

Supplementary Figure 3. 22: Genome-wide P-values from the mixed model method based on shoot potassium content on fresh weight basis (µmoles/gFW) in 0.1 NPK plants. The X-axis shows the location of the identified SNPs along the 12 chromosomes of the rice genome, the Y-axis indicates the -log10 (P-value) which determines the significance of the association between SNPs and traits. The horizontal line indicates the genome-wide significance threshold (FDR <10%). To the right, Q-Q plot for the corresponding trait shows the distribution of the observed P-values alongside their expected values.

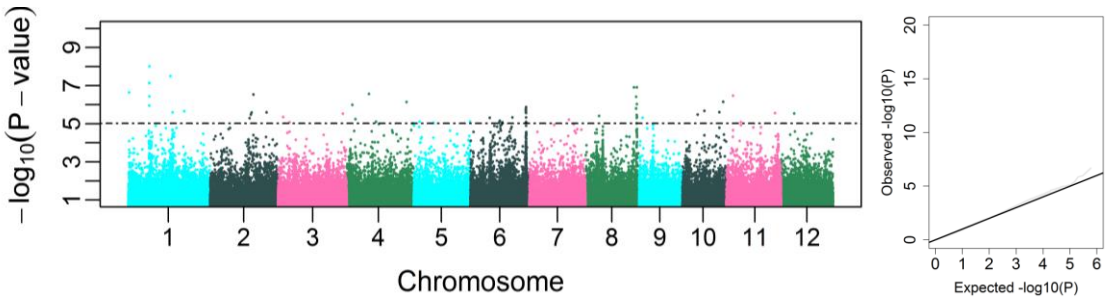

Supplementary Figure 3. 23: Genome-wide P-values from the mixed model method based on shoot sodium content on fresh weight basis (µmoles/gFW) in 0.1 NPK plants. The X-axis shows the location of the identified SNPs along the 12 chromosomes of the rice genome, the Y-axis indicates the -log10 (P-value) which determines the significance of the association between SNPs and traits. The horizontal line indicates the genome-wide significance threshold (FDR <10%). To the right, Q-Q plot for the corresponding trait shows the distribution of the observed P-values alongside their expected values.

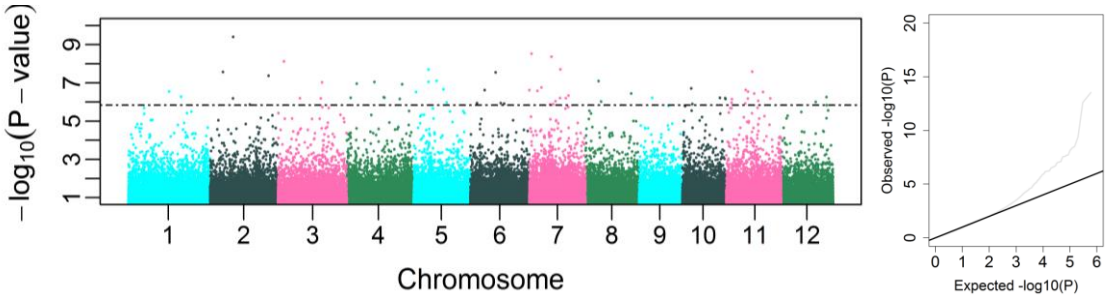

Supplementary Figure 3. 24: Genome-wide P-values from the mixed model method based on shoot zinc content on fresh weight basis (µmoles/gFW) in 0.1 NPK plants. The X-axis shows the location of the identified SNPs along the 12 chromosomes of the rice genome, the Y-axis indicates the -log10 (P-value) which determines the significance of the association between SNPs and traits. The horizontal line indicates the genome-wide significance threshold (FDR <10%). To the right, Q-Q plot for the corresponding trait shows the distribution of the observed P-values alongside their expected values.

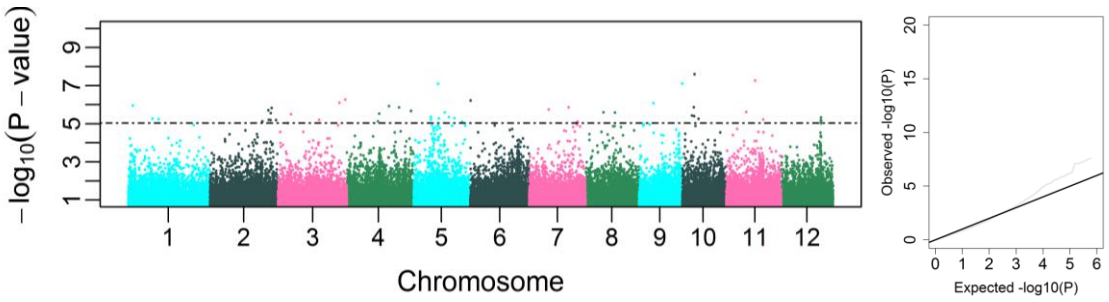

Supplementary Figure 3. 25: Genome-wide P-values from the mixed model method based on shoot iron content on fresh weight basis (µmoles/gFW) in 0.1 NPK plants. The X-axis shows the location of the identified SNPs along the 12 chromosomes of the rice genome, the Y-axis indicates the -log10 (P-value) which determines the significance of the association between SNPs and traits. The horizontal line indicates the genome-wide significance threshold (FDR <10%). To the right, Q-Q plot for the corresponding trait shows the distribution of the observed P-values alongside their expected values.

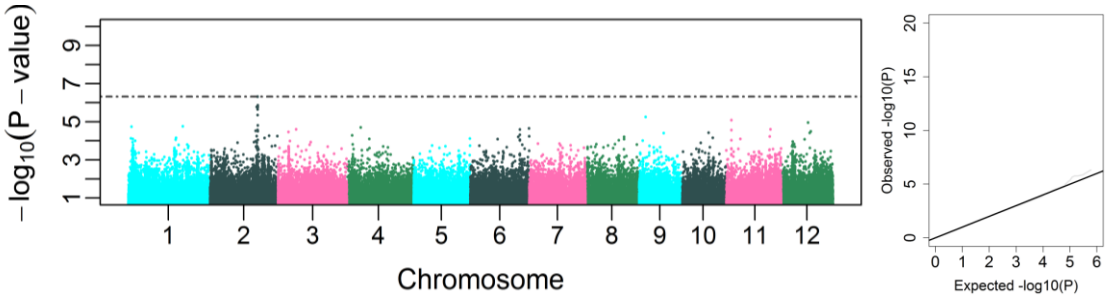

Supplementary Figure 3. 26: Genome-wide P-values from the mixed model method based on shoot boron content on fresh weight basis (µmoles/gFW) in 0.1 NPK plants. The X-axis shows the location of the identified SNPs along the 12 chromosomes of the rice genome, the Y-axis indicates the -log10 (P-value) which determines the significance of the association between SNPs and traits. The horizontal line indicates the genome-wide significance threshold (FDR <10%). To the right, Q-Q plot for the corresponding trait shows the distribution of the observed P-values alongside their expected values.

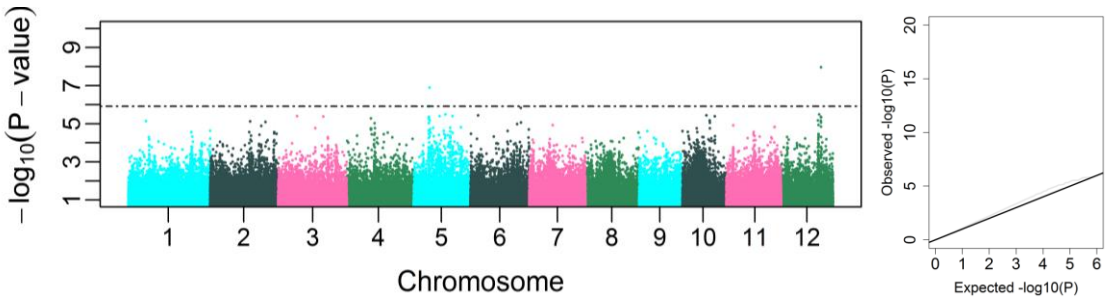

Supplementary Figure 3. 27: Genome-wide P-values from the mixed model method based on shoot carbon content on fresh weight basis (µmoles/gFW) in 0.1 NPK plants. The X-axis shows the location of the identified SNPs along the 12 chromosomes of the rice genome, the Y-axis indicates the -log10 (P-value) which determines the significance of the association between SNPs and traits. The horizontal line indicates the genome-wide significance threshold (FDR <10%). To the right, Q-Q plot for the corresponding trait shows the distribution of the observed P-values alongside their expected values.

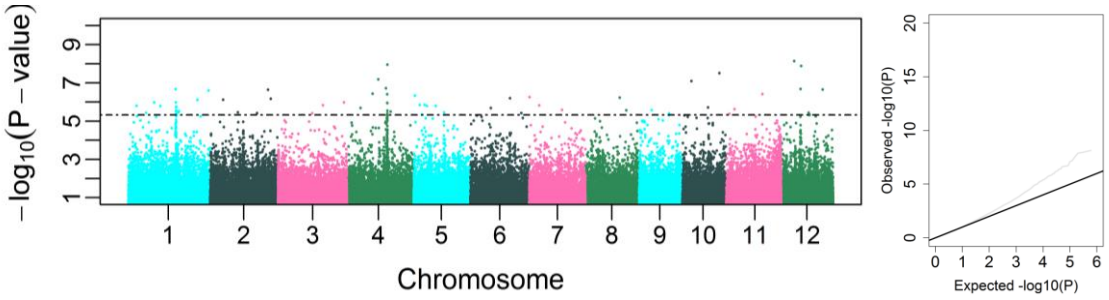

Supplementary Figure 3. 28: Genome-wide P-values from the mixed model method based on shoot magnesium content on fresh weight basis (µmoles/gFW) in 0.1 NPK plants. The X-axis shows the location of the identified SNPs along the 12 chromosomes of the rice genome, the Y-axis indicates the -log10 (P-value) which determines the significance of the association between SNPs and traits. The horizontal line indicates the genome-wide significance threshold (FDR <10%). To the right, Q-Q plot for the corresponding trait shows the distribution of the observed P-values alongside their expected values.

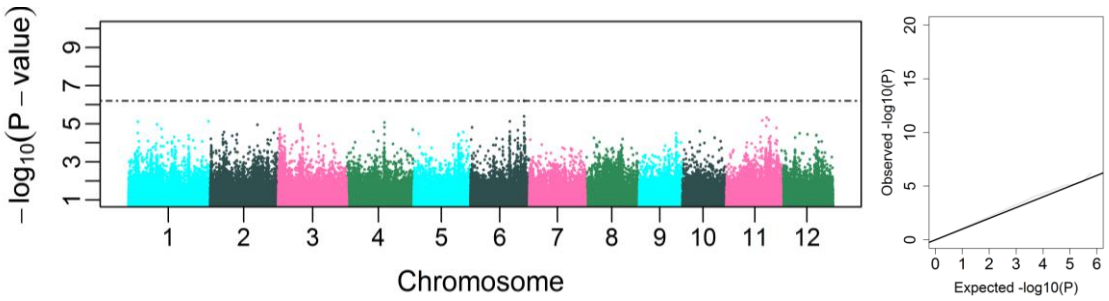

Supplementary Figure 3. 29: Genome-wide P-values from the mixed model method based on shoot calcium content on fresh weight basis (µmoles/gFW) in 0.1 NPK plants. The X-axis shows the location of the identified SNPs along the 12 chromosomes of the rice genome, the Y-axis indicates the -log10 (P-value) which determines the significance of the association between SNPs and traits. The horizontal line indicates the genome-wide significance threshold (FDR <10%). To the right, Q-Q plot for the corresponding trait shows the distribution of the observed P-values alongside their expected values.

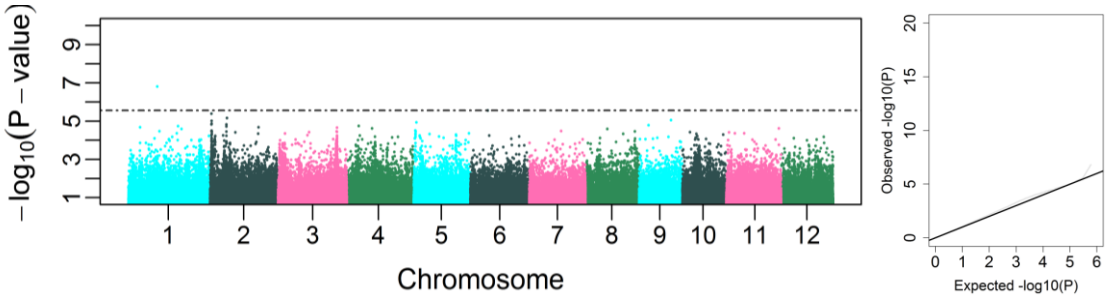

Supplementary Figure 3. 30: Genome-wide P-values from the mixed model method based on shoot nitrogen content (µmoles/gDW)/RGR in 0.1 NPK plants. The X-axis shows the location of the identified SNPs along the 12 chromosomes of the rice genome, the Y-axis indicates the -log10 (P-value) which determines the significance of the association between SNPs and traits. The horizontal line indicates the genome-wide significance threshold (FDR <10%). To the right, Q-Q plot for the corresponding trait shows the distribution of the observed P-values alongside their expected values.

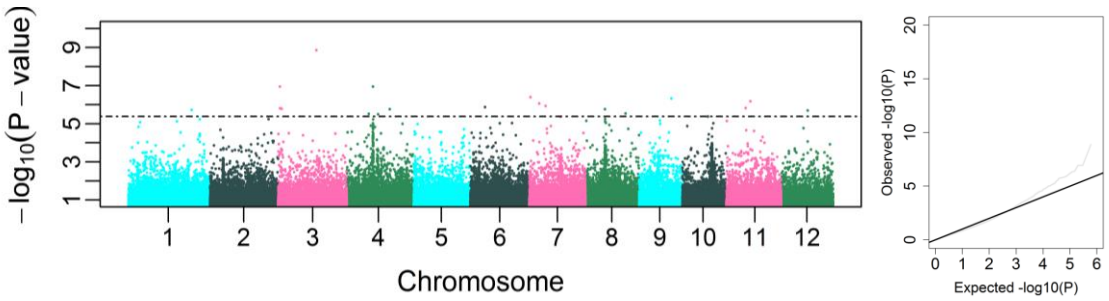

Supplementary Figure 3. 31: Genome-wide P-values from the mixed model method based on shoot phosphorus content (µmoles/gDW)/RGR in 0.1 NPK plants. The X-axis shows the location of the identified SNPs along the 12 chromosomes of the rice genome, the Y-axis indicates the -log10 (P-value) which determines the significance of the association between SNPs and traits. The horizontal line indicates the genome-wide significance threshold (FDR <10%). To the right, Q-Q plot for the corresponding trait shows the distribution of the observed P-values alongside their expected values.

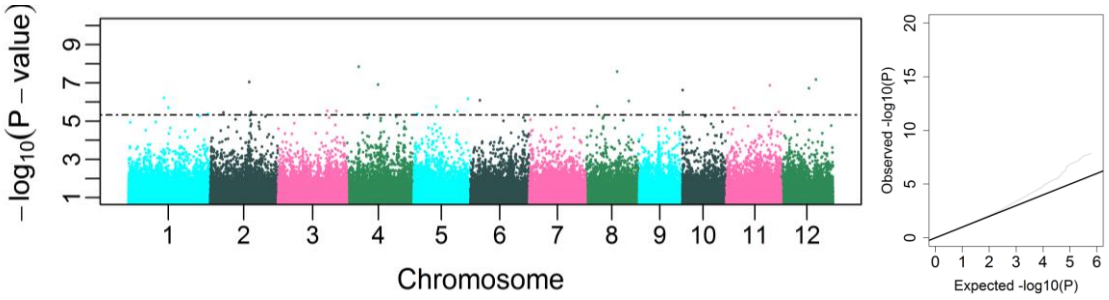

Supplementary Figure 3. 32: Genome-wide P-values from the mixed model method based on shoot potassium content (µmoles/gDW)/RGR in 0.1 NPK plants. The X-axis shows the location of the identified SNPs along the 12 chromosomes of the rice genome, the Y-axis indicates the -log10 (P-value) which determines the significance of the association between SNPs and traits. The horizontal line indicates the genome-wide significance threshold (FDR <10%). To the right, Q-Q plot for the corresponding trait shows the distribution of the observed P-values alongside their expected values.

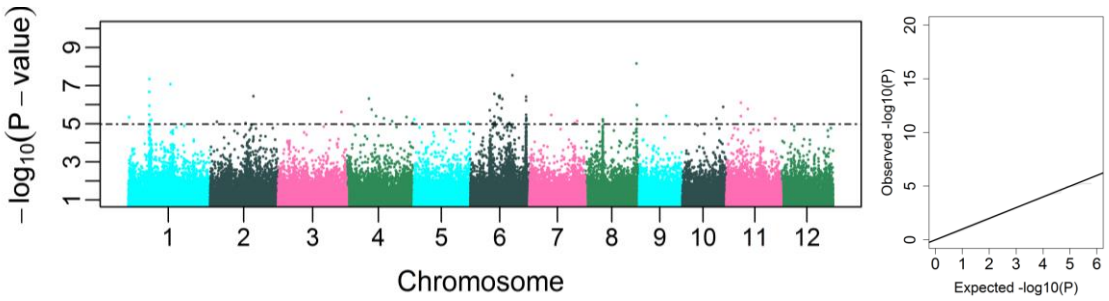

Supplementary Figure 3. 33: Genome-wide P-values from the mixed model method based on shoot sodium content (µmoles/gDW)/RGR in 0.1 NPK plants. The X-axis shows the location of the identified SNPs along the 12 chromosomes of the rice genome, the Y-axis indicates the -log10 (P-value) which determines the significance of the association between SNPs and traits. The horizontal line indicates the genome-wide significance threshold (FDR <10%). To the right, Q-Q plot for the corresponding trait shows the distribution of the observed P-values alongside their expected values.

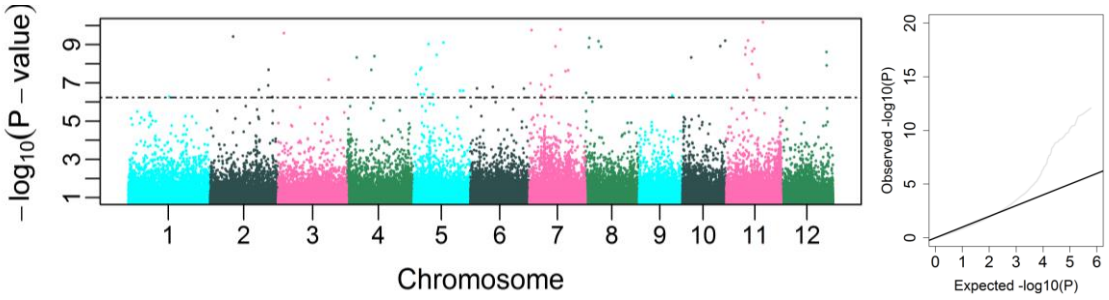

Supplementary Figure 3. 34: Genome-wide P-values from the mixed model method based on shoot zinc content (µmoles/gDW)/RGR in 0.1 NPK plants. The X-axis shows the location of the identified SNPs along the 12 chromosomes of the rice genome, the Y-axis indicates the -log10 (P-value) which determines the significance of the association between SNPs and traits. The horizontal line indicates the genome-wide significance threshold (FDR <10%). To the right, Q-Q plot for the corresponding trait shows the distribution of the observed P-values alongside their expected values.

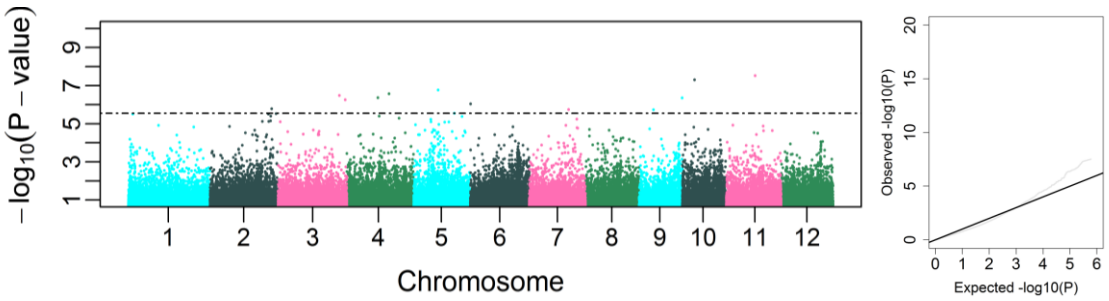

Supplementary Figure 3. 35: Genome-wide P-values from the mixed model method based on shoot iron content (µmoles/gDW)/RGR in 0.1 NPK plants. The X-axis shows the location of the identified SNPs along the 12 chromosomes of the rice genome, the Y-axis indicates the -log10 (P-value) which determines the significance of the association between SNPs and traits. The horizontal line indicates the genome-wide significance threshold (FDR <10%). To the right, Q-Q plot for the corresponding trait shows the distribution of the observed P-values alongside their expected values.

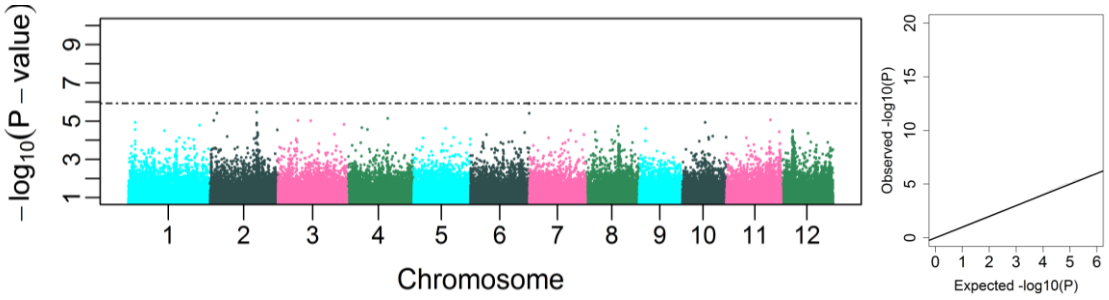

Supplementary Figure 3. 36: Genome-wide P-values from the mixed model method based on shoot boron content (µmoles/gDW)/RGR in 0.1 NPK plants. The X-axis shows the location of the identified SNPs along the 12 chromosomes of the rice genome, the Y-axis indicates the -log10 (P-value) which determines the significance of the association between SNPs and traits. The horizontal line indicates the genome-wide significance threshold (FDR <10%). To the right, Q-Q plot for the corresponding trait shows the distribution of the observed P-values alongside their expected values.

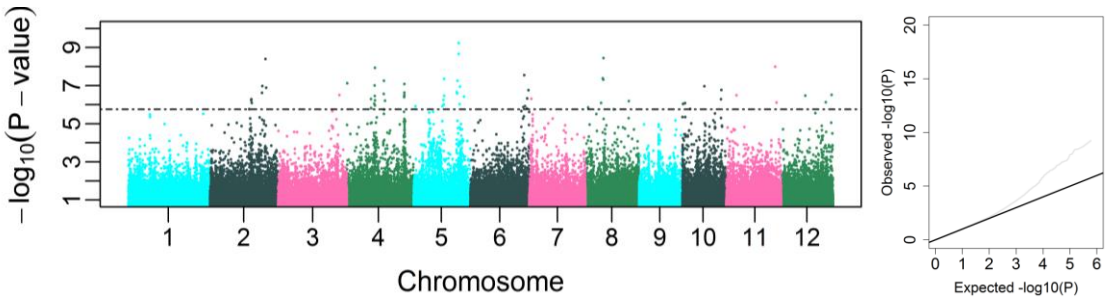

Supplementary Figure 3. 37: Genome-wide P-values from the mixed model method based on shoot carbon content (µmoles/gDW)/RGR in 0.1 NPK plants. The X-axis shows the location of the identified SNPs along the 12 chromosomes of the rice genome, the Y-axis indicates the -log10 (P-value) which determines the significance of the association between SNPs and traits. The horizontal line indicates the genome-wide significance threshold (FDR <10%). To the right, Q-Q plot for the corresponding trait shows the distribution of the observed P-values alongside their expected values.

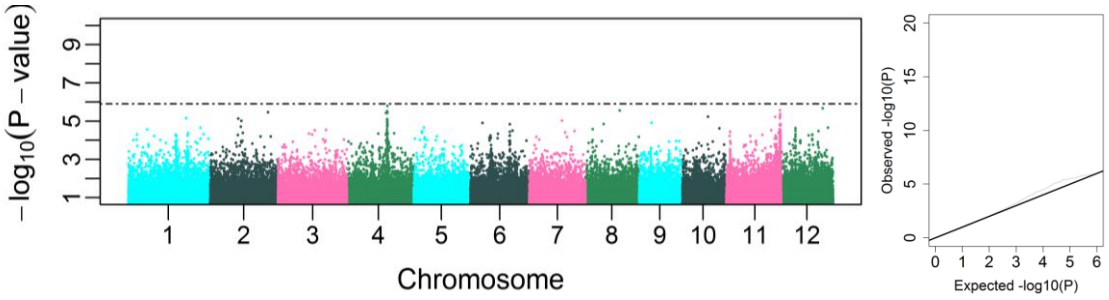

Supplementary Figure 3. 38: Genome-wide P-values from the mixed model method based on shoot magnesium content (µmoles/gDW)/RGR in 0.1 NPK plants. The X-axis shows the location of the identified SNPs along the 12 chromosomes of the rice genome, the Y-axis indicates the -log10 (P-value) which determines the significance of the association between SNPs and traits. The horizontal line indicates the genome-wide significance threshold (FDR <10%). To the right, Q-Q plot for the corresponding trait shows the distribution of the observed P-values alongside their expected values.

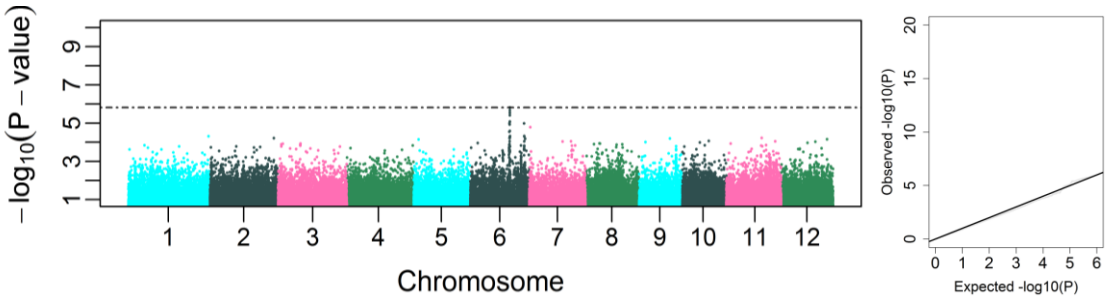

Supplementary Figure 3. 39: Genome-wide P-values from the mixed model method based on shoot calcium content (µmoles/gDW)/RGR in 0.1 NPK plants. The X-axis shows the location of the identified SNPs along the 12 chromosomes of the rice genome, the Y-axis indicates the -log10 (P-value) which determines the significance of the association between SNPs and traits. The horizontal line indicates the genome-wide significance threshold (FDR <10%). To the right, Q-Q plot for the corresponding trait shows the distribution of the observed P-values alongside their expected values.

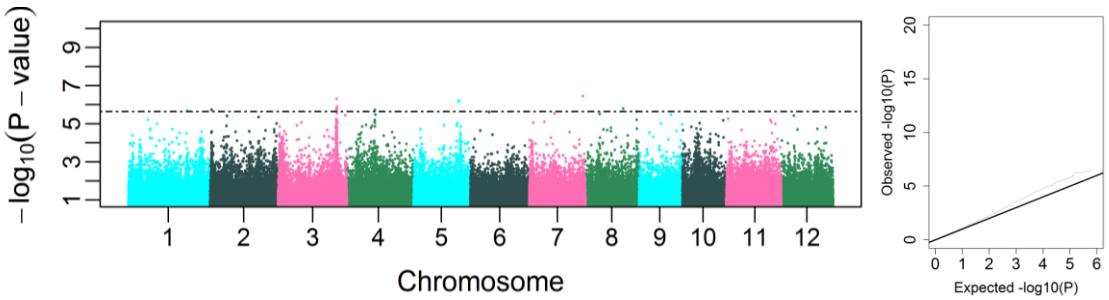

Supplementary Figure 3. 40: Genome-wide P-values from the mixed model method based on shoot nitrogen content (µmoles/gFW)/RGR in 0.1 NPK plants. The X-axis shows the location of the identified SNPs along the 12 chromosomes of the rice genome, the Y-axis indicates the -log10 (P-value) which determines the significance of the association between SNPs and traits. The horizontal line indicates the genome-wide significance threshold (FDR <10%). To the right, Q-Q plot for the corresponding trait shows the distribution of the observed P-values alongside their expected values.

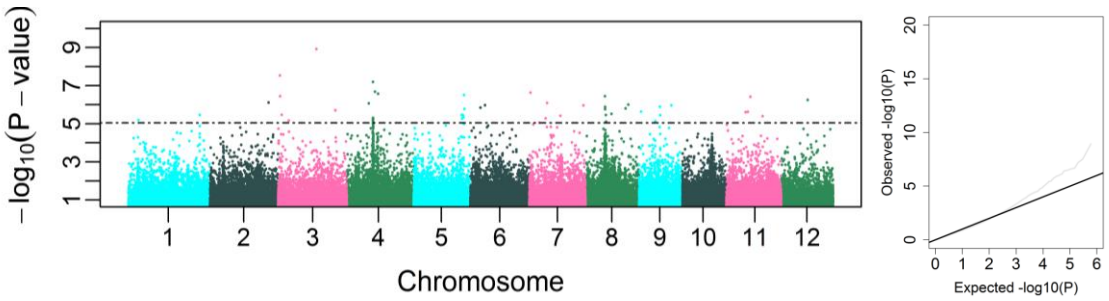

Supplementary Figure 3. 41: Genome-wide P-values from the mixed model method based on shoot phosphorus content (µmoles/gFW)/RGR in 0.1 NPK plants. The X-axis shows the location of the identified SNPs along the 12 chromosomes of the rice genome, the Y-axis indicates the -log10 (P-value) which determines the significance of the association between SNPs and traits. The horizontal line indicates the genome-wide significance threshold (FDR <10%). To the right, Q-Q plot for the corresponding trait shows the distribution of the observed P-values alongside their expected values.

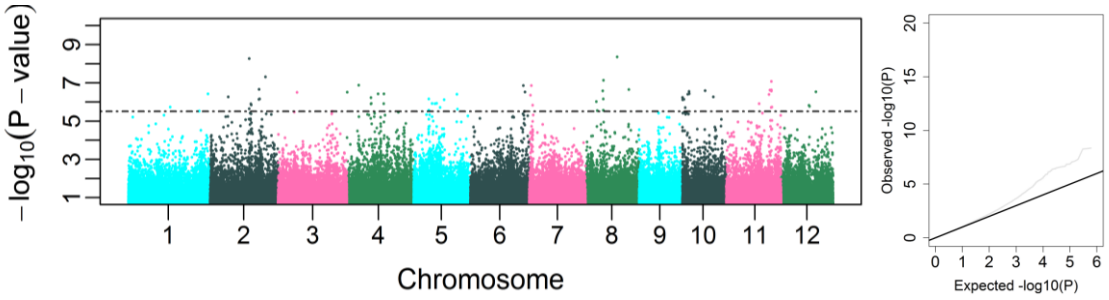

Supplementary Figure 3. 42: Genome-wide P-values from the mixed model method based on shoot potassium content (µmoles/gFW)/RGR in 0.1 NPK plants. The X-axis shows the location of the identified SNPs along the 12 chromosomes of the rice genome, the Y-axis indicates the -log10 (P-value) which determines the significance of the association between SNPs and traits. The horizontal line indicates the genome-wide significance threshold (FDR <10%). To the right, Q-Q plot for the corresponding trait shows the distribution of the observed P-values alongside their expected values.

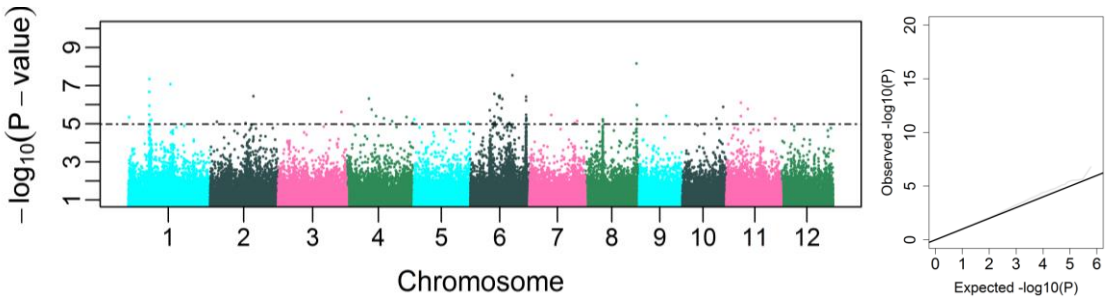

Supplementary Figure 3. 43: Genome-wide P-values from the mixed model method based on shoot sodium content (µmoles/gFW)/RGR in 0.1 NPK plants. The X-axis shows the location of the identified SNPs along the 12 chromosomes of the rice genome, the Y-axis indicates the -log10 (P-value) which determines the significance of the association between SNPs and traits. The horizontal line indicates the genome-wide significance threshold (FDR <10%). To the right, Q-Q plot for the corresponding trait shows the distribution of the observed P-values alongside their expected values.

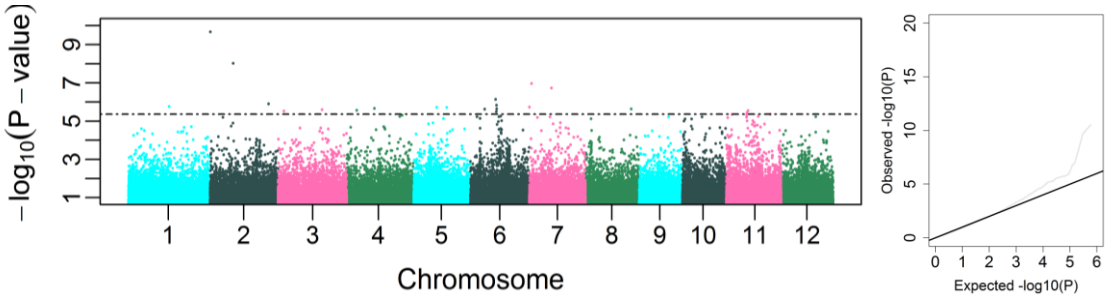

Supplementary Figure 3. 44: Genome-wide P-values from the mixed model method based on shoot zinc content (µmoles/gFW)/RGR in 0.1 NPK plants. The X-axis shows the location of the identified SNPs along the 12 chromosomes of the rice genome, the Y-axis indicates the -log10 (P-value) which determines the significance of the association between SNPs and traits. The horizontal line indicates the genome-wide significance threshold (FDR <10%). To the right, Q-Q plot for the corresponding trait shows the distribution of the observed P-values alongside their expected values.

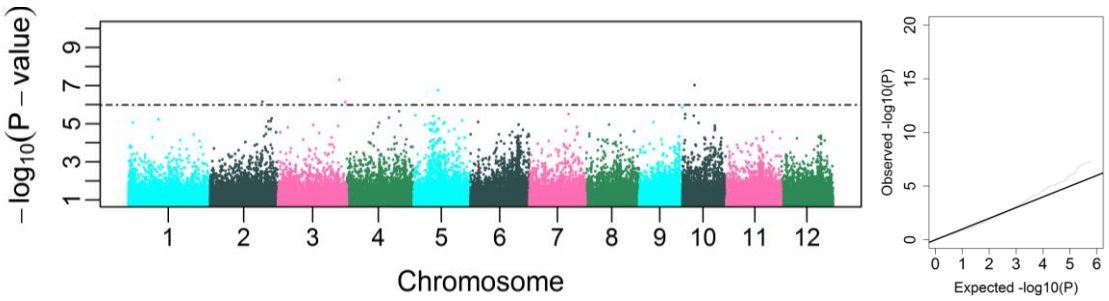

Supplementary Figure 3. 45: Genome-wide P-values from the mixed model method based on shoot iron content (µmoles/gFW)/RGR in 0.1 NPK plants. The X-axis shows the location of the identified SNPs along the 12 chromosomes of the rice genome, the Y-axis indicates the -log10 (P-value) which determines the significance of the association between SNPs and traits. The horizontal line indicates the genome-wide significance threshold (FDR <10%). To the right, Q-Q plot for the corresponding trait shows the distribution of the observed P-values alongside their expected values.

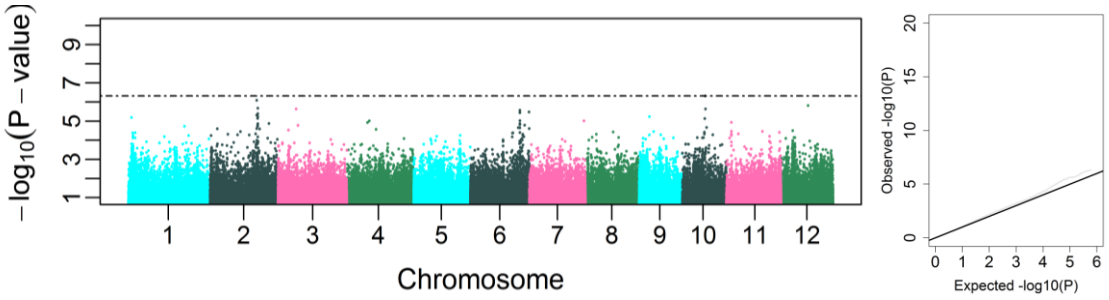

Supplementary Figure 3. 46: Genome-wide P-values from the mixed model method based on shoot boron content (µmoles/gFW)/RGR in 0.1 NPK plants. The X-axis shows the location of the identified SNPs along the 12 chromosomes of the rice genome, the Y-axis indicates the -log10 (P-value) which determines the significance of the association between SNPs and traits. The horizontal line indicates the genome-wide significance threshold (FDR <10%). To the right, Q-Q plot for the corresponding trait shows the distribution of the observed P-values alongside their expected values.

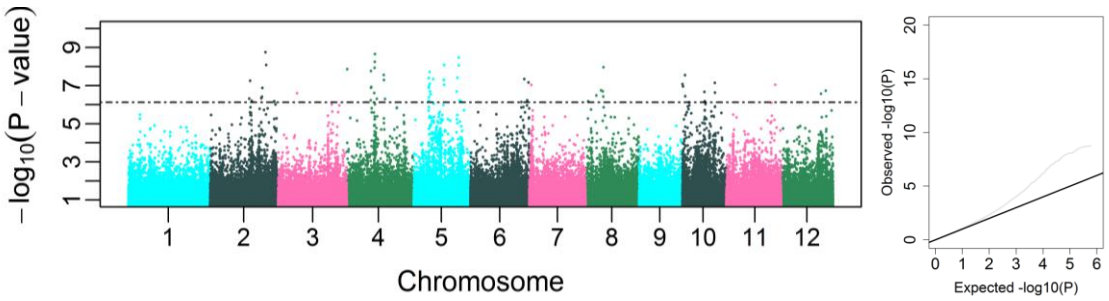

Supplementary Figure 3. 47: Genome-wide P-values from the mixed model method based on shoot carbon content (µmoles/gFW)/RGR in 0.1 NPK plants. The X-axis shows the location of the identified SNPs along the 12 chromosomes of the rice genome, the Y-axis indicates the -log10 (P-value) which determines the significance of the association between SNPs and traits. The horizontal line indicates the genome-wide significance threshold (FDR <10%). To the right, Q-Q plot for the corresponding trait shows the distribution of the observed P-values alongside their expected values.

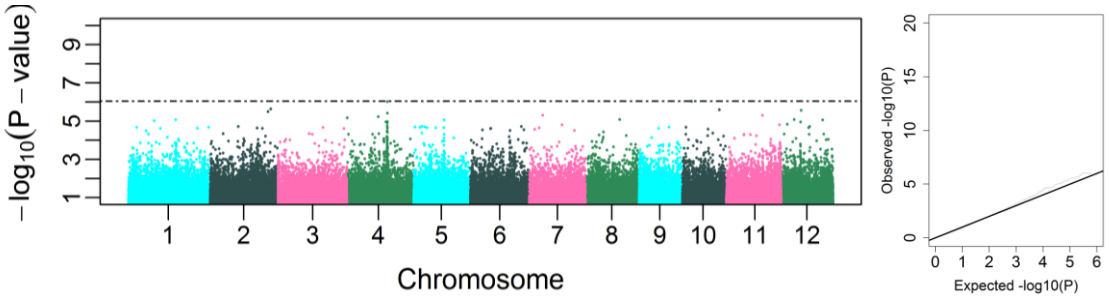

Supplementary Figure 3. 48: Genome-wide P-values from the mixed model method based on shoot magnesium content (µmoles/gFW)/RGR in 0.1 NPK plants. The X-axis shows the location of the identified SNPs along the 12 chromosomes of the rice genome, the Y-axis indicates the -log10 (P-value) which determines the significance of the association between SNPs and traits. The horizontal line indicates the genome-wide significance threshold (FDR <10%). To the right, Q-Q plot for the corresponding trait shows the distribution of the observed P-values alongside their expected values.

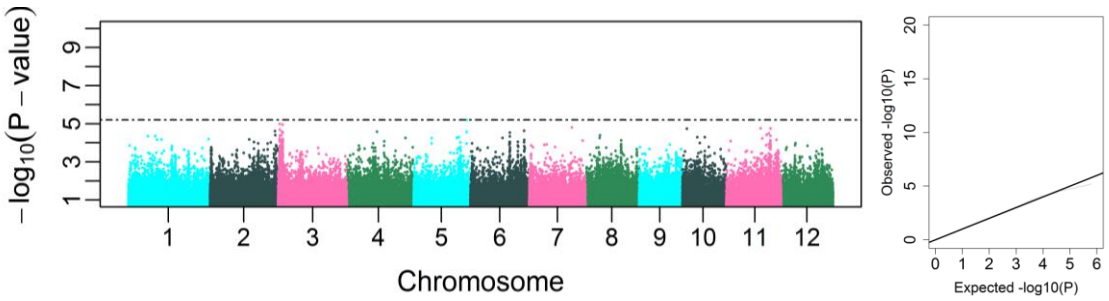

Supplementary Figure 3. 49: Genome-wide P-values from the mixed model method based on shoot calcium content (µmoles/gFW)/RGR in 0.1 NPK plants. The X-axis shows the location of the identified SNPs along the 12 chromosomes of the rice genome, the Y-axis indicates the -log10 (P-value) which determines the significance of the association between SNPs and traits. The horizontal line indicates the genome-wide significance threshold (FDR <10%). To the right, Q-Q plot for the corresponding trait shows the distribution of the observed P-values alongside their expected values.

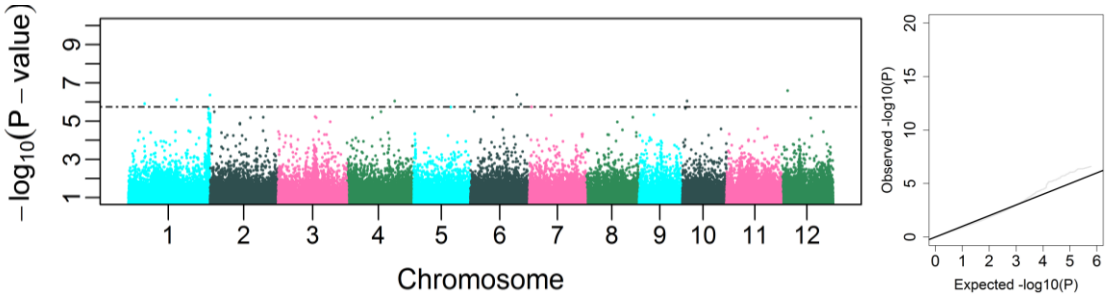

Supplementary Figure 3. 50: Genome-wide P-values from the mixed model method based on total final fresh weight reduction in 0.1 NPK plants. The X-axis shows the location of the identified SNPs along the 12 chromosomes of the rice genome, the Y-axis indicates the -log10 (P-value) which determines the significance of the association between SNPs and traits. The horizontal line indicates the genome-wide significance threshold (FDR <10%). To the right, Q-Q plot for the corresponding trait shows the distribution of the observed P-values alongside their expected values.

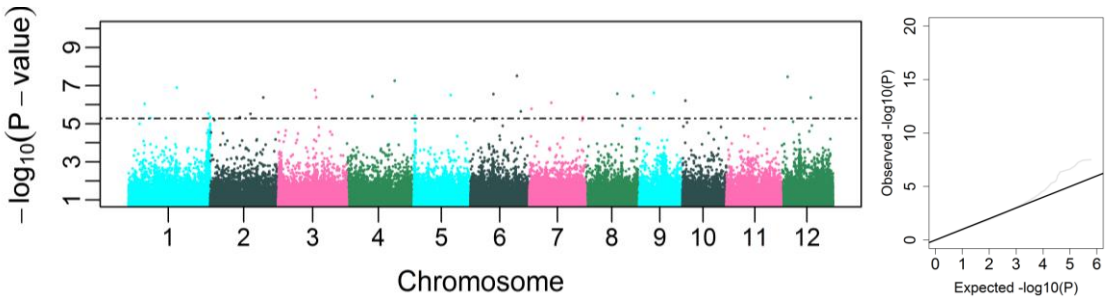

Supplementary Figure 3. 51: Genome-wide P-values from the mixed model method based on shoot fresh weight reduction in 0.1 NPK plants. The X-axis shows the location of the identified SNPs along the 12 chromosomes of the rice genome, the Y-axis indicates the -log10 (P-value) which determines the significance of the association between SNPs and traits. The horizontal line indicates the genome-wide significance threshold (FDR <10%). To the right, Q-Q plot for the corresponding trait shows the distribution of the observed P-values alongside their expected values.

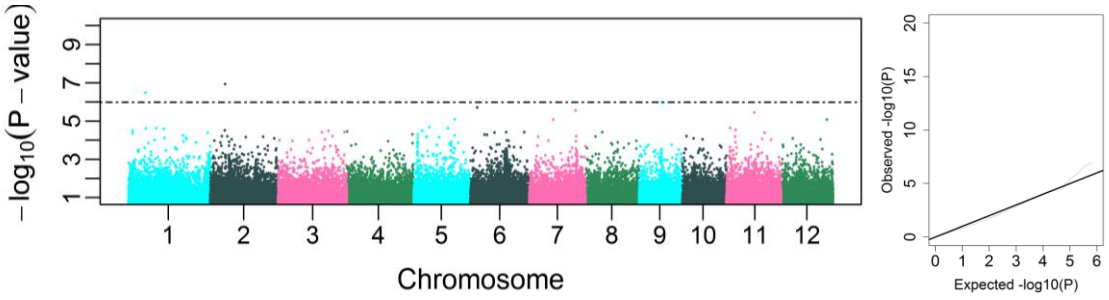

Supplementary Figure 3. 52: Genome-wide P-values from the mixed model method based on root fresh weight reduction in 0.1 NPK plants. The X-axis shows the location of the identified SNPs along the 12 chromosomes of the rice genome, the Y-axis indicates the -log10 (P-value) which determines the significance of the association between SNPs and traits. The horizontal line indicates the genome-wide significance threshold (FDR <10%). To the right, Q-Q plot for the corresponding trait shows the distribution of the observed P-values alongside their expected values.

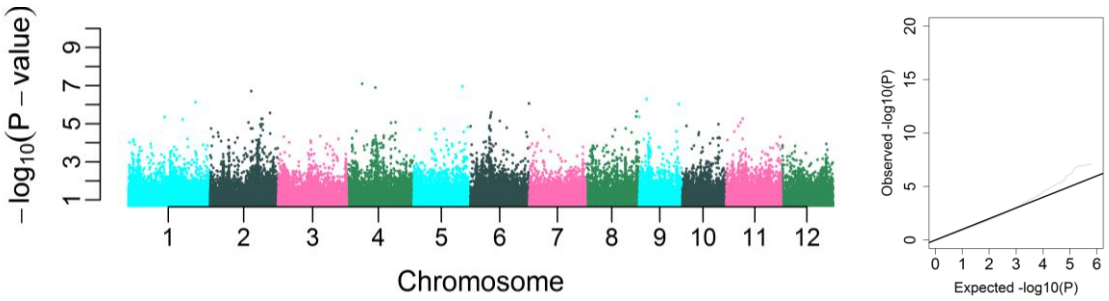

Supplementary Figure 3. 53: Genome-wide P-values from the mixed model method based on fresh weight shoot-to-root ratio reduction in 0.1 NPK plants. The X-axis shows the location of the identified SNPs along the 12 chromosomes of the rice genome, the Y-axis indicates the -log10 (P-value) which determines the significance of the association between SNPs and traits. The horizontal line indicates the genome-wide significance threshold (FDR <10%). To the right, Q-Q plot for the corresponding trait shows the distribution of the observed P-values alongside their expected values.

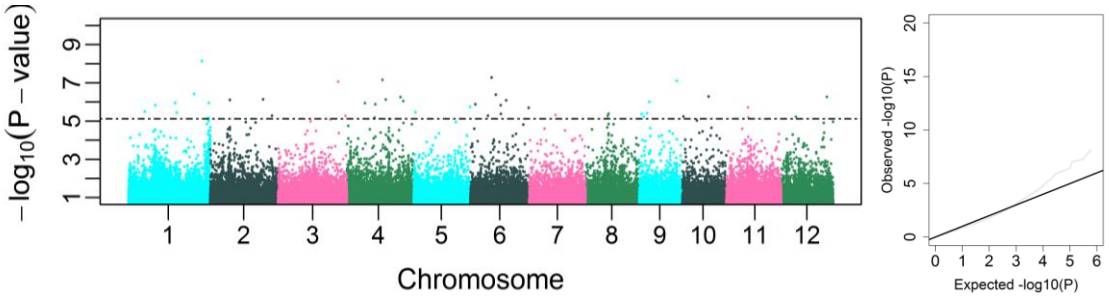

Supplementary Figure 3. 54: Genome-wide P-values from the mixed model method based on dry weight reduction in 0.1 NPK plants. The X-axis shows the location of the identified SNPs along the 12 chromosomes of the rice genome, the Y-axis indicates the -log10 (P-value) which determines the significance of the association between SNPs and traits. The horizontal line indicates the genome-wide significance threshold (FDR <10%). To the right, Q-Q plot for the corresponding trait shows the distribution of the observed P-values alongside their expected values.

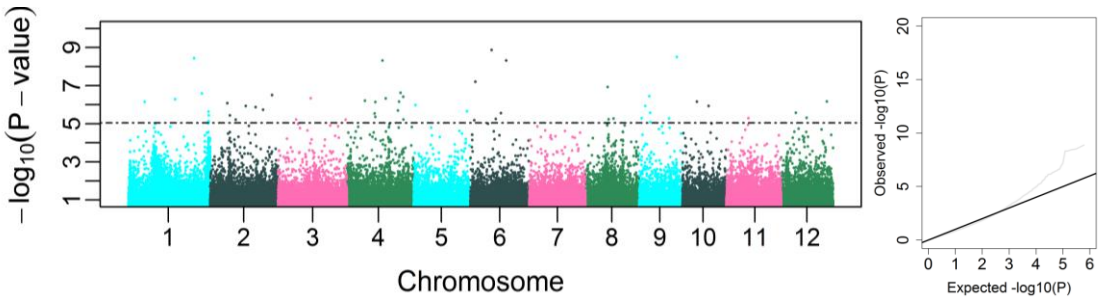

Supplementary Figure 3. 55: Genome-wide P-values from the mixed model method based on shoot dry weight reduction in 0.1 NPK plants. The X-axis shows the location of the identified SNPs along the 12 chromosomes of the rice genome, the Y-axis indicates the -log10 (P-value) which determines the significance of the association between SNPs and traits. The horizontal line indicates the genome-wide significance threshold (FDR <10%). To the right, Q-Q plot for the corresponding trait shows the distribution of the observed P-values alongside their expected values.

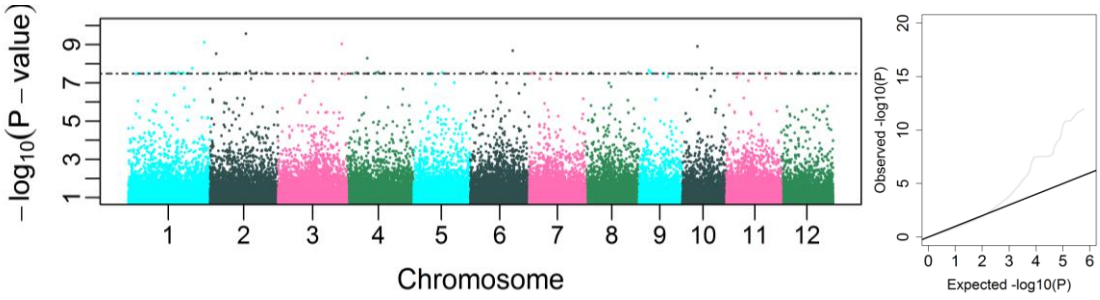

Supplementary Figure 3. 56: Genome-wide P-values from the mixed model method based on root dry weight reduction in 0.1 NPK plants. The X-axis shows the location of the identified SNPs along the 12 chromosomes of the rice genome, the Y-axis indicates the -log10 (P-value) which determines the significance of the association between SNPs and traits. The horizontal line indicates the genome-wide significance threshold (FDR <10%). To the right, Q-Q plot for the corresponding trait shows the distribution of the observed P-values alongside their expected values.

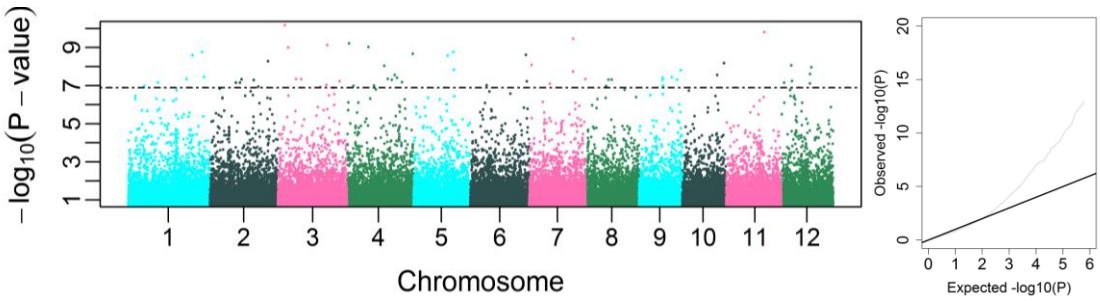

Supplementary Figure 3. 57: Genome-wide P-values from the mixed model method based on dry weight shoot-to-root ratio reduction in 0.1 NPK plants. The X-axis shows the location of the identified SNPs along the 12 chromosomes of the rice genome, the Y-axis indicates the -log10 (P-value) which determines the significance of the association between SNPs and traits. The horizontal line indicates the genome-wide significance threshold (FDR <10%). To the right, Q-Q plot for the corresponding trait shows the distribution of the observed P-values alongside their expected values.

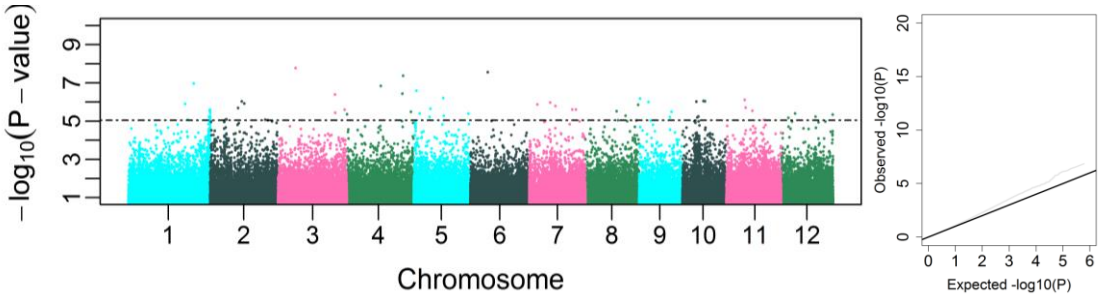

Supplementary Figure 3. 58: Genome-wide P-values from the mixed model method based on shoot nitrogen content on dry weight basis (µmoles/gDW) reduction in 0.1 NPK plants. The X-axis shows the location of the identified SNPs along the 12 chromosomes of the rice genome, the Y-axis indicates the -log10 (P-value) which determines the significance of the association between SNPs and traits. The horizontal line indicates the genome-wide significance threshold (FDR <10%). To the right, Q-Q plot for the corresponding trait shows the distribution of the observed P-values alongside their expected values.

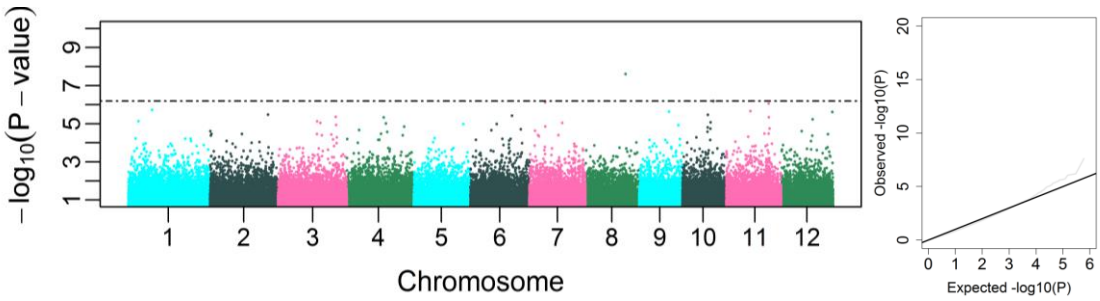

Supplementary Figure 3. 59: Genome-wide P-values from the mixed model method based on shoot phosphorus content on dry weight basis (µmoles/gDW) reduction in 0.1 NPK plants. The X-axis shows the location of the identified SNPs along the 12 chromosomes of the rice genome, the Y-axis indicates the -log10 (P-value) which determines the significance of the association between SNPs and traits. The horizontal line indicates the genome-wide significance threshold (FDR <10%). To the right, Q-Q plot for the corresponding trait shows the distribution of the observed P-values alongside their expected values.

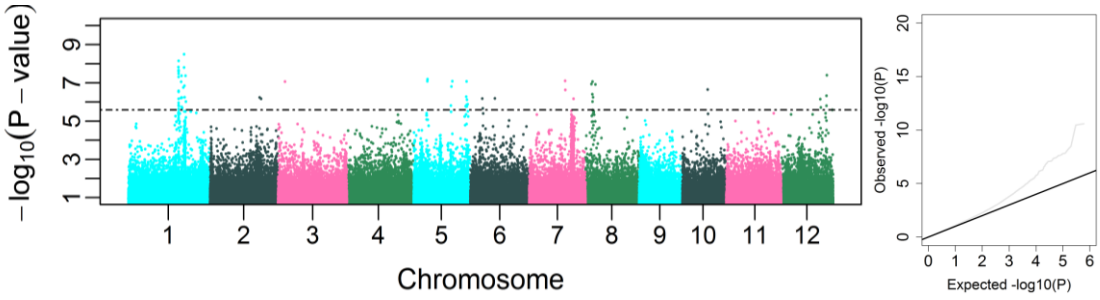

Supplementary Figure 3. 60: Genome-wide P-values from the mixed model method based on shoot potassium content on dry weight basis (µmoles/gDW) reduction in 0.1 NPK plants. The X-axis shows the location of the identified SNPs along the 12 chromosomes of the rice genome, the Y-axis indicates the -log10 (P-value) which determines the significance of the association between SNPs and traits. The horizontal line indicates the genome-wide significance threshold (FDR <10%). To the right, Q-Q plot for the corresponding trait shows the distribution of the observed P-values alongside their expected values.

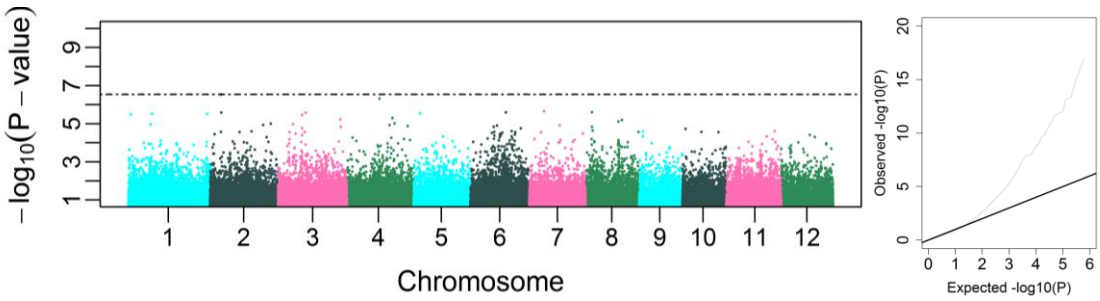

Supplementary Figure 3. 61: Genome-wide P-values from the mixed model method based on shoot sodium content on dry weight basis (µmoles/gDW) reduction in 0.1 NPK plants. The X-axis shows the location of the identified SNPs along the 12 chromosomes of the rice genome, the Y-axis indicates the -log10 (P-value) which determines the significance of the association between SNPs and traits. The horizontal line indicates the genome-wide significance threshold (FDR <10%). To the right, Q-Q plot for the corresponding trait shows the distribution of the observed P-values alongside their expected values.

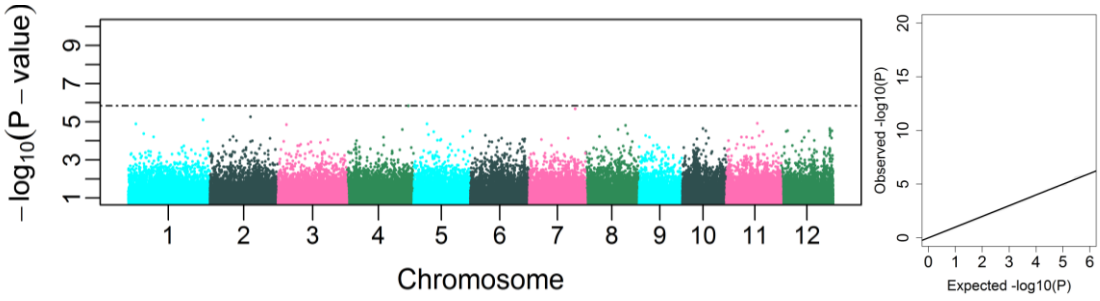

Supplementary Figure 3. 62: Genome-wide P-values from the mixed model method based on shoot zinc content on dry weight basis (µmoles/gDW) reduction in 0.1 NPK plants. The X-axis shows the location of the identified SNPs along the 12 chromosomes of the rice genome, the Y-axis indicates the -log10 (P-value) which determines the significance of the association between SNPs and traits. The horizontal line indicates the genome-wide significance threshold (FDR <10%). To the right, Q-Q plot for the corresponding trait shows the distribution of the observed P-values alongside their expected values.

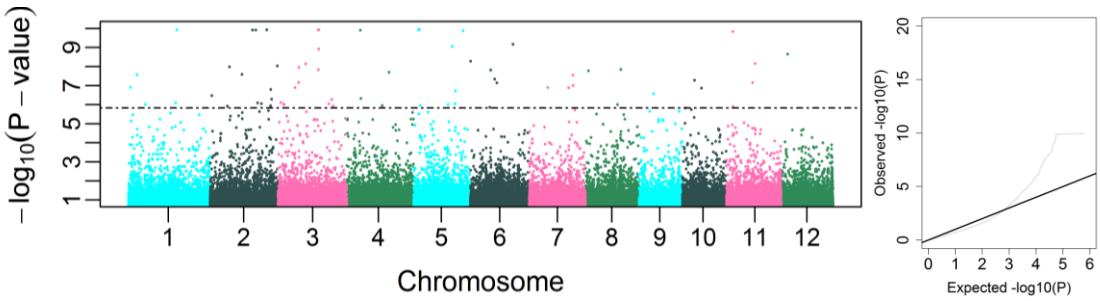

Supplementary Figure 3. 63: Genome-wide P-values from the mixed model method based on shoot iron content on dry weight basis (µmoles/gDW) reduction in 0.1 NPK plants. The X-axis shows the location of the identified SNPs along the 12 chromosomes of the rice genome, the Y-axis indicates the -log10 (P-value) which determines the significance of the association between SNPs and traits. The horizontal line indicates the genome-wide significance threshold (FDR <10%). To the right, Q-Q plot for the corresponding trait shows the distribution of the observed P-values alongside their expected values.

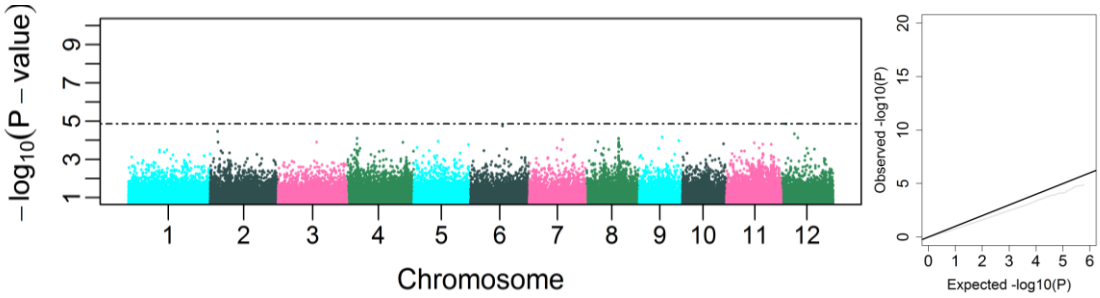

Supplementary Figure 3. 64: Genome-wide P-values from the mixed model method based on shoot boron content on dry weight basis (µmoles/gDW) reduction in 0.1 NPK plants. The X-axis shows the location of the identified SNPs along the 12 chromosomes of the rice genome, the Y-axis indicates the -log10 (P-value) which determines the significance of the association between SNPs and traits. The horizontal line indicates the genome-wide significance threshold (FDR <10%). To the right, Q-Q plot for the corresponding trait shows the distribution of the observed P-values alongside their expected values.

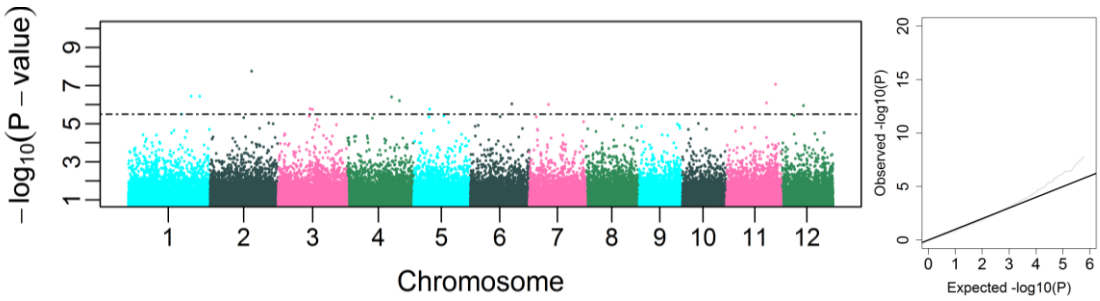

Supplementary Figure 3. 65: Genome-wide P-values from the mixed model method based on shoot carbon content on dry weight basis (µmoles/gDW) reduction in 0.1 NPK plants. The X-axis shows the location of the identified SNPs along the 12 chromosomes of the rice genome, the Y-axis indicates the -log10 (P-value) which determines the significance of the association between SNPs and traits. The horizontal line indicates the genome-wide significance threshold (FDR <10%). To the right, Q-Q plot for the corresponding trait shows the distribution of the observed P-values alongside their expected values.

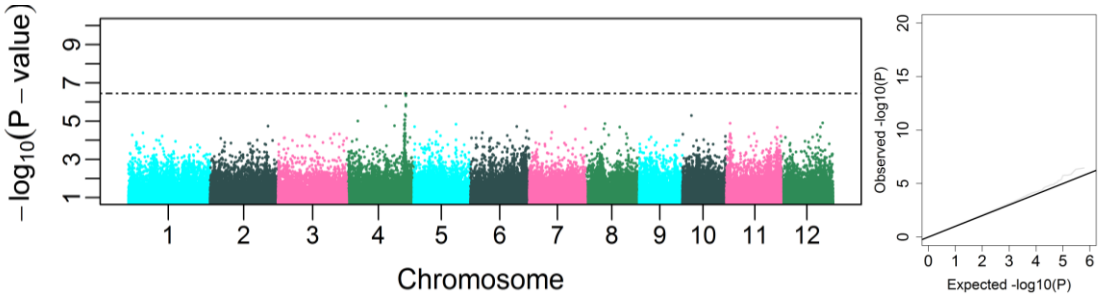

Supplementary Figure 3. 66: Genome-wide P-values from the mixed model method based on shoot magnesium content on dry weight basis (µmoles/gDW) reduction in 0.1 NPK plants. The X-axis shows the location of the identified SNPs along the 12 chromosomes of the rice genome, the Y-axis indicates the -log10 (P-value) which determines the significance of the association between SNPs and traits. The horizontal line indicates the genome-wide significance threshold (FDR <10%). To the right, Q-Q plot for the corresponding trait shows the distribution of the observed P-values alongside their expected values.

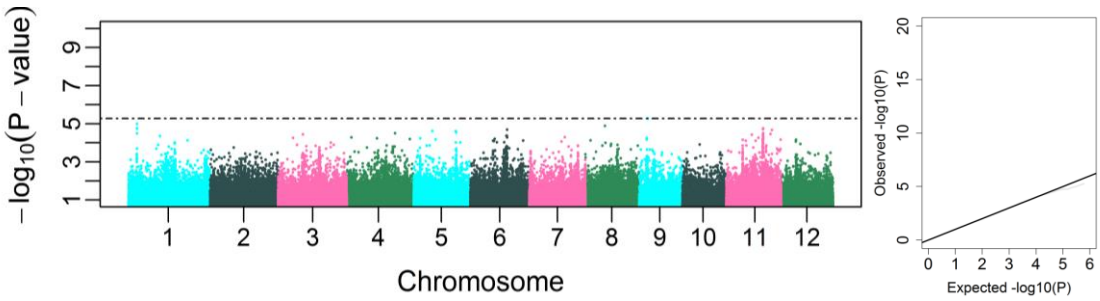

Supplementary Figure 3. 67: Genome-wide P-values from the mixed model method based on shoot calcium content on dry weight basis (µmoles/gDW) reduction in 0.1 NPK plants. The X-axis shows the location of the identified SNPs along the 12 chromosomes of the rice genome, the Y-axis indicates the -log10 (P-value) which determines the significance of the association between SNPs and traits. The horizontal line indicates the genome-wide significance threshold (FDR <10%). To the right, Q-Q plot for the corresponding trait shows the distribution of the observed P-values alongside their expected values.

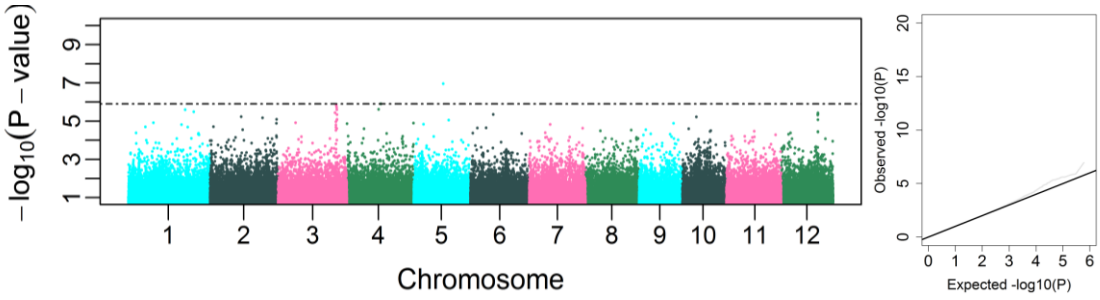

Supplementary Figure 3. 68: Genome-wide P-values from the mixed model method based on shoot nitrogen content on fresh weight basis (µmoles/gFW) reduction in 0.1 NPK plants. The X-axis shows the location of the identified SNPs along the 12 chromosomes of the rice genome, the Y-axis indicates the -log10 (P-value) which determines the significance of the association between SNPs and traits. The horizontal line indicates the genome-wide significance threshold (FDR <10%). To the right, Q-Q plot for the corresponding trait shows the distribution of the observed P-values alongside their expected values.

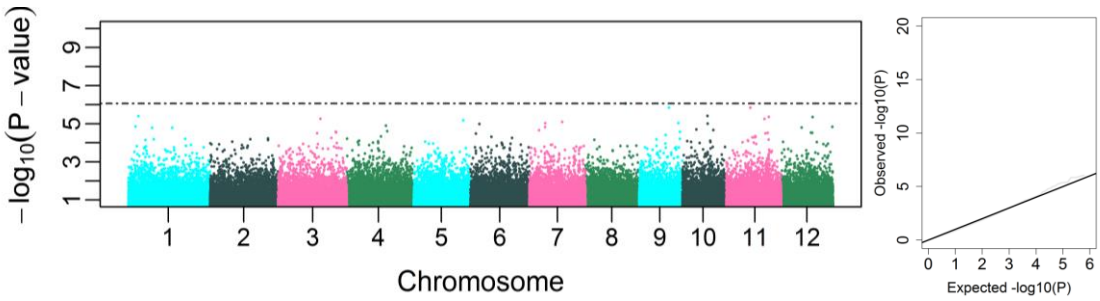

Supplementary Figure 3. 69: Genome-wide P-values from the mixed model method based on shoot phosphorus content on fresh weight basis (µmoles/gFW) reduction in 0.1 NPK plants. The X-axis shows the location of the identified SNPs along the 12 chromosomes of the rice genome, the Y-axis indicates the -log10 (P-value) which determines the significance of the association between SNPs and traits. The horizontal line indicates the genome-wide significance threshold (FDR <10%). To the right, Q-Q plot for the corresponding trait shows the distribution of the observed P-values alongside their expected values.

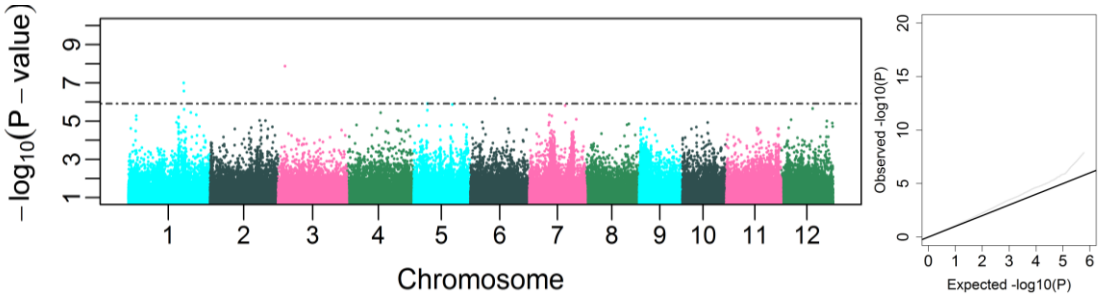

Supplementary Figure 3. 70: Genome-wide P-values from the mixed model method based on shoot potassium content on fresh weight basis (µmoles/gFW) reduction in 0.1 NPK plants. The X-axis shows the location of the identified SNPs along the 12 chromosomes of the rice genome, the Y-axis indicates the -log10 (P-value) which determines the significance of the association between SNPs and traits. The horizontal line indicates the genome-wide significance threshold (FDR <10%). To the right, Q-Q plot for the corresponding trait shows the distribution of the observed P-values alongside their expected values.

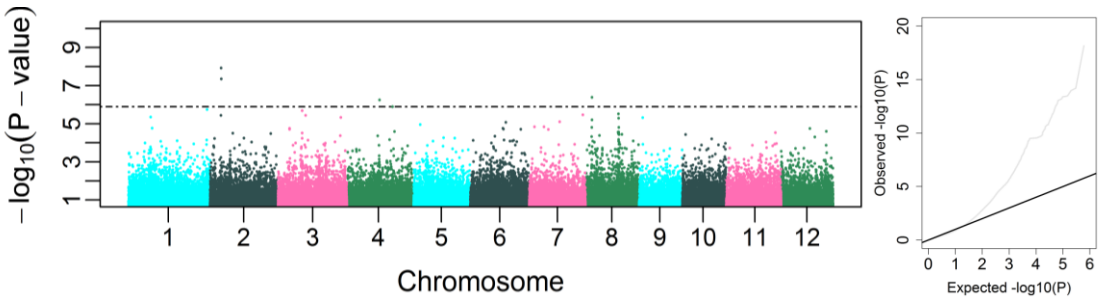

Supplementary Figure 3. 71: Genome-wide P-values from the mixed model method based on shoot sodium content on fresh weight basis (µmoles/gFW) reduction in 0.1 NPK plants. The X-axis shows the location of the identified SNPs along the 12 chromosomes of the rice genome, the Y-axis indicates the -log10 (P-value) which determines the significance of the association between SNPs and traits. The horizontal line indicates the genome-wide significance threshold (FDR <10%). To the right, Q-Q plot for the corresponding trait shows the distribution of the observed P-values alongside their expected values.

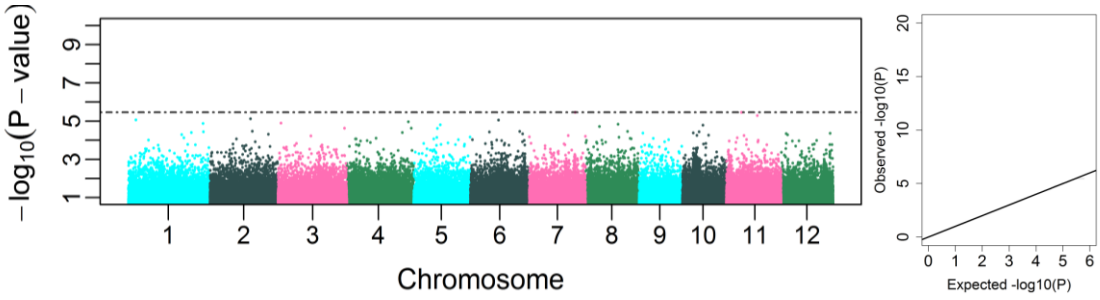

Supplementary Figure 3. 72: Genome-wide P-values from the mixed model method based on shoot zinc content on fresh weight basis (µmoles/gFW) reduction in 0.1 NPK plants. The X-axis shows the location of the identified SNPs along the 12 chromosomes of the rice genome, the Y-axis indicates the -log10 (P-value) which determines the significance of the association between SNPs and traits. The horizontal line indicates the genome-wide significance threshold (FDR <10%). To the right, Q-Q plot for the corresponding trait shows the distribution of the observed P-values alongside their expected values.

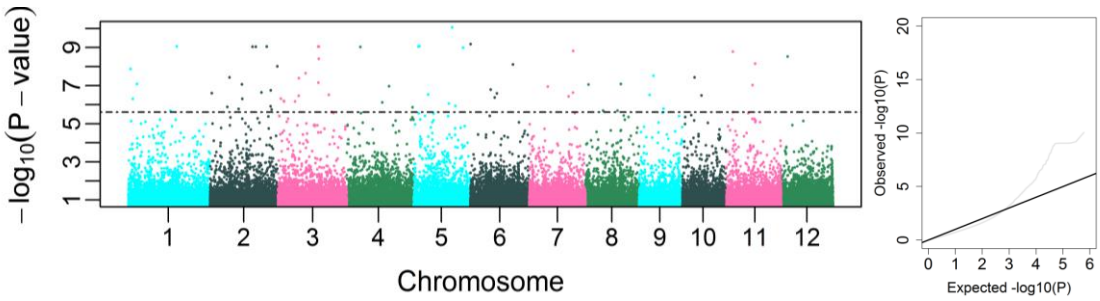

Supplementary Figure 3. 73: Genome-wide P-values from the mixed model method based on shoot iron content on fresh weight basis (µmoles/gFW) reduction in 0.1 NPK plants. The X-axis shows the location of the identified SNPs along the 12 chromosomes of the rice genome, the Y-axis indicates the -log10 (P-value) which determines the significance of the association between SNPs and traits. The horizontal line indicates the genome-wide significance threshold (FDR <10%). To the right, Q-Q plot for the corresponding trait shows the distribution of the observed P-values alongside their expected values.

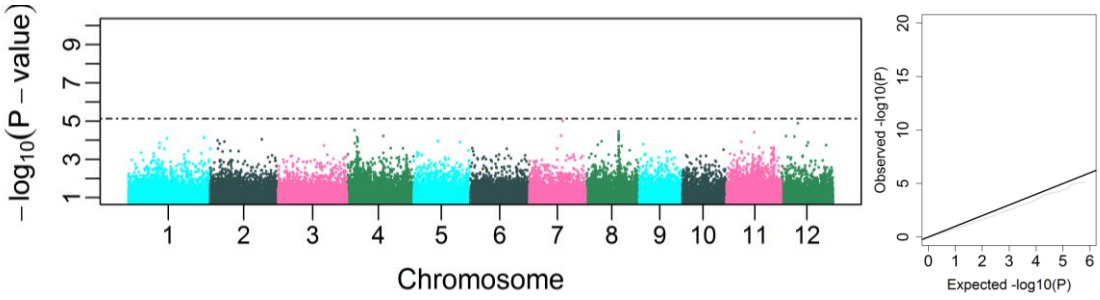

Supplementary Figure 3. 74: Genome-wide P-values from the mixed model method based on shoot boron content on fresh weight basis (µmoles/gFW) reduction in 0.1 NPK plants. The X-axis shows the location of the identified SNPs along the 12 chromosomes of the rice genome, the Y-axis indicates the -log10 (P-value) which determines the significance of the association between SNPs and traits. The horizontal line indicates the genome-wide significance threshold (FDR <10%). To the right, Q-Q plot for the corresponding trait shows the distribution of the observed P-values alongside their expected values.

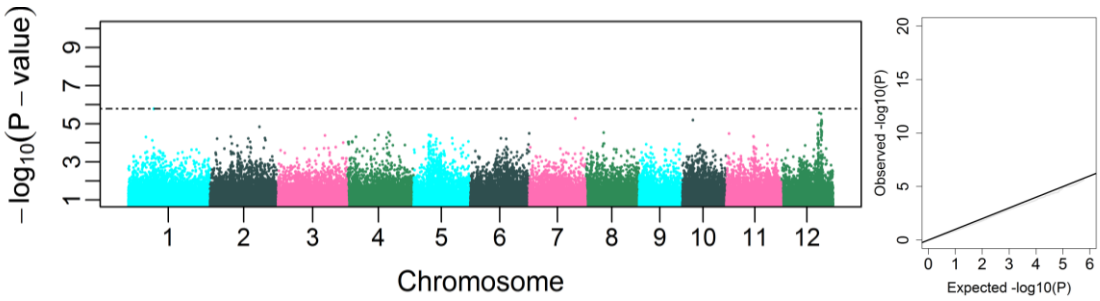

Supplementary Figure 3. 75: Genome-wide P-values from the mixed model method based on shoot carbon content on fresh weight basis (µmoles/gFW) reduction in 0.1 NPK plants. The X-axis shows the location of the identified SNPs along the 12 chromosomes of the rice genome, the Y-axis indicates the -log10 (P-value) which determines the significance of the association between SNPs and traits. The horizontal line indicates the genome-wide significance threshold (FDR <10%). To the right, Q-Q plot for the corresponding trait shows the distribution of the observed P-values alongside their expected values.

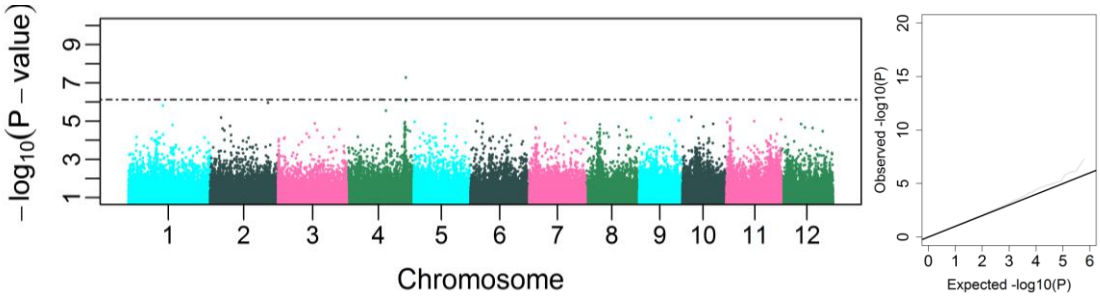

Supplementary Figure 3. 76: Genome-wide P-values from the mixed model method based on shoot magnesium content on fresh weight basis (µmoles/gFW) reduction in 0.1 NPK plants. The X-axis shows the location of the identified SNPs along the 12 chromosomes of the rice genome, the Y-axis indicates the -log10 (P-value) which determines the significance of the association between SNPs and traits. The horizontal line indicates the genome-wide significance threshold (FDR <10%). To the right, Q-Q plot for the corresponding trait shows the distribution of the observed P-values alongside their expected values.

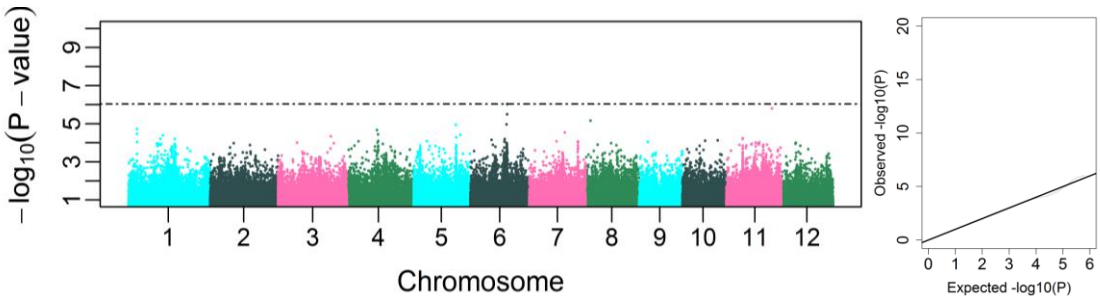

Supplementary Figure 3. 77: Genome-wide P-values from the mixed model method based on shoot calcium content on fresh weight basis (µmoles/gFW) reduction in 0.1 NPK plants. The X-axis shows the location of the identified SNPs along the 12 chromosomes of the rice genome, the Y-axis indicates the -log10 (P-value) which determines the significance of the association between SNPs and traits. The horizontal line indicates the genome-wide significance threshold (FDR <10%). To the right, Q-Q plot for the corresponding trait shows the distribution of the observed P-values alongside their expected values.

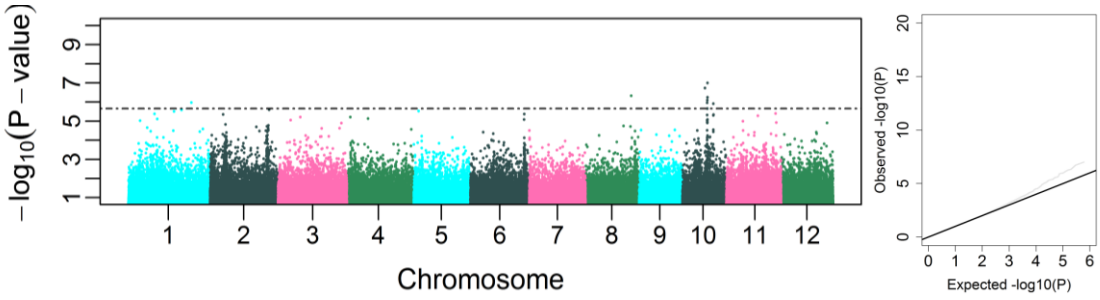

Supplementary Figure 3. 78: Genome-wide P-values from the mixed model method based on nitrogen use efficiency in 0.1 NPK plants. The X-axis shows the location of the identified SNPs along the 12 chromosomes of the rice genome, the Y-axis indicates the -log10 (P-value) which determines the significance of the association between SNPs and traits. The horizontal line indicates the genome-wide significance threshold (FDR <10%). To the right, Q-Q plot for the corresponding trait shows the distribution of the observed P-values alongside their expected values.

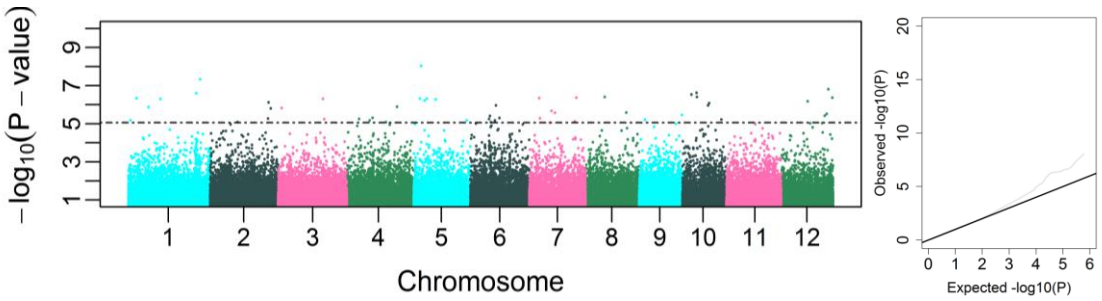

Supplementary Figure 3. 79: Genome-wide P-values from the mixed model method based on phosphorus use efficiency in 0.1 NPK plants. The X-axis shows the location of the identified SNPs along the 12 chromosomes of the rice genome, the Y-axis indicates the -log10 (P-value) which determines the significance of the association between SNPs and traits. The horizontal line indicates the genome-wide significance threshold (FDR <10%). To the right, Q-Q plot for the corresponding trait shows the distribution of the observed P-values alongside their expected values.

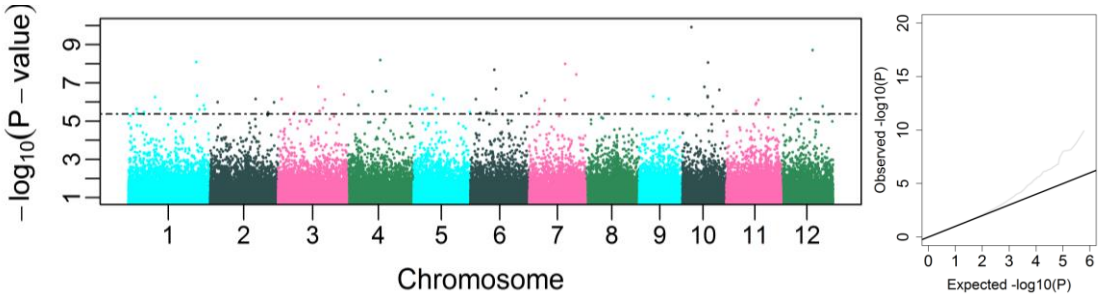

Supplementary Figure 3. 80: Genome-wide P-values from the mixed model method based on potassium use efficiency in 0.1 NPK plants. The X-axis shows the location of the identified SNPs along the 12 chromosomes of the rice genome, the Y-axis indicates the -log10 (P-value) which determines the significance of the association between SNPs and traits. The horizontal line indicates the genome-wide significance threshold (FDR <10%). To the right, Q-Q plot for the corresponding trait shows the distribution of the observed P-values alongside their expected values.

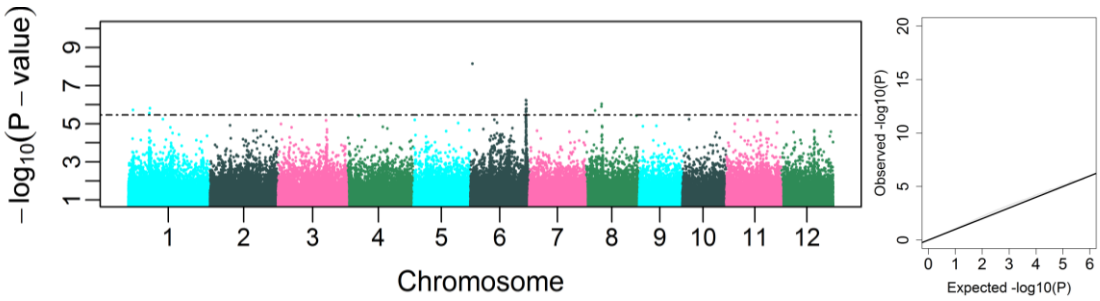

Supplementary Figure 3. 81: Genome-wide P-values from the mixed model method based on sodium use efficiency in 0.1 NPK plants. The X-axis shows the location of the identified SNPs along the 12 chromosomes of the rice genome, the Y-axis indicates the -log10 (P-value) which determines the significance of the association between SNPs and traits. The horizontal line indicates the genome-wide significance threshold (FDR <10%). To the right, Q-Q plot for the corresponding trait shows the distribution of the observed P-values alongside their expected values.

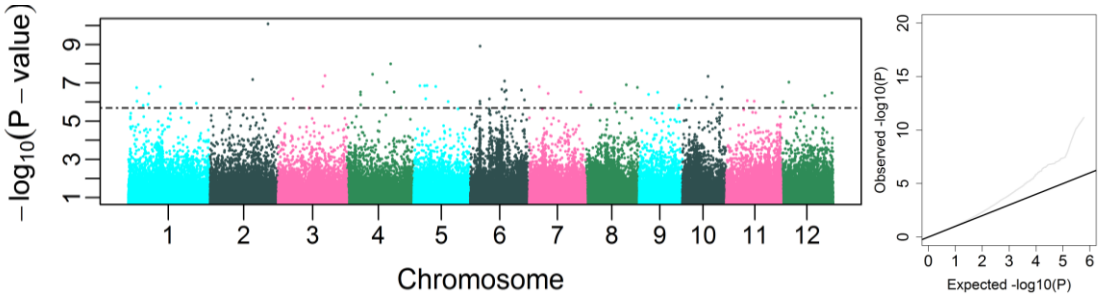

Supplementary Figure 3. 82: Genome-wide P-values from the mixed model method based on zinc use efficiency in 0.1 NPK plants. The X-axis shows the location of the identified SNPs along the 12 chromosomes of the rice genome, the Y-axis indicates the -log10 (P-value) which determines the significance of the association between SNPs and traits. The horizontal line indicates the genome-wide significance threshold (FDR <10%). To the right, Q-Q plot for the corresponding trait shows the distribution of the observed P-values alongside their expected values.

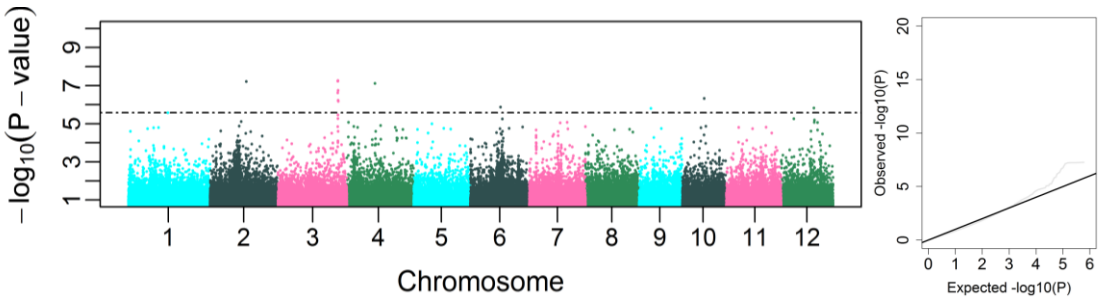

Supplementary Figure 3. 83: Genome-wide P-values from the mixed model method based on iron use efficiency in 0.1 NPK plants. The X-axis shows the location of the identified SNPs along the 12 chromosomes of the rice genome, the Y-axis indicates the -log10 (P-value) which determines the significance of the association between SNPs and traits. The horizontal line indicates the genome-wide significance threshold (FDR <10%). To the right, Q-Q plot for the corresponding trait shows the distribution of the observed P-values alongside their expected values.

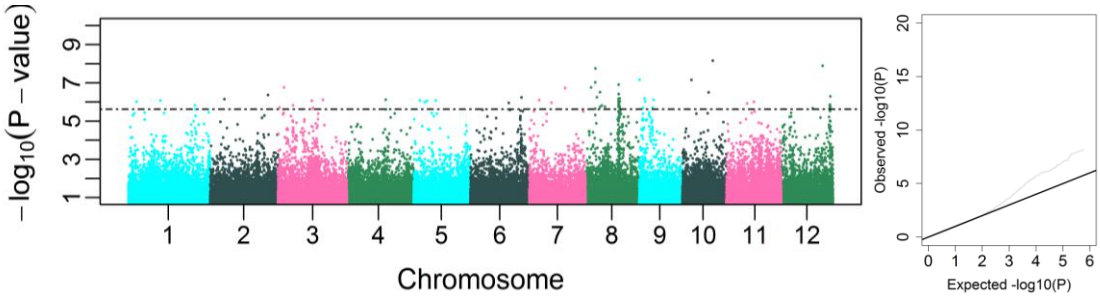

Supplementary Figure 3. 84: Genome-wide P-values from the mixed model method based on boron use efficiency in 0.1 NPK plants. The X-axis shows the location of the identified SNPs along the 12 chromosomes of the rice genome, the Y-axis indicates the -log10 (P-value) which determines the significance of the association between SNPs and traits. The horizontal line indicates the genome-wide significance threshold (FDR <10%). To the right, Q-Q plot for the corresponding trait shows the distribution of the observed P-values alongside their expected values.

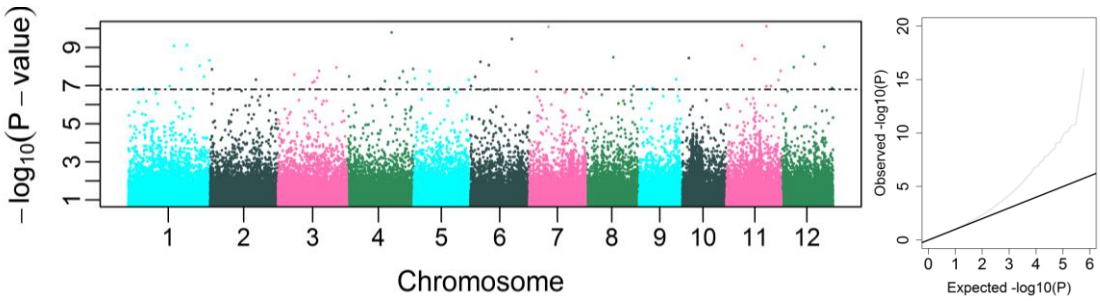

Supplementary Figure 3. 85: Genome-wide P-values from the mixed model method based on carbon use efficiency in 0.1 NPK plants. The X-axis shows the location of the identified SNPs along the 12 chromosomes of the rice genome, the Y-axis indicates the -log10 (P-value) which determines the significance of the association between SNPs and traits. The horizontal line indicates the genome-wide significance threshold (FDR <10%). To the right, Q-Q plot for the corresponding trait shows the distribution of the observed P-values alongside their expected values.

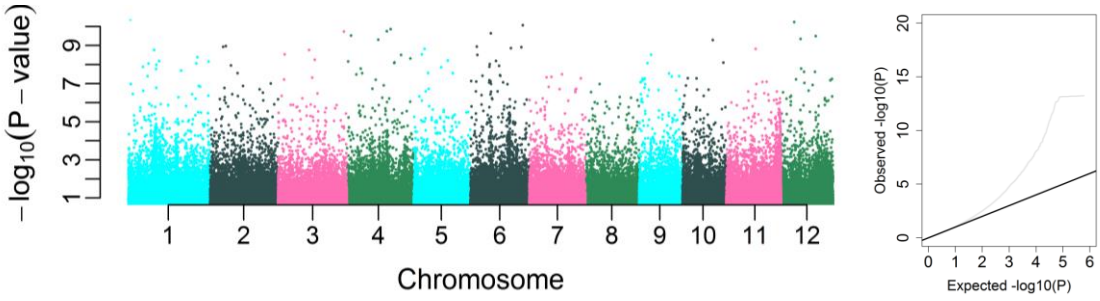

Supplementary Figure 3. 86: Genome-wide P-values from the mixed model method based on magnesium use efficiency in 0.1 NPK plants. The X-axis shows the location of the identified SNPs along the 12 chromosomes of the rice genome, the Y-axis indicates the -log10 (P-value) which determines the significance of the association between SNPs and traits. The horizontal line indicates the genome-wide significance threshold (FDR <10%). To the right, Q-Q plot for the corresponding trait shows the distribution of the observed P-values alongside their expected values.

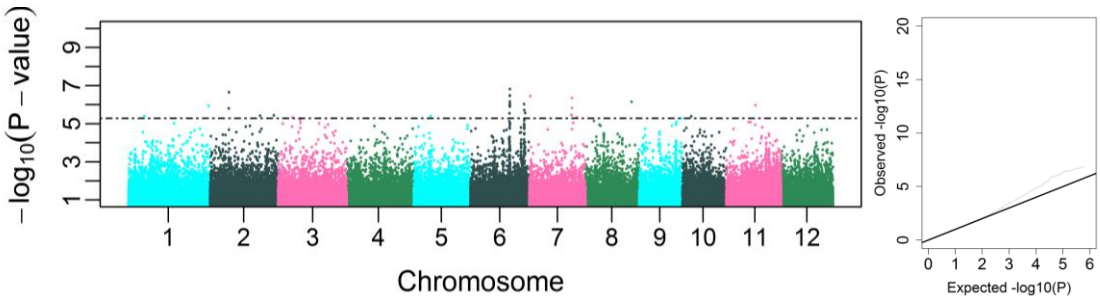

Supplementary Figure 3. 87: Genome-wide P-values from the mixed model method based on calcium use efficiency in 0.1 NPK plants. The X-axis shows the location of the identified SNPs along the 12 chromosomes of the rice genome, the Y-axis indicates the -log10 (P-value) which determines the significance of the association between SNPs and traits. The horizontal line indicates the genome-wide significance threshold (FDR <10%). To the right, Q-Q plot for the corresponding trait shows the distribution of the observed P-values alongside their expected values.

Abbreviations

ADI: admixed indica

ADJ: admixed japonica

ADM: admixed

ANOVA: analysis of variance

ARO: aromatic

bp: base pairs

BUE: boron use efficiency

CaUE: calcium use efficiency

Chr.: chromosome

CRISPR clustered regularly interspaced short palindromic repeats

CRM: certified reference material

CT: control treatment

CUE: carbon use efficiency

DW: total dry weight

DWSR: dry weight shoot to root ratio

FAO: Food and Agricultural Organization of the United Nations

FASTA: Family-Based Score Test for Association

FeUE: iron use efficiency

FW: total final fresh weight

FWSR: fresh weight shoot to root ratio

GO: gene ontology

gRNA: guide RNA

GWAS: genome-wide association study

HDRA: high density rice array

ICP-OES: inductively coupled plasma optical emission spectrometry

IND: indica

IW: initial weight

KUE: potassium use efficiency

LMM: linear mixed model

LT: low treatment

MgUE: magnesium use efficiency

NaUE: sodium use efficiency

nm: nanometer

nsSNPs: Nonsynonymous SNPs

NUE: nitrogen use efficiency

PC: principal component

PCA: principal component analysis

PUE: phosphorususe efficiency

QQ: Quantile-quantile

QTL: Quantitative trait loci

RDP1: rice diversity panel 1

RDP2: rice diversity panel 2

RDW: root dry weight

RED: reduction

RFW: root fresh weight

RGR: relative growth rate

RGRRED: relative growth rate reduction

SDW: shoot dry weight

SFW: shoot fresh weight

SNP: single nucleotide polymorphism

TEJ: temperate japonica

TRJ: tropical japonica

UE: nutrient use efficiency

ZnUE: zinc use efficiency

References

Ahmad, I., Devonshire, J., Mohamed, R., Schultze, M. & Maathuis, F. J. M. (2016a). Overexpression of the potassium channel TPKb in small vacuoles confers osmotic and drought tolerance to rice. *New Phytologist* 209: 1040-1048.

Ahmad, I., Mian, A. & Maathuis, F. J. (2016b). Overexpression of the rice AKT1 potassium channel affects potassium nutrition and rice drought tolerance. *Journal of Experimental Botany* 67: 2689-2698.

Ai, P., Sun, S., Zhao, J., Fan, X., Xin, W., Guo, Q., Yu, L., Shen, Q., Wu, P., Miller, A. J. & Xu, G. (2009). Two rice phosphate transporters, OsPht1;2 and OsPht1;6, have different functions and kinetic properties in uptake and translocation. *The Plant Journal* 57: 798-809.

Amrani, N., Dong, S., He, F., Ganesan, R., Ghosh, S., Kervestin, S., Li, C., Mangus, D., Spatrick, P. & Jacobson, A. (2006). Aberrant termination triggers nonsense-mediated mRNA decay. *Biochemical Society Transactions* 34: 39-42.

Amtmann, A., Troufflard, S., and Armengaud, P. (2008). The effect of potassium nutrition on pest and disease resistance in plants (Oxford, UK), pp. 682-691.

Araki, R. & Hasegawa, H. (2006). Expression of rice (*Oryza sativa* L.) genes involved in high- affinity nitrate transport during the period of nitrate induction. *Breeding Science* 56: 295-302.

Ashley, M. K., Grant, M. & Grabov, A. (2006). Plant responses to potassium deficiencies: A role for potassium transport proteins. *Journal of Experimental Botany* 57, 425-436.

Atkinson, N. J. & Urwin, P. E. (2012). The interaction of plant biotic and abiotic stresses: from genes to the field. *Journal of Experimental Botany* 63: 3523-3543.

Aulakh, M. S. & Malhi, S. S. (2005). Interactions of nitrogen with other nutrients and water: effect on crop yield and quality, nutrient use efficiency, carbon sequestration, and environmental pollution. *Advances in Agronomy* 86: 341-409.

Aulchenko, Y. S., Ripke, S., Isaacs, A. & Van Duijn, C. M. (2007). GenABEL: an R library for genome-wide association analysis. *Bioinformatics* 23(10): 1294-1296.

Baligar, V. & Bennett, O. (1986a). NPK-fertilizer efficiency—a situation analysis for the tropics. *Fertilizer Research* 10: 147-164.

Baligar, V. & Bennett, O. (1986b). Outlook on fertilizer use efficiency in the tropics. *Fertilizer Research* 10: 83-96.

Baligar, V. C., Fageria, N. K. & He, Z. L. (2001). Nutrient use efficiency in plants. *Communications in Soil Science and Plant Analysis* 32: 921-950.

Baligar, V., Fageria, N. & Elrashidi, M. (1998). Toxicity and nutrient constraints on root growth. *HortScience* 33: 960-965.

Bañuelos, M. a. A., Garciadeblas, B., Cubero, B. & Rodríguez-Navarro, A. (2002). Inventory and functional characterization of the HAK potassium transporters of rice. *Plant Physiology* 130: 784-795.

Bao, A., Liang, Z., Zhao, Z. & Cai, H. (2015). Overexpressing of OsAMT1-3, a high affinity ammonium transporter gene, modifies rice growth and carbon-nitrogen metabolic status. *International Journal of Molecular Sciences* 16: 9037-9063.

Barneix, A. J. & Breteler, H. (1985). Effect of cations on uptake, translocation and reduction of nitrate in wheat seedlings. *New Phytologist* 99: 367-379.

Bates, D., Mächler, M., Bolker, B. & Walker, S. (2015). Fitting linear mixed-effects models using lme4. *Journal of Statistical Software* 67: 1-48.

Baunsgaard, L., Venema, K., Axelsen, K. B., Villalba, J. M., Welling, A., Wollenweber, B. & Palmgren, M. G. (1996). Modified plant plasma membrane H^+-ATPase with improved transport coupling efficiency identified by mutant selection in yeast. *Plant Journal* 10: 451-458.

Baxter, I., Tchieu, J., Sussman, M. R., Boutry, M., Palmgren, M. G., Gribskov, M., Harper, J. F. & Axelsen, K. B. (2003). Genomic comparison of P-type ATPase ion pumps in Arabidopsis and rice. *Plant Physiology* 132: 618-628.

Belhaj, K., Chaparro-Garcia, A., Kamoun, S. & Nekrasov, V. (2013). Plant genome editing made easy: targeted mutagenesis in model and crop plants using the CRISPR/Cas system. *Plant Methods* 9: 39.

Belhaj, K., Chaparro-Garcia, A., Kamoun, S., Patron, N. J. & Nekrasov, V. (2015). Editing plant genomes with CRISPR/Cas9. *Current Opinion in Biotechnology* 32: 76-84.

Benjamini, Y. & Hochberg, Y. (1995). Controlling the false discovery rate: a practical and powerful approach to multiple testing. *Journal of the Royal Statistical Society. Series B (Methodological)* 57: 289-300.

Bethlenfalvay, G. J. (1992). Mycorrhizae and Crop Productivity. *Mycorrhizae in Sustainable Agriculture* 54:1-27.

Bhattacharjee, S. & Sharma, G. D. (2011). The vesicular arbuscular mycorrhiza associated with three cultivars of rice (*Oryza sativa* L.). *Indian Journal of Microbiology* 51: 377-383.

Bin, H., Wei, W., Shujun, O., Jiuyou, T., Hua, L., Ronghui, C., Zhihua, Z., Xuyang, C., Hongru, W., Yiqin, W., Chengzhen, L., Linchuan, L., Zhongze, P., Qiyun, D., Kun, D., Chi, X., Yan, L., Lianhe, Z., Legong, L. & Chengcai, C. (2015). Variation in NRT1.1B contributes to nitrate-use divergence between rice subspecies. *Nature Genetics* 47: 834-838.

Borlaug, N. (1994). Feeding a human population that increasing crowds a fragile planet. *Acapulco, MX: International Society of Soil Science*.

Bortesi, L. & Fischer, R. (2015). The CRISPR/ Cas9 system for plant genome editing and beyond. *Biotechnology Advances* 33: 41-52.

Brueck, H. (2008). Effects of nitrogen supply on water- use efficiency of higher plants. Journal of Plant Nutrition and Soil Science 171, 210-219.

Brueck, H., and Senbayram, M. (2009). Low nitrogen supply decreases water- use efficiency of oriental tobacco. Journal of Plant Nutrition and Soil Science 172, 216-223.

Bush, W. S. & Moore, J. H. (2012). Genome-wide association studies. *PLoS Computational Biology* 8: e1002822.

Campbell, M.T., Bandillo, N., Al Shiblawi, F.R.A., Sharma, S., Liu, K., Du, Q., Schmitz, A.J., Zhang, C., Very, A.A., Lorenz, A.J., et al. (2017). Allelic variants of OsHKT1;1 underlie the divergence between indica and japonica subspecies of rice (Oryza sativa) for root sodium content.(Research Article)(Report). PLoS Genetics 13, e1006823.

Chapman, N., Miller, A. J., Lindsey, K. & Whalley, W. R. (2012). Roots, water, and nutrient acquisition: let's get physical. *Trends Plant Sci.* 17: 701-710.

Chauhan, B.S., Jabran, K., and Mahajan, G. (2017). Rice production worldwide, Vol 247 (Springer).

Chen, G., Feng, H., Hu, Q., Qu, H., Chen, A., Yu, L. & Xu, G. (2015a). Improving rice tolerance to potassium deficiency by enhancing OsHAK16p: WOX11-controlled root development. *Plant Biotechnology Journal* 13: 833-848.

Chen, G., Hu, Q., Luo, L., Yang, T., Zhang, S., Hu, Y., Yu, L. & Xu, G. (2015b). Rice potassium transporter OsHAK1 is essential for maintaining potassium-mediated growth and functions in salt tolerance over low and high potassium concentration ranges. *Plant, Cell & Environment* 38: 2747-2765.

Chen, J., Liu, Y., Ni, J., Wang, Y., Bai, Y., Shi, J., Gan, J., Wu, Z. & Wu, P. (2011). OsPHF1 regulates the plasma membrane localization of low- and high-affinity inorganic phosphate transporters and determines inorganic phosphate uptake and translocation in rice. *Plant Physiology* 157: 269-278.

Chen, L., Lin, L., Cai, G., Sun, Y., Huang, T., Wang, K. & Deng, J. (2014). Identification of nitrogen, phosphorus, and potassium deficiencies in rice based on static scanning technology and hierarchical identification method. *PloS one* 9: e113200.

Chen, W.-M. & Abecasis, G. R. (2007). Family-based association tests for genomewide association scans. *The American Journal of Human Genetics* 81: 913-926.

Cheng, D., Wu, G., and Zheng, Y. (2015). Positive correlation between potassium uptake and salt tolerance in wheat. Photosynthetica 53, 447-454.

Chiou, T.-J. & Lin, S.-I. (2011). Signaling network in sensing phosphate availability in plants. *Annual Review of Plant Biology* 62: 185-206.

Cho, Y. I., Jiang, W., Chin, J. H., Piao, Z., Cho, Y. G., McCouch, S. R. & Koh, H. J. (2007). Identification of QTLs associated with physiological nitrogen use efficiency in rice. *Molecules and Cells* 23: 72-79.

Clark, R. B. & Baligar, V. C. (2000). Acidic and alkaline soil constraints on plant mineral nutrition. In: Plant Environment Interactions II, Marcel Dekker Inc, NY, pp. 133-177.

Clark, R. B. 1982. Plant response to mineral element toxicity and deficiency. In: M. N. Christiansen and C. F. Lewis (eds), Breeding Plants for Less Favorable Environments. John Wiley and Sons, New York, NY, pp. 71–73.

Collard, B. & Mackill, D. (2008). Marker-assisted selection: an approach for precision plant breeding in the twenty-first century. *Philos. Trans. R. Soc. B-Biol. Sci.* 363: 557-572.

Cong, L., Ran, F. A., Cox, D., Lin, S., Barretto, R., Habib, N., Hsu, P. D., Wu, X., Jiang, W. & Marraffini, L. (2013). Multiplex genome engineering using CRISPR/Cas systems. *Science*: 339: 819-823.

Cormier, F., Gouis, J., Dubreuil, P., Lafarge, S., and Praud, S. (2014). A genome- wide identification of chromosomal regions determining nitrogen use efficiency components in wheat (*Triticum aestivum* L.). Theoretical and Applied Genetics 127, 2679-2693.

Cotsaftis, O., Plett, D., Shirley, N., Tester, M. & Hrmova, M. (2012). A two-staged model of Na^+ exclusion in rice explained by 3D modeling of HKT transporters and alternative splicing. *PLoS ONE* 7: e39865.

De Datta, S., Samson, M., Obcemea, W., Real, J. & Buresh, R. (1991). Direct measurement of ammonia and denitrification fluxes from urea applied to rice. *Soil Science Society of America Journal* 55: 543-548.

De Datta, S.K. (1981). Principles and practices of rice production (Int. Rice Res. Inst.).
de Oliveira, L. F. V., Christoff, A. P., de Lima, J. C., de Ross, B. C. F., Sachetto-Martins, G., Margis-Pinheiro, M. & Margis, R. (2014). The Wall-associated Kinase gene family in rice genomes. *Plant Science* 229: 181-192.
Deeken, R., Geiger, D., Fromm, J., Koroleva, O., Ache, P., Langenfeld-Heyser, R., Sauer, N., May, S. T. & Hedrich, R. (2002). Loss of the AKT2/3 potassium channel affects sugar loading into the phloem of Arabidopsis. *Planta* 216: 334-344.
Dibb, D. & Thompson Jr, W. (1985). Interaction of potassium with other nutrients. In: *Potassium in Agriculture* pp. 515-533.
Dobermann, A. (2000). Rice: Nutrient disorders & nutrient management, Vol 1 (Int. Rice Res. Inst.).
Doench, J. G., Hartenian, E., Graham, D. B., Tothova, Z., Hegde, M., Smith, I., Sullender, M., Ebert, B. L., Xavier, R. J. & Root, D. E. (2014). Rational design of highly active sgRNAs for CRISPR-Cas9–mediated gene inactivation. *Nature Biotechnology* 32: 1262-1267.
Du, Z., Zhou, X., Ling, Y., Zhang, Z. & Su, Z. (2010). agriGO: a GO analysis toolkit for the agricultural community. *Nucleic Acids Research* 38: W64-W70.
Duan, Y.-H., Shi, X.-J., Li, S.-L., Sun, X.-F. & He, X.-H. (2014). Nitrogen use efficiency as affected by phosphorus and potassium in long- term rice and wheat experiments. *Journal of Integrative Agriculture* 13: 588-596.
Duby, G. & Boutry, M. (2009). The plant plasma membrane proton pump ATPase: a highly regulated P-type ATPase with multiple physiological roles. *Pflügers Archiv - European Journal of Physiology* 457: 645-655.
Edwards, K., Johnstone, C. & Thompson, C. (1991). A simple and rapid method for the preparation of plant genomic DNA for PCR analysis. *Nucleic Acids Research* 19: 1349.
Engler, C., Kandzia, R. & Marillonnet, S. (2008). A one pot, one step, precision cloning method with high throughput capability. *Plos One* 3: e3647.
Engler, C., Youles, M., Gruetzner, R., Ehnert, T.-M., Werner, S., Jones, J. D., Patron, N. J. & Marillonnet, S. (2014). A golden gate modular cloning toolbox for plants. *ACS Synthetic Biology* 3: 839-843.
Fageria, N. & Baligar, V. (2001). Lowland rice response to nitrogen fertilization. *Communications in Soil Science and Plant Analysis* 32: 1405-1429.
Fageria, N. & Baligar, V. (2005). Properties of termite mound soils and responses of rice and bean to nitrogen, phosphorus, and potassium fertilization on such soil. *Communications in Soil Science and Plant Analysis* 35: 2097-2109.
Fageria, N. & Gheyi, H. (1999). *Efficient crop production.* Universidade Federal.
Fageria, N. & Press, C. (2009). The use of nutrients in crop plants. *Cereal Res Commun* 37: 149-150.
Fageria, N. (2003). Plant tissue test for determination of optimum concentration and uptake of nitrogen at different growth stages in lowland rice. *Communications in Soil Science and Plant Analysis* 34: 259-270.
Fageria, N. K. & Baligar, V. C. (1997). Upland rice genotypes evaluation for phosphorus use efficiency. *Journal of Plant Nutrition* 20: 499-509.
Fageria, N. K. (1983). Ionic interactions in rice plants from dilute solutions. *Plant and Soil* 70: 309-316.
Fageria, N. K. (1992). *Maximizing crop yields.* CRC Press.

Fageria, N. K. (2008). *The use of nutrients in crop plants.* CRC Press.
Fageria, N. K. (2012). *The role of plant roots in crop production.* CRC Press.
Fageria, N. K., Baligar, V. C. & Clark, R. B. (2006). *Physiology of Crop Production.* Haworth Press Inc.
Fageria, N. K., Baligar, V. C. & Jones, C. A. (2010). *Growth and Mineral Nutrition of Field Crops.* CRC Press.
Fageria, N. K., De Morais, O. P., Dos Santos, A. B. & Vasconcelos, M. J. (2013a). Phosphorus use efficiency in upland rice genotypes under field conditions. *Journal of Plant Nutrition*. 37: 633-642.
Fageria, N. K., De Morais, O. P., Dos Santos, A. B. & Vasconcelos, M. J. (2014). Phosphorus use efficiency in upland rice genotypes under field conditions. *Journal of Plant Nutrition* 37: 633-642.
Fageria, N. K., Moreira, A. & dos Santos, A. B. (2013b). Phosphorus uptake and use efficiency in field crops. *Journal of Plant Nutrition* 36: 2013-2022.
Fageria, N. K., Moreira, A., Ferreira, E. P. B. & Knupp, A. M. (2013c). Potassium use efficiency in upland rice genotypes. *Communications in Soil Science and Plant Analysis*. 44: 2656-2665.
Fageria, N., Baligar, V. & Hillel, D. (2005). Nutrient availability. *Encyclopedia of Soils in the Environment* 3: 63-71.
Fageria, N., Baligar, V. & Li, Y. (2008). The role of nutrient efficient plants in improving crop yields in the twenty first century. *Journal of Plant Nutrition* 31: 1121-1157.
Fageria, N., Barbosa Filho, M., Stone, L., Guimães, C. (2004). Phosphorus nutrition for upland rice production. In: *Phosphorus in Brazilian Agriculture* (T. Yamada and S.R.S. Abdalla, eds), Brazilian Phosphorus and Potassium Institute, pp. 401-418.
Fageria, N., Slaton, N. & Baligar, V. (2003). Nutrient management for improving lowland rice productivity and sustainability. *Advances in Agronomy* 80: 63-152.
Falhof, J., Pedersen, Jesper t., Fuglsang, Anja t. & Palmgren, M. (2016). Plasma membrane H^+-ATPase regulation in the center of plant physiology. *Molecular Plant* 9: 323-337.
Fan, X., Tang, Z., Tan, Y., Zhang, Y., Luo, B., Yang, M., Lian, X., Shen, Q., Miller, A. J. & Xu, G. (2016). Overexpression of a pH-sensitive nitrate transporter in rice increases crop yields. *Proceedings of the National Academy of Sciences of the United States of America* 113: 7118-7123.
Fang, Y., Wu, W., Zhang, X., Jiang, H., Lu, W., Pan, J., Hu, J., Guo, L., Zeng, D. & Xue, D. (2015). Identification of quantitative trait loci associated with tolerance to low potassium and related ions concentrations at seedling stage in rice (*Oryza sativa* L.). *Plant Growth Regulation* 77: 157-166.
FAO (2013). Food and Agricultural Organization. FAOSTAT. http://faostat.fao.org/Rome.
FAO (2017). World fertilizer trends and outlook to 2020. Roma, Italy: FAO.
Faye, I., Diouf, O., Guissé, A., Sene, M. & Diallo, N. (2006). Characterizing root responses to low phosphorus in pearl millet [*Pennisetum glaucum* (L.) R. Br.]. *Agronomy Journal* 98: 1187-1194.
Fellbaum, C. R., Gachomo, E. W., Beesetty, Y., Choudhari, S., Strahan, G. D., Pfeffer, P. E., Kiers, E. T. & Bücking, H. (2012). Carbon availability triggers fungal nitrogen uptake and transport in arbuscular mycorrhizal symbiosis. *Proceedings of the National Academy of Sciences of the United States of America* 109: 2666- 2671.

Feng, H., Yan, M., Fan, X., Li, B., Shen, Q., Miller, A. J. & Xu, G. (2011). Spatial expression and regulation of rice high- affinity nitrate transporters by nitrogen and carbon status. *Journal of Experimental Botany* 62: 2319-2332.

Feng, Y., Cao, L. Y., Wu, W. M., Shen, X. H., Zhan, X. D., Zhai, R. R., Wang, R. C., Chen, D. B. & Cheng, S. H. (2010). Mapping QTLs for nitrogen- deficiency tolerance at seedling stage in rice (*Oryza sativa* L. *Plant Breeding* 129: 652-656.

Feng, Z., Mao, Y., Xu, N., Zhang, B., Wei, P., Yang, D.-L., Wang, Z., Zhang, Z., Zheng, R., Yang, L., Zeng, L., Liu, X. & Zhu, J.-K. (2014). Multigeneration analysis reveals the inheritance, specificity, and patterns of CRISPR/ Cas-induced gene modifications in Arabidopsis. *Proceedings of the National Academy of Sciences of the United States of America* 111: 4632- 4637.

Feng, Z., Zhang, B., Ding, W., Liu, X., Yang, D.-L., Wei, P., Cao, F., Zhu, S., Zhang, F. & Mao, Y. (2013). Efficient genome editing in plants using a CRISPR/Cas system. *Cell Research* 23: 1229.

Fuglsang, A. T., Paez-Valencia, J. & Gaxiola, R. (2011). Plant proton pumps: regulatory circuits involving H^+-ATPase and H^+-PPase. In: *Transporters and Pumps in Plant Signaling*, (M. Geisler and K. Venema, eds) Springer Verlag, pp. 39-64.

Fukuda, A., Nakamura, A., Tagiri, A., Tanaka, H., Miyao, A., Hirochika, H. & Tanaka, Y. (2004). Function, intracellular localization and the importance in salt tolerance of a vacuolar Na^+/H^+ antiporter from rice. *Plant and Cell Physiology* 45: 146-159.

Gajdanowicz, P., Michard, E., Sandmann, M., Rocha, M., Corrêa, L. G. G., Ramírez-Aguilar, S. J., Gomez-Porras, J. L., González, W., Thibaud, J.-B., Van Dongen, J. T. & Dreyer, I. (2011). Potassium (K^+) gradients serve as a mobile energy source in plant vascular tissues. *Proceedings of the National Academy of Sciences of the United States of America* 108: 864-869.

Garciadeblás, B., Senn, M. E., Bañuelos, M. A. & Rodríguez-Navarro, A. (2003). Sodium transport and HKT transporters: the rice model. *The Plant Journal* 34: 788-801.

Gattward, J. N., Almeida, A. A. F., Souza, J. O., Gomes, F. P. & Kronzucker, H. J. (2012). Sodium–potassium synergism in *Theobroma cacao*: stimulation of photosynthesis, water-use efficiency and mineral nutrition. *Physiologia Plantarum* 146: 350-362.

Gaur, V., Singh, U., Gupta, A. & Kumar, A. (2012). Understanding the differential nitrogen sensing mechanism in rice genotypes through expression analysis of high and low affinity ammonium transporter genes. *Molecular Biology Reports* 39: 2233-2241.

Gazipur, B. (2004). Effect of potassium on salinity tolerance of mungbean (*Vigana radiata* L. *Wilczek*). Journal of Biological Sciences 4, 103-110.

Gericke, W. F. (1937). Hydroponics- crop production in liquid culture media. *Science* 85: 177-178.

Gévaudant, F., Duby, G. & Zhao, R. (2007). Expression of a constitutively activated plasma membrane H^+-ATPase alters plant development and increases salt tolerance. *Plant Physiology* 144: 1763-1776.

Gianinazzi-Pearson, V., Arnould, C., Oufattole, M., Arango, M. & Gianinazzi, S. (2000). Differential activation of H^+-ATPase genes by an arbuscular mycorrhizal fungus in root cells of transgenic tobacco. *Planta* 211: 609-613.

Glass, A. D. (2003). Nitrogen use efficiency of crop plants: physiological constraints upon nitrogen absorption. *Critical Reviews in Plant Sciences* 22: 453-470.

Glaszmann, J. C. (1987). Isozymes and classification of asian rice varieties. *Theoretical and Applied Genetics* 74: 21-30.

Godfray, H. C. J., Beddington, J. R., Crute, I. R., Haddad, L., Lawrence, D., Muir, J. F., Pretty, J., Robinson, S., Thomas, S. M. & Toulmin, C. (2010). Food security: the challenge of feeding 9 billion people. *Science* 327: 812-818.

Gong, D.-S., Xiong, Y.-C., Ma, B.-L., Wang, T.-M., Ge, J.-P., Qin, X.-L., Li, P.-F., Kong, H.-Y., Li, Z.-Z. & Li, F.-M. (2010). Early activation of plasma membrane H^+-ATPase and its relation to drought adaptation in two contrasting oat (*Avena sativa* L.) genotypes. *Environmental and Experimental Botany* 69: 1-8.

Gourley, C., Allan, D. & Russelle, M. (1994). Plant nutrient efficiency: A comparison of definitions and suggested improvement. *Plant and Soil* 158: 29-37.

Grabov, A. (2007). Plant KT/ KUP/ HAK potassium transporters: Single family - multiple functions. *Annals of Botany* 99: 1035-1041.

Guo, M., Ruan, W., Li, C., Huang, F., Zeng, M., Liu, Y., Yu, Y., Ding, X., Wu, Y., Wu, Z., Mao, C., Yi, K., Wu, P. & Mo, X. (2015). Integrative comparison of the role of the PHOSPHATE RESPONSE1 subfamily in phosphate signaling and homeostasis in rice. *Plant Physiology* 168: 1762-1776.

Guo, S., Zhou, Y., Li, Y., Gao, Y., and Shen, Q. (2008). Effects of different Nitrogen forms and osmotic stress on water use efficiency of rice (*Oryza sativa*). Annals Of Applied Biology 153, 127-134.

Gupta, M., Qiu, X., Wang, L., Xie, W., Zhang, C., Xiong, L., Lian, X. & Zhang, Q. (2008). KT/HAK/KUP potassium transporters gene family and their whole-life cycle expression profile in rice (*Oryza sativa*). *Molecular Genetics and Genomics* 280: 437-452.

Halewood, M., Chiurugwi, T., Sackville Hamilton, R., Kurtz, B., Marden, E., Welch, E., Michiels, F., Mozafari, J., Sabran, M. & Patron, N. (2018). Plant genetic resources for food and agriculture: opportunities and challenges emerging from the science and information technology revolution. *New Phytologist*. 217: 1407-1419.

Halliday, D., and Trenkel, M. (1992). IFA world fertilizer use manual.

Hammond-Kosack, K. & Jones, J. D. (2000). Responses to plant pathogens. *Biochemistry and Molecular Biology of Plants* 1: 1102-1156.

Hartley, T. (2018). Increasing the potassium use efficiency of Crops. *PhD thesis*: University of York.

He, Y., Liao, H. & Yan, X. (2003). Localized supply of phosphorus induces root morphological and architectural changes of rice in split and stratified soil cultures. *Plant and Soil* 248: 247-256.

Heffer, P. (2013). Assessment of Fertilizer Use by Crop at the Global Level 2010-2010/11. International Fertilizer Industry Association, Paris.

Hermans, C., Hammond, J. P., White, P. J. & Verbruggen, N. (2006). How do plants respond to nutrient shortage by biomass allocation? *Trends in Plant Science* 11: 610-617.

Hill, W. & Morrill, L. (1975). Boron, calcium, and potassium interactions in Spanish peanuts. *Soil Science Society of America Journal* 39: 80-83.

Hittalmani, S., Huang, N., Courtois, B., Venuprasad, R., Shashidhar, H., Zhuang, J. Y., Zheng, K. L., Liu, G. F., Wang, G. C., Sidhu, J., Srivantaneeyakul, S., Singh, V., Bagali, P., Prasanna, H., McLaren, G. & Khush, G. (2003). Identification of QTL for growth- and grain yield-related traits in rice across nine locations of Asia. *Theoretical and Applied Genetics* 107: 679-690.

Hoffmann, W. & Poorter, H. (2002). Avoiding bias in calculations of relative growth rate. *Annals of Botany* 90: 37-42.

Hong, J. P., Takeshi, Y., Kondou, Y., Schachtman, D. P., Matsui, M. & Shin, R. (2013). Identification and characterization of transcription factors regulating Arabidopsis HAK5. *Plant and Cell Physiology* 54: 1478-1490.

Horie, T., Brodsky, D. E., Costa, A., Kaneko, T., Lo Schiavo, F., Katsuhara, M. & Schroeder, J. I. (2011). K^+ transport by the OsHKT2;4 transporter from rice with atypical Na^+ transport properties and competition in permeation of K^+ over Mg^{2+} and Ca^{2+} ions. *Plant Physiology* 156: 1493-1507.

Horie, T., Costa, A., Kim, T. H., Han, M. J., Horie, R., Leung, H. Y., Miyao, A., Hirochika, H., An, G. & Schroeder, J. I. (2007). Rice OsHKT2; 1 transporter mediates large Na^+ influx component into K+-starved roots for growth. *The EMBO Journal* 26: 3003-3014.

Horie, T., Yoshida, K., Nakayama, H., Yamada, K., Oiki, S. & Shinmyo, A. (2001). Two types of HKT transporters with different properties of Na^+ and K^+ transport in Oryza sativa. *The Plant Journal* 27: 129-138. https://doi.org/10.1080/00380768.2017.1412238

Hu, B., Wang, W., Ou, S., Tang, J., Li, H., Che, R., Zhang, Z., Chai, X., Wang, H. & Wang, Y. (2015). Variation in NRT1.1B contributes to nitrate-use divergence between rice subspecies. *Nature Genetics* 47: 834-838.

Hu, J., Lin, X., Wang, J., Dai, J., Cui, X., Chen, R. & Zhang, J. (2009). Arbuscular mycorrhizal fungus enhances crop yield and P-uptake of maize (*Zea mays* L.): A field case study on a sandy loam soil as affected by long-term P-deficiency fertilization. *Soil Biology and Biochemistry* 41: 2460-2465.

Huang, S., Zhao, C., Zhang, Y. & Wang, C. (2018). Nitrogen Use Efficiency in Rice. In *Nitrogen in Agriculture-Updates*: InTech.

Huang, W.-y. (2009). *Factors contributing to the recent increase in US fertilizer prices, 2002-08.* DIANE Publishing.

Hui, L., Zhiyu, P., Xiaohong, Y., Weidong, W., Junjie, F., Jianhua, W., Yingjia, H., Yuchao, C., Tingting, G., Ning, Y., et al. (2012). Genome- wide association study dissects the genetic architecture of oil biosynthesis in maize kernels. Nature Genetics 45, 43.

Hwang, H., Yoon, J., Kim, H. Y., Min, M. K., Kim, J.-A., Choi, E.-H., Lan, W., Bae, Y.-M., Luan, S. & Cho, H. (2013). Unique features of two potassium channels, OsKAT2 and OsKAT3, expressed in rice guard cells. *PLoS ONE* 8: e72541.

Inghelandt, D., Reif, J., Dhillon, B., Flament, P., and Melchinger, A. (2011). Extent and genome-wide distribution of linkage disequilibrium in commercial maize germplasm. Theoretical and Applied Genetics 123, 11-20.

Isayenkov, S., Isner, J.-C. & Maathuis, F. (2011). Rice two-pore K^+ channels are expressed in different types of vacuoles. *Plant Cell* 23: 756-768.

Itoh, J., Nonomura, K., Ikeda, K., Yamaki, S., Inukai, Y., Yamagishi, H., Kitano, H. & Nagato, Y. (2005). Rice plant development: from zygote to spikelet. *Plant and Cell Physiology* 46: 23-47.

Ivashikina, N. V. & Feyziev, Y. M. (1998). Regulation of nitrate uptake in maize seedlings by accompanying cations. *Plant Science* 131: 25-34.

Jahn, T., Fuglsang, A. T., Olsson, A., Bruntrup, I. M., Collinge, D. B., Volkmann, D., Sommarin, M., Palmgren, M. G. & Larsson, C. (1997). The 14-3-3 protein interacts

directly with the C-terminal region of the plant plasma membrane H^+-ATPase. *The Plant Cell* 9: 1805-1814.

Janicka-Russak, M., Kabala, K., Wdowikowska, A. & Klobus, G. (2013). Modification of plasma membrane proton pumps in cucumber roots as an adaptation mechanism to salt stress. *Journal of Plant Physiology* 170: 915-922.

Jarzyniak, K. M. & Jasiński, M. (2014). Membrane transporters and drought resistance – a complex issue. *Frontiers in Plant Science* 5: Article 687.

Jeong, K., Mattes, N., Catausan, S., Chin, J. H., Paszkowski, U. & Heuer, S. (2015). Genetic diversity for mycorrhizal symbiosis and phosphate transporters in rice. *Journal of Integrative Plant Biology* 57: 969-979.

Jia, H., Zhang, S., Wang, L., Yang, Y., Zhang, H., Cui, H., Shao, H. & Xu, G. (2017). OsPht1;8, a phosphate transporter, is involved in auxin and phosphate starvation response in rice. *Journal of Experimental Botany* 68: 5057-5068.

Jia, Y.-b., Yang, X.-e., Feng, Y. & Jilani, G. (2008). Differential response of root morphology to potassium deficient stress among rice genotypes varying in potassium efficiency. *Journal of Zhejiang University Science B* 9: 427-434.

Jian-chang, X. (2004). Potassium nutrition of the rice–wheat cropping system. Advances in Agronomy 81, 203.

Jian-Feng, L., Julie, E. N., John, A., Matthew, M., Dandan, Z., Jenifer, B., George, M. C. & Jen, S. (2013). Multiplex and homologous recombination– mediated genome editing in *Arabidopsis* and *Nicotiana benthamiana* using guide RNA and Cas9. *Nature Biotechnology* 31: 688-691

Jin, M., Dongshu, G., Jinzhe, Z., Qingpei, H., Genji, Q., Xin, Z., Jianmin, W., Hongya, G. & Li-Jia, Q. (2013). Targeted mutagenesis in rice using CRISPR-Cas system. *Cell Research* 23: 1233-1236.

Johansen, C., Edwards, D. & Loneragan, J. (1968). Interactions between potassium and calcium in their absorption by intact barley plants. I. Effects of potassium on calcium absorption. *Plant Physiology* 43: 1717-1721.

Ju, J., Yamamoto, Y., Wang, Y., Shan, Y., Dong, G., Yoshida, T. & Miyazaki, A. (2006). Genotypic differences in grain yield, and nitrogen absorption and utilization in recombinant inbred lines of rice under hydroponic culture. *Soil Science and Plant Nutrition* 52: 321-330.

Kamburova, V. S., Nikitina, E. V., Shermatov, S. E., Buriev, Z. T., Kumpatla, S. P., Emani, C. & Abdurakhmonov, I. Y. (2017). Genome editing in plants: an overview of tools and applications. *International Journal of Agronomy* 2017. Article ID 7315351.

Kant, S., Bi, Y. M. & Rothstein, S. J. (2011). Understanding plant response to nitrogen limitation for the improvement of crop nitrogen use efficiency. *Journal of Experimental Botany* 62: 1499-1509.

Katayama, H., Mori, M., Kawamura, Y., Tanaka, T., Mori, M. & Hasegawa, H. (2009). Production and characterization of transgenic rice plants carrying a high-affinity nitrate transporter gene (OsNRT2.1). *Breeding Science* 59: 237-243.

Kim, H. Y., Choi, E.-H., Min, M. K., Hwang, H., Moon, S.-J., Yoon, I., Byun, M.-O. & Kim, B.-G. (2015). Differential gene expression of two outward-rectifying shaker-like potassium channels OsSKOR and OsGORK in rice. *Journal of Plant Biology* 58: 230-235.

Kobae, Y. & Hata, S. (2010). Dynamics of periarbuscular membranes visualized with a fluorescent phosphate transporter in arbuscular mycorrhizal roots of rice. *Plant and Cell Physiology* 51: 341-353.

Kobayashi, N. I., Yamaji, N., Yamamoto, H., Okubo, K., Ueno, H., Costa, A., Tanoi, K., Matsumura, H., Fujii-Kashino, M., Horiuchi, T., Nayef, M. A., Shabala, S., An, G., Ma, J. F. & Horie, T. (2017). OsHKT1;5 mediates Na^+ exclusion in the vasculature to protect leaf blades and reproductive tissues from salt toxicity in rice. *Plant Journal* 91: 657-670.

Korte, A. & Farlow, A. (2013). The advantages and limitations of trait analysis with GWAS: a review. *Plant Methods* 9: 29.

Kraakman, A.T.W., Niks, R.E., Van Den Berg, P.M.M.M., Stam, P., and Van Eeuwijk, F.A. (2004). Linkage disequilibrium mapping of yield and yield stability in modern spring barley cultivars. Genetics 168, 435-446.

Krajinski, F., Courty, P.-E., Sieh, D., Franken, P., Zhang, H., Bucher, M., Gerlach, N., Kryvoruchko, I., Zoeller, D., Udvardi, M. & Hause, B. (2014). The H^+-ATPase HA1 of *Medicago truncatula* is essential for phosphate transport and plant growth during arbuscular mycorrhizal symbiosis. *The Plant Cell* 26: 1808-1817.

Krajinski, F., Hause, B., Gianinazzi-Pearson, V. & Franken, P. (2002). Mtha1, a plasma membrane H^+-ATPase gene from Medicago truncatula, shows arbuscule-specific induced expression in mycorrhizal tissue. *Plant Biology* 4: 754-761.

Krapp, A., Berthomé, R., Orsel, M., Mercey-Boutet, S., Yu, A., Castaings, L., Elftieh, S., Major, H., Renou, J.-P. & Daniel-Vedele, F. (2011). Arabidopsis roots and shoots show distinct temporal adaptation patterns toward nitrogen starvation. *Plant Physiology* 157: 1255-1282.

Krapp, A., David, L. C., Chardin, C., Girin, T., Marmagne, A., Leprince, A. S., Chaillou, S., Ferrario-Méry, S., Meyer, C. & Daniel-Vedele, F. (2014). Nitrate transport and signalling in Arabidopsis. *Journal Of Experimental Botany* 65: 789-798.

Kristen, L.K., Peter, J.B., Randall, J.W., Edward, S.B., Araby, R.B., Marco, A.O.-R., John, C.Z., Stephen, K., Michael, D.M., Doreen, W., et al. (2011). Genome- wide association study of quantitative resistance to southern leaf blight in the maize nested association mapping population. Nature Genetics 43, 163.

Kumar, A., and Yadav, D. (2001). Long-Term Effects of Fertilizers on the Soil Fertility and Productivity of a Rice–Wheat System. Journal of Agronomy and Crop science 186, 47-54.

Kumar, V., Singh, A., Mithra, S.V.A., Krishnamurthy, S.L., Parida, S.K., Jain, S., Tiwari, K.K., Kumar, P., Rao, A.R., Sharma, S.K., et al. (2015). Genome- wide association mapping of salinity tolerance in rice (Oryza sativa). DNA research : an international journal for rapid publication of reports on genes and genomes 22, 133.

Lan, W.-Z., Wang, W., Wang, S.-M., Li, L.-G., Buchanan, B. B., Lin, H.-X., Gao, J.-P. & Luan, S. (2010a). A rice high-affinity potassium transporter (HKT) conceals a calcium-permeable cation channel. *Proceedings of the National Academy of Sciences USA* 107: 7089-7094.

Leon, V. K. (2012). Plant nutrition: Rooting for more phosphorus. *Nature* 488: 466-467.

Li, G. & Zhu, H. (2013). Genetic studies: the linear mixed models in genome-wide association studies. *Open Bioinformatics Journal* 7: 27-33.

Li, J., Long, Y., Qi, G.-N., Li, J., Xu, Z.-J., Wu, W.-H. & Wang, Y. (2014). The Os-AKT1 Channel Is Critical for K+ Uptake in rice roots and is modulated by the rice CBL1-CIPK23 complex. *The Plant Cell* 26: 3387-3402.

Li, S. M. & Shi, W. M. (2006). Quantitative characterization of nitrogen regulation of OsAMT1;1, OsAMT1;2, and OsAMT2;2 expression in rice seedlings. *Russian Journal of Plant Physiology* 53: 837-843.

Li, S.-M., Li, B.-Z. & Shi, W.-M. (2012). Expression patterns of nine ammonium transporters in rice in response to N status. *Pedosphere* 22: 860-869.

Li, W., Xu, G., Alli, A. & Yu, L. (2017). Plant HAK/ KUP/KT K^+ transporters: Function and regulation. *Seminars in Cell and Developmental Biology*.

Lian, X., Xing, Y., Yan, H., Xu, C., Li, X. & Zhang, Q. (2005). QTLs for low nitrogen tolerance at seedling stage identified using a recombinant inbred line population derived from an elite rice hybrid. *Theoretical and Applied Genetics* 112: 85-96.

Liang, S., Wu, L., Ren, G., Zhao, X., Zhou, M., McNeil, D., and Ye, G. (2016). Genome-wide association study of grain yield and related traits using a collection of advanced indica rice breeding lines for irrigated ecosystems. Field Crops Research 193, 70-86.

Lin, W. Y., Lin, S. I. & Chiou, T. J. (2009). Molecular regulators of phosphate homeostasis in plants. *Journal of Experimental Botany* 60: 1427-1438.

Liu, F., Wang, Z., Ren, H., Shen, C., Li, Y., Ling, H. Q., Wu, C., Lian, X. & Wu, P. (2010). OsSPX1 suppresses the function of OsPHR2 in the regulation of expression of OsPT2 and phosphate homeostasis in shoots of rice. *Plant Journal* 62: 508-517.

Liu, G., Li, Y. & Porterfield, D. M. (2009). Genotypic differences in potassium nutrition in lowland rice hybrids. *Communications in Soil Science and Plant Analysis* 40: 1803-1821.

Lopez-Bucio, J., Hernandez-Abreu, E., Sanchez-Calderon, L., Perez-Torres, A., Rampey, R. A., Bartel, B. & Herrera-Estrella, L. (2005). An auxin transport independent pathway is involved in phosphate stress-induced root architectural alterations in Arabidopsis. Identification of BIG as a mediator of auxin in pericycle cell activation. *Plant Physiology* 137, 681-691.

Loqué, D. (2004). Regulatory levels for the transport of ammonium in plant roots. *Journal of Experimental Botany* 55: 1293-1305.

Lynch, J. P. & Brown, K. M. (2001). Topsoil foraging–an architectural adaptation of plants to low phosphorus availability. *Plant and Soil* 237: 225-237.

Ma, T. L., Wu, W. H. & Wang, Y. (2012). Transcriptome analysis of rice root responses to potassium deficiency. *BMC Plant Biology* 12: 161.

Ma, X., Zhang, Q., Zhu, Q., Liu, W., Chen, Y., Qiu, R., Wang, B., Yang, Z., Li, H., Lin, Y., Xie, Y., Shen, R., Chen, S., Wang, Z., Chen, Y., Guo, J., Chen, L., Zhao, X., Dong, Z. & Liu, Y.-G. (2015). A robust CRISPR/Cas9 system for convenient, high-efficiency multiplex genome editing in monocot and dicot plants. *Molecular Plant* 8: 1274-1284.

Maathuis, F. (2013). Plant Mineral Nutrients Methods and Protocols. In *Methods in Molecular Biology*, (Ed J. Walker, ed.). Human press. p. 290.

Maathuis, F. J. & Podar, D. (2011). Uptake, distribution, and physiological functions of potassium, calcium, and magnesium. *The Molecular and Physiological Basis of Nutrient Use Efficiency in Crops* pp. 265-293.

Maathuis, F. J. M. (2009). Physiological functions of mineral macronutrients. *Current Opinion in Plant Biology* 12: 250-258.

Maclean, J., Hardy, B. & Hettel, G. (2013). *Rice Almanac: Source book for one of the most important economic activities on earth.* IRRI.

Magnus, N., Justin, O.B., Joy, B., Charles, C.B., Joanne, C., Jenny, H., Martin, K., Julin, N.M., Tina, N., Peter, J.O., et al. (2002). The extent of linkage disequilibrium in Arabidopsis thaliana. Nature Genetics 30, 190.

Malvi, U. R. (2011). Interaction of micronutrients with major nutrients with special reference to potassium. *Karnataka Journal of Agricultural Sciences* 24: 106-109.

Marschner, H. & Dell, B. (1994). Nutrient uptake in mycorrhizal symbiosis. *Plant and Soil* 159: 89-102.

Maruyama, H. & Wasaki, J. (2018).Transgenic approaches for improving phosphorus use efficiency in plants. In: *Plant Macronutrient Use Efficiency*, pp. 323-338: Elsevier.

Mather, K. A., Caicedo, A. L., Polato, N. R., Olsen, K. M., McCouch, S. & Purugganan, M. D. (2007). The extent of linkage disequilibrium in rice (*Oryza sativa* L.). *Genetics* 177: 2223-2232.

Matsubara, K., Yamamoto, E., Kobayashi, N., Ishii, T., Tanaka, J., Tsunematsu, H., Yoshinaga, S., Matsumura, O., Yonemaru, J. I., Mizobuchi, R., Yamamoto, T., Kato, H. & Yano, M. (2016). Improvement of rice biomass yield through QTL-based selection. *PLoS ONE* 11: e0151830.

May, A. (2017). Base editing on the rise. *Nature Biotechnology* 35: 428-429

McCouch, S. R., Wright, M. H., Tung, C.-W., Maron, L. G., McNally, K. L., Fitzgerald, M., Singh, N., DeClerck, G., Agosto-Perez, F. & Korniliev, P. (2016). Open access resources for genome-wide association mapping in rice. *Nature Communications* 7: 10532.

McNally, K. L., Childs, K. L., Bohnert, R., Davidson, R. M., Zhao, K., Ulat, V. J., Zeller, G., Clark, R. M., Hoen, D. R. & Bureau, T. E. (2009). Genomewide SNP variation reveals relationships among landraces and modern varieties of rice. *Proceedings of the National Academy of Sciences USA* 106: 12273-12278.

Mekawy, A. M. M., Assaha, D. V. M., Yahagi, H., Tada, Y., Ueda, A. & Saneoka, H. (2015). Growth, physiological adaptation, and gene expression analysis of two Egyptian rice cultivars under salt stress. *Plant Physiology and Biochemistry* 87: 17-25.

Miyamoto, T., Ochiai, K., Nonoue, Y., Matsubara, K., Yano, M. & Matoh, T. (2015). Expression level of the sodium transporter gene OsHKT2;1 determines sodium accumulation of rice cultivars under potassium-deficient conditions. *Soil Science and Plant Nutrition* 61: 481-492

Miyamoto, T., Ochiai, K., Takeshita, S. & Matoh, T. (2012). Identification of quantitative trait loci associated with shoot sodium accumulation under low potassium conditions in rice plants. *Soil Science and Plant Nutrition* 58: 728-736.

Morsomme, P. & Boutry, M. (2000). The plant plasma membrane H^+-ATPase: structure, function and regulation. *BBA - Biomembranes* 1465: 1-16.

Muthayya, S., Sugimoto, J. D., Montgomery, S. & Maberly, G. F. (2014). An overview of global rice production, supply, trade, and consumption. *Annals of the New York Academy of Sciences* 1324: 7-14.

Namai, S., Toriyama, K. & Fukuta, Y. (2009). Genetic variations in dry matter production and physiological nitrogen use efficiency in rice (*Oryza sativa* L.) varieties. *Breeding Science* 59: 269-276.

Nath, M. & Tuteja, N. (2016). NPKS uptake, sensing, and signaling and miRNAs in plant nutrient stress. *Protoplasma* 253: 767-786.

Neumann, K., Kobiljski, B., Denčić, S., Varshney, R., and Börner, A. (2011). Genome-wide association mapping: a case study in bread wheat (Triticum aestivum L.). Molecular Breeding 27, 37-58.

Nguyen, N. (2002). Global climate changes and rice food security. *Ed, Vol FAO, Rome, Italy*: pp. 24-30.

Nguyen, T. H., Huang, S., Meynard, D., Chaine, C., Michel, R., Roelfsema, M. R. G., Guiderdoni, E., Sentenac, H. & Véry, A.-A. (2017). A dual role for the OsK5.2 ion channel in stomatal movements and K^+ loading into xylem sap. *Plant Physiology* 174: 2409-2418.

Nieves-Cordones, M., Alemán, F., Martínez, V. & Rubio, F. (2010). The Arabidopsis thaliana HAK5 K^+ transporter is required for plant growth and K^+ Acquisition from low K^+ solutions under saline conditions. *Molecular Plant* 3: 326-333.

Nishida, S., Dissanayaka, D. M. S. B., Honda, S., Tateishi, Y., Chuba, M., Maruyama, H., Tawaraya, K. & Wasaki, J. (2017). Identification of genomic regions associated with low phosphorus tolerance in japonica rice (*Oryza sativa* L.) by QTL-Seq. *Soil Science and Plant Nutrition*

Nishimura, A., Aichi, I. & Matsuoka, M. (2006). A protocol for *Agrobacterium*-mediated transformation in rice. *Nature Protocols* 1: 2796-2802.

Obata, T., Kitamoto, H. K., Nakamura, A., Fukuda, A. & Tanaka, Y. (2007). Rice shaker potassium channel OsKAT1 confers tolerance to salinity stress on yeast and rice cells. *Plant Physiology* 144: 1978-1985.

Okada, T., Nakayama, H., Shinmyo, A. & Yoshida, K. (2008). Expression of OsHAK genes encoding potassium ion transporters in rice. *Plant Biotechnology* 25: 241-245.

Parniske, M. (2008). Arbuscular mycorrhiza: the mother of plant root endosymbioses. *Nature Reviews Microbiology* 6: 763-775.

Pasam, R., Sharma, R., Malosetti, M., van Eeuwijk, F., Haseneyer, G., Kilian, B., and Graner, A. (2012). Genome- wide association studies for agronomical traits in a world wide spring barley collection. BMC Plant Biology 12, 16.

Paszkowski, U., Kroken, S., Roux, C. & Briggs, S. P. (2002). Rice phosphate transporters include an evolutionarily divergent gene specifically activated in arbuscular mycorrhizal symbiosis. *Proceedings of the National Academy of Sciences* 99: 13324-13329.

Poirier, Y. & Bucher, M. (2002). Phosphate Transport and Homeostasis in Arabidopsis. *The Arabidopsis Book* 1.

Price, A. L., Patterson, N. J., Plenge, R. M., Weinblatt, M. E., Shadick, N. A. & Reich, D. (2006). Principal components analysis corrects for stratification in genome-wide association studies. *Nature Genetics* 38: 904-909.

Price, A. L., Zaitlen, N. A., Reich, D. & Patterson, N. (2010). New approaches to population stratification in genome-wide association studies. *Nature Reviews Genetics* 11: 459-463.

Prinzenberg, A., Barbier, H., Salt, D., Stich, B. & Reymond, M. (2010). Relationships between growth, growth response to nutrient supply, and ion content using a recombinant inbred line population in Arabidopsis. *Plant Physiology* 154: 1361-1371.

Qiwei, S., Yanpeng, W., Jun, L., Yi, Z., Kunling, C., Zhen, L., Kang, Z., Jinxing, L., Jianzhong Jeff, X., Jin-Long, Q. & Caixia, G. (2013). Targeted genome modification of crop plants using a CRISPR-Cas system. *Nature Biotechnology* 31: 686-688.

Raghothama, K. & Karthikeyan, A. (2005). Phosphate acquisition. *Plant and Soil* 274: 37-49.

Rakshit, S., Rakshit, A., Matsumura, H., Takahashi, Y., Hasegawa, Y., Ito, A., Ishii, T., Miyashita, N. T. & Terauchi, R. (2007). Large-scale DNA polymorphism study of Oryza sativa and O. rufipogon reveals the origin and divergence of Asian rice. *Theoretical and Applied Genetics* 114: 731-743.

Ramensky, V., Bork, P. & Sunyaev, S. (2002). Human non- synonymous SNPs: server and survey. *Nucleic Acids Research* 30: 3894.

Ranathunge, K., El-Kereamy, A., Gidda, S., Bi, Y. & Rothstein, S. J. (2014). AMT1;1 transgenic rice plants with enhanced NH_4 permeability show superior growth and higher yield under optimal and suboptimal NH_4 conditions. *Journal Of Experimental Botany* 65(4): 965-979.

Raun, W. R. & Johnson, G. V. (1999). Improving nitrogen use efficiency for cereal production. *Agronomy Journal* 91: 357-363.

Regenberg, B., Villalba, J. M., Lanfermeijer, F. C. & Palmgren, M. G. (1995). C-terminal deletion analysis of plant plasma membrane H^+-ATPase: yeast as a model system for solute transport across the plant plasma membrane. *The Plant Cell* 7: 1655-1666.

Ren, B., Wang, M., Chen, Y., Sun, G., Li, Y., Shen, Q., and Guo, S. (2015). Water absorption is affected by the nitrogen supply to rice plants. Plant And Soil 396, 397-410.

Ristova, D., and Busch, W. (2014). Natural variation of root traits: from development to nutrient uptake. Plant physiology 166, 518.

Rothstein, S. J. (2007). Returning to our roots: Making plant biology research relevant to future challenges in agriculture. *Plant Cell* 19: 2695-2699.

Ruan, W., Guo, M., Wu, P. & Yi, K. (2017). Phosphate starvation induced OsPHR4 mediates Pi-signaling and homeostasis in rice. *Plant Molecular Biology* 93: 327-340.

Ryan, P. R., Delhaize, E. & Jones, D. L. (2001). Function and mechanism of organic anion exudation from plant roots. *Annual Review of Plant Biology* 52: 527-560.

Sales, M. A., Burgos, N. R., Shivrain, V. K., Murphy, B. & Gbur, E. E. (2011). Morphological and physiological responses of weedy red rice (*Oryza sativa* L.) and cultivated rice (*O. sativa*) to N supply. *American Journal of Plant Sciences* 2: 569-577.

Samonte, S. O. P., Wilson, L. T., Medley, J. C., Pinson, S. R., McClung, A. M. & Lales, J. S. (2006). Nitrogen utilization efficiency. *Agronomy Journal* 98: 168-176.

Samuel, C., Pavel, K., Alexandre, F., Abdelbagi, I., Glenn, G., Jason, M. & Susan, M. (2016). Genome- wide association and high- resolution phenotyping link *Oryza*

sativa panicle traits to numerous trait-specific QTL clusters. *Nature Communications* 7: 10527.
Sanyal, P., Malczynski, L. A. & Kaplan, P. (2015). Impact of energy price variability on global fertilizer price: application of alternative volatility models. *Sustainable Agriculture Research* 04(4).
Sassi, A., Mieulet, D., Khan, I., Moreau, B., Gaillard, I., Sentenac, H. & Véry, A.-A. (2012). The rice monovalent cation transporter OsHKT2;4: revisited ionic selectivity. *Plant Physiology* 160: 498-510.
Sauer, N. J., Mozoruk, J., Miller, R. B., Warburg, Z. J., Walker, K. A., Beetham, P. R., Schöpke, C. R. & Gocal, G. F. W. (2016). Oligonucleotide-directed mutagenesis for precision gene editing. *Plant Biotechnology Journal* 14: 496-502.
Schaller, A. & Oecking, C. (1999). Modulation of plasma membrane H^+-ATPase activity differentially activates wound and pathogen defense reponses in tomato plants. *Plant Cell* 11: 263-272.
Scheible, W. R., Lauerer, M., Schulze, E. D., Caboche, M. & Stitt, M. (1997). Accumulation of nitrate in the shoot acts as a signal to regulate shoot-root allocation in tobacco†. *The Plant Journal* 11: 671-691.
Secco, D., Baumann, A. & Poirier, Y. (2010). Characterization of the rice PHO1 gene family reveals a key role for OsPHO1; 2 in phosphate homeostasis and the evolution of a distinct clade in dicotyledons. *Plant Physiology* 152: 1693-1704.
Secco, D., Wang, C., Arpat, B. A., Wang, Z., Poirier, Y., Tyerman, S. D., Wu, P., Shou, H. & Whelan, J. (2012a). The emerging importance of the SPX domain-containing proteins in phosphate homeostasis. *New Phytologist* 193: 842-851.
Secco, D., Wang, C., Shou, H. & Whelan, J. (2012b). Phosphate homeostasis in the yeast Saccharomyces cerevisiae, the key role of the SPX domain-containing proteins. *FEBS Letters* 586: 289-295.
Shan, Y.-H., Wang, Y.-L. & Pan, X.-B. (2005). Mapping of QTLs for nitrogen use efficiency and related traits in rice (*Oryza sativa* L.). *Agricultural Sciences in China* 4: 721-727.
Shankar, A., Singh, A., Kanwar, P., Srivastava, A. K., Pandey, A., Suprasanna, P., Kapoor, S. & Pandey, G. K. (2013). Gene expression analysis of rice seedling under potassium deprivation reveals major changes in metabolism and signaling components. *PLoS ONE* 8: e70321.
Sharma, S., Kaur, R. & Singh, A. (2017). Recent advances in CRISPR/Cas mediated genome editing for crop improvement. *Plant Biotechnology Reports* 11: 193-207.
Shimizu, A., Kato, K., Komatsu, A., Motomura, K. & Ikehashi, H. (2008). Genetic analysis of root elongation induced by phosphorus deficiency in rice (*Oryza sativa* L.): fine QTL mapping and multivariate analysis of related traits. *Theoretical and Applied Genetics* 117: 987-996.
Shin, J. & Lee, C. (2015). A mixed model reduces spurious genetic associations produced by population stratification in genome-wide association studies. *Genomics* 105: 191-196.
Sinclair, T. (1992). Mineral nutrition and plant growth response to climate change. *Journal of Experimental Botany* 43: 1141-1146.
Singh, B. & Singh, R. (1985). Zinc-deficiency symptoms in lowland rice as induced by modified-urea materials applied at different rates of nitrogen in calcareous soil. *Plant and soil* 87: 439-440.

Smith, A. P., Nagarajan, V. K. & Raghothama, K. G. (2011). Arabidopsis Pht1; 5 plays an integral role in phosphate homeostasis. *Plant Signaling & Behavior* 6: 1676-1678.
Smith, S. E. & Read, D. (2008). *Mycorrhizal Symbiosis.*
Smith, S. E. & Read, D. J. (2010). *Mycorrhizal symbiosis.* Academic press.
Somers, D.J., Banks, T., DePauw, R., Fox, S., Clarke, J., Pozniak, C., and McCartney, C. (2007). Genome-wide linkage disequilibrium analysis in bread wheat and durum wheat. Genome 50, 557-567.
Sondergaard, T. E., Schulz, A. & Palmgren, M. G. (2004). Energization of transport processes in plants. Roles of the plasma membrane H^+-ATPase. *Plant Physiology* 136: 2475-2482.
Song, G., Jia, M., Chen, K., Kong, X., Khattak, B., Xie, C., Li, A. & Mao, L. (2016). CRISPR/Cas9: a powerful tool for crop genome editing. *The Crop Journal* 4: 75-82.
Song, Z., Yang, S., Zuo, J. & Su, Y. (2014). Over-expression of ApKUP3 enhances potassium nutrition and drought tolerance in transgenic rice. *Biologia Plantarum* 58: 649-658.
Sonoda, Y., Ikeda, A., Saiki, S., Wirén, N. v., Yamaya, T. & Yamaguchi, J. (2003a). Distinct expression and function of three ammonium transporter genes (OsAMT1;1 – 1;3) in rice. *Plant and Cell Physiology* 44: 726-734.
Sonoda, Y., Ikeda, A., Saiki, S., Yamaya, T. & Yamaguchi, J. (2003b). Feedback regulation of the ammonium transporter gene family AMT1 by glutamine in rice. *Plant and Cell Physiology* 44: 1396-1402.
Speth, C., Jaspert, N., Marcon, C. & Oecking, C. (2010). Regulation of the plant plasma membrane H^+-ATPase by its C-terminal domain: what do we know for sure? *European Journal of Cell Biology* 89: 145-151.
Spindel, J. E. & McCouch, S. R. (2016). When more is better: how data sharing would accelerate genomic selection of crop plants. *New Phytologist* 212: 814-826.
Stephanie, K. & Allan, J. (2012). NMD: a multifaceted response to premature translational termination. *Nature Reviews Molecular Cell Biology* 13: 700.
Subbarao, G. V., Wheeler, R. M., Stutte, G. W. & Levine, L. H. (1999). How far can sodium substitute for potassium in red beet? *Journal of Plant Nutrition* 22: 1745-1761.
Suenaga, A., Moriya, K., Sonoda, Y., Ikeda, A., Von Wirn, N., Hayakawa, T., Yamaguchi, J. & Yamaya, T. (2003). Constitutive expression of a novel-type ammonium transporter OsAMT2 in rice plants. *Plant and Cell Physiology* 44: 206-211.
Sukumaran, S., Dreisigacker, S., Lopes, M., Chavez, P., and Reynolds, M. (2015). Genome- wide association study for grain yield and related traits in an elite spring wheat population grown in temperate irrigated environments. Theoretical and Applied Genetics 128, 353-363.
Sun, J., Zou, D., Luan, F., Zhao, H., Wang, J., Liu, H., Xie, D., Su, D., Ma, J. & Liu, Z. (2014). Dynamic QTL analysis of the Na^+ content, K^+ content, and Na^+/K^+ ratio in rice roots during the field growth under salt stress. *Biologia Plantarum* 58: 689-696.
Sun, S., Gu, M., Cao, Y., Huang, X., Zhang, X., Ai, P., Zhao, J., Fan, X. & Xu, G. (2012). A Constitutive Expressed Phosphate Transporter, OsPht1;1, Modulates Phosphate Uptake and Translocation in Phosphate-Replete Rice. *Plant Physiology* 159: 1571-1581.

Sun, Y., Kong, X., Li, C., Liu, Y., and Ding, Z. (2015). Potassium Retention under Salt Stress Is Associated with Natural Variation in Salinity Tolerance among Arabidopsis Accessions. PLoS One 10, e0124032.

Sung, K., Vincent, P., Tina, T.H., Christopher, T., Richard, M.C., Stephan, O., Joseph, R.E., Detlef, W., and Magnus, N. (2007). Recombination and linkage disequilibrium in Arabidopsis thaliana. Nature Genetics 39, 1151.

Suzuki, K., Yamaji, N., Costa, A., Okuma, E., Kobayashi, N. I., Kashiwagi, T., Katsuhara, M., Wang, C., Tanoi, K. & Murata, Y. (2016). OsHKT1;4-mediated Na^+ transport in stems contributes to Na^+ exclusion from leaf blades of rice at the reproductive growth stage upon salt stress. *BMC Plant Biology* 16: 1.

Taiz, L. & Zeiger, E. (2010). Plant Physiology. Sinauer Associates.

Takehisa, H., Sato, Y., Antonio, B. A. & Nagamura, Y. (2013). Global transcriptome profile of rice root in response to essential macronutrient deficiency. *Plant Signaling & Behavior* 8: e24409.

Tang, Z., Fan, X., Li, Q., Feng, H., Miller, A. J., Shen, Q. & Xu, G. (2012). Knockdown of a rice stelar nitrate transporter alters long- distance translocation but not root influx. *Plant physiology* 160: 2052.

Teng, W., He, X. & Tong, Y.-P. (2017). Transgenic approaches for improving use efficiency of nitrogen, phosphorus and potassium in crops. *Journal of Integrative Agriculture* 16: 2657-2673.

Tian, F., Bradbury, P.J., Brown, P.J., Hung, H., Sun, Q., Flint-Garcia, S., Rocheford, T.R., McMullen, M.D., Holland, J.B., and Buckler, E.S. (2011). Genome-wide association study of leaf architecture in the maize nested association mapping population. Nature genetics 43, 159.

Toriyama, K. (2005). *Rice is Life Scientific Perspectives for the 21st Century.* Int. Rice Res. Inst.

Tsay, Y. F., Chiu, C. C., Tsai, C. B., Ho, C. H. & Hsu, P. K. (2007). Nitrate transporters and peptide transporters. *FEBS Letters* 581: 2290-2300.

Vaughan, D. A., Morishima, H. & Kadowaki, K. (2003). Diversity in the *Oryza* genus. *Current Opinion in Plant Biology* 6: 139-146.

Venuprasad, R., Bool, M., Quiatchon, L., Sta Cruz, M., Amante, M. & Atlin, G. (2012). A large-effect QTL for rice grain yield under upland drought stress on chromosome 1. *Molecular Breeding* 30: 535-547.

Wan, T., Xue, H. & Tong, Y.-P. (2017). Transgenic approaches for improving use efficiency of nitrogen, phosphorus and potassium in crops. *Journal of Integrative Agriculture* 16: 2657-2673.

Wang, C., Huang, W., Ying, Y., Li, S., Secco, D., Tyerman, S., Whelan, J. & Shou, H. (2012). Functional characterization of the rice SPX-MFS family reveals a key role of OsSPX-MFS1 in controlling phosphate homeostasis in leaves. *New Phytologist* 196: 139-148.

Wang, D., Lv, S., Jiang, P. & Li, Y. (2017). Roles, Regulation, and Agricultural Application of Plant Phosphate Transporters. *Frontiers in Plant Science* 8(817).

Wang, E., Yu, N., Bano, A., Liu, C., Miller, A. J., Cousins, D., Zhang, X., Ratet, P., Tadege, M., Mysore, K. S., Downie, J. A., Murray, J. D., Oldroyd, G. E. D. & Schultze, M. (2014a). A H^+-ATPase that energizes nutrient uptake during mycorrhizal symbioses in rice and *Medicago truncatula. Plant Cell*: 26: 1818–1830.

Wang, M., Zheng, Q., Shen, Q., and Guo, S. (2013). The Critical Role of Potassium in Plant Stress Response (Basel), pp. 7370-7390.
Wang, N., Long, T., Yao, W., Xiong, L., Zhang, Q. & Wu, C. (2013). Mutant resources for the functional analysis of the rice genome. *Molecular plant* 6: 596-604.
Wang, R., Jing, W., Xiao, L., Jin, Y., Shen, L. & Zhang, W. (2015). The rice high-affinity potassium transporter1;1 is involved in salt tolerance and regulated by an MYB-type transcription factor. *Plant Physiology* 168: 1076-1090.
Wang, W., Vinocur, B. & Altman, A. (2003). Plant responses to drought, salinity and extreme temperatures: towards genetic engineering for stress tolerance. *Planta* 218: 1-14.
Wang, X., Wang, Y., Piñeros, M. A., Wang, Z., Wang, W., Li, C., Wu, Z., Kochian, L. V. & Wu, P. (2014b). Phosphate transporters OsPHT1; 9 and OsPHT1; 10 are involved in phosphate uptake in rice. *Plant, Cell & Environment* 37: 1159-1170.
Wang, Z., Hu, H., Huang, H., Duan, K., Wu, Z. & Wu, P. (2009). Regulation of OsSPX1 and OsSPX3 on expression of OsSPX domain genes and Pi-starvation signaling in rice. *Journal of Integrative Plant Biology* 51: 663-674.
Waters, S., Gilliham, M. & Hrmova, M. (2013). Plant High-Affinity Potassium (HKT) Transporters Involved in Salinity Tolerance: Structural Insights to Probe Differences in Ion Selectivity. *International Journal of Molecular Sciences* 14: 7660-7680.
Wei, D., Cui, K., Ye, G., Pan, J., Xiang, J., Huang, J. & Nie, L. (2012). QTL mapping for nitrogen- use efficiency and nitrogen-deficiency tolerance traits in rice. *Plant and Soil* 359: 281-295.
Werner, K. (2004). Biology, structure and mechanism of P-type ATPases. *Nature Reviews Molecular Cell Biology* 5: 282.
White, P. J. (2013). Improving potassium acquisition and utilisation by crop plants. *Journal of Plant Nutrition and Soil Science* 176: 305-316.
Wilkinson, S., Grunes, D. & Sumner, M. (2000). Nutrient interactions in soil and plant nutrition. *Handbook of Soil Sscience*: pp. 89-112.
Wilson, C., Wells, B., and Norman, R. (1994). Fertilizer nitrogen uptake by rice from urea-ammonium nitrate solution vs. granular urea. Soil Science Society of America Journal 58, 1825-1828.
Wissuwa, M. & Ae, N. (2001). Genotypic variation for tolerance to phosphorus deficiency in rice and the potential for its exploitation in rice improvement. *Plant Breeding* 120: 43-48.
Wissuwa, M., Kretzschmar, T., and Rose, T.J. (2016). From promise to application: root traits for enhanced nutrient capture in rice breeding. Journal Of Experimental Botany 67, 3605-3615.
Wissuwa, M., Yano, M. & Ae, N. (1998). Mapping of QTLs for phosphorus- deficiency tolerance in rice (*Oryza sativa* L.). *Theoretical and Applied Genetics* 97: 777-783.
Wissuwa, Wegner, Ae & Yano (2002). Substitution mapping of Pup1 : a major QTL increasing phosphorus uptake of rice from a phosphorus-deficient soil. *Theoretical and Applied Genetics* 105: 890-897.
Wu, P. & Wang, X. M. (2008). Role of OsPHR2 on phosphorus homoestasis and root hairs development in rice (*Oryza sativa* L.). *Plant Signaling & Behavior* 3: 674-675.
Xie, K. & Yang, Y. (2013). RNA- Guided Genome Editing in Plants Using a CRISPR-Cas System. *Molecular Plant* 6: 1975-1983.

Xuehui, H., Xinghua, W., Tao, S., Qiang, Z., Qi, F., Yan, Z., Canyang, L., Chuanrang, Z., Tingting, L., Zhiwu, Z., et al. (2010). Genome- wide association studies of 14 agronomic traits in rice landraces. Nature Genetics 42, 961.

Yan, M., Fan, X., Feng, H., Miller, A. J., Shen, Q. & Xu, G. (2011). Rice OsNAR2.1 interacts with OsNRT2.1, OsNRT2.2 and OsNRT2.3a nitrate transporters to provide uptake over high and low concentration ranges. *Plant, Cell & Environment* 34: 1360.

Yang, H., Wu, J.-J., Tang, T., Liu, K.-D. & Dai, C. (2017a). CRISPR/Cas9-mediated genome editing efficiently creates specific mutations at multiple loci using one sgRNA in Brassica napus. *Scientific reports* 7: 7489.

Yang, S.-Y., Grønlund, M., Jakobsen, I., Grotemeyer, M. S., Rentsch, D., Miyao, A., Hirochika, H., Kumar, C. S., Sundaresan, V., Salamin, N., Catausan, S., Mattes, N., Heuer, S. & Paszkowski, U. (2012). Nonredundant regulation of rice arbuscular mycorrhizal symbiosis by two members of the *phosphate transporter1* gene family. *The Plant Cell* 24: 4236-4251.

Yang, T., Zhang, S., Hu, Y., Wu, F., Hu, Q., Chen, G., Cai, J., Wu, T., Moran, N. & Yu, L. (2014a). The role of a potassium transporter OsHAK5 in potassium acquisition and transport from roots to shoots in rice at low potassium supply levels. *Plant Physiology* 166: 945-959.

Yang, T., Zhang, S., Hu, Y., Wu, F., Hu, Q., Chen, G., Cai, J., Wu, T., Moran, N., Yu, L. & Xu, G. (2014b). The role of a potassium transporter OsHAK5 in potassium acquisition and transport from roots to shoots in rice at low potassium supply levels. *Plant Physiology* 166: 945-959.

Yang, X. E., Liu, J. X., Wang, W. M., Li, H., Luo, A. C., Ye, Z. Q. & Yang, Y. (2003). Genotypic differences and some associated plant traits in potassium internal use efficiency of lowland rice (*Oryza sativa* L.). *Nutrient Cycling in Agroecosystems* 67: 273-282.

Yang, X., Xia, X., Zhang, Z., Nong, B., Zeng, Y., Xiong, F., Wu, Y., Gao, J., Deng, G. & Li, D. (2017b). QTL Mapping by Whole Genome Re-sequencing and Analysis of Candidate Genes for Nitrogen Use Efficiency in Rice. *Frontiers in Plant Science* 8: 1634.

Yang, Z., Gao, Q., Sun, C., Li, W., Gu, S. & Xu, C. (2009). Molecular evolution and functional divergence of HAK potassium transporter gene family in rice (*Oryza sativa* L.). *Journal of Genetics and Genomics* 36: 161-172.

Yao, X., Horie, T., Xue, S., Leung, H.-Y., Katsuhara, M., Brodsky, D. E., Wu, Y. & Schroeder, J. I. (2010). Differential sodium and potassium transport selectivities of the rice OsHKT2; 1 and OsHKT2; 2 transporters in plant cells. *Plant Physiology* 152: 341-355.

Ye, Y., Yuan, J., Chang, X., Yang, M., Zhang, L., Lu, K. & Lian, X. (2015). The phosphate transporter gene OsPht1;4 is involved in phosphate homeostasis in rice. *PLoS One* 10: e0126186.

Yoshida, S., Forno, D. A., Cock, J. H. & Gomez, K. A. (1976). *Laboratory Manual for Physiological Studies of Rice.* Los Baños, Laguna, Philippines: The International Rice Research Institute.

Yu, C., Liu, Y., Zhang, A., Su, S., Yan, A., Huang, L., Ali, I., Liu, Y., Forde, B. G. & Gan, Y. (2015). MADS-box transcription factor OsMADS25 regulates root development through affection of nitrate accumulation in rice. *PLoS One* 10(8).

Yu, J. & Buckler, E. S. (2006). Genetic association mapping and genome organization of maize. *Current Opinion in Biotechnology* 17: 155-160.

Yu, J., Pressoir, G., Briggs, W. H., Bi, I. V., Yamasaki, M., Doebley, J. F., McMullen, M. D., Gaut, B. S., Nielsen, D. M. & Holland, J. B. (2006). A unified mixed-model method for association mapping that accounts for multiple levels of relatedness. *Nature Genetics* 38: 203-208.

Zhang, B., Yang, X., Yang, C., Li, M. & Guo, Y. (2016). Exploiting the CRISPR/ Cas9 System for Targeted Genome Mutagenesis in Petunia. *Scientific Reports* 6: 20315-20315.

Zhang, F., Sun, Y., Pei, W., Jain, A., Sun, R., Cao, Y., Wu, X., Jiang, T., Zhang, L., Fan, X., Chen, A., Shen, Q., Xu, G. & Sun, S. (2015a). Involvement of OsPht1;4 in phosphate acquisition and mobilization facilitates embryo development in rice. *The Plant Journal* 82: 556-569.

Zhang, F., Wu, X.-N., Zhou, H.-M., Wang, D.-F., Jiang, T.-T., Sun, Y.-F., Cao, Y., Pei, W.-X., Sun, S.-B. & Xu, G.-H. (2014a). Overexpression of rice phosphate transporter gene OsPT6 enhances phosphate uptake and accumulation in transgenic rice plants. *Plant and Soil* 384: 259-270.

Zhang, H., Wang, Z., Wang, S., and Li, H. (2012). Progress of genome wide association study in domestic animals. In J Anim Sci Biotechnol.

Zhang, H., Zhang, J., Wei, P., Zhang, B., Gou, F., Feng, Z., Mao, Y., Yang, L., Zhang, H. & Xu, N. (2014b). The CRISPR/Cas9 system produces specific and homozygous targeted gene editing in rice in one generation. *Plant Biotechnology Journal* 12: 797-807.

Zhang, Y., Tan, L., Zhu, Z., Yuan, L., Xie, D. & Sun, C. (2015b). TOND1 confers tolerance to nitrogen deficiency in rice. *Plant Journal* 81: 367-376.

Zhao, D., Reddy, K. R., Kakani, V. G. & Reddy, V. (2005). Nitrogen deficiency effects on plant growth, leaf photosynthesis, and hyperspectral reflectance properties of sorghum. *European Journal of Agronomy* 22: 391-403.

Zhao, K., Tung, C. W., Eizenga, G. C., Wright, M. H., Ali, M. L., Price, A. H., Norton, G. J., Islam, M. R., Reynolds, A., Mezey, J., McClung, A. M., Bustamante, C. D. & McCouch, S. R. (2011). Genome-wide association mapping reveals a rich genetic architecture of complex traits in Oryza sativa. *Nature Communications* 2: 10.

Zhao, R., Dielen, V., Kinet, J.-M. & Boutry, M. (2000). Cosuppression of a plasma membrane H^+-ATPase Isoform impairs sucrose translocation, stomatal opening, plant growth, and male fertility. *The Plant Cell* 12: 535-546.

Zhong-Hai, R., Ji-Ping, G., Le-Gong, L., Xiu-Ling, C., Wei, H., Dai-Yin, C., Mei-Zhen, Z., Zong-Yang, W., Sheng, L. & Hong-Xuan, L. (2005). A rice quantitative trait locus for salt tolerance encodes a sodium transporter. *Nature Genetics* 37: 1141-1146.

Zhou, H., Liu, B., Weeks, D. P., Spalding, M. H. & Yang, B. (2014). Large chromosomal deletions and heritable small genetic changes induced by CRISPR/Cas9 in rice. *Nucleic Acids Research* 42: 10903-10914.